



## Speciation of Long-Lived Radionuclides in the Environment

Hou, Xiaolin

*Publication date:*  
2008

*Document Version*  
Publisher's PDF, also known as Version of record

[Link back to DTU Orbit](#)

*Citation (APA):*  
Hou, X. (2008). *Speciation of Long-Lived Radionuclides in the Environment*. Danmarks Tekniske Universitet, Risø Nationallaboratoriet for Bæredygtig Energi. Denmark. Forskningscenter Risoe. Risoe-R No. 1677(EN)

---

### General rights

Copyright and moral rights for the publications made accessible in the public portal are retained by the authors and/or other copyright owners and it is a condition of accessing publications that users recognise and abide by the legal requirements associated with these rights.

- Users may download and print one copy of any publication from the public portal for the purpose of private study or research.
- You may not further distribute the material or use it for any profit-making activity or commercial gain
- You may freely distribute the URL identifying the publication in the public portal

If you believe that this document breaches copyright please contact us providing details, and we will remove access to the work immediately and investigate your claim.

# Chemical Speciation of Long-Lived Radionuclides in the Environment

Xiaolin Hou

Risø-R-1677(EN)

**Author:** Xiaolin Hou  
**Title:** Chemical Speciation of Long-Lived Radionuclides in the Environment  
**Division:** Radiation Research Division

**Abstract (max. 2000 char.):**

This project started in November 2005 and ended in November 2008, the work and research approaches are summarized in this report.

This project studied the speciation of radionuclides in environment. A number of speciation analytical methods are developed for determination of species of  $^{129}\text{I}$ ,  $^{99}\text{Tc}$ , isotopes of Pu, and  $^{237}\text{Np}$  in seawater, fresh water, soil, sediment, vegetations, and concrete. The developed methods are used for the investigation of the chemical speciation of these radionuclides as well as their environmental behaviours, especially in Danish environment. In addition the speciation of Pu isotopes in waste samples from the decommissioning of Danish nuclear facilities is also investigated. The report summarizes these works completed in this project. Through this research project, a number of research papers have been published in the scientific journals, the research results has also been presented in the Nordic and international conference/meeting and communicated to international colleagues. Some publications are also enclosed to this report.

**Participants of this project:**

Xiaolin Hou (Risø-DTU, project leader))  
Per Roos (Risø-DTU)  
Sven P. Nielsen (Risø-DTU)  
Jussi Jernstroem (Risø-DTU)  
Svend Olsen (Risø-DTU)  
Violeta Hansen (Risø-DTU)  
Ala Aldahan (Uppsala University, Sweden)  
Göran Possnert (Uppsala University, Sweden)  
Susanne Persson (Uppsala University, Sweden)  
Edvard Englund (Uppsala University, Sweden)

**Acknowledgement:**

We like to thank the Villum Kann Rasmussen Foundation for the finical support to complete this project.

We also like to thank all stuffs in Radioecology and Tracer Program, Radiation Research Division, Risø National laboratory for Sustainable Energy, Technical University of Denmark for their contributions to this work.

**Risø-R-1677(EN)**  
**November 2008**

**ISSN 0106-2840**  
**ISBN 978-87-550-3730-4**

**Contract no.:**

**Group's own reg. no.:**

**Sponsorship:**  
Supported by the Villum  
Kann Rasmussen Foundation

**Cover :**

**Pages: 145**

Information Service Department  
Risø National Laboratory for  
Sustainable Energy  
Technical University of Denmark  
P.O.Box 49  
DK-4000 Roskilde  
Denmark  
Telephone +45 46774004  
[bibl@risoe.dk](mailto:bibl@risoe.dk)  
Fax +45 46774013  
[www.risoe.dtu.dk](http://www.risoe.dtu.dk)

## **Contents:**

1. Objectives of the project
2. Instrumentations
  - 2.1 X Series<sup>II</sup> ICP-MS and HPLC
  - 2.2 Air sampler for iodine species collection from atmosphere
  - 2.3 Combustion furnace
3. Development of analytical methods
  - 3.1 Determination of  $^{127}\text{I}$  in environmental samples using ICP-MS
    - 3.1.1 Separation of iodine from solid sample using combustion
    - 3.1.2 Measurement of iodine using ICP-MS
  - 3.2 Determination of  $^{129}\text{I}$  using accelerator mass spectrometry (AMS)
  - 3.3 Determination of Pu isotopes and  $^{237}\text{Np}$  in environment
    - 3.3.1 Separation of Pu and Np from environmental samples
    - 3.3.2 Measurement of  $^{238}\text{Pu}$ ,  $^{239,240}\text{Pu}$  and  $^{237}\text{Np}$  using alpha spectrometry
    - 3.3.3 Measurement of  $^{239}\text{Pu}$ ,  $^{240}\text{Pu}$ ,  $^{241}\text{Pu}$  and  $^{237}\text{Np}$  using ICP-MS
    - 3.3.4 Measurement of  $^{241}\text{Pu}$  using liquid scintillation counting
  - 3.4 Determination of  $^{99}\text{Tc}$  and Pu/Am in environmental samples using HPLC coupled with ICP-MS.
    - 3.4.1 Separation of Pu and Am using ion chromatography HPLC
      - 3.4.1.1 Extraction chromatography for separating trivalent light lanthanides and actinides
      - 3.4.1.2 Cation exchange column for pre-concentrating trivalent actinides
      - 3.4.1.3 Ion chromatography column for final separation of trivalent actinides
    - 3.4.2 Separation of Tc using ion chromatography HPLC
      - 3.4.2.1 Separation procedure
      - 3.4.2.2 Elution of technetium from ion chromatography column
  - 3.5 Method for the speciation of  $^{129}\text{I}$  and  $^{127}\text{I}$  in water samples
    - 3.5.1 Speciation separation of iodine in water samples using ion exchange chromatography.
    - 3.5.2 Speciation of  $^{129}\text{I}$  in water using extraction and co-precipitation
    - 3.5.2 Speciation/fractionation of  $^{129}\text{I}$  and  $^{127}\text{I}$  in soil/sediment samples
    - 3.5.3. Speciation method for  $^{129}\text{I}$  and  $^{127}\text{I}$  in atmosphere
  - 3.6 Speciation/fractionation of plutonium isotopes,  $^{237}\text{Np}$  and  $^{241}\text{Am}$  in soil, sediment and concrete samples using dynamic sequential extraction
  - 3.7 Analytical method for the determination of rhenium

- 3.8 Investigation on Re-absorption of Pu during the fractionation of Pu in soil and sediment
4. Investigation of speciation of the radionuclides in environmental samples
  - 4.1 Speciation of  $^{129}\text{I}$  in North Sea surface water
  - 4.2 Speciation of  $^{129}\text{I}$  in precipitation collected in Roskilde, Denmark 2001-2006
  - 4.3. Partition of  $^{137}\text{Cs}$  and  $^{129}\text{I}$  in the Nordic lake sediment, pore-water and lake water
  - 4.4  $^{129}\text{I}$  and  $^{127}\text{I}$  and their speciation in lake sediment
  - 4.5 Iodine isotopes ( $^{127}\text{I}$  and  $^{129}\text{I}$ ) in aerosols
  - 4.6. Speciation of Pu in soil, sediment and concrete samples from decommissioning of Danish nuclear reactor
  - 4.7 Speciation of  $^{99}\text{Tc}$  and Re in seaweed samples
  - 4.8 Speciation of Pu isotopes and  $^{237}\text{Np}$  in water samples collected from Framvaren fjord
  - 4.9 Speciation of  $^{129}\text{I}$  and  $^{127}\text{I}$  in atmosphere for investigation of geochemical cycle of iodine using reprocessing  $^{129}\text{I}$  as tracer.
5. Conclusion and perspective
6. List of papers published and to be published
7. Papers presented in conferences and meetings

#### **Appendix: Some published materials**

Paper-1-EST-129I-NorthSea-2007.pdf  
 Paper-2-JER-Dynamic adsorption2008.pdf  
 Paper-3-129I-speciation-review-ACA2008.pdf  
 Paper-4-ACA-review-article-2008.pdf  
 Paper-5-Handbook of Iodine-CH015-iodine speciation-2009.pdf  
 Paper-6-EST-modeling129I-2008.pdf  
 Paper-7- Jussi-PuAm.pdf

## 1. Objectives of the project:

The aim of the project is to study the chemical speciation of the radionuclides iodine-129 ( $^{129}\text{I}$ ), plutonium-238, -239, -240, -241 ( $^{238,239,240,241}\text{Pu}$ ), technetium-99 and neptunium-237 ( $^{237}\text{Np}$ ) in order to obtain information on their behaviour in the environment. Once released to the environment these radionuclides and their radioactive decay products remain for a long time due to their very long half-lives. The results of the project will provide understanding and data for the quantification of the environmental processes governing the dispersion and biological transfer of these radionuclides and thus enable reliable assessments to be made of the associated risks to man and environment.

Specific aims of the project include:

- 1) To examine the chemical speciation of the radionuclides in environmental samples with emphasis on the radioactive contamination and nuclear waste repositories covering
  - Speciation analysis of Pu isotopes in contaminated environmental samples from Thule, Greenland,
  - Speciation analysis of Pu isotopes,  $^{129}\text{I}$  and  $^{99}\text{Tc}$  in samples related to nuclear waste from the operation and decommissioning of nuclear facilities in Denmark
  - Environmental behaviour study of Pu isotopes,  $^{129}\text{I}$  and  $^{99}\text{Tc}$  related to their transfer in the environment and to humans with an emphasis on the Danish environment.
- 2) To develop analytical methods for the chemical speciation of  $^{129}\text{I}$ , isotopes of Pu,  $^{99}\text{Tc}$  and  $^{237}\text{Np}$  in relation to risk assessment involving
  - Development of ultra-trace analysis methods for  $^{99}\text{Tc}$ ,  $^{129}\text{I}$ , isotopes of Pu and  $^{237}\text{Np}$  with inductively-coupled plasma mass spectrometry, accelerator mass spectrometry, alpha spectrometry and liquid scintillation counting techniques.
  - Development of separation methods for the chemical speciation of  $^{129}\text{I}$ , isotopes of Pu,  $^{99}\text{Tc}$ , and  $^{237}\text{Np}$  in environmental samples using chromatographic techniques as well as extraction, and sequential extraction.

The project focuses on a quantitative understanding of the chemical speciation of radionuclides in the environment that can be used for risk assessment of the plutonium contamination in Thule, Greenland, issues related to a Danish repository for nuclear waste and radionuclides in Danish waters from European reprocessing facilities.

## 2. Instrumentations

### 2.1 X Series<sup>II</sup> ICP-MS and HPLC

An X Series<sup>II</sup> ICP-MS and HPLC equipments were purchased from Thermo Electron Corporation, the instruments have been installed and tested in July 2006 (Figure 1). The performance of the instruments have been tested and optimized for the determination of the target radionuclides and speciation separation-determination. Satisfied results (sensitivity, detection limit, stability, etc.) have been obtained for the determination of  $^{127}\text{I}$ ,  $^{99}\text{Tc}$ , isotopes of Pu, and  $^{237}\text{Np}$ . The HPLC has been coupled to ICP-MS for the automated separation and speciation of analytes including  $^{127}\text{I}$ ,  $^{99}\text{Tc}$ , and isotopes of Pu and  $^{237}\text{Np}$ .



Figure 1 Thermo X Series<sup>II</sup> ICP-MS coupled with HPLC for speciation analysis of nuclides

### 2.2 Air sampler for iodine species collection from atmosphere

Two sets of air sampler was designed and manufactured by a commercial company (Staplex, USA), which has been used to collect different chemical speciation of iodine from atmosphere, such as particle, inorganic gaseous iodine, and organic gaseous iodine. The equipments have been installed and tested (Figure 2). A satisfied performance has been obtained, except the problems of vacuum pump, in which carbon brush has to be replaced every 150 hours operation. The equipment has been successfully applied to collect atmospheric samples from different location in Denmark, Sweden and Lithuania.



Figure 2 Air sampler setup for collecting particulates associated, in organic gaseous and organic gaseous iodine



### 2.3 Combustion furnace

A specific combustion furnace was designed and manufactured by a commercial company (Carbolite, UK), which is used to separate iodine from various solid samples such as soil, sediment, vegetation, tissues, air particles, filters, and active charcoal. The furnace has been installed and tested (Figure 3), a good separation efficiency (>80%) was obtained. The equipment has been successfully used for the analysed the samples for  $^{129}\text{I}$  and  $^{127}\text{I}$  in solid samples.

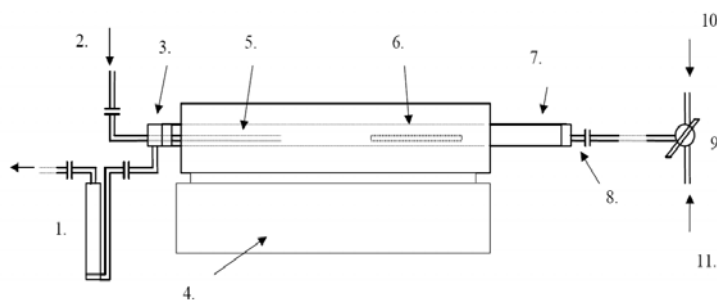


Figure 3 Schematic diagram and picture of combustion facility (Carbolite, UK) for the separation of iodine from solid sample. 1) Gas bubbler (filling with NaOH solution for trapping iodine); 2) Oxygen supply; 3) Exhaust gas manifold; 4) Temperature controller of combustion furnace; 5) Second furnace (for complete combustion of residue from first furnace); 6) sample boat in the first furnace; 7) Quartz working tube; 8) gas inlet adaptor; 9) Three ways valve; 10) main oxygen supply; 11) Compressed air supply (In the beginning of combustion, air is supplied to avoid a violet combustion under pure oxygen condition)



## 3. Development of analytical method for the speciation analysis of radionuclides

### 3.1 Determination of $^{127}\text{I}$ in environmental samples using ICP-MS

An analytical method was developed for the determination of stable iodine in various environmental samples. For the solid samples such as soil, sediment, plants, tissues and filters, the samples were first decomposed using combustion method using the furnace established (Figure 3), the separated iodine in NaOH solution is measured by ICP-MS. For seawater samples, the samples is first diluted with  $0.15 \text{ mol mL}^{-1} \text{ NH}_4\text{OH}$  solution and then iodine is measured using ICP-MS. For fresh water samples (rain, lake, river, and ground water),  $6 \text{ mol mL}^{-1} \text{ NH}_4\text{OH}$  is first added to the samples to a concentration of  $\text{NH}_4\text{OH}$  of  $0.15 \text{ mol mL}^{-1}$ , iodine in the samples is then measured by ICP-MC.



### **3.1.1 Separation of iodine from solid sample using combustion**

The dried solid sample is weighted to the samples boat, a maximum of 50 grams of soil and sediment, 10 grams of grass, lichens, leaves, wood, seaweed, or tissues, and 20 g of active charcoal can used, the filter paper of size less than 50cm × 50 cm can be used.  $^{125}\text{I}$  tracer is then added to the samples for monitoring the recovery of iodine during the separation procedure including combustion. The boat with sample is then put in to the furnace.

In the combustion facility, there are two furnaces; the sample is put in the middle of the first furnace. The second furnace is used for completely burn out the particles and organics, which is turn on and increasing the temperature to 850 °C in 30 minutes. Oxygen gas is supply in this furnace from the beginning to assist the complete combustion of materials in this furnace. The compressed air is passed through the combustion tube until the temperature is increased to 800 °C. This is necessary to avoid a violet combustion of the samples, articulately for organic samples. The oxygen gas may cause a explosion due to fast combustion and fast production of gases. The temperature in the first furnace is gradually increased, first to 100 °C and keep for 15 minutes to remove the water content in the samples, then slowly increased the temperature to 400 °C in the speed of 3-5°C per minute, this step is important, especially for organic samples such as grass, lichens, leaves, wood, seaweed, and tissue, active charcoal impregnated with TEHA also require a slowly increasing of temperature. The temperature is kept at 400 °C for 30 minutes to complete the carbonation of the organic in the samples. Afterwards the temperature is increased to 850-900 °C in 30 minutes, the supplied gas is then switch to oxygen, and finally the temperature is kept for 1 hour at this temperature. Iodine released as elemental iodine ( $\text{I}_2$ ) from the sample during the combustion is trapped in the bubbler which is filled with 0.4 mol mL<sup>-1</sup> NaOH with 0.02 mol mL<sup>-1</sup> NaHSO<sub>3</sub>. The trapping efficiency is checked using measuring  $^{125}\text{I}$  in the trapping solution. Recovery of iodine monitored using  $^{125}\text{I}$  in the soil and sediment samples is 95-99% with an average of 98%, the recovery of iodine in filter, and active charcoal is also higher (90-98%), while the recovery of iodine in organic samples (grass, lichens seaweeds, tissues etc.) is normally lower (50-70%).

### **3.1.2 Measurement of iodine using ICP-MS.**

For the trapping solution from the combustion, since the high salt content (18 g L<sup>-1</sup>), the sample is diluted 10 time with 0.15 mol L<sup>-1</sup> NH<sub>4</sub>OH. Cs as CsCl is added to a concentration about 2 ng mL<sup>-1</sup>, Cs is used as internal standard for monitoring and harmonizing the sampling introduction efficiency. The standard of iodine was prepared using KIO<sub>3</sub> and KI in 0.15 mol L<sup>-1</sup> NH<sub>4</sub>OH and 0.04 mol L<sup>-1</sup> NaOH solution. The results (Figure 4) show a good linearity of iodine prepared and the measured in a concentration range from 0.1 ng mL<sup>-1</sup> to 50 ng mL<sup>-1</sup>. In addition, no different of the single intensity for iodide and iodate was observed (Fig. 4).

It means that in routine analysis, one standard is enough for the determination of the total iodine the samples. Due to high stability, iodate is normally used as the routine standard of iodine for ICP-MS analysis.

In the ICP-MS analysis of iodine, hot plasma is always used due to high ionization potential of iodine. The Xt skimmer cone is used due to its good stability for “dirty” samples with high salt content to avoid the block of the small Xs cones, although the analytical sensitivity is lower by using Xt cone comparing with Xs cone. Various parameters is tuned to the optimal value to get the best sensitivity, the normal parameter tuned are shown in Table 1. The sensitivity of  $15100 \pm 450$  cps for  $1 \text{ ng mL}^{-1}$  iodine was obtained, and the blank ( $0.15 \text{ mol mL}^{-1} \text{ NH}_4\text{OH}$ ) counts of  $1750 \pm 110$  cps was measured. It is there a detection limit of  $0.02 \text{ ng mL}^{-1}$  is calculated.

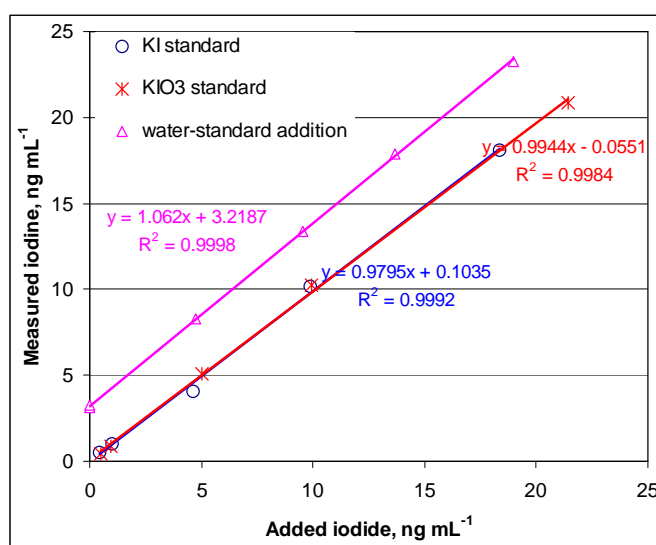


Figure 4 Standard curves of iodine measured using ICP-MS (Thermo, X Series<sup>II</sup>). KI and KIO<sub>3</sub> are prepared in  $0.15 \text{ mol mL}^{-1} \text{ NH}_4\text{OH}$  solution, standard addition of iodate to rain water and  $\text{NH}_4\text{OH}$  was added to a concentration of  $0.15 \text{ mol mL}^{-1}$ .

Table 1 Setup of ICP-MS for the measurement of iodine.

<u>Parameter</u>	<u>Value</u>	<u>Parameter</u>	<u>Value</u>
Skimmer cone	Xt	Dwell time ( <sup>127</sup> I)	25 ms
RF forward power	1400 W	Dwell time ( <sup>133</sup> Cs)	10 ms
Plasma gas flow rate	14.0 L min <sup>-1</sup>	Sweeps	1200
Nebulizer gas flow rate	1.00 L min <sup>-1</sup>	Channel space	0.02
Auxiliary gass flow rate	1.10 L min <sup>-1</sup>	Acquistion duration	64000 ms
Vacuum pressure	$5.3 \times 10^{-8}$ mbar	Integration time	5 min.
Pole Bias	-6.0	Evaluation software	PlasmaLab
Scan mode	Peak hopping		

### 3.2 Determination of $^{129}\text{I}$ using accelerator mass spectrometry (AMS)

An AMS analytical method was developed in Uppsala University for the determination of  $^{129}\text{I}$ . The separated iodine in AgI form is first to be dried and then mixed with twice amount by mass of niobium powder and pressed into a copper holder for the AMS measurement. A Pelletron (NEC) machine and the AMS system at the Tandem Laboratory, Uppsala University was used to measure  $^{129}\text{I}$  at a terminal voltage of 3.5 MV. The  $^{129}\text{I}$  standard NIST-SRM 4949C with  $^{129}\text{I}/^{127}\text{I}$  ratios of  $1.1 \times 10^{-11}$  was used. Blank samples were prepared using the same procedure as for samples for total iodine, iodide and iodate. The measured  $^{129}\text{I}/^{127}\text{I}$  ratio in blank samples ( $1.5 \pm 0.5 \times 10^{-13}$ ) was two orders of magnitude lower than that in samples ( $0.5\text{--}15 \times 10^{-11}$ ), which was subtracted from the measured value in the samples. Instrumental background for the AMS system was controlled by measurement of natural AgI (iodargyrite) crystal, which gave  $^{129}\text{I}/^{127}\text{I}$  value of  $4 \times 10^{-14}$ . The statistical error of the measurements at one standard deviation was  $< 10\%$ . During this project, the analytical accuracy and analytical speed was significantly improved. The detection limit of method to  $^{129}\text{I}$  was improved to be  $10^5$  atoms, and analytical capacity was increased to 50-70 samples per day.

### 3.3 Determination of Pu isotopes and $^{237}\text{Np}$ in environment

There are 4 isotopes of Pu which normally exist in environment, they are  $^{238}\text{Pu}$ ,  $^{239}\text{Pu}$ ,  $^{240}\text{Pu}$ , and  $^{241}\text{Pu}$  the concentration of other isotopes of Pu is very low, so the analysis of environmental samples normally only address to these three isotopes.  $^{241}\text{Pu}$  is a beta emitter, it can be measured by beta counting. By measuring its daughter  $^{241}\text{Am}$  it can be also determined, but a long waiting time for growth of  $^{241}\text{Am}$  is needed). Other isotopes of Pu are alpha emitters, it can be measured by alpha spectrometry. In addition, all these isotopes can be measured by mass spectrometry including ICP-MS. However because of higher isobaric interference of  $^{238}\text{U}$  to the mass spectrometric measurement of  $^{238}\text{Pu}$ , the measurement of  $^{238}\text{Pu}$  by mass spectrometry is very difficult, so it has to be measured by alpha spectrometry.  $^{237}\text{Np}$  is an alpha emitter, it is therefore can be measured by alpha spectrometry. However, due to its very long half-life (2.144 My), the detection limit of ICP-MS is better than alpha spectrometry.  $^{242}\text{Pu}$  is normally used as a tracer for the monitoring the chemical yield during separation and measurement.

Since the concentration of isotopes of Pu and  $^{237}\text{Np}$  is very low in the environmental samples, and interferences of other alpha emitters for the measurement by alpha spectrometry, and isobaric interference and molecular ions interference in the ICP-MS, Pu and Np has to be separated and concentrated from the samples before measurement.

### 3.3.1 Separation of Pu and Np from environmental samples

A chemical procedure has been developed in our lab for the separation of Pu and Np from various samples, including soil, sediment, plants, water, tissue and urine, which consists of a few steps including decomposition of samples, pre-concentration using co-precipitation, purification using ion exchange chromatography, source preparation for measurement.

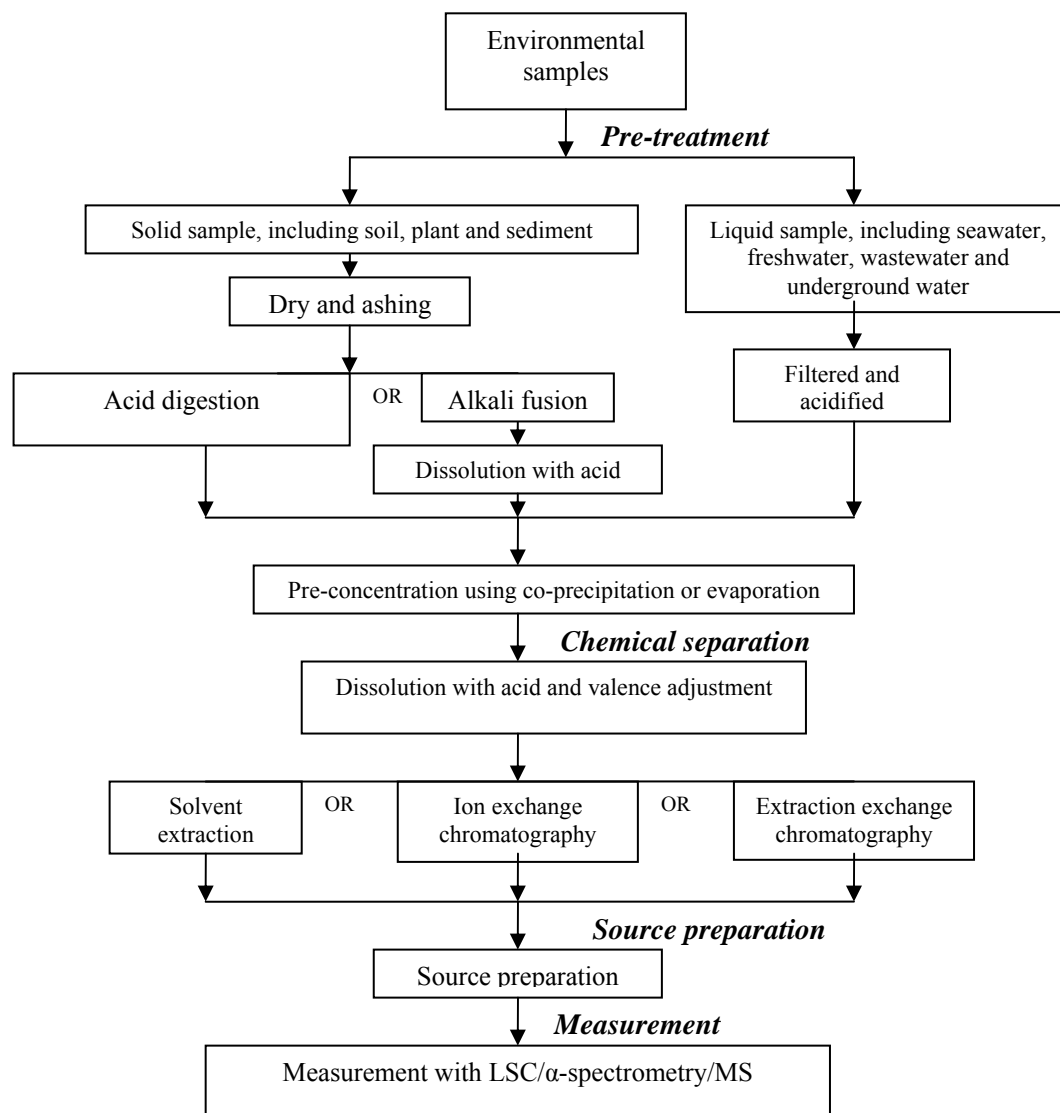


Figure. 4 Flow chart of the analytical procedure for the determination of Pu in environmental samples

Figure 4 shows a general procedure used for the separation of Pu from environment. Figure 5 shows the procedure for the chromatographic separation and purification of Pu. In addition an extraction chromatography method was also developed for the separation of Pu, which can replace the anion exchange chromatography. The results show that both methods are good for the separation and purification of Pu. The chemical yield of Pu and Np during the separation was measured using  $^{242}\text{Pu}$  to be 80-95%, and the decontamination factors for most of interferences are higher than  $10^4$ . Due to the similar chemical properties, Np is separated with Pu,  $^{242}\text{Pu}$  can be also used as yield tracer for  $^{237}\text{Np}$ .

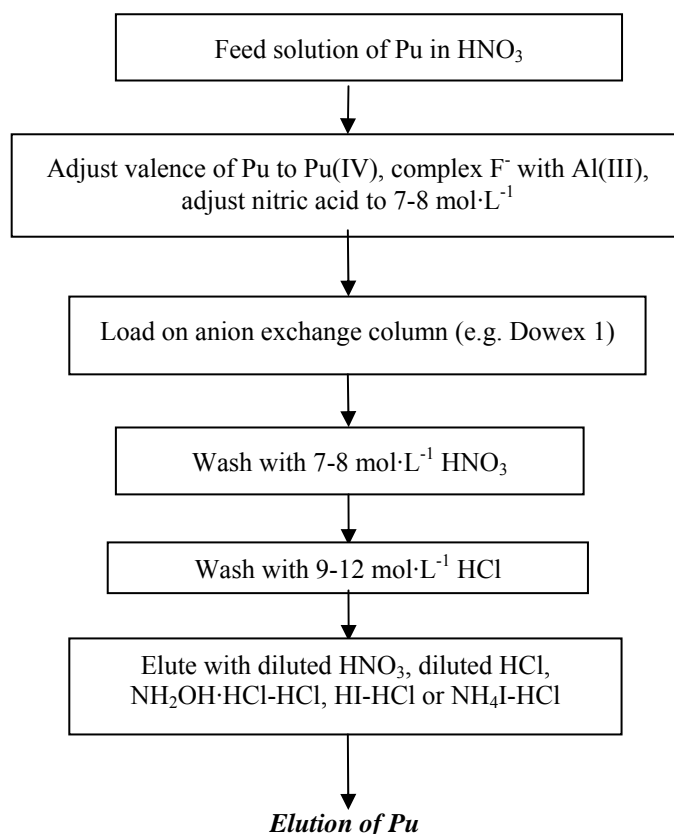


Figure. 5. General flow sheet for separation of Pu using anion exchange chromatography

### 3.3.2 Measurement of <sup>238</sup>Pu, <sup>239,240</sup>Pu and <sup>237</sup>Np using alpha spectrometry

The eluate of Pu and Np was evaporated to dryness, the residue was then dissolved with 0.05 mol L<sup>-1</sup> H<sub>2</sub>SO<sub>4</sub>, the solution was transferred to an electrodeposition cell, NH<sub>4</sub>OH solution is added to adjust pH to 2.5. Pu was finally electrodeposited on a stainless steel disc at a current of 0.7 A cm<sup>-2</sup> for 4-5 hours. Pu isotopes on electrodeposition disc were measured by alpha spectrometry (Canberra, USA). Detection limits of <sup>238</sup>Pu, <sup>239,240</sup>Pu, and <sup>242</sup>Pu, in this work are 0.1 mBq. A spectrum of alpha spectrometry of Pu isotopes is shown in Figure 6.

### 3.3.3 Measurement of <sup>239</sup>Pu, <sup>240</sup>Pu, <sup>241</sup>Pu and <sup>237</sup>Np using ICP-MS

For the measurement of isotopes of Pu and Np, eluted Pu solution is evaporated to dryness and prepared in 0.5 mol mL<sup>-1</sup> HNO<sub>3</sub> solution for the ICP-MS measurement. <sup>242</sup>Pu used as chemical yield tracer can be also used as an internal standard for the counting efficiency. Some times, In solution can be also used as a international standard. In this case, the chemical yield of Pu during the chemical separation can be obtained. The Xs- cone is always used as skimmer cone to get a high sensitivity. For increasing the instruction efficiency, consequently the analytical sensitivity, an Ultrasonic nebuliser is used to replace the ordinary concentric nebuliser. In this case the introduction of Pu can be improved by a factor of 5-10.

For ordinary concentric nebuliser, a sensitivity of 450 cps per  $\text{pg mL}^{-1}$  Pu is obtained, with a blank ( $0.5 \text{ mol mL}^{-1} \text{ HNO}_3$ ) count of  $0.8 \pm 0.2$  cps, a detection limit of Pu and Np of  $1.3 \text{ fg mL}^{-1}$  can be achieved, if 5 ml of sample solution is used, an absolute detection limit of 6.5 fg of Pu or Np can be obtained. It is corresponding to a detection limit of 15  $\mu\text{Bq}$ , 55  $\mu\text{Bq}$  25 mBq and 0.17  $\mu\text{Bq}$  for  $^{239}\text{Pu}$ ,  $^{240}\text{Pu}$ ,  $^{241}\text{Pu}$  and  $^{237}\text{Np}$  respectively.

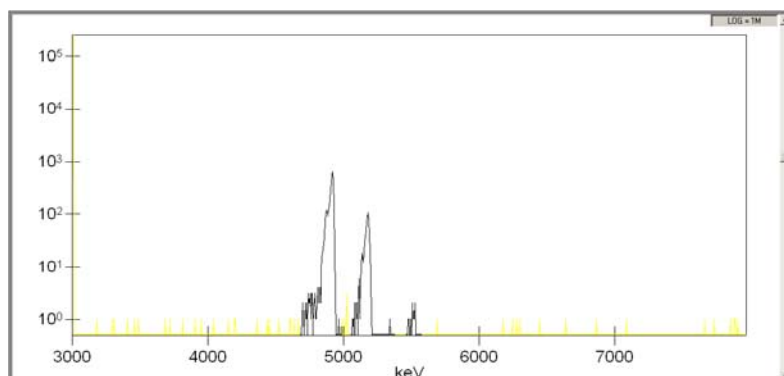


Figure.6 Alpha spectra of Pu isotopes measured using a alpha spectrometry after chemical separation.

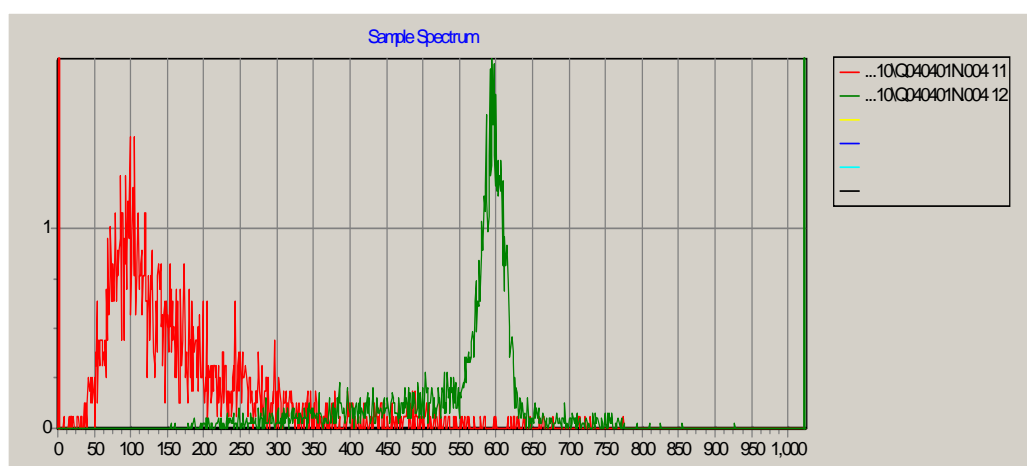


Figure 7 LSC spectrum of  $^{241}\text{Pu}$  (also with alpha emitting Pu ( $^{239,240}\text{Pu}$  in another window , green colour)

### 3.3.4 Measurement of $^{241}\text{Pu}$ using liquid scintillation counting

The separated sample can be directly used for the measurement of  $^{241}\text{Pu}$  using liquid scintillation counting (LSC). However, it is normally carried out by using the same sample after alpha counting. In this case, the Pu electrodeposited on the disc is stripped using acid, and then purified again using anion exchange chromatography, and then used for the measurement of  $^{241}\text{Pu}$ . A method has been developed for the determination of  $^{241}\text{Pu}$  using an ultra low level liquid scintillation counter. The interference from other Pu isotopes was corrected, a detection limits of 30 mBq  $^{241}\text{Pu}$  (8 fg) was obtained. Figures 7 shows a spectra LSC for  $^{241}\text{Pu}$ .

### ***3.4 Determination of $^{99}\text{Tc}$ and Pu/Am in environmental samples using HPLC coupled with ICP-MS.***

Ion chromatography (IC) is a form of liquid chromatography that uses ion exchange resins to separate atomic or molecular ions based on their interaction with the resin. It is a versatile, selective and sensitive method for the determination of a variety of anions and cations at trace and ultra trace levels. In the IC process, a stoichiometric chemical reaction occurs between ions in a solution and a solid substance carrying functional groups that can fix ions through electrostatic forces. In anion chromatography these are quaternary ammonium groups, and in cation chromatography sulfonic acid groups. In theory, ions with the same charge can be exchanged completely reversibly between the two phases. The process of ion exchange leads to a condition of equilibrium, the side to which the equilibrium lies depending on the affinity of the participating ions to the functional groups of the stationary phases .

#### ***3.4.1 Separation of Pu and Am using ion chromatography HPLC***

Work was focused on developing a method for the separation of plutonium and americium by using chromatographic columns together with HPLC pump. In the procedure plutonium is reduced to trivalent oxidation state and is recovered in the various separation steps together with trivalent americium. The method consists of three separation steps: 1) Light lanthanides and trivalent actinides are separated with TEVA extraction chromatographic resin in thiocyanate/formic acid media. 2) Trivalent plutonium and americium are pre-concentrated in a TCC-II cation-exchange column. 3) The separation of Pu and Am is performed in CS5A ion chromatography column by using two different eluents. Finally, plutonium is eluted from the column with dipicolinic acid (PDCA) eluent and americium is eluted with oxalic acid eluent. Radiochemical and chemical purity of the eluted plutonium and americium fractions were ensured with alpha-spectrometry. The separation procedure is visualized in Figure 8.

In the following chapters the main results of the work are described and shortly discussed.

##### ***3.4.1.1 Extraction chromatography for separating trivalent light lanthanides and actinides***

Soil and sediment samples usually contain major amounts of lanthanide elements. Lanthanides exist mostly in trivalent oxidation state in solutions, and exhibit similar chemical behavior than americium and other trivalent actinides. Sources prepared for measurement by alpha-spectrometry need to be chemically pure. Impurities in the sources absorb the energy of the emitting alpha-particles, and therefore, degrade the spectral resolution. Because of their chemical similarity, trivalent lanthanides and actinides are frequently recovered together in chromatographic separations. Therefore, removal of lanthanides from the sample prior to alpha-spectrometry is required. TEVA extraction chromatographic resin, which contains quaternary

ammonium salt (Aliquat-336, general formula  $R_3CH_3NCl$ ) as the extractant, has been applied in separating americium from lanthanide elements in thiocyanate/dilute acid media .

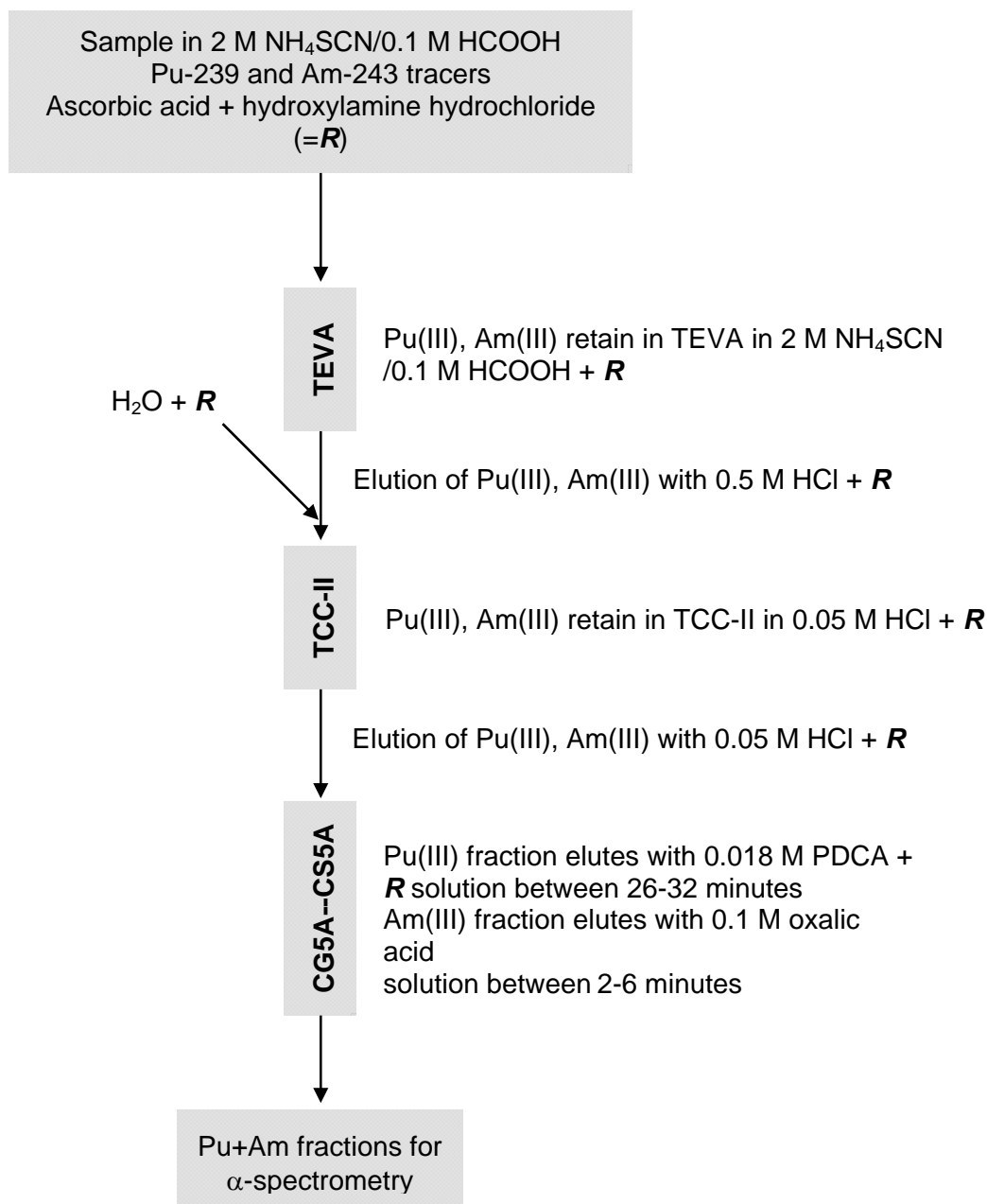


**Figure 8.** A scheme of the separation procedure for plutonium and americium. The symbol **R** denotes reducing agents.

Based on earlier work with americium (Perna et al., 2003) it was assumed that trivalent plutonium would behave similarly to americium in the TEVA/thiocyanate/acid system. As Figure 8 presents, practically all of plutonium (98.5–99.1%) was sorbed in TEVA resin during loading and washing. For elution of plutonium from TEVA resin, and subsequent preconcentration in the cation exchange resin (TCC-II),



the elution needed to be performed with dilute acid. By eluting with hydrochloric acid it was found out that for quantitative elution of Pu(III) from TEVA resin the concentration and volume of hydrochloric acid should be no less than 0.25 M and 6 ml, respectively (Figure 2).

The use of nitric acid as eluent was out of question due to the sorption of trivalent actinides in the quaternary ammonium resin in nitrate solution .

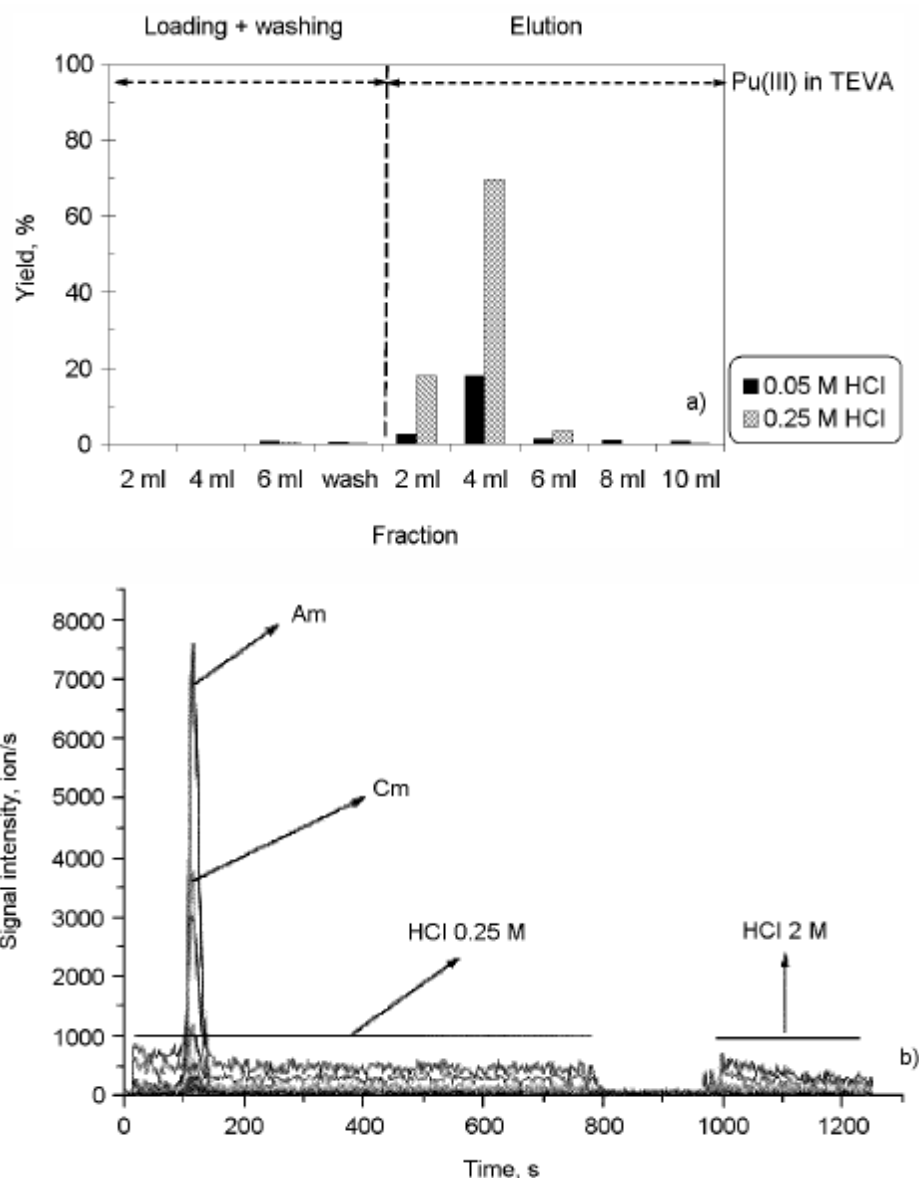


**Figure 9.** a) Elution profiles of Pu(III) being eluted from TEVA resin with two different HCl molarities. The loading volume was 6 ml and washing volume 2 ml. b) Sharp elution peak of Am(Cm) being eluted with 0.25 M HCl. The position of the peak is within 150 s, which corresponds to 2.5 ml of HCl. The detector in the experiment with Pu was LSC and with Am(Cm) ICP-MS. The experiment with Am(Cm) did not contain any added reducing agents.

The behavior of americium was studied previously in similar conditions except without the presence of the added reducing agents, as reported by Perna et al. (2003) Americium was found to elute from TEVA resin with 2.5 ml (150 s, 1 ml/min) of 0.25 M hydrochloric acid (Figure 8).

### 3.4.1.2 Cation exchange column for pre-concentrating trivalent actinides

The function of TCC-II column (Dionex, USA) in the procedure is to remove the trivalent ions from solution during the elution from TEVA resin, and to concentrate the cations in a compact band in the head of the column. The subsequent elution of the trivalent ions from the TCC-II column is done countercurrentwise, which enables rapid release of cations into following ion-chromatography column (IonPac, 1998). In the investigated procedure the load solution volume was 100 ml, therefore, as the elution of plutonium and americium occurred in the first 2 ml fraction, a concentration factor of minimum of 50 was achieved.

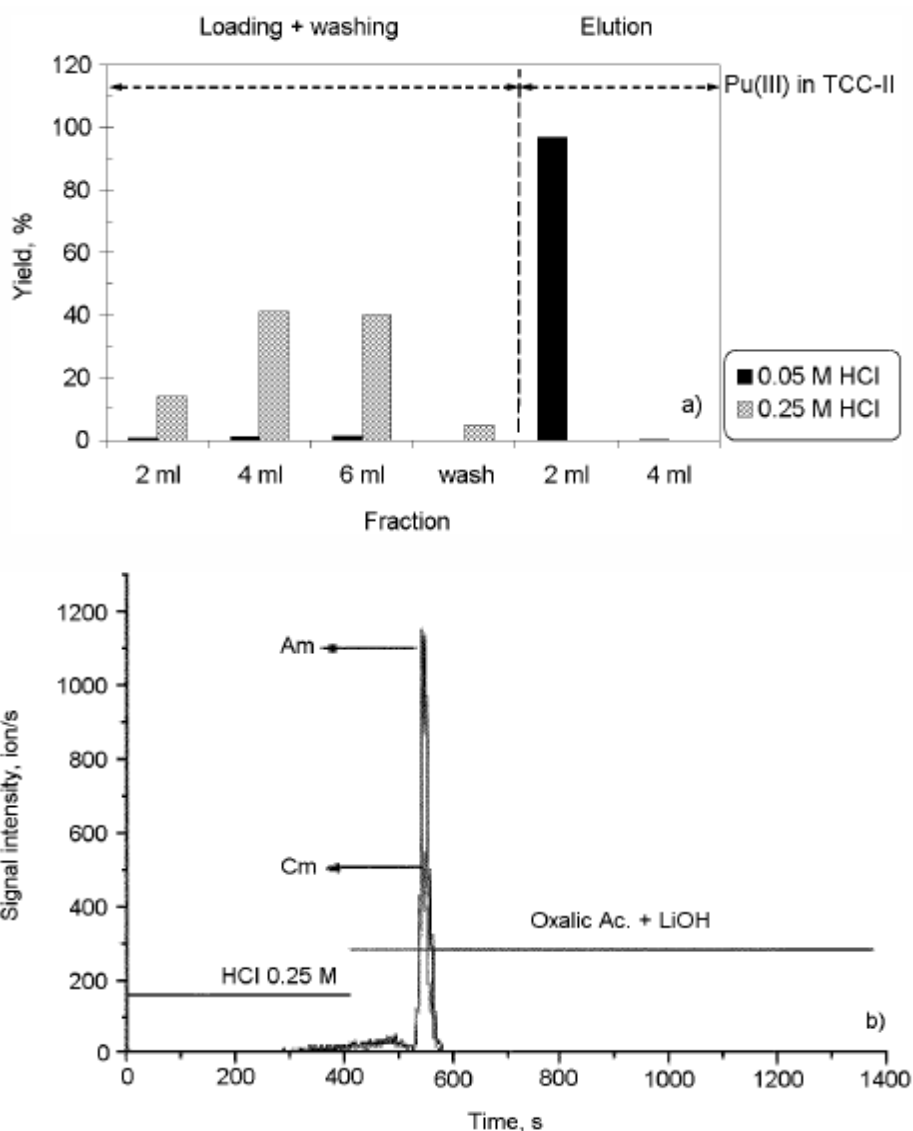


**Figure 10.** a) Pu(III) is quantitatively sorbed on TCC-II column in 0.05 M HCl but elutes through completely in 0.25 M HCl. The eluent consisted of 0.006 M PDCA/0.04 M NaOH/0.09 M CH<sub>3</sub>COOH. b) Am was found to be sorbed on TCC-II column in 0.25 M HCl. The experiment with Am did not contain any added reducing agents.

As can be seen in the Figure 10, plutonium did not retain in the TCC-II column in 0.25 M hydrochloric acid, which was needed for quantitative elution of Pu from the

TEVA resin. However, by diluting the acid concentration to 0.05 M quantitative concentration of plutonium in the TCC-II column was attained. The water flow for dilution was pumped with an external peristaltic pump.

As reported by Perna et al. (2003) in similar conditions except without the added reducing agents americium was found to be sorbed on TCC-II column in 0.25 M hydrochloric acid. The sorption was quantitative except of the end of the loading when some breakthrough was observed (Figure 10).

### 3.4.1.3 Ion chromatography column for final separation of trivalent actinides

A mixture of 0.1 M oxalic acid in 0.19 M lithium hydroxide has been used in the separation method developed for environmental samples in order to elute a pure fraction of americium from CS5A column for measurement by alpha-spectrometry. The same eluent additionally containing the ascorbic acid and hydroxyl amine hydrochloride reduction agents was tested for trivalent plutonium. However, no sign of elution of plutonium was observed in the time frame of 60 minutes, while americium eluted quantitatively (~98%) between 2 and 6 minutes. Increasing the oxalate concentration up to 0.5 M did not have any effect on elution of plutonium. The database of NIST reports the  $\log \beta_3$  of 11.15 for  $\text{Am}(\text{C}_2\text{O}_4)_3^{3-}$  (Smith et al., 2004) as the corresponding  $\log \beta_3$  for  $\text{Pu}(\text{C}_2\text{O}_4)_3^{3-}$  has been determined as 9.39/10.65 (Table 1). In case of elution behavior of oxalate complexes of Pu(III) and Am(III) in CS5A column follows that of lanthanides plutonium should have eluted prior to americium. The reason why trivalent plutonium was not observed to elute with oxalic acid is not clear.

Table 2. Various stability constants of oxalate and dipicolinate ligands of trivalent light actinides and lanthanides

Cation	Oxalate			Dipicolinate		
	$\log \beta_1$	$\log \beta_2$	$\log \beta_3$	$\log \beta_1$	$\log \beta_2$	$\log \beta_3$
Ac(III)	4.36 <sup>1</sup>	7.08 <sup>1</sup>				
Pu(III)	—	—	9.39 <sup>5</sup> 10.65 <sup>6</sup>	—	—	—
Am(III)	5.25 <sup>1</sup>	8.85 <sup>1</sup>	11.15 <sup>2</sup>	—	—	—
Cm(III)	5.25 <sup>1</sup>	8.85 <sup>1</sup>	—	—	—	—
Bk(III)	5.45 <sup>1</sup>	9.14 <sup>1</sup>	—	—	—	—
Cf(III)	5.50 <sup>1</sup>	9.37 <sup>1</sup>	—	—	—	—
La(III)	4.71 <sup>1</sup>	7.83 <sup>1</sup>	10.3 <sup>2</sup>	7.94 <sup>3</sup>	13.71 <sup>3</sup>	17.95 <sup>3</sup>
Ce(III)	4.90 <sup>1</sup>	8.26 <sup>1</sup>	10.2 <sup>4</sup>	8.29 <sup>3</sup>	14.33 <sup>3</sup>	18.67 <sup>3</sup>
Pr(III)	—	—	—	8.58 <sup>3</sup>	15.00 <sup>3</sup>	19.80 <sup>3</sup>
Nd(III)	—	—	—	8.73 <sup>3</sup>	15.40 <sup>3</sup>	20.41 <sup>3</sup>
Pm(III)	5.18 <sup>1</sup>	8.78 <sup>1</sup>	—	—	—	—
Sm(III)	—	—	—	8.81 <sup>3</sup>	15.77 <sup>3</sup>	21.06 <sup>3</sup>
Eu(III)	5.36 <sup>1</sup>	9.04 <sup>1</sup>	11.4 <sup>2</sup>	8.79 <sup>3</sup>	15.86 <sup>3</sup>	21.32 <sup>3</sup>
Gd(III)	4.77 <sup>3</sup>	8.66 <sup>3</sup>	—	8.68 <sup>3</sup>	15.95 <sup>3</sup>	21.66 <sup>3</sup>

As oxalic acid did not elute plutonium from the CS5A column another eluent was needed. Like oxalic acid, 2,6-pyridinedicarboxylic acid (dipicolinic acid or PDCA;  $\log K_{a1,2}$ : 2.07, 4.66, 25 °C, 0.1 M) has been applied in separating transition and heavy metals in CS5A column. The dipicolinate (2,6 pyridinecarboxylate) ligand is a tridentate ligand which is able to coordinate by an oxygen of each carboxylate group

and by the nitrogen of the pyridine ring. Dipicolinate reacts with transition and heavy metal cations, and lanthanide cations forming stable anionic complexes.

A mixture of 0.012 M PDCA/0.08 M NaOH/0.18 M CH<sub>3</sub>COOH (pH 4.62) was found to elute Pu(III) from the column between 44 and 50 minutes. By increasing dipicolinate concentration up to 0.018 M faster elution of plutonium between 26 and 32 minutes was observed. Further increase of PDCA concentration within a same pH range was not feasible as the viscosity of the eluent increased too much for stable elution rate with the used HPLC pump.

No americium was found to elute with PDCA during 60 minutes. Observing the stability constants of anionic dipicolinate complexes of light lanthanides, collected in Table 2, a steady increase in log  $\beta$  values from La to Gd is seen. No equivalent information on trivalent actinide complexes was found in the literature nor was found any experimental data dealing with elution behavior of trivalent lanthanides or actinides in CS5A column in dipicolinate media. However, in the case of the stability order of anionic dipicolinate complexes of trivalent actinides follows that of trivalent lanthanides, as is the case with oxalate complexes, Pu(III) should form weaker complexes with dipicolinate than Am(III). Consequently, assuming that the elution behavior of anionic dipicolinate complexes of trivalent actinides follows the order observed by Perna et al. (2002) with respect to oxalate complexes of trivalent americium and lanthanides Pu(III) should elute before Am(III) with PDCA eluent. In the experiments no elution of americium was observed, before or after the elution of plutonium. However, as the elution dynamics of americium in the studied PDCA system are not known it is possible that elution of americium would have taken place beyond the time (60 minutes) used in the experiments.

Based on the experiments; in order to quantitatively separate trivalent plutonium and americium in CS5A column it was therefore, necessary to use two different eluents. ~99% of Pu eluted from the column between 26 and 32 minutes by using dipicolinic acid eluent; ~98% of Am eluted between 2 and 6 minutes with oxalic acid eluent (Figure 11). The elution of plutonium was followed by rinsing the column for 10 minutes with dipicolinic acid solution, after which the elution of americium followed. The eluted plutonium and americium fractions were measured with alpha-spectrometry, and were found to be radiochemically pure.

The developed method is based on reducing plutonium to trivalent oxidation state so that it follows americium throughout the separation processes. The elution of Pu and Am from the final separation column was done with two different eluents, and radiochemically pure quantitative separation of both elements was achieved. Further studies are needed for testing the method with environmental samples.

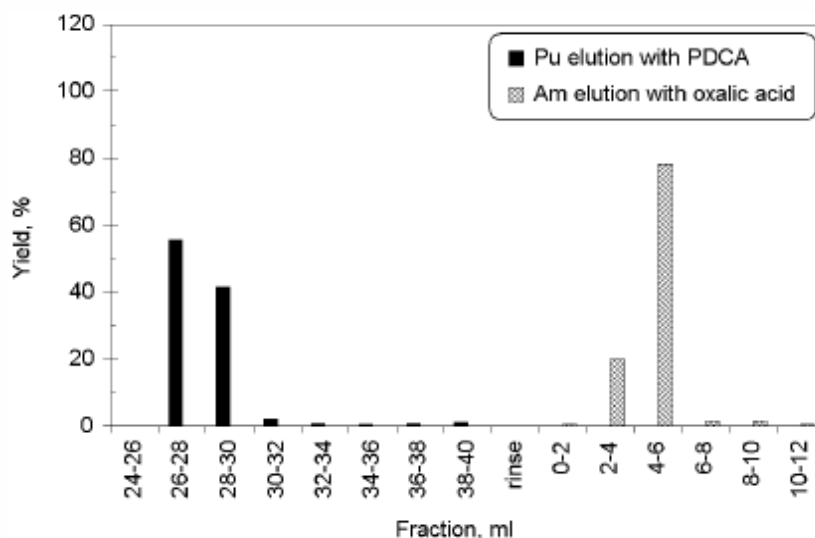


Figure 11. Separation of Pu(III) and Am(III) in ion chromatography CS5A column. Plutonium is firstly eluted with 0.018 M PDCA/0.12 M NaOH/0.27 M CH<sub>3</sub>COOH solution including the reduction agents. After washing the column americium is eluted with reductant-free solution of 0.1 M oxalic acid in 0.19 M LiOH.

### 3.4.2 Separation of Tc using ion chromatography HPLC

Measurement of <sup>99</sup>Tc with ICP-MS is feasible due to low determination limit. When compared to classical method beta counting the modern ICP-MS instruments reach even three orders of magnitude lower determination limits. However, for efficient analysis the sample needs to be free of interfering agents such as isotopes of other elements and polyatomics. The main interferences in the mass spectra of <sup>99</sup>Tc are <sup>99</sup>Ru and, to some extent, <sup>98</sup>MoH, <sup>59</sup>Co<sup>40</sup>Ar, <sup>87</sup>Sr<sup>12</sup>C, <sup>87</sup>Rb<sup>12</sup>C, <sup>43</sup>Ca<sup>16</sup>O<sup>40</sup>Ar, <sup>40</sup>Ar<sub>2</sub><sup>18</sup>OH and <sup>40</sup>Ca<sup>18</sup>OH<sup>40</sup>Ar. These can be removed in the chemical separation procedure, for example, by using TEVA resin (Eichrom Industries), but when working with large samples and using large amounts of reagents, absolute clean up can be difficult. The amount of Ru in the sample can be calculated from its relatively undisturbed isotope <sup>101</sup>Ru, however, this decreases the determination limit of <sup>99</sup>Tc which is problematic with samples of low <sup>99</sup>Tc concentration. Large amounts of Mo in samples create a problem for measurement of Tc via the interference of <sup>98</sup>Mo-hydride. Another issue with Mo is the interference of <sup>97</sup>Mo isotope when <sup>97</sup>Tc is used as yield tracer.

The aim of this work was to use ion chromatography column (CS5A) for separating Tc from Mo and Ru in the end of chemical separation chain which also includes iron hydroxide precipitation and anion exchange. The following chapters introduce the separation procedure and results obtained with ion chromatography column used for purification of Tc fraction. The purified fraction can be measured straight with ICP-MS or by other methods.

### **3.4.2.1 Separation procedure**

The separation procedure is visualized in Figure 12. After acid digestion of the soil sample (10 g) in 8 M HNO<sub>3</sub> the sample is filtered and made alkaline by adding ammonium hydroxide. Iron hydroxide precipitation is the first cleanup step which removes several elements such as transition metals, lanthanides and actinides from solution phase. After vacuum filtration the solution phase is collected and acidified to pH 5-6 and added to column containing AG1×4 anion exchange resin (Biorad). The resin is washed with 7 bed volumes of 0.5 M HNO<sub>3</sub>, after which Tc is eluted with 6 bed volumes of 10 M HNO<sub>3</sub>. By using 10 M instead of 14 M nitric acid the amount of Ru eluting from the resin is lowered (Keith-Roach et al., 2002). The eluted sample is evaporated to dryness on a hot plate of temperature of +140 °C. For the last few milliliters of solution the temperature of the hot plate is reduced to +80 °C. This is done to prevent any possible volatilization of Tc during drying of the sample. The dried sample is then treated and evaporated to dryness three times with 5 ml of concentrated HNO<sub>3</sub> and few drops of concentrated hydrogen peroxide to destroy all organic material employed from the anion exchange resin.

For the separation with ion chromatography the sample is dissolved in 2 ml of 0.2 M oxalic acid which contains 20 mM of ascorbic acid and 20 mM of hydroxylamine hydrochloride as reducing agents. After 30 minutes reduction time the sample is injected in CG5A-CS5A column for the final purification of Tc fraction.

### **3.4.2.2 Elution of technetium from ion chromatography column**

Different oxalate concentrations were tested and solution pH was changed to find out differences in the elution behaviour of technetium and molybdenum/ruthenium. Increasing oxalate concentration did have an effect on retention time of Tc; when using 0.2 M oxalate solution instead of 0.1 M the retention time of Tc decreased 200 seconds (Figure 10-12). As can be seen from Figure 13-15, decreasing pH of elution solution closer to the pK<sub>a2</sub> value of oxalic acid (4.28) further decreased retention time of Tc but also had an effect of retention times of Mo and Ru. A clear separation between Tc and Mo/Ru with moderate retention time of Tc was achieved in oxalic acid solution pH of 3.50.

Some further work is needed for finalizing the method. The suitability of the method for different kinds of environmental samples has to be examined. The chemical yield of the ion chromatography separation step has been tested by using <sup>99m</sup>Tc tracer and found to be quantitative. However, the chemical yield of the whole procedure needs to be determined. Also, the determination limit of the method with respect to low-concentration environmental samples needs to be determined.

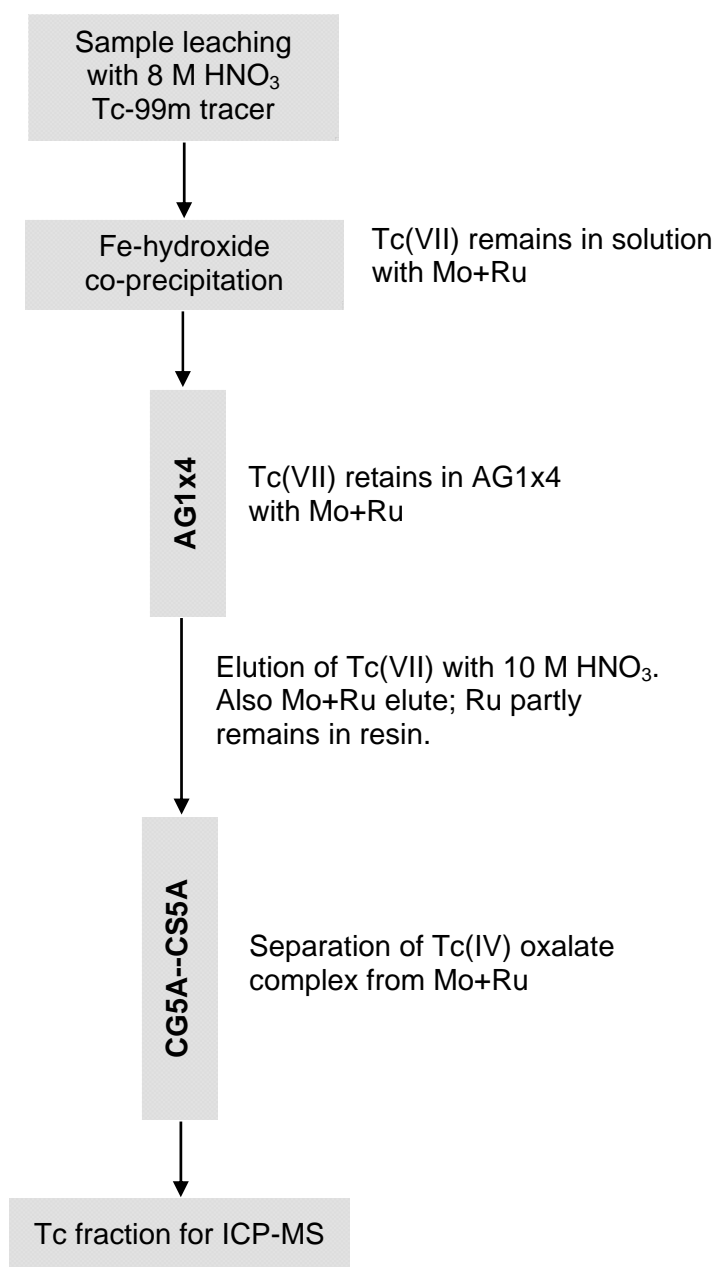


Figure 12. A scheme of the separation procedure for technetium.

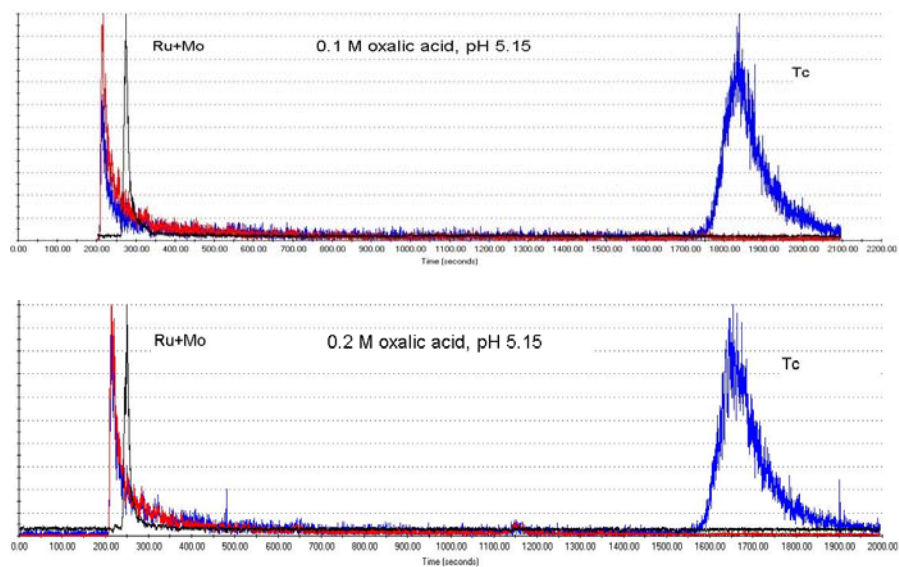


Figure 13. Effect of oxalate concentration on elution of Tc.

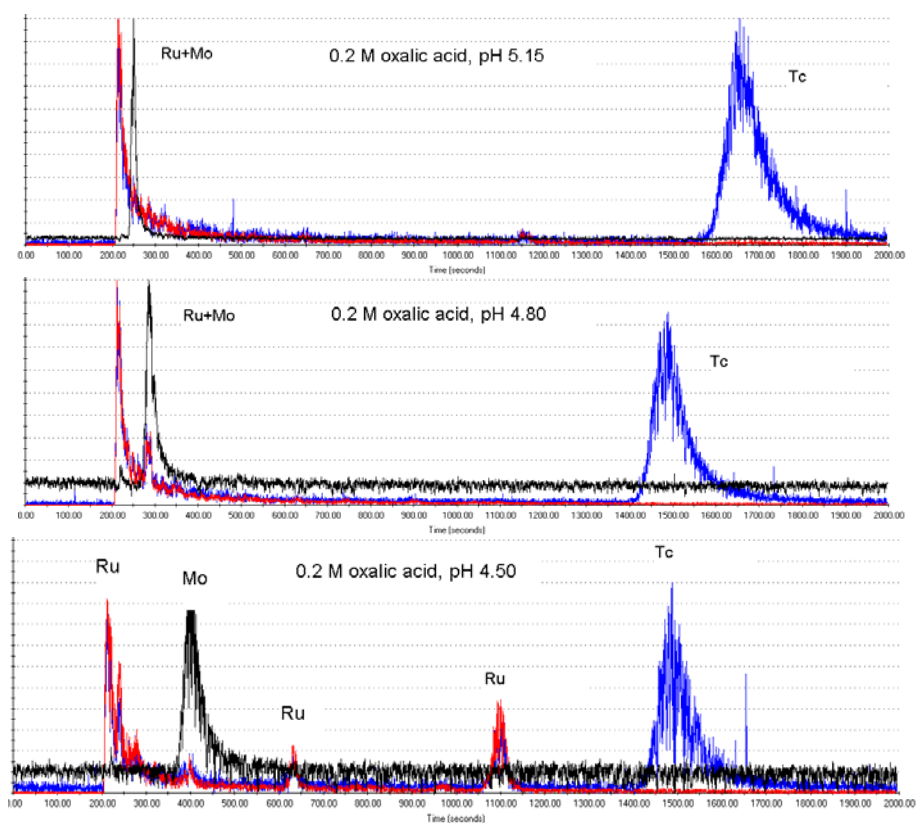


Figure 14. Effect of pH on elution of Tc.



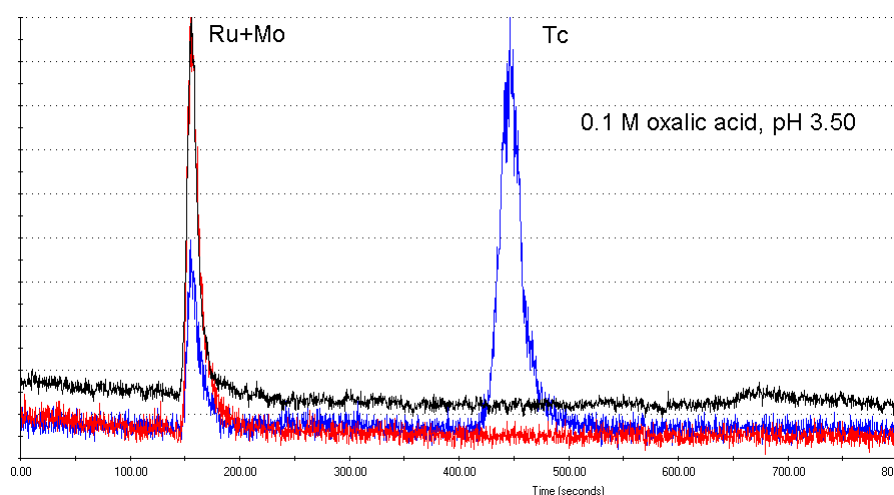


Figure 15. Separation of Tc from Mo and Ru in ion chromatography CS5A column.

It has been observed that ion chromatography column (CS5A) can be used in purifying Tc fraction from Mo and Ru which are disturbing elements when measuring Tc by using ICP-MS. Some further investigations are needed to finalize the method to be suitable for different kinds of samples, and also to find out the efficiency of the method.

### 3.5 Method for the speciation of $^{129}\text{I}$ and $^{127}\text{I}$ in water samples

In water samples, iodine mainly exist as iodide, iodate and minor organic iodine, the work mainly focused on the analysis of iodide and iodate in the water samples. A method for the organic iodine was also investigated. But the method is still on the way to be completed.

#### 3.5.1 Speciation separation of iodine in water samples using ion exchange chromatography

A method has been developed and improved in this work for the speciation of  $^{129}\text{I}$ , a separation scheme is shown in Figure 16. The method is brief described below. 100-1000 ml of filtered water sample was transferred to a beaker,  $^{125}\text{I}^-$  and  $^{131}\text{IO}_3^-$  tracers are added to the sample and stirring to 10 minutes. The water sample was then loaded to a pre-prepared AG1 $\times$ 4 anion exchange column ( $\text{Ø}1.0 \times 20$  cm,  $\text{NO}_3^-$  column) with a flow rate 2-4 ml/min. The column was then washed using 50 mL of  $0.2 \text{ mol L}^{-1} \text{ NaNO}_3$  solution. The effluent and wash were collected and combined, 20 ml of this solution was taken to a vial for determination of iodate plus non-ionic iodine ( $^{127}\text{I}$ ) using inductively coupled plasma mass spectrometry (ICP-MS), and the remained solution is used for the separation of iodate and non-ionic iodine. Iodide adsorbed on the column was then eluted using 150 ml of  $2.0 \text{ mol L}^{-1} \text{ NaNO}_3$  solution.

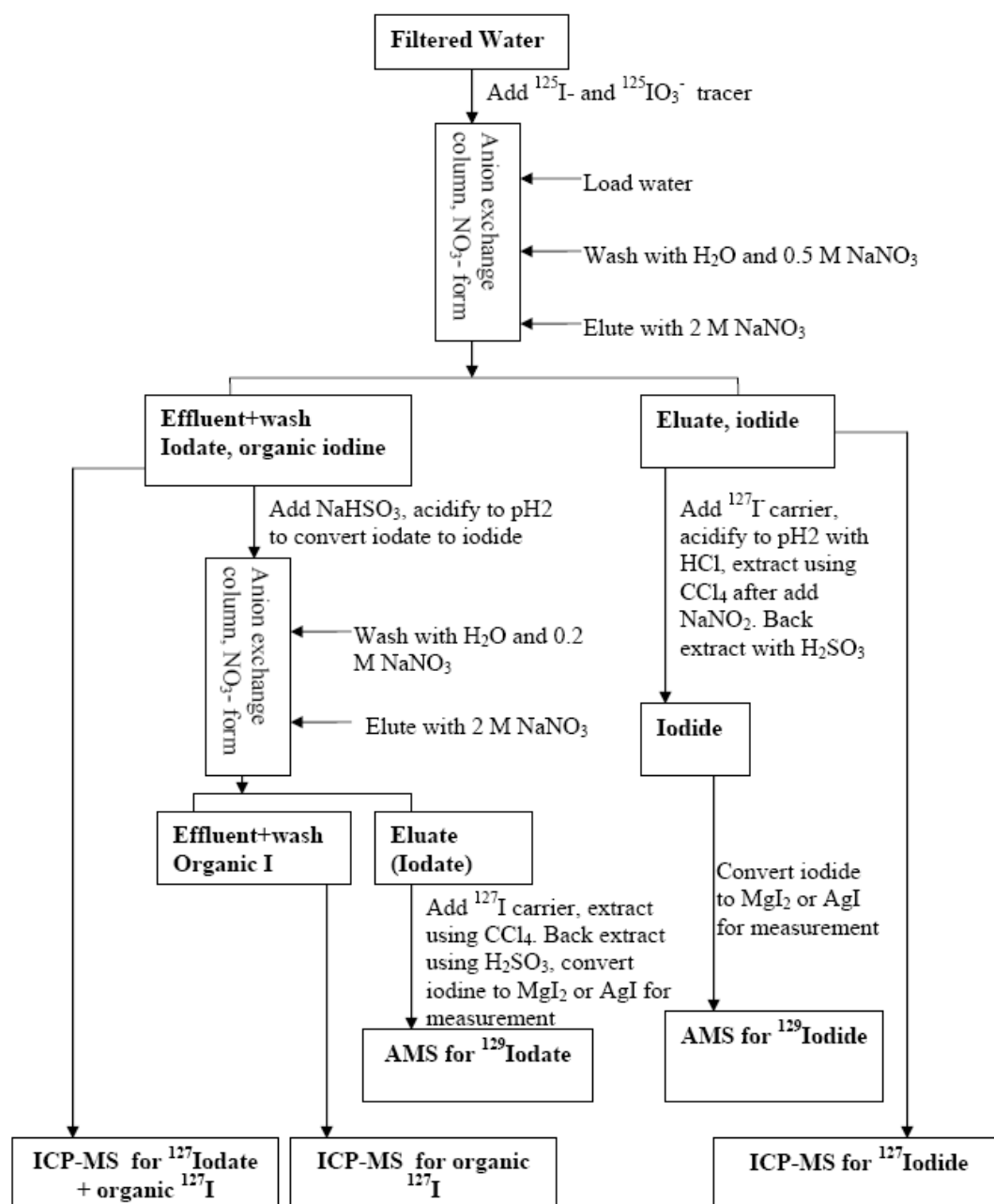


Figure 16 Chemical separation procedure for speciation analysis of  $^{129}\text{I}$  in water samples

Thirty ml of the collected effluent and wash was taken to a beaker,  $1.0\text{ ml}$  of  $1.0\text{ mol L}^{-1}\text{ NaHSO}_3$  was added, and the solution is acidified to pH 1-2 using  $\text{HCl}$  and stirred for 10 minutes. The solution was then loaded to another AG  $1\times 4$  column, washing the column with  $15\text{ ml}$  of  $0.5\text{ mol L}^{-1}\text{ NaNO}_3$ . The effluent and wash were combined;  $9.8\text{ ml}$  of this solution was taken to a vial for determination of non-ionic iodine ( $^{127}\text{I}$ ).

For separation of iodine from water matrix, 2.0 mg of low-background iodine (Woodward Corporation, USA) and 1.0 ml of 1.0 mol mL<sup>-1</sup> NaHSO<sub>3</sub> (freshly prepared within 5 days) were added to 100 mL of original precipitation sample, 150 ml of iodide eluate, or remained effluent plus wash, the pH of the solution was then adjusted to pH1-2 using HCl. The solution was transferred to a reparatory funnel, CCl<sub>4</sub> was added to the funnel and then 1.0 mol mL<sup>-1</sup> NaNO<sub>2</sub> solution was added to extract iodine as I<sub>2</sub> to CCl<sub>4</sub> phase, extraction step with CCl<sub>4</sub> was repeated. The CCl<sub>4</sub> phases were combined, iodine (I<sub>2</sub>) in the CCl<sub>4</sub> was then back extracted with 20-30 ml of 0.01 mol mL<sup>-1</sup> NaHSO<sub>3</sub> solution. The extraction and back extraction were repeated, and finally back extracted iodine solution (5-7 mL) was transferred to a vial; 0.1 ml of 25% NH<sub>4</sub>OH was added to keep iodide stable. <sup>125</sup>I and <sup>131</sup>I in the final solution were measured using a NaI gamma detector (well type, Risø National Laboratory, Denmark) with a Canberra Series 20 Multichannel analyzer by measuring X- and gamma rays of <sup>125</sup>I in 26-36 keV. The chemical yield of iodide, iodate and total iodine during the separation procedure were calculated by comparing with the amount added to the sample before separation to be 80-85%, 90-95% and 94-98%, respectively.

The separated iodine solution was then transferred to a 10 ml centrifuge tube, 1 ml of 3 mol L<sup>-1</sup> HNO<sub>3</sub> and 0.2 ml of 1.0 M AgNO<sub>3</sub> were added to precipitate iodine as AgI, which was separated by centrifuge. The AgI precipitate was further washed with 3 mol L<sup>-1</sup> HNO<sub>3</sub> and centrifuged to remove any remained Ag<sub>2</sub>SO<sub>3</sub> and Ag<sub>2</sub>SO<sub>4</sub>, followed by H<sub>2</sub>O washing and drying at 70°C (<5 h).

### ***3.5.2 Speciation of <sup>129</sup>I in water using extraction and co-precipitation***

Two new chemical procedures were developed in this work to separate iodide and iodate from water sample using solvent extraction and co-precipitation of AgI with AgCl. For separation of iodide-129, iodide carrier (1-2mg) is first added to the seawater (0.1-2 liters), and pH is adjusted to 5-7 using HCl, and then 0.2-2 ml of 1mol/L AgNO<sub>3</sub> is added (Cl:Ag >10 mol/mol), the solution is stirred for 30 min. and the precipitate is separated by centrifuge. 25% of NH<sub>3</sub> is then added to the precipitate to dissolve the AgCl, and the separated AgI is directly used for AMS analysis of iodide-129. For total I-129, after addition of iodine carrier and HCl to pH<2, NaHSO<sub>3</sub> solution is added to reduce iodate to iodide, then total iodine is separated by the same procedure as for iodide. The iodate-129 is calculated by the difference between iodide-129 and total iodine-129. The procedure is shown in Figure 17. The analytical results showed that the recovery of iodine is more than 80% and the crossover of iodate in the iodide fraction is less than 2%. Because more samples can be treated simultaneously (>10 sample /h), the method is rapid and very suitable for the in situ separation on board.

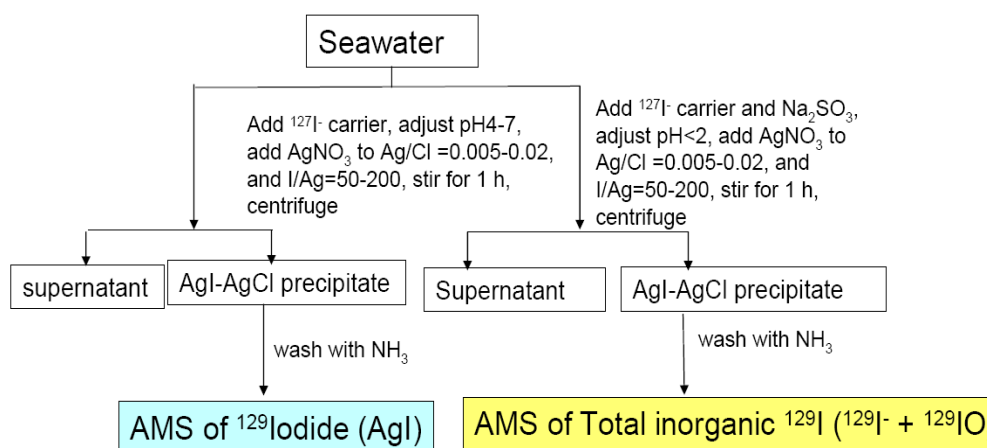


Figure 17 Chemical procedure for speciation of  $^{129}\text{I}$  using AgI-AgCl coprecipitation

Another method is based on the specific oxidation of iodide to  $\text{I}_2$  at pH4-7 using  $\text{NaClO}$  and then extracting  $\text{I}_2$  using  $\text{CCl}_4$  to separate iodide from other species of iodine. After reducing iodate to iodide using  $\text{NaHSO}_3$ , and then used the same procedure as iodide, the total inorganic iodine can be separated. the difference between total inorganic iodine and iodide is iodate. The results show that the cross contamination of iodate to iodide is less than 3%, and recovery of iodine is higher than 85%. The separation procedure is shown in Figure 18.

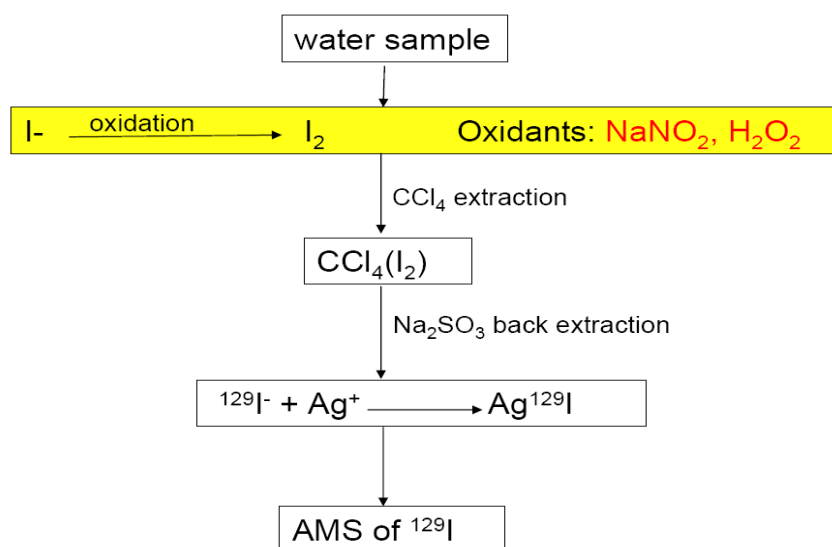


Figure 18 Chemical procedure for the speciation of  $^{129}\text{I}$  using reagent extraction

### 3.5.2 Speciation/fractionation of $^{129}\text{I}$ and $^{127}\text{I}$ in soil/sediment samples

A sequential extraction was developed and improved for the speciation of  $^{129}\text{I}$  and  $^{127}\text{I}$  in soil and sediment samples, water soluble, exchangeable, carbonate, oxides, organic and minerals associated iodine was separated with different reagents and iodine was then separated from the fractions for the determination of  $^{129}\text{I}$  and  $^{127}\text{I}$ . A diagram of the separation procedure is shown in Figure 17.

Scheme of the sequential extraction of iodine (both isotopes)

Speciation	Reagent	Temperature	Time
1. Leachable	1.0 M NaAc in 25% HAc (v/v), pH = 4	20° C	1 h.
2. Organic material*	0.3 M NaOH	60° C	4 h.
	5 - 6% NaOCl, pH = 12	96° C	1 h.
	0.3 M NaOH	60° C	30 min.
3. Reducible (Oxides)	0.04 M $\text{NH}_2\text{OH} \cdot \text{HCl}$ and 0.01 M $\text{NaHSO}_3$ in 25% HAc (v/v)	80° C	6 h.
4. Residue*	NaOH fusion	550° C	8 h.

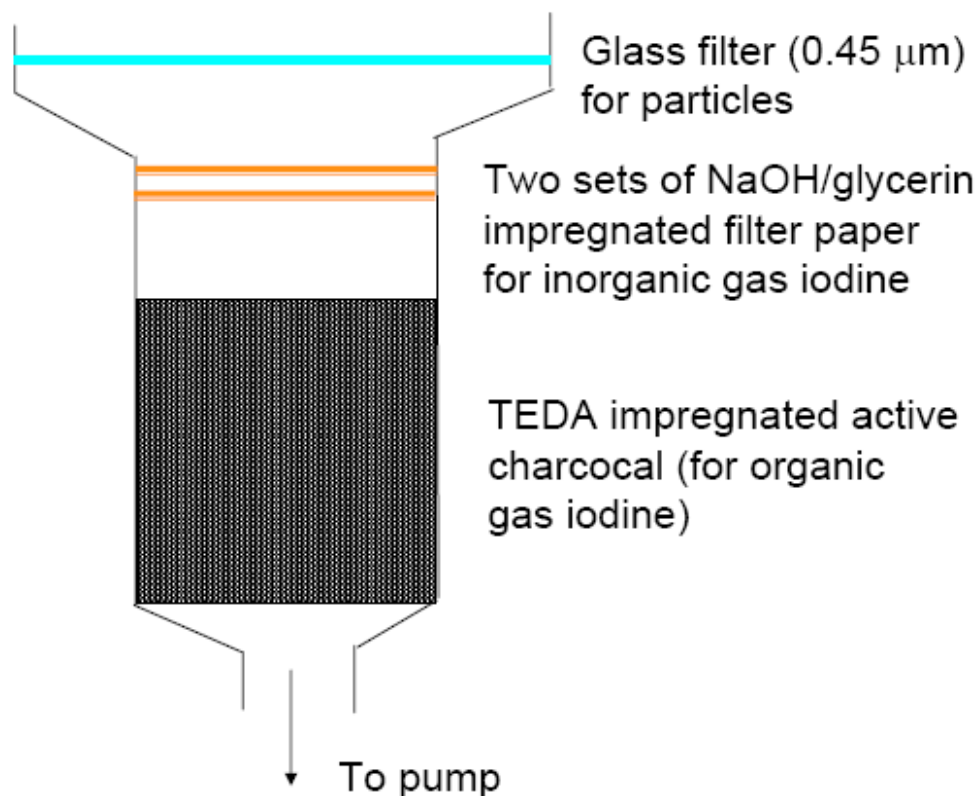
\* Iodine tracer ( $^{125}\text{I}$ ) was added for establishing recovery

Figure 17 Sequential extraction procedure for speciation of  $^{129}\text{I}$  in sediment and soil

### 3.5.3. Speciation method for $^{129}\text{I}$ and $^{127}\text{I}$ in atmosphere

A method for the collection and separation of different species of iodine in atmosphere was developed. In this method, particle associated iodine, inorganic gaseous iodine and organic gaseous iodine was collected by pumping the air through air sampler with sequential air filters as show in Fig. 18. In which the particle associated iodine was first collected on a glass fibre filter with pore size of 0.45  $\mu\text{m}$ , the gas components passed through the filter. Inorganic gaseous iodine, such as  $\text{I}_2$ , HI, HIO are then trapped by cellulous filter which was impregnated in NaOH/glycerol and dried. Finally the organic gaseous iodine, mainly alkane iodide, such as  $\text{CH}_3\text{I}$  and  $\text{CH}_3\text{CH}_2\text{I}$  was trapped in a column filled with active charcoal

which was impregnated with TEDA. The air sampler for the collecting air sample is shown in Figure 2.



*Figure 18 Air sampler for the collecting particle associated iodine, inorganic gas iodine and organic gas iodine.*

The collected different species of iodine were then separated by a combustion method (Figure 3). In this method, the collected sample was put into a quartz boat, and  $^{125}\text{I}$  as yield tracer was added to the sample. The sample boat was then put in a quartz tube which was heated by a tube oven, compressed air and oxygen gas pass through the tube during heating. The iodine released during heating up to  $800\text{ }^{\circ}\text{C}$  was then trapped by two sets of bubbler filled with  $0.2\text{ mol/l NaOH}$  solution. One ml of trapped solution was taken for the determination of  $^{127}\text{I}$  by ICP-MS. The remained solution was used for the separation of iodine and AMS determination of  $^{129}\text{I}$  by solvent extraction method and AgI precipitation method as the same as for water sample.

### ***3.6 Speciation/fractionation of plutonium isotopes, $^{237}\text{Np}$ and $^{241}\text{Am}$ in soil, sediment and concrete samples using dynamic sequential extraction***

A dynamic extraction system (Figure 19) exploiting sequential injection (SI) for sequential extractions incorporating a specially designed extraction column (Figure) was developed to fractionate radionuclides such as Pu, Am, Np and  $^{137}\text{Cs}$  in environmental solid samples such as soils and sediments. The extraction column can

contain a large amount of soil sample (up to 5 g), and under optimal operational conditions it does not give rise to creation of back pressure. The purpose of developing such a dynamic system for fractionation of radionuclides is to reduce the readsorption problems during sequential extraction using a modified Standards, Measurements and Testing (SM&T) scheme with 4-step sequential extractions. In addition, the dynamic system is more similar as the situation occurring in nature.

A modified sequential extraction scheme of the Standards, Measurements and Testing (SM&T) program of the European Commission (formerly BCR) (Rauret et al., 1999; Mossop et al., 2003) was employed using the following solutions:

Step I: 1 mol l<sup>-1</sup> NH<sub>4</sub>OAc (i.e. for radionuclides weakly bound to soil surfaces by electrostatic interactions, or readily released by ion-exchange processes, or the so called exchangeable fraction)

Step II: 0.11 mol l<sup>-1</sup> CH<sub>3</sub>COOH (i.e. for radionuclides bound to carbonates, or the so-called acid soluble fraction).

Step III: 0.1 mol l<sup>-1</sup> NH<sub>2</sub>OH·HCl (radionuclides bound to Fe–Mn oxides, or the so-called reducible fraction).

Step IV: 8.8 mol l<sup>-1</sup> H<sub>2</sub>O<sub>2</sub> (radionuclides bound to organic matter, or the so called oxidizable fraction).

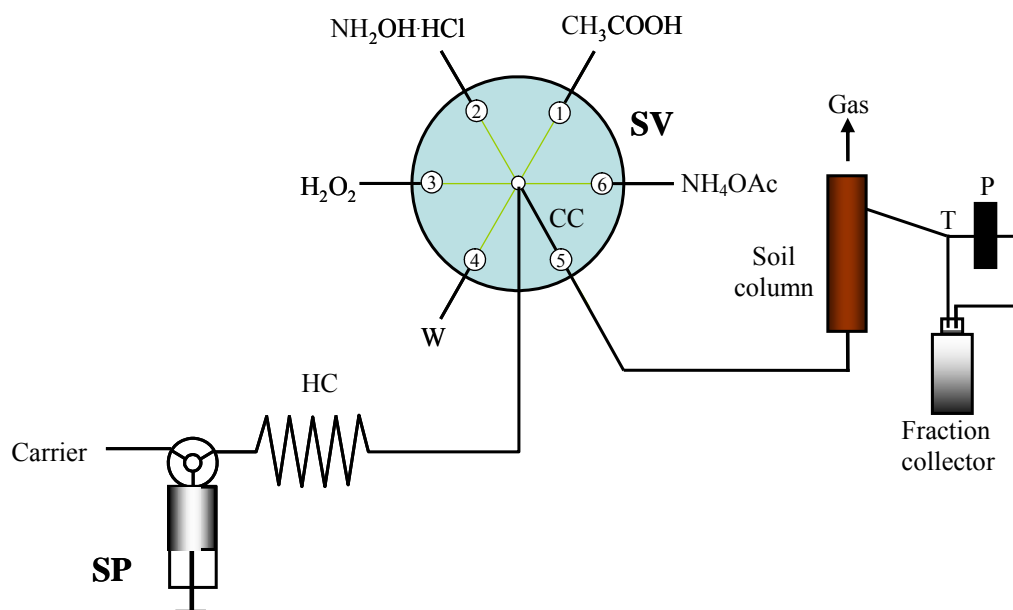
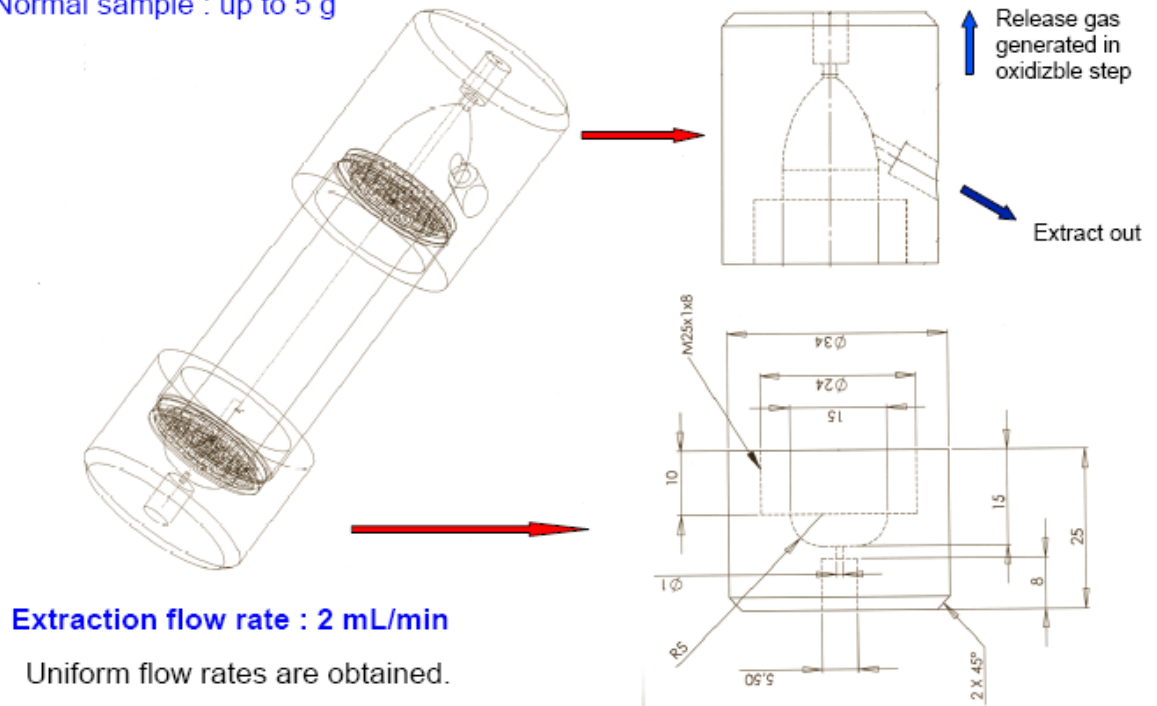


*Figure 19 Schematic diagram of the dynamic sequential extraction systems; SP, syringe pump; HC, holding coil; SV, selection valve; CC, central communication channel; W, waste; carrier, Milli-Q water; T, three ways valve; P, peristaltic pump.*

### Sample size

Contaminated sample : ca. 0.5-1 g

Normal sample : up to 5 g



Extraction flow rate : 2 mL/min

Uniform flow rates are obtained.

Figure 20 Extraction column used for dynamic sequential extraction of radionuclides from soil and sediment samples

### 3.7 Analytical method for the determination of rhenium

A method suitable for the analysis of rhenium in sediments and seaweed by ICP-MS was developed. Due to the volatility of rhenium (as  $\text{Re}_2\text{O}_7$ ) wet-ashing and dry ashing at 450 C of seaweed and sediments were compared. In no cases (n=10) could any loss of rhenium due to dry-ashing be detected.

The amount of seaweed used for a typical analysis was around 0.5g dry weight and 50-200mg of dry sediment. About 0.5 ng of a  $^{185}\text{Re}$  standard (enriched to 96% with respect to  $^{185}\text{Re}$ ) was added. Rhenium was separated using anion exchange (AG 1x4, 100-200 mesh resin). The sample was loaded onto a 1ml column in 0.1M HCl and beaker and column washed with 10ml 0.1M HCl and the major and trace elements washed from the column by 10ml 0.5M HCl and 10ml 1.5M HCl respectively. Rhenium was eluted from the column using 15ml 4M  $\text{HNO}_3$ . All HCl and  $\text{HNO}_3$  solutions were prepared from ultrapure acids and ELGA 18 Mohm water.



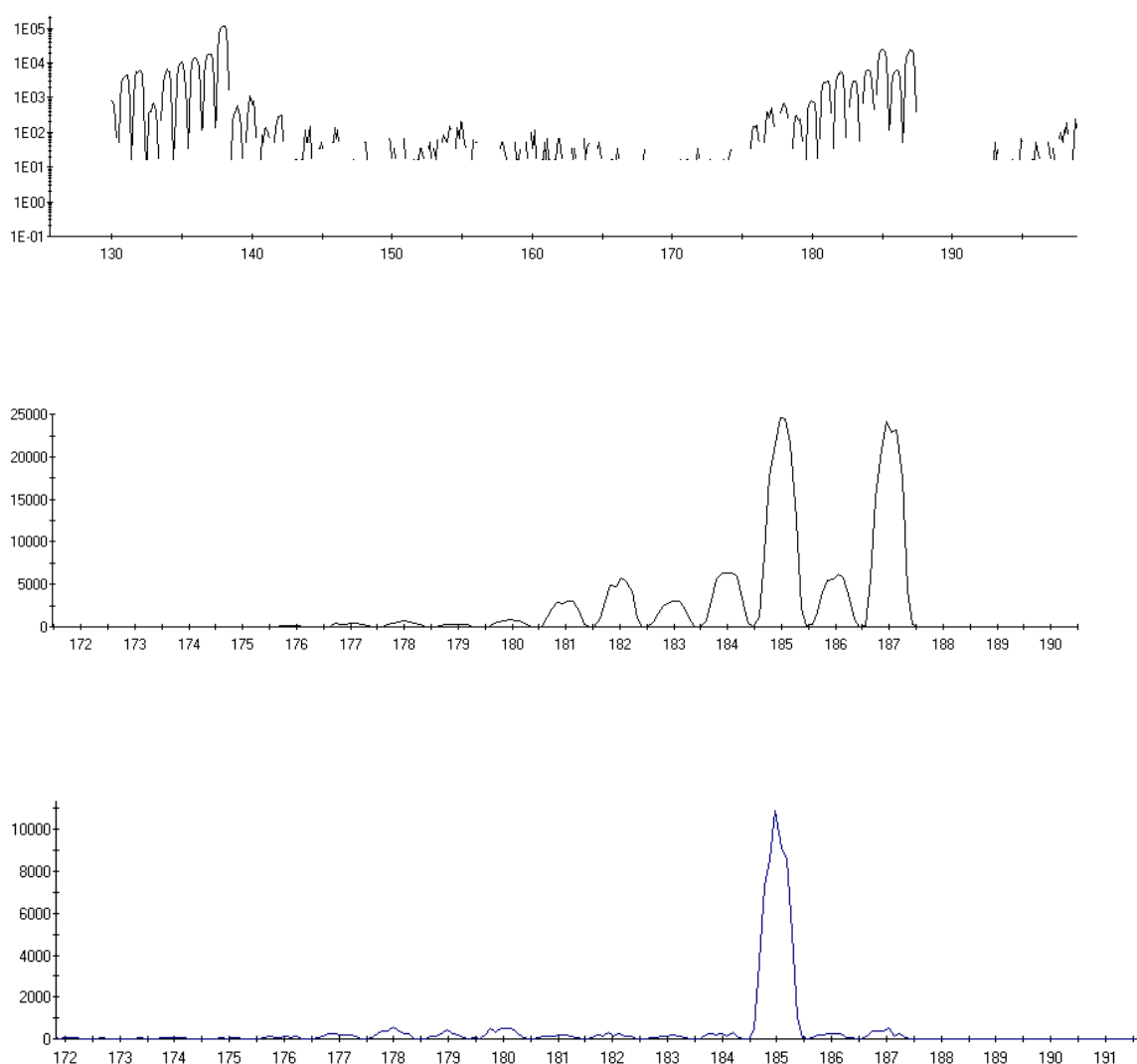


**Figure 21** Mass-spectra of rhenium isolated from a 100mg sediment sample as described in the text. The presence of tungsten and REE is negligible. The lowermost mass-spectra show a procedure blank including the  $^{185}\text{Re}$  spike.

There are three major concerns to take into account in the separation of rhenium. Tungsten (W), rare earth elements and blank contribution from chemicals and labware. The major problem is usually tungsten due to the hydrides  $^{184}\text{WH}$  and  $^{186}\text{WH}$ . Since the abundance of tungsten is in the order of  $10^3$ - $10^5$  times that of rhenium in typical sediments and the WH/W ratio varies with ICP-MS instrumental setup the chemical removal of tungsten as well as measurements of the WH/W ratio is essential. Typical WH/W ratios are around  $10^{-4}$  when using standard Meinhard nebuliser but may be reduced by a factor of 3-4 by desolvation techniques such as USN. In seaweed the tungsten problem is far less due to the relatively low concentrations while at the same time rhenium concentrations are high.

During specific conditions the presence of REE may create problems in the analysis of rhenium. The oxides, nitrides and argides of some REE ends up at the rhenium mass range. In the chemical procedure described above REE are efficiently removed which also may be seen in the figure below. The interference of the very rare isotope  $^{187}\text{Os}$  (1.6% abundance) is in all cases negligible. Figure 21 show the ICP-MS spectra of Re from sediment samples.

### ***3.8 Investigation on Re-absorption of Pu during the fractionation of Pu in soil and sediment***

One of the most important problems with sequential extraction techniques is redistribution as a result of readsorption of dissolved metals onto the remaining solid phases during extraction. It has been recommended that the extraction time or contact time between the solid phase and the extracting reagent of the earlier steps of sequential extractions should be kept as short as possible to minimize the risk of readsorption to take place. Our previous work with dynamic extraction system incorporating the microextraction column to fractionate stable metals in soils and sediments has shown many advantages over the batch system, and one of the major ones is less readsorption.

It was expected that the dynamic extraction system developed in this work would also reduce readsorption of radionuclides (Pu and Am) during fractionation in comparison with the conventional batch methods.

A double spiking technique was used to determine the extent of Pu and Am readsorption during sequential extraction. Known activities of  $^{242}\text{Pu}$  and  $^{243}\text{Am}$  tracers were spiked to the extractant in order to measure the degree of readsorption. Recoveries and the distributions of  $^{242}\text{Pu}$  and  $^{243}\text{Am}$  among different fractions are shown in Figure 21 and Figure 22, respectively. The results showed that recoveries of  $^{242}\text{Pu}$  and  $^{243}\text{Am}$  in different spiked steps in the batch and dynamic extraction systems are similar, except recovery of  $^{243}\text{Am}$  at step I for dynamic system showed lower percentage (ca. 2%) in comparison with the batch system (ca. 9%). It was found that a very significant readsorption occurred in all steps.

For example, recovery of spiked  $^{242}\text{Pu}$  in the exchangeable step was 24% in average and less than 10% for  $^{243}\text{Am}$ . In the acid soluble and the reducible fractions, recoveries of  $^{242}\text{Pu}$  and  $^{243}\text{Am}$  were less than 4% and 8%, respectively. A relatively low degree of readsorption in comparison with other steps was observed in the exchangeable fraction for Pu (ca. 76%, both methods) and for Am (ca. 90%, batch method).

The main reason for these is probably because ammonium acetate entails a high complexing capacity due to the acetate ion which may prevent readsorption or precipitation of the released ions from the soil sample.

From the results (Figure 22, 23), it was found that  $^{242}\text{Pu}$  and  $^{243}\text{Am}$  are redistributed among the remaining phases, especially to the oxidizable and residual fractions. The distribution of spiked Pu and Am showed similar patterns for both the dynamic and the batch procedures. Major amount of spiked  $^{242}\text{Pu}$  (ca. 59%) and

<sup>243</sup>Am (ca. 64%) were mainly redistributed to the oxidizable fraction (organic matter phase, step IV).

It should be borne in mind that in the oxidizable phase (step IV), the proposed dynamic extraction system was operated at room temperature by passing the extractant slowly through the soil column, which provided 4 h extraction time. The batch extraction was performed at room temperature (1 h) and at 85 °C (2 h). Therefore, the results from the dynamic system indicated that the percentages of leachability of radionuclides in this step were slightly lower than the batch system. However, the extractable amounts of Pu and Am in this step were higher than our expectation. It might be because the newly readsorbed radionuclides were loosely bound to the organic matter.

This result indicates that the readsorption of Pu and Am occurs in a very short time scale. Even though extracts are rapidly removed from contact with the remaining solid phase in the dynamic system, the degree of readsorption is still high. However, based on the experimental results, it can be concluded that extractions performed by the dynamic approach are, still, preferable to those obtained with the batch procedures. The dynamic extraction system is a closed system providing no sample loss, less risk of personal errors, and eliminates external contamination. Therefore, it gives higher recoveries of the spiked radionuclides (ca. 89% as compared to ca. 67% recovery with the batch procedure). Besides, the continuous extraction approach mimics much better the real environmental conditions.

The system is fully automated and computer-controlled. Uniform flow rates are obtained under the optimal operational conditions. Tedious procedures such as solid-liquid phase separation by centrifugation and manual filtration are completely eliminated. Washing between steps can be implemented simply by dispensing pure water to the column between extraction steps.

The extraction time for the 4 steps comprises totally ca. 8 h as compared to ca. 50 h in the batch systems (even without considering the separation procedure by centrifuge and filtration). And it is possible to obtain more detailed knowledge of the leaching kinetics when highly contaminated samples are applied. Further studies are required to understand more about the readsorption events themselves, including factors affecting the degree of readsorption such as soil properties and how to solve or reduce this problem when performing dynamic sequential extraction procedures.

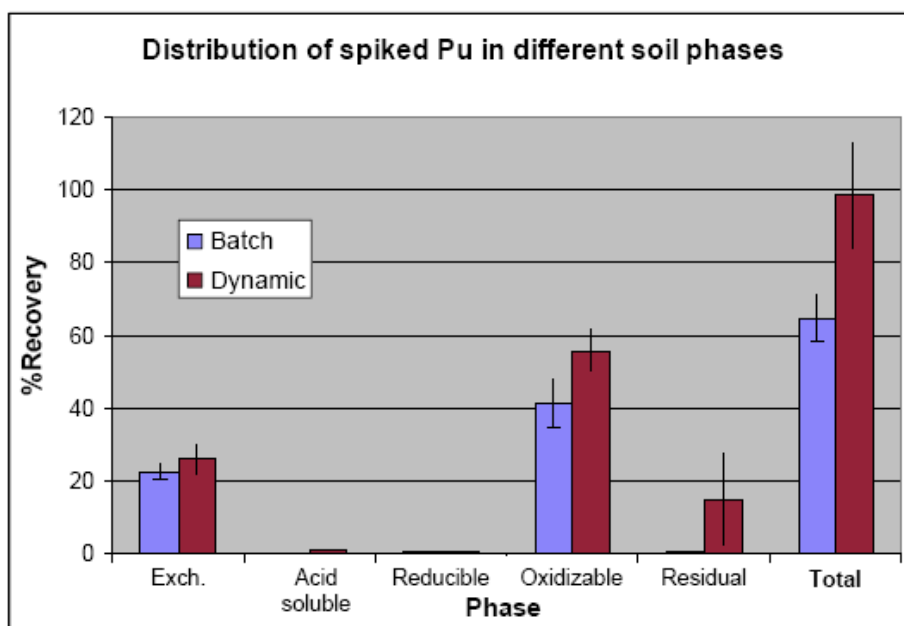


Figure 22 Recoveries of spiked  $^{242}\text{Pu}$  in each extraction step when comparing the dynamic and the batch extraction systems

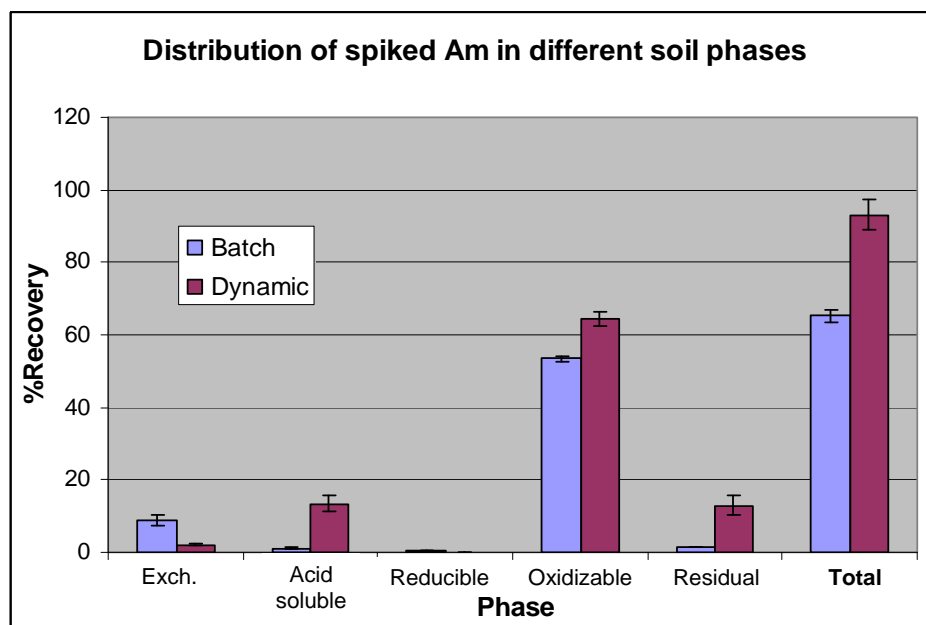


Figure 23 Recoveries of spiked  $^{243}\text{Am}$  in each extraction step when comparing the dynamic and the batch extraction systems

## 4. Investigation of speciation of the radionuclides in environmental samples

The developed methods have been successfully used for the investigation of speciation of radionuclides including  $^{129}\text{I}$ , Pu isotopes, and  $^{99}\text{Tc}$  in Danish environment and contaminated region in Thule, Greenland. In addition, the nuclear waste from the decommissioning of Danish nuclear facility was also studied to investigation of speciation of Pu isotopes.

### 4.1 Speciation of $^{129}\text{I}$ in North Sea surface water

Surface seawater samples collected from the North Sea and English Channel were analyzed for total  $^{129}\text{I}$  and  $^{127}\text{I}$  as well as for iodide and iodate. The results (Figure 24, 25) show that relatively high  $^{129}\text{I}$  concentrations ( $2\text{--}3 \times 10^{11}$  atoms/L) were observed in the northern part of the English Channel and in the south-eastern North Sea. The atomic ratio of  $^{129}\text{I}/^{127}\text{I}$  decreases from the eastern ( $1.0\text{--}1.9 \times 10^{-6}$ ) to the western ( $4\text{--}6 \times 10^{-8}$ ) parts of the North Sea and from the north-eastern ( $1.5 \times 10^{-6}$ ) to south-western ( $1\text{--}5 \times 10^{-8}$ ) parts of the English Channel. The ratios of iodide to iodate are (0.1–0.5) and (0.5–1.6) for the  $^{127}\text{I}$  and  $^{129}\text{I}$ , respectively, in open seawaters, whereas these ratios range at (0.6–1.3) and (0.8–2.2) in coastal waters.

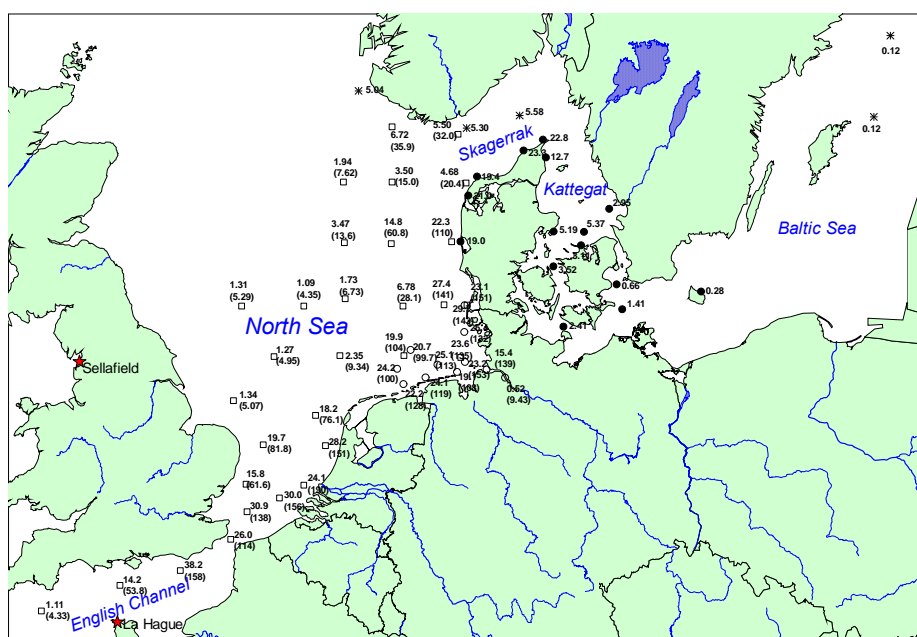


Figure. 24 Distribution of  $^{129}\text{I}$  concentration ( $10^{10}$  atoms/L, the upper number) and  $^{129}\text{I}/^{127}\text{I}$  ratio ( $10^{-8}$  mol/mol, in parentheses) in the North Sea in Aug. 2005 (○, ✱) and Skagerrak, Kattegat and Baltic Sea in 1999 and 2000 (□) measured in this work, and in June 1999 (◊, Alfimov et al., 2004)

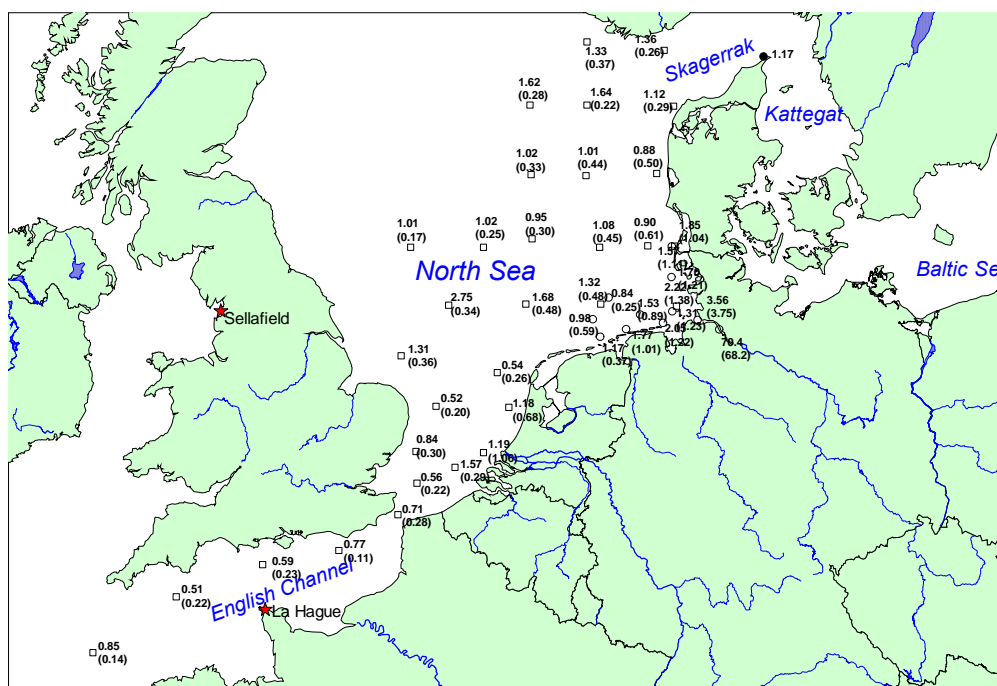


Figure 25 Distribution of iodide/iodate ratios for  $^{129}\text{I}$  (upper number) and  $^{127}\text{I}$  (in parentheses) in surface seawater from the English Channel and North Sea

The results suggest that: (1) Imprints of the La Hague facility dominates the  $^{129}\text{I}$  distribution in the surface water of the North Sea; (2) Reduction of iodate to iodide is relatively fast during the transport to the European continental coast; (3) Oxidation of newly produced  $^{129}\text{I}$  to  $^{129}\text{IO}_3^-$  is insignificant during water exchange between the coastal area and open sea, and reduction of iodate; (4) Oxidation of iodide in the open sea seems to be a slow process.

#### 4.2 Speciation of $^{129}\text{I}$ in precipitation collected in Roskilde, Denmark 2001-2006

Speciation analysis of  $^{129}\text{I}$  and  $^{127}\text{I}$  in precipitations collected from Roskilde, Denmark in 2001 to 2006 was completed, the variation of concentrations of iodide, iodate, total iodine for  $^{129}\text{I}$  and  $^{127}\text{I}$  are shown in Figures 26-29. The concentrations of total  $^{129}\text{I}$  in precipitation vary from  $0.28$  to  $5.63 \times 10^9$  atoms  $\text{L}^{-1}$  with an average of  $(2.34 \pm 1.43) \times 10^9$  atoms  $\text{L}^{-1}$ , and the annual deposition flux of  $^{129}\text{I}$  is  $(1.25 \pm 0.30) \times 10^{12}$  atoms  $\text{m}^{-2}$ . Iodide is the major species of  $^{129}\text{I}$ , which accounts for 50-99% of total  $^{129}\text{I}$  with an average of 92%.

The concentrations of total  $^{127}\text{I}$  vary from  $0.78$  to  $2.70$  ng  $\text{mL}^{-1}$  with an average of  $1.63 \pm 0.47$  ng  $\text{mL}^{-1}$ , and annual deposition of  $^{127}\text{I}$  is  $0.95 \pm 0.26$  mg  $\text{m}^{-2}$ . Unlike  $^{129}\text{I}$ , iodate is the major species of  $^{127}\text{I}$ , which accounts for 43-93% of total  $^{127}\text{I}$  with an average of 68%, and the concentrations of non-ionic iodine and iodate are lower. The  $^{129}\text{I}/^{127}\text{I}$  atomic values for total iodine vary from  $5.04$  to  $76.5 \times 10^{-8}$  atom/atom with an average of  $(30.1 \pm 16.8) \times 10^{-8}$ , while these values are 10 times lower for iodate with an average of  $(2.95 \pm 3.13) \times 10^{-8}$ . A similar seasonally variations of  $^{129}\text{I}/^{127}\text{I}$  values as well as  $^{129}\text{I}$  concentration are observed with higher value in spring and lower one in summer-autumn period.

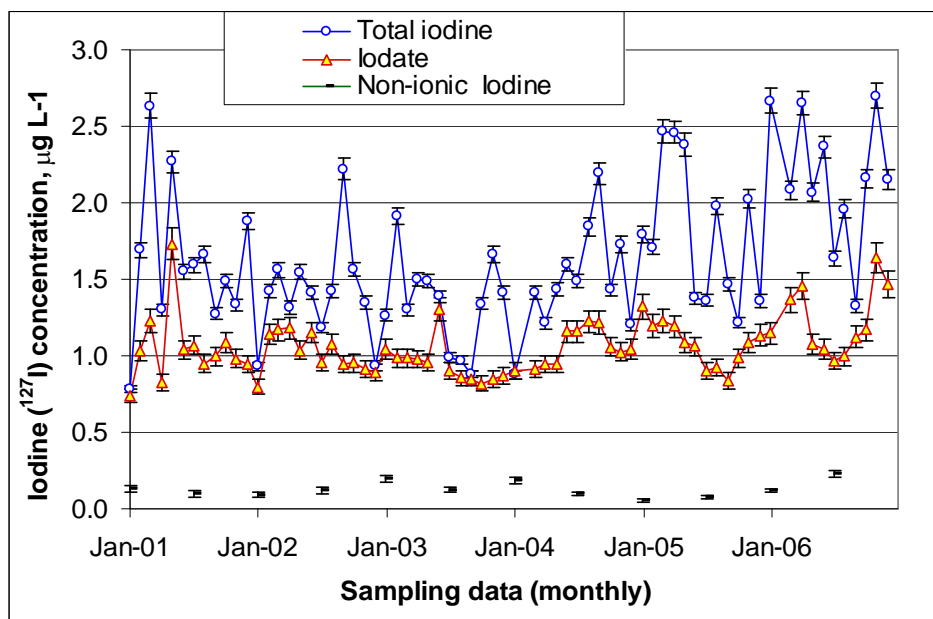


Figure 26 Variation of concentrations of  $^{127}\text{IO}_3^-$ , and non-ionic and total  $^{127}\text{I}$  in precipitation from Roskilde, Denmark in 2001-2006 (the error bar shows the analytical uncertainty).

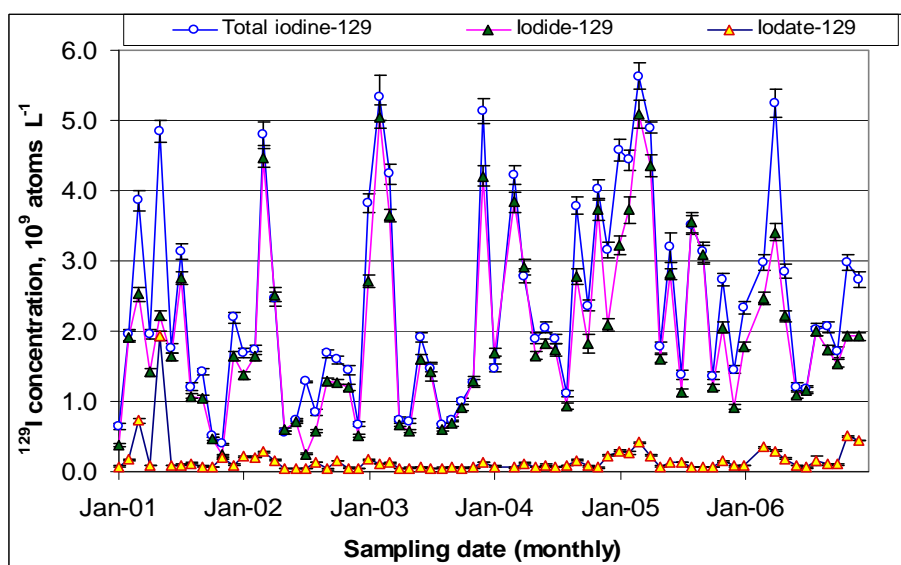


Figure 27 Variation of concentrations of  $^{129}\text{I}$ ,  $^{129}\text{IO}_3^-$ , and total inorganic  $^{129}\text{I}$  in precipitation from Roskilde, Denmark in 2001-2006 (the error bar shows the analytical uncertainty).

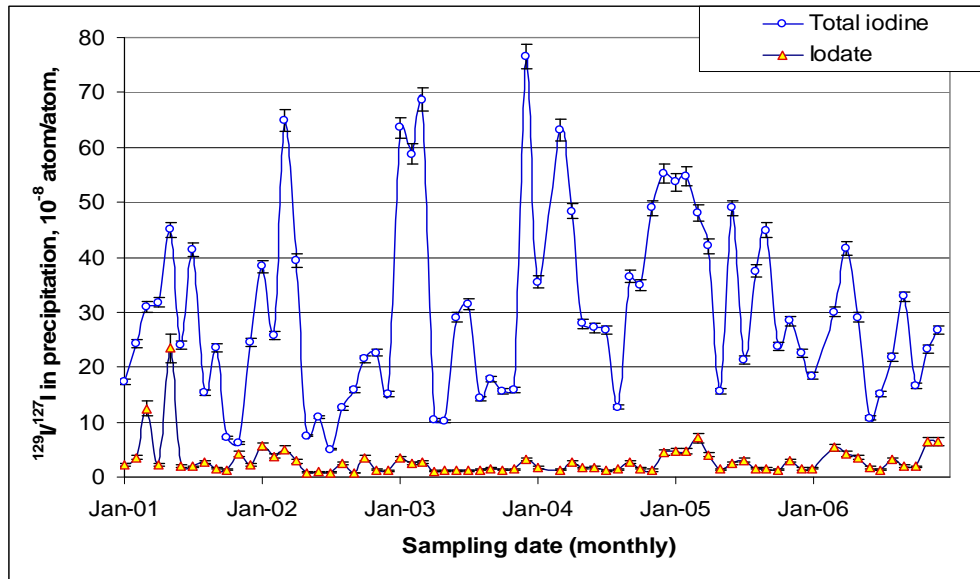


Figure 28 Variation of  $^{129}\text{I}/^{127}\text{I}$  values ( $10^{-8}$  stoms/atoms) for iodate and total iodine in precipitation from Roskilde, Denmark in 2001-2006 (the error bar shows the analytical uncertainty).

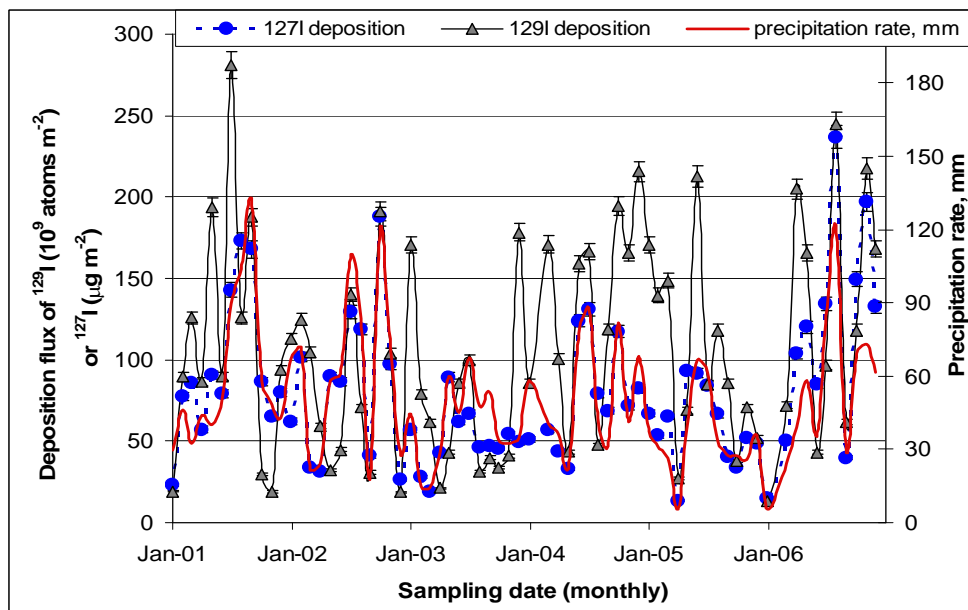


Figure 29 Variation of deposition flux of  $^{129}\text{I}$  and  $^{127}\text{I}$  ( $10^9$  atoms  $\text{m}^{-2}$ ) by precipitation collected with a  $1 \text{ m}^2$  collector at Roskilde, Denmark in 2001-2006, the deposition rates (mm) are show as a solid line (red).



Based on the results it is concluded that (1) an increased  $^{129}\text{I}$  level in precipitation is attributed to the release of  $^{129}\text{I}$  from reprocessing plants at La Hague and Sellafield, in which marine discharges is the major source of  $^{129}\text{I}$  through the re-emission of  $^{129}\text{I}$  discharged to the seas, particularly from the coastal areas. (2) Iodide as the dominant species of  $^{129}\text{I}$  is mainly attributed to the re-emission of  $^{129}\text{I}$  from the coastal water in the English Channel, Irish Sea, North Sea, Kattegat and Norwegian Sea. While, iodate, as the major species of  $^{127}\text{I}$  in the precipitation, might result from its multi-origins, i.e. emission from the ocean as well as emission from terrestrial plants. (3)

Based on the deposition flux of  $^{129}\text{I}$  and  $^{127}\text{I}$  measured in this work, an annual deposition of  $^{129}\text{I}$  over Europe can be estimated to be  $3.0 \text{ kg y}^{-1}$  in 2001-2006, and a total annual deposition of stable iodine on the surface of the earth to be about  $0.5 \times 10^{12} \text{ g y}^{-1}$ . (4) High concentrations of  $^{129}\text{I}$  in the coastal areas in the European seas and its specific origin from marine discharges of two European reprocessing plants supply a unique environmental tracer, this work shows the potential application of  $^{129}\text{I}$  as tracer for the investigation of geochemical cycle and complicated atmospheric chemistry of iodine.

#### ***4.3. Partition of $^{137}\text{Cs}$ and $^{129}\text{I}$ in the Nordic lake sediment, pore-water and lake water***

To quantify partitioning of the radioactive isotopes between solid and liquid phases and estimation of the isotope migration within soil and lake sediment profiles. Sediment cores were collected from a small lake in central Sweden (Loppesjön); a region characterised by relatively high Chernobyl fallout. With the view that a period of about 20 years has passed since the Chernobyl fallout, we aimed at investigating whether the fallout horizon has been stationary or if it has migrated within the sediment column. Furthermore, we explored interaction between the pore water and enclosing sediment and possible dispersion within the sediment profile and to the sediment-water inter-phase.

The sampling was done during winter of 2006 from a frozen lake surface and through direct core slicing. Sediment and pore water were separated and used to evaluate these hypotheses. Although we have measured the distribution of  $^{137}\text{Cs}$ , our main focus was on the distribution of  $^{129}\text{I}$ . The  $^{129}\text{I}$  occurs in minute quantities ( $10^{7-9}$  atoms/g sediment or water) in nature and thus is measured with the accelerator mass spectrometry technique (AMS). Some improvement of the analytical techniques for the determination of  $^{129}\text{I}$  by AMS was carried out, which includes minimizing the amount of sample to a degree that a few mm-wide sediment layers as well as a few ml of the pore water in a core can be sampled and measured. Furthermore, because of the rather heavy contamination of the Nordic atmosphere with anthropogenic releases of  $^{129}\text{I}$ , ultra clean laboratory conditions, preparation procedure and chemicals have been established. In addition, to increase detection limit of the AMS system a time of flight detector is used for near background concentration values.

Our preliminary results on the distribution of  $^{137}\text{Cs}$  and  $^{129}\text{I}$  in the lake sediment, pore-water and lake water show interesting partitioning behaviour. The data suggest a rather constant and conservative behaviour of the  $^{137}\text{Cs}$ -rich sediment layer (Chernobyl) without observable migration compared to previous measurement, during 1996, at the same part of the lake. This  $^{137}\text{Cs}$  coincidence was used to estimate possible migration in the  $^{129}\text{I}$  isotope through the sediment profile. The data show indication of an upward migration of the  $^{129}\text{I}$ -Chernobyl related layer. Data on the  $^{129}\text{I}$  distribution in the pore water also support an upward migration of the isotope. However, the partition between pore-water and sediment was relatively small (a few %) suggesting that most of the  $^{129}\text{I}$  was kept in immobile speciation forms in sediment particles.

The amount of  $^{129}\text{I}$  in the lake water along the sediment-water inter-phase is about several times higher than what is found in the lake water. This observation indicates that some fraction of  $^{129}\text{I}$  are released from the sediment to the water through possible decomposition of organic matters (an iodine-rich source).

The next stage of our project is to exactly specify the type of iodine speciation in all sediment-water compartments as well as in the biota (animals and vegetation). This approach is vital in order to investigate the rate of  $^{129}\text{I}$  mobility and the speciation forms that are most appealing to nutrient chain and the bio-availability of the isotope in the ecosystem.

#### **4.4 $^{129}\text{I}$ and $^{127}\text{I}$ and their speciation in lake sediment**

Iodine is a biophilic element commonly occurring in trace to minor amounts in marine and terrestrial biota. Several radioactive isotopes of iodine have been released to the environment in relatively large amounts since the start of the atomic era during the 1940s. Although most of these isotopes decay within a short time, the long half-life (15.7 Myr) of I-129 makes its geochemical behaviour comparable to the stable iodine. Presently, there are few data about the partitioning of the iodine isotopes in continental environment, which represent a large reservoir of the isotope.

In the aim of capturing both the historical changes in I-129 deposition since the start of the nuclear era and understand possible occurrence modes of iodine, we have measured I-127 and I-129 in a sequence of lake sediment located in central Sweden. The varve structure together with a well-defined Cs-137 Chernobyl peak provided constrained chronology of the sediment, which covers the period 1942-2006. All samples were measured for I-129 and 9 selected samples were used for the sequential leaching procedure and measurement of I-129 and I-127 in four fractions of each sample.

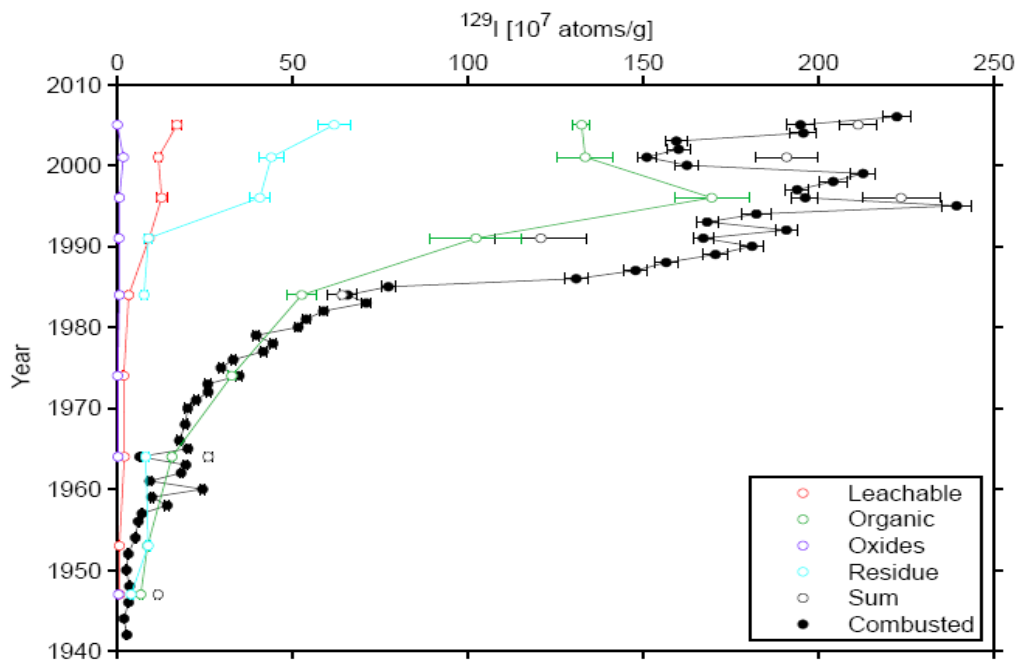


Figure 30 Depth profile of  $^{129}\text{I}$  concentrations for total iodine and different species of  $^{129}\text{I}$

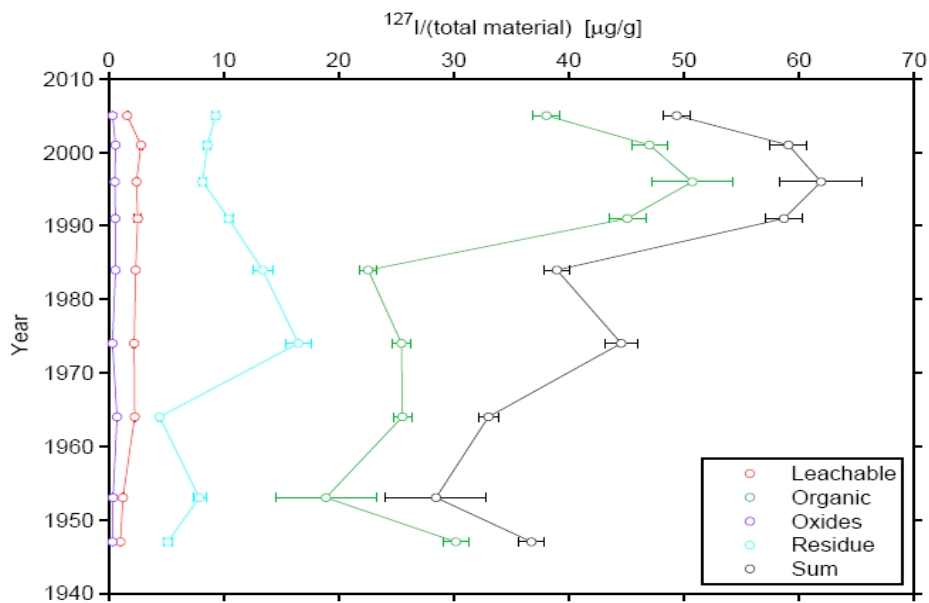


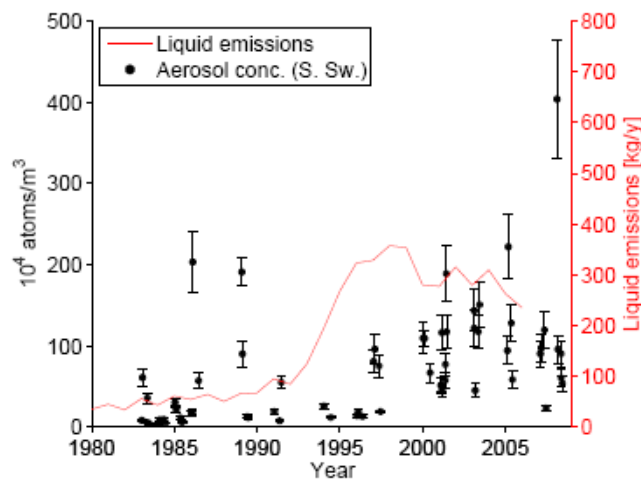
Figure 31 Depth profiles of  $^{127}\text{I}$  concentrations for total iodine and different species of  $^{127}\text{I}$

The I-129 profile (Figure 30) reflects impacts of the emission from the European nuclear reprocessing facilities since the early 1950's as well as that of the Chernobyl fallout in 1986. Results of the sequential leaching show that major part of both I-129 and I-127 is found within the organic fraction, whereas the reducible oxides fraction contains the lowest values (Figure 31). The leachable and carbonate partitions show appreciable concentrations of both isotopes, but the values are lower than that found in the residual partition.

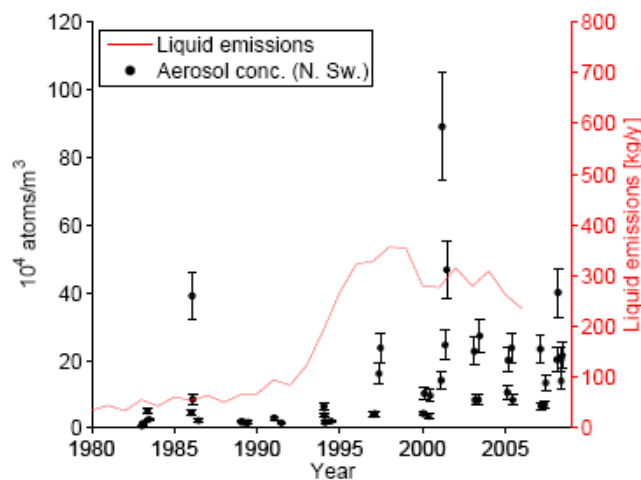
The ratio of I-129/I-127 in the different partitions shows a wide range reflecting mainly the two orders of magnitude difference in I-129 between post- and pre-Chernobyl period.

#### 4.5 Iodine isotopes ( $^{127}\text{I}$ and $^{129}\text{I}$ ) in aerosols

Aerosols represent a potential carrier of iodine in the continental atmosphere where aerosol contribution to the iodine budget is scarce and even lacking for most parts of the world. We here present data on distribution of iodine isotopes (I-127 and I-129) in aerosols covering the period 1983 to 2000 from two sites (67.84°N, 20.34°E and 56.08°N, 13.23°E) in Sweden. Aerosols have been collected by the Swedish Defence Research Institute (FOI) for the surveillance program of radioactivity in airborne particulate matters. Aerosols were weekly trapped in glass fiber filters (0.58 m×0.58 m) at an air-flow rate of 84 cm/s and a trapping efficiency > 99% for the > 0.3  $\mu\text{m}$  particles.



(a)



(b)

Figure 32.  $^{129}\text{I}$  concentration in (1) southern Sweden (Ljunghed) and (b) northern Sweden (Kiruna) together with the liquid  $^{129}\text{I}$  discharge from reprocessing plants at Sellafield and La Hague

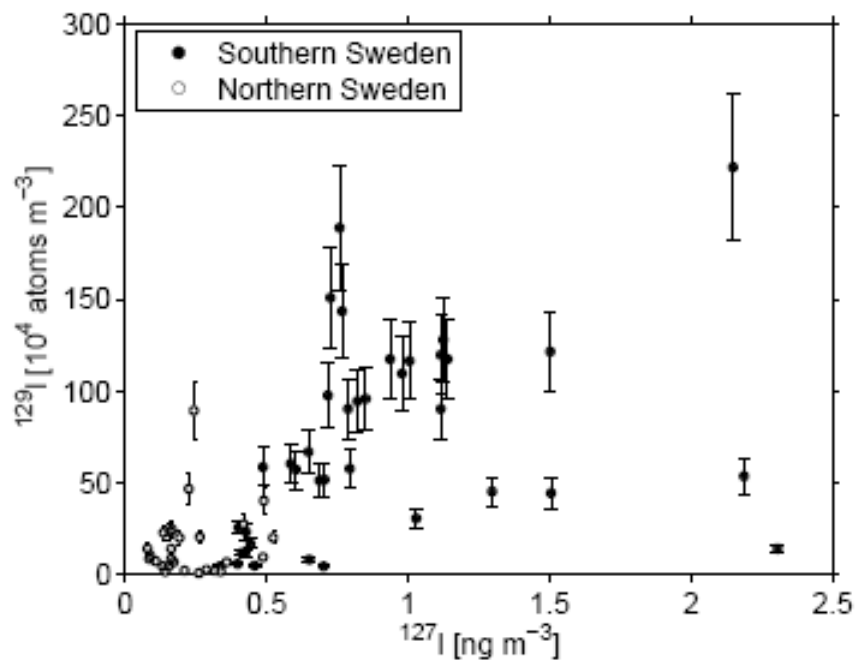


Figure 33 Variation of  $^{129}\text{I}$  concentrations with  $^{127}\text{I}$  in aerosol collected in Sweden.

Figure 32 and 33 show the variations of concentrations of  $^{129}\text{I}$  and  $^{127}\text{I}$  in the aerosol collected in Sweden from 1980 to 2008. Concentrations of I-127 in the two sites vary between 0.14 and 2.31 ng/cubic m air while the range of I-129 is  $(1 - 203) \times 10^4$  atoms/cubic m air and isotopic ratios of I-129I/I-127 [atoms/atoms] range at  $(1 \text{ and } 23.9) \times 10^{-8}$ . Annual mean concentrations are consistently higher at the southern site with a significant difference in the relative concentrations between the sites, being 9 times higher for I-129 and only 2 times for I-127.

There is no clearly observable temporal trend and the correlation between the two isotopes is not strong ( $r^2=0.6$ ) suggesting effects from variable sources and complex atmospheric recycling. Both isotopes have anthropogenic sources (mainly fertilizers for I-127 and nuclear fuel reprocessing for I-129), but the natural source is dominant for I-127 compared to I-129. A mixed proportion of sea surface volatilization and gaseous emission, particularly for the I-129 suggest that aerosols fallout comprises not more than 35% and 25% of I-127 and I-129, respectively, of the total fallout which is dominated by the wet (precipitation) component.

#### 4.6. Speciation of Pu in soil, sediment and concrete samples from decommissioning of Danish nuclear reactor

The developed dynamic extraction method has been used to investigate the fractionation of Pu in soil collected from Thule, Greenland and heavy contamination area near Chernobyl power plant, sediment samples collected from Thule, Greenland, Palomares, Spain and Irish Sea, and concrete samples from the concrete shielding in Danish DK-2 research reactor which was decommissioned.

The result (Table 3) shows that most of Pu was associated to organic and oxides fractions and small fraction of Pu exists as mobile or bioavailable form (exchangeable and carbonate) in soil and sediment. However, in concrete sample, a large fraction of Pu exist as mobile for (carbonate), very less associated to organic fraction. To our best knowledge, this is the first investigation of the Pu fractionation in concrete, the results is very important in the view of waste disposal.

**Table 3** Sequential fractionation of  $^{239,240}\text{Pu}$  (Bq/kg) in soil, sediment, and concrete samples using dynamic sequential extraction system.

Sample	Rep.	Step 1 <sup>a</sup> ( $\text{NH}_4\text{OAc}$ )	Step 2 <sup>a</sup> ( $\text{CH}_3\text{COOH}$ )	Step 3 <sup>a</sup> ( $\text{NH}_2\text{OH}\cdot\text{HCl}$ )	Step 4 <sup>a</sup> ( $\text{H}_2\text{O}_2$ )	Step 5 <sup>a</sup> (Aqua regia)	Total <sup>a</sup> (1+2+3+4+5)	Total <sup>b</sup> (Aqua regia)
Thule Soil	1	0.37	0.26	20.5	0.76	27.9	49.8	56.5 ± 1.5
	2	0.30	0.34	17.6	0.60	35.1	53.9	
Chernobyl Soil	1	0.08	0.07	0.04	0.39	0.46	1.04	0.86 ± 0.18
	2	0.04	0.06	0.04	0.45	0.86	1.46	
Thule Sediment	1	<DL	<DL	<DL	<DL	3.71	3.71	3.90 8.60
	2	<DL	<DL	1.13	3.45	23.5	28.1	
Palomares Sediment	1	11.6	14.8	52.8	6.9	3481	3568	4006 ± 46
	2	10.1	11.8	36.5	20.4	2458	2537	
Irish Sea Sediment	1	1.49	3.02	44.6	213	46.8	309	344 ± 7.5
	2	1.90	2.26	52.0	0.90	282.4	339	
Concrete no.5	1	0.10	0.44	0.40	<DL	<DL	0.94	NA
Concrete no.6	1	<DL	0.07	0.17	<DL	<DL	0.24	0.23 ± 0.08
	2	<DL	0.05	0.11	0.16	<DL	0.32	

#### 4.7 Speciation of $^{99}\text{Tc}$ and Re in seaweed samples

Since rhenium is an analogue to technetium and similarly has a redox sensitive behaviour a pilot tests has been undertaken to study if the behaviour of the two elements in the important bioindicator *Fucus Vesiculosus* is similar. A 10g dry sample from the Swedish west coast collected in 2001 was used for this study. The total  $^{99}\text{Tc}$  concentration in this sample was determined to be 135 Bq kg<sup>-1</sup> and the rhenium concentration determined to 43 ppb. The sample was gently heated in 100ml 2M NaOH overnight on a hotplate. Following this treatment the slightly

coloured solution was filtered through a 0.45 µm filter and divided in to equal parts.  $^{99m}\text{Tc}$  and  $^{185}\text{Re}$  tracer were added to respectively solution. Rhenium was sorbed onto a AG1×4 column and treatment was then as above for sediments. The analysis of Tc was done by radiometric analysis, briefly this method is based on isolation of Tc by ion-exchange and solvent extraction followed by electrodeposition and betacounting. Results from this study showed that extraction of Tc was only about 15% while for Re it was 35%. The difference in extraction may be due to several factors such as different timing in the uptake and allocation to different parts of the plant.

#### ***4.8 Speciation of Pu isotopes and $^{237}\text{Np}$ in water samples collected from Framvaren fjord***

Water samples for Pu-isotopes and  $^{237}\text{Np}$  was collected from Framvaren fjord, Norway. For Pu-isotopes four methods were used to identify speciation (Figure 34). The first made used of ultrafiltration which enabled colloidal and “dissolved” plutonium to be isolated from each other. A 10kD membrane was used and samples were ultrafiltered to produce a retentate and a permeate that consisted of equal volumes. Two methods were used to investigate the oxidation state of Pu. The first consist of co-precipitation onto REE-fluorides from acidic solutions which carries the reduced Pu(III) & Pu(IV) species. From the deepest part of the fjord having the highest Pu concentrations a 3 litre sample was acidified with HCl to make it 8 M where after it was passed through an anion exchange column. Since only Pu(IV), Pu(V) and Pu(VI) species are sorbed onto the anion exchanger from strong HCl solutions and it was known that reduced plutonium dominates the experiment was a method to determine if Pu(III) or Pu(IV) dominates. Finally an extraction method using Thenoyltrifluoreacetone (TTA) was used to determine if reduced Pu consisted of Pu (III) or Pu (IV) since Pu(III) is not extracted. The results are shown in Table 4.

***Table 4 Results of speciation analysis of Pu isotopes in water samples collected from Framvaren fjord***

Method	Adsorbed or extracted oxidation state	$^{239+240}\text{Pu}$ [µB l <sup>-1</sup> ]	Sum of fractions [µB l <sup>-1</sup> ]
LaF <sub>3</sub> precipitate (10 l);	Pu(III+IV)	275±11	na
TTA extracted (8 l)	Pu(IV)	12±4	-
Not extracted (water phase)		271±13	283±15
Adsorbed on AG 1x4 , 8 M HCL. (3 l)	Pu(IV,V,VI)	14±6	-
Not adsorbed		290±17	304±20

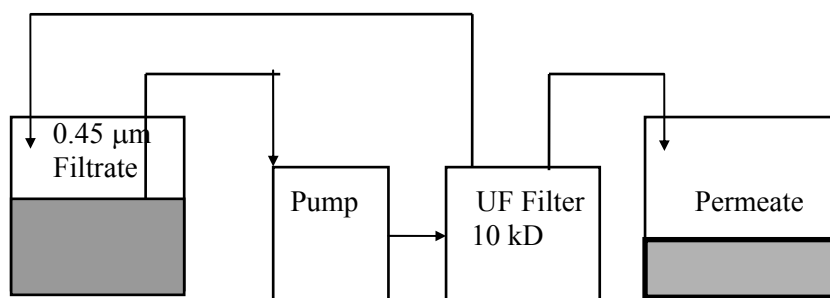


Figure 34: Schematic view of the Millipore Pellicon ultrafiltration system used in this work.

#### 4.9 Speciation of $^{129}\text{I}$ and $^{127}\text{I}$ in atmosphere for investigation of geochemical cycle of iodine using reprocessing $^{129}\text{I}$ as tracer.

Air samples at 8 locations with different distance to the North Sea (0, 5, 50, 100, 250, 500, 1000 km) in Denmark, Sweden, and Lithuania (Figure 35) have been collected in March and September 2007 using a air sampler (Figure 2) for directly collect different chemical speciation of iodine from atmosphere, such as particle, inorganic gaseous iodine, and organic gaseous iodine (Figure 18). Total 45 samples have been collected. Near the air sampling station, lichen, pine needle, surface water, and rain water samples have also been collected, total 25 lichen and pine needle samples, and 40 water samples was collected. Iodine in 25 lichen and pine needle samples has been separated using the combustion furnace (Figure 3), the separated iodine has been determined by ICP-MS for stable iodine, and prepared as AgI for AMS measurement for  $^{129}\text{I}$ . The results show a high  $^{129}\text{I}/^{127}\text{I}$  ratio in air sample as well as lichen samples in the short distance to the North Sea, especially those collected in a 10 km distance to the North Sea. The lowest value was observed in the Lithuania, where is 1000 km far from the North Sea.



Figure 25 Sampling locations for atmosphere(⊙), lichens(≡) and surface water with a distance to the North Sea from 0 km to 1000 km



## 5. Conclusion and perspective

Through this project, a number of analytical methods were developed for the speciation analysis of radionuclides including  $^{99}\text{Tc}$ ,  $^{129}\text{I}$ , plutonium isotopes and  $^{237}\text{Np}$ , as well as some relative stable element and isotopes such as  $^{127}\text{I}$  and rhenium. The speciation method are designed for the different environmental samples including seawater, fresh water, soil, sediment, atmosphere, as well as nuclear waste from the decommissioning of Danish nuclear facilities.

The developed method have been successfully used for the investigation of the environmental behaviours of radionuclides. A number of significant investigations have been completed, they are summarized below: (1) The speciation of Pu isotopes in radioactive concrete from the decommissioning of Danish nuclear reactor DK2 was observed to be very much different with those in environmental samples such as soil and sediment, Pu in the concrete is more mobile than that in soil and sediment, which means that a specially attention should be given during the repository of such nuclear waste. (2) Speciation analysis of Pu isotopes in the soil and sediment from the contaminated area in Thule Greenland shows that Pu is less mobile in this samples, and therefore less bioavailable, the more risk of radiation exposure of Pu in this circumstance will be the inhalation of aerosols. (3)  $^{129}\text{I}$  speciation is very successfully applied to investigate the dispersion of pollution in the North Sea, Kattegat, and Baltic Sea, as well as for the investigation of marine geochemical cycle of stable iodine by measure the different species of  $^{129}\text{I}$  and  $^{127}\text{I}$ .

The investigation show that iodate is reduced in the European continental coast, especially the Dutch coast and German Bight, the reduction of iodate to iodide and oxidation of iodide to iodate in the open sea is a slow process. (4)  $^{129}\text{I}$  level in the precipitation in Denmark has increased to  $10^9 \text{ atom L}^{-1}$  which is 3-4 orders magnitude higher than other lotions in Asia, American and Africa, this is mainly attributed to the releases from the reprocessing plant in Sellafield and La Hague.  $^{129}\text{I}$  in the precipitation in Denmark dominates by iodide, while the dominant species of  $^{127}\text{I}$  is iodate, it indicates that  $^{129}\text{I}$  and  $^{127}\text{I}$  have a different source. (5)  $^{129}\text{I}$  is mainly associated to organic phase in the sediment and soil, which is not mobile. It is therefore the organic mater in the sea and lake is the main sink of  $^{129}\text{I}$ . (6) In seaweed (*Fucus*), only small fraction of  $^{99}\text{Tc}$  is leachable with water and alkaline solution, and absorbed on anion exchange column. This indicates that  $^{99}\text{Tc}$  is mainly bound to organic molecules, and some fraction of  $^{99}\text{Tc}$  exist as  $\text{TcO}_4^-$  ions.

Speciation of radionuclides is becoming more and more attractive and important topic for the radiation protection, dose assessment, as well as tracer application. However, the speciation is much more complicate comparing to the total concentration of radionuclides. Although many works have been done during this project, but it is a good start, a lot questions need to be answered and plenty of application worth to be investigated. We will keep this research line to go further investigations.

## 6. List of papers published and to be published

1. Hou, X.L., Aldahan, A., Nielsen, S.P., Possnert, G., Niels, H., Speciation of  $^{129}\text{I}$  and  $^{127}\text{I}$  in seawater and implications for sources and transport pathways in the North Sea, *Environ. Sci. Tech.*, 41(2007)4993-5999.
2. Xiaolin Hou, Violeta Hansen, Ala Aldahan, Göran Possnert, Ole Christian Lind, Galina Lujaniene, Speciation of Iodine-129 in the Environment, *Anal. Chim. Acta*, 632(2009) 181-196
3. Petersen R.; Hou X.L.; Hansen, E.H. Evaluation of the readsorption of plutonium and americium in dynamic fractionations of environmental solid sample, *J. Environ. Radioact.* 99 (2008)1165-1174.
4. E.Englund, A.Aldahan, G. Possnert, X.L. Hou, I. Renberg, I. Saarinen, Modeling fallout of anthropogenic  $^{129}\text{I}$ , *Environ. Sci. Tech.*, 42 (2008) 9225-9230.
5. Hou, X.L.; Roos P. Critical Comparison of Radiometric and Mass Spectrometric Methods for the Determination of Radionuclides in Environmental, Biological and Nuclear Waste samples, *Anal. Chim. Acta*, 608(2008) 105-139.
6. Jixin Qiao, Xiaolin Hou, Manuel Miro, Per Roos, Determination of plutonium isotopes in environmental samples: a review, *Anal. Chim. Acta*, 2009, in press
7. Hou, X.L. Iodine Speciation in Foodstuff, Tissues and Environmental samples, -- Iodine species and analytical method, *Comprehensive Handbook of Iodine*, Academic Press, 2009.Chapter 16
8. Persson, S., Aldahan, A., Possnert, G., Alfimov, V., Hou, X.L.,  $^{129}\text{I}$  Variability in precipitation over Europe, *Nuclear Instruments and Methods in Physics Research Section B*, 259(2007)508-512.
9. Aldahan, A.; Englund, E.; Possnert, G.; Cato, I.; Hou, X.L., Iodine-129 enrichment in sediment of the Baltic Sea. *Appl. Geochem.* 22(2007)637-647
10. J. Jernström, J. Lehto, M. Betti, On-line separation of Pu(III) and Am(III) using extraction and ion chromatography, *J. Radioanal. Nucl. Chem.*, 274 (2007) 95-102
11. Aldahan A., Persson P., Possnert G., Hou X.L. Distribution of  $^{127}\text{I}$  and  $^{129}\text{I}$  in precipitation at high European Latitudes, *Geophys. Res. Lett.*, (2009) accepted
12. Xiaolin Hou, Ala Aldahan, S.P. Nielsen, Göran Possnert, (2008). Speciation of  $^{129}\text{I}$  and  $^{127}\text{I}$  in precipitation in Denmark: Source term of  $^{129}\text{I}$  and its application as a tracer, *Environ. Sci. Technol.*, 2008, to be submitted
13. Xiaolin Hou, Violeta Hansen, Ala Aldahan, Göran Possnert, A simple and novel method for chemical speciation of  $^{129}\text{I}$  in seawater, *Anal. Chem.*, 2008, to be submitted
14. Xiaolin Hou, S.P. Nilesen, Ala Aldahan, S.P. Nielsen, Göran Possnert, Speciation of  $^{129}\text{I}$  and  $^{127}\text{I}$  in atmosphere, potential application for geochemical cycle study of stable iodine, *Environ. Sci. Technol.*, 2008, to be submitted.
15. Jussi Jernstroem, Per Roos, Using ion chromatography in separation of technetium in environmental samples, *the Analyst*, 2008, to be submitted

## 7. Papers presented in conferences and meetings

1. Hou, X.L., Aldahan, A., Nielsen, S.P., Possnert, G., Niels, H., Chemical speciation of  $^{129}\text{I}$  in North Sea water and its application for the study of marine geochemical cycle of stable iodine, Proceedings of NKS speciation seminar, April. 2007.
2. Pertersen R., Dynamic Chemical Fractionation of Metals and Radionuclides in Soils and Sediments, Proceedings of NKS speciation seminar, April. 2007.
3. Aldahan, A.; Possnert, G.; Hou, X., Iodine (I-127 and I-129) in aerosols. In: Book of abstracts. 11. International conference on accelerator mass spectrometry, Rome (IT), 14-19 Sep 2008. (University of Salento, Lecce, 2008) p. 115
4. Englund, E.; Hou, X.; Petersen, R.; Aldahan, A.; Possnert, G., Sequential extraction of I-127 and I-129 in sediment. In: Book of abstracts. 11. International conference on accelerator mass spectrometry, Rome (IT), 14-19 Sep 2008. (University of Salento, Lecce, 2008) p. 114-114
5. Hou, X.; Hansen, V.; Aldahan, A.; Possnert, G.; Fievet, B.; Nies, H., Iodine-129 chemical forms in the surface water of the English Channel. In: Book of abstracts. 11. International conference on accelerator mass spectrometry, Rome (IT), 14-19 Sep 2008. (University of Salento, Lecce, 2008) p. 133-133
6. Hou, X.; Hansen, V.; Aldahan, A.; Possnert, G., A simple method for the speciation analysis of  $^{129}\text{I}$  in seawater. In: Book of abstracts. 11. International conference on accelerator mass spectrometry, Rome (IT), 14-19 Sep 2008. (University of Salento, Lecce, 2008) p. 18-18
7. Hou, X., Radiochemical analysis in decommissioning of nuclear facilities. In: Book of abstracts. 7. International conference on nuclear and radiochemistry, Budapest (HU), 24-29 Aug 2008. (Committee on Radiochemistry of the Hungarian Academy of Sciences, Budapest, 2008) p. 91-91
8. Hou, X., Critical comparison of radiometric and mass spectrometric methods for the determination of radionuclides. In: Program. Abstract book. 2. International nuclear chemistry congress, Cancun (MX), 13-18 Apr 2008. Navarrete, M. (ed.), (National University of Mexico, Cancun, 2008) p. 63-63
9. Hou, X.; Aldahan, A.; Nielsen, S.P.; Possnert, G.; Nies, H., Speciation of  $^{129}\text{I}$  and  $^{127}\text{I}$  in seawater. In: Proceedings. Oral and oral poster presentations. Part 2. International conference on radiowcology and environmental radioactivity, Bergen (NO), 15-20 Jun 2008. Strand, P.; Brown, J.; Jølle, T. (eds.), (Norwegian Radiation Protection Authority, Østerås, 2008) p. 82-87.

# Speciation of $^{129}\text{I}$ and $^{127}\text{I}$ in Seawater and Implications for Sources and Transport Pathways in the North Sea

XIAOLIN HOU,<sup>\*,†</sup> ALA ALDAHAN,<sup>‡</sup> SVEN P. NIELSEN,<sup>†</sup> GÖRAN POSSNERT,<sup>§</sup> HARTMUT NIES,<sup>||</sup> AND JIM HEDFORS<sup>‡</sup>

*Risø National Laboratory, NUK-202, Technical University of Denmark, DK-4000 Roskilde, Denmark, Department of Earth Sciences, Uppsala University, SE-752 36 Uppsala, Sweden, Tandem Laboratory, Uppsala University, SE-751 21 Uppsala, Sweden, and Bundesamt fuer Seeschifffahrt und Hydrographie, D-22589 Hamburg, Germany*

Surface seawater samples collected from the North Sea and English Channel were analyzed for total  $^{129}\text{I}$  and  $^{127}\text{I}$ , as well as for iodide and iodate. Relatively high  $^{129}\text{I}$  concentrations ( $2\text{--}3 \times 10^{11}$  atoms/L) were observed in the northern part of the English Channel and in the southeastern North Sea. The atomic ratio of  $^{129}\text{I}/^{127}\text{I}$  decreases from the eastern ( $1.0\text{--}1.9 \times 10^{-6}$ ) to the western ( $4\text{--}6 \times 10^{-8}$ ) parts of the North Sea and from the northeastern ( $1.5 \times 10^{-6}$ ) to southwestern ( $1\text{--}5 \times 10^{-8}$ ) parts of the English Channel. The ratios of iodide to iodate are 0.1–0.5 and 0.5–1.6 for  $^{127}\text{I}$  and  $^{129}\text{I}$ , respectively, in open seawaters, whereas these ratios range from 0.6 to 1.3 and 0.8 to 2.2, respectively, in coastal waters. The results suggest that (1) imprints of the La Hague facility dominates the  $^{129}\text{I}$  distribution in the surface water of the North Sea, (2) reduction of iodate to iodide is relatively fast during the transport to the European continental coast, (3) oxidation of newly produced  $^{129}\text{I}^-$  to  $^{129}\text{IO}_3^-$  is insignificant during water exchange between the coastal area and open sea, (4) reduction of iodate and oxidation of iodide in the open sea seems to be a slow process.

## Introduction

Iodine exists in the ocean surface waters predominantly as dissolved iodate, iodide, and a minute amount of organic iodine (*I*). Iodide is a thermodynamically unfavorable species in oxygenated water, so its formation through the reduction of iodate cannot occur spontaneously by chemical means alone. Although iodate is a thermodynamically favorable species of iodine in seawater, the kinetic barrier prevents the direct oxidation of iodide to iodate (*I*). Numerous studies have been carried out to investigate the origin of iodide, the conversion of iodine between different species, and the marine geochemical cycle of iodine by determination of the concentrations of various species of iodine in seawater in

certain areas (1–4). However, the mechanism of conversion among iodine species is still not clear because of the difficulties associated with distinguishing the origin of newly produced and converted iodine species.

Isotopic tracers are an excellent tool for the distinction and detection of the source of chemical species. Laboratory research on the conversion of different chemical species of iodine using short-lived isotopes of iodine has been carried out (5–6), but the results are only qualitative because of inadequate simulation of the real seawater environment and consideration of complex interactions among a variety of minor and trace components in seawater.  $^{129}\text{I}$  ( $T_{1/2} \approx 15.7$  Ma) is a naturally produced long-lived radioisotope of iodine, which has a natural atomic ratio ( $^{129}\text{I}/^{127}\text{I}$ ) of about  $10^{-12}$  in the ocean (7). Releases from human nuclear activities dominate the present  $^{129}\text{I}$  level in the environment (8–11), where the nuclear reprocessing facilities at Sellafield (U.K.) and La Hague (France) are responsible for about 90% of the anthropogenic releases (9, 10, 12). These sources and their rapid increase since 1990 (Figure S-1) provide a unique temporal and spatial field tracer for the investigation of the iodine marine geochemical cycle by chemical speciation of  $^{129}\text{I}$  combined with that of stable iodine.

The occurrence of a relatively huge anthropogenic  $^{129}\text{I}$  input in marine waters has been used to trace ocean currents and water transport in the North Atlantic and Arctic Oceans and related seas (9–10, 13–17). However, none of these studies have used the chemical speciation of iodine to further quantify effects on the mixing of water masses and fingerprinting of transport mechanisms. Schwehr et al. (18) showed a potential application of  $^{129}\text{I}$  and  $^{127}\text{I}$  speciation in the estuarine surface waters of Galveston Bay for tracing terrestrial organic carbon.

A main objective of this study was to investigate the source of iodide in the coastal water and interconversion process of iodide and iodate by chemical speciation of  $^{129}\text{I}$  and  $^{127}\text{I}$  in surface seawater collected from the English Channel and the North Sea. A second objective of this study was to investigate the distribution and transport pathways of different species of  $^{129}\text{I}$  and  $^{127}\text{I}$  in the North Sea surface waters. Such knowledge will provide significant information about the use of  $^{129}\text{I}$  as an environmental tracer.

## Experimental Section

Surface water was collected from 42 sites in the English Channel and the North Sea in August–September 2005 (Table S-1 and Figure 1). The samples were filtered through a  $\Phi$  0.45  $\mu\text{m}$  membrane (Sartorius AG, Göttingen, Germany) on site and then tightened and stored in clean polyethylene containers under normal laboratory conditions until analysis.

A modified method of Hou et al. (19–20) was used for the separation of iodine species. Wet AG1- $\times$ 4 resin (Bio-Rad laboratories) in  $\text{NO}_3^-$  form was packed in column of  $\phi$  10  $\times$  200 mm. A 50–100 mL of seawater spiked with 50 Bq of  $^{125}\text{I}^-$  and  $^{125}\text{IO}_3^-$  tracers was loaded onto the column, and the column was washed with 30 mL of deionized water and then 50 mL of 0.2 M  $\text{KNO}_3$ . The effluent and the washes were combined for the determination of iodate. Iodide on the column was eluted by 150 mL of 2.0 M  $\text{KNO}_3$ . One milliliter of separated iodide, iodate solution, or original seawater was diluted to 20 mL with 0.15 M  $\text{NH}_4\text{OH}$ , and  $\text{Cs}^+$  as ( $\text{CsCl}$ ) was added as an internal standard. The concentration of iodine ( $^{127}\text{I}$ ) was determined using an X Series<sup>II</sup> ICP-MS (Thermal Electron Corporation). The detection limit, calculated as 3SD of blanks, was 0.27 nM.

\* Corresponding author fax: +45 4677 5347; e-mail: xiaolin.hou@risoe.dk.

<sup>†</sup> Risø National Laboratory, NUK-202, Technical University of Denmark.

<sup>‡</sup> Department of Earth Sciences, Uppsala University.

<sup>§</sup> Tandem Laboratory, Uppsala University.

<sup>||</sup> Bundesamt fuer Seeschifffahrt und Hydrographie.

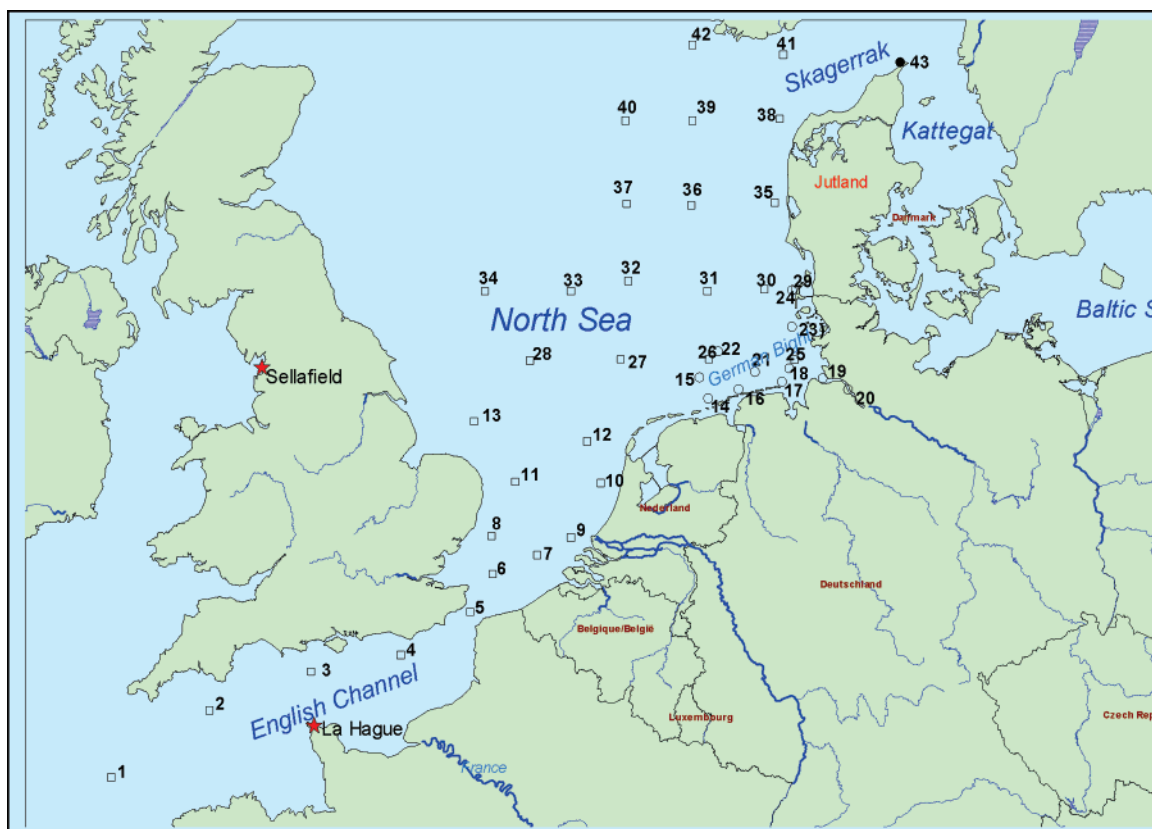


**FIGURE 1.** Sampling locations of surface water from the North Sea (□) and German Bight (○) in August 2005 and Danish coast in November 1999 (●).

About 50 Bq of a  $^{125}\text{I}^-$  solution was added to 20 mL of original seawater as chemical yield tracer. About 2.0 mg of stable iodine (as NaI prepared from Woodward iodine) was added as a carrier. To convert all iodine to iodide, 0.2 mL of 2.0 M  $\text{NaHSO}_3$  and 3 mL of 3.0M  $\text{HNO}_3$  were added to the solution. Iodine was first extracted with  $\text{CCl}_4$  after oxidation using  $\text{NaNO}_2$ , and then back-extracted with  $\text{NaHSO}_3$  solution.  $^{125}\text{I}$  in the separated solution was measured using an NaI  $\gamma$ -detector, and the chemical yield of iodide, iodate, and total iodine was 80–85, 90–95, and 94–98%, respectively. Iodine in the separated solution (as iodide) was precipitated as AgI. The dried AgI precipitate was mixed with niobium powder, pressed into a copper holder, and analyzed for  $^{129}\text{I}$  using a Pelletron (NEC machine) and the AMS system at the Tandem Laboratory, Uppsala University. A diluted  $^{129}\text{I}$  standard NIST-SRM 4949C with an  $^{129}\text{I}/^{127}\text{I}$  ratio of  $1.1 \times 10^{-11}$  was used. Blank samples were prepared using the same procedure as for samples for total iodine, iodide, and iodate. The measured  $^{129}\text{I}/^{127}\text{I}$  ratio in blanks ( $1.5 \pm 0.5 \times 10^{-13}$ ), which was subtracted from the measured value in the samples, was 30–1000 times lower than that in the samples ( $0.5\text{--}15 \times 10^{-11}$ ). The statistical error of the measurements at 1 standard deviation was <10%. An analytical scheme is given in Figure S-2. All chemical reagents used were of analytical grade, and all solutions were prepared using deionized water. The analytical accuracy and stability of the iodine chemical species during storage are discussed in the Supporting Information.

## Results

**Distribution of Total  $^{127}\text{I}$  and  $^{129}\text{I}$ .** The concentrations of  $^{129}\text{I}$  and  $^{127}\text{I}$  and the ratios of  $^{129}\text{I}/^{127}\text{I}$  in seawater are shown in Table 1 and Figure 2. The distribution of  $^{127}\text{I}$  concentration in the studied region seems to strongly follow the salinity values with even better resolution for the incursion of fresh

water (Figures 3, S-3, and S-4). The concentration of  $^{129}\text{I}$  in the investigated area shows up to 150 times difference between the low and high values. The highest  $^{129}\text{I}$  level occurred in the northeastern English Channel and along the European continental coast in the southern North Sea with values reaching  $20\text{--}38 \times 10^{10}$  atoms/L or  $1.0\text{--}1.6 \times 10^{-6}$  atom/atom for  $^{129}\text{I}$  and  $^{129}\text{I}/^{127}\text{I}$ . As one moves away from the Cap de La Hague across the English Channel toward the southwest, the  $^{129}\text{I}$  concentration decreases dramatically from about  $38 \times 10^{10}$  atoms/L (or  $1.6 \times 10^{-6}$  atoms/atom for  $^{129}\text{I}/^{127}\text{I}$ ) near the La Hague reprocessing plants to  $0.26 \times 10^{10}$  atoms/L (or  $1.05 \times 10^{-8}$  atom/atom for  $^{129}\text{I}/^{127}\text{I}$ ). This pattern agrees well with distribution of other radionuclides discharged from the La Hague reprocessing plant (16, 21–23).

Within the North Sea, the  $^{129}\text{I}$  concentration decreases from  $20\text{--}30 \times 10^{10}$  atoms/L in the east side along the European continental coast to about  $1.3 \times 10^{10}$  atoms/L in the central part and west side. Relatively higher  $^{129}\text{I}$  concentrations ( $15\text{--}20 \times 10^{10}$  atoms/L) occur in the west side of the southern North Sea close to the English coast. A slightly low  $^{129}\text{I}$  concentration ( $15 \times 10^{10}$  atoms/L) is found in seawater from location 19 compared to the surrounding locations ( $20\text{--}25 \times 10^{10}$  atoms/L). The  $^{129}\text{I}$  concentration decreases significantly in samples from the northern North Sea and Skagerrak (locations 38, 41, and 42) to be  $5\text{--}7 \times 10^{10}$  atoms/L with a  $^{129}\text{I}/^{127}\text{I}$  of  $2\text{--}4 \times 10^{-7}$ . An especially low  $^{129}\text{I}$  concentration is observed (location 20 to be only  $0.52 \times 10^{10}$  atoms/L with a  $^{129}\text{I}/^{127}\text{I}$  atom ratio of  $9.4 \times 10^{-8}$ ) in samples from the Elbe River.

**Distribution of Chemical Species of  $^{129}\text{I}$  and  $^{127}\text{I}$ .** Data on  $^{129}\text{I}$  and  $^{127}\text{I}$  in iodide ( $\text{I}^-$ ) and iodate ( $\text{IO}_3^-$ ) forms in the investigated seawater samples are listed in Table 1. Figures 2 and S-4 show the distribution of iodide and iodate, as well as iodide/iodate ratios for  $^{129}\text{I}$  and  $^{127}\text{I}$ . In general, the ratios of iodide to iodate for  $^{129}\text{I}$  are higher than those for  $^{127}\text{I}$  and

**TABLE 1. Analytical Result of  $^{127}\text{I}$  and  $^{129}\text{I}$  in Surface Seawater from the English Channel and North Sea for Total Iodine, Iodide, and Iodate<sup>a</sup>**

sample	$^{127}\text{I}$ ( $\mu\text{M}$ )			$^{129}\text{I}$ ( $\times 10^{10}$ atoms/L)			$^{129}\text{I}/^{127}\text{I}$ ( $\times 10^{-8}$ atom/atom)		
	total I	iodide	iodate	total I	iodide	iodate	total I	iodate	iodide
1	0.416	0.047	0.340	0.26	0.12	0.14	1.05	4.27	0.69
2	0.426	0.076	0.350	1.11	0.38	0.74	4.33	8.25	3.52
3	0.440	0.083	0.356	14.24	5.32	9.05	53.80	106.05	42.20
4	0.401	0.039	0.362	38.17	17.51	22.69	158.27	744.13	104.26
5	0.380	0.084	0.296	26.01	11.29	16.00	113.79	223.48	89.86
6	0.372	0.070	0.324	30.86	11.10	19.77	137.85	262.21	101.34
7	0.385	0.086	0.297	36.03	21.99	14.04	155.47	424.15	78.64
8	0.426	0.092	0.310	15.82	7.22	8.60	61.65	129.74	46.13
9	0.231	0.122	0.115	24.15	13.10	11.04	173.84	178.07	159.29
10	0.310	0.116	0.172	28.17	15.24	12.93	150.99	217.47	124.94
11	0.399	0.063	0.323	19.66	6.77	12.90	81.81	178.21	66.24
12	0.394	0.076	0.297	18.02	6.35	11.67	76.05	139.20	65.35
13	0.438	0.109	0.305	1.34	0.81	0.61	5.07	12.28	3.35
14	0.288	0.072	0.197	22.20	11.98	10.22	127.95	275.87	86.14
15	0.400	0.142	0.242	24.15	11.98	12.17	100.26	140.13	83.39
16	0.335	0.169	0.166	24.08	14.71	8.31	119.31	144.75	82.95
17	0.307	0.169	0.138	19.91	13.89	6.25	107.66	136.73	75.00
18	0.252	0.158	0.128	23.24	13.19	10.06	153.39	139.01	130.13
19	0.185	0.148	0.040	15.42	12.04	3.38	138.67	135.05	142.09
20	0.091	0.082	0.001	0.52	0.51	0.01	9.43	10.32	10.00
21	0.367	0.177	0.200	25.07	15.15	9.91	113.39	141.89	82.52
22	0.346	0.066	0.267	20.73	9.46	11.28	99.66	236.85	70.03
23	0.319	0.172	0.142	25.41	16.00	9.40	132.21	154.48	109.92
24	0.344	0.167	0.151	29.68	18.14	11.54	143.43	180.21	126.72
25	0.290	0.156	0.113	23.59	16.26	7.32	135.29	172.90	107.53
26	0.317	0.097	0.201	19.92	11.34	8.57	104.39	194.56	70.80
27	0.417	0.127	0.264	2.35	1.28	1.07	9.34	19.22	5.51
28	0.425	0.099	0.295	1.27	0.65	0.62	4.95	15.62	1.90
29	0.255	0.126	0.121	23.14	14.78	8.00	150.63	194.55	109.50
30	0.324	0.114	0.188	27.44	12.61	14.05	140.69	183.76	124.01
31	0.401	0.114	0.252	6.78	3.36	3.11	28.08	49.07	20.50
32	0.426	0.093	0.307	1.73	0.79	0.84	6.73	14.15	4.53
33	0.414	0.080	0.315	1.09	0.55	0.54	4.35	11.51	2.85
34	0.413	0.055	0.333	1.31	0.64	0.64	5.29	19.38	3.19
35	0.337	0.105	0.210	22.28	9.83	11.17	109.70	154.94	88.23
36	0.407	0.115	0.259	14.90	7.50	7.39	60.76	108.37	47.41
37	0.424	0.097	0.297	3.47	1.75	1.72	13.59	29.94	9.61
38	0.380	0.078	0.266	4.68	2.47	2.20	20.44	52.58	13.75
39	0.388	0.063	0.290	3.50	2.17	1.33	14.98	57.67	7.58
40	0.422	0.086	0.313	1.94	1.20	0.74	7.62	23.05	3.93
41	0.285	0.062	0.241	5.50	3.17	2.34	32.04	36.60	28.52
42	0.311	0.091	0.243	6.72	3.84	2.89	35.89	70.27	19.76
43-1	0.283	0.150	0.133	21.44	11.67	9.85	122.80	129.20	116.54
43-2	0.303	0.165	0.143	22.80	11.98	10.87	126.25	124.38	128.97

<sup>a</sup> Sample 43-1 was analyzed in August 2006, and sample 43-2 was analyzed in September 2000. The values in *italic* are calculated by the difference between total iodine and iodide. The analytical uncertainties are 3–7% for  $^{127}\text{I}$  and 4–10% for  $^{129}\text{I}$ .

a marked difference can be observed between open sea and coastal area (Figure 2e and f). Except along the Dutch coastal area and the German Bight where  $^{127}\text{I}^-/^{127}\text{IO}_3^-$  values reach 3.75, the ratio of these species does not exceed 0.48 in the North Sea and the English Channel (Figure 2 and Table S-2).

The lowest  $^{129}\text{I}^-/^{129}\text{IO}_3^-$  value (0.5–0.77) was observed in waters from the English Channel, which continues further northeastward along the British coast and part of the offshore southern North Sea (Figure 2). A significant increase of  $^{129}\text{I}^-/^{129}\text{IO}_3^-$  values (1.0–1.6) occurs in the Dutch coastal seawater (sampling locations 7, 9, and 10) compared to the range (0.5–0.6) in the relatively  $^{129}\text{I}$ -poor (Figure 2, Table S-2) offshore waters (sampling locations 11 and 12). The later waters have  $^{129}\text{I}^-/^{129}\text{IO}_3^-$  values rather similar to those in the English Channel and southern North Sea (sampling locations 1–6 and 8). An interesting observation found in this investigation is the similarity of  $^{129}\text{I}^-/^{129}\text{IO}_3^-$  values (0.9–1.6) between the offshore waters (locations 22, 26, 31, 36, and 38) and the coastal waters in the northern North Sea (Figure 2 and Table S-2). In the central North Sea (locations 27, 28, 32, 33, 34, 37, 39, and 40), the  $^{129}\text{I}^-/^{129}\text{IO}_3^-$  values (0.9–1.6) show a range

comparable to that observed in the offshore water. A higher  $^{129}\text{I}^-/^{129}\text{IO}_3^-$  (3.6), compared to that in other coastal waters (0.9–2.2), was observed in samples from the estuary of Elbe River at location 19. The highest  $^{129}\text{I}^-/^{129}\text{IO}_3^-$  (70) occurred in the water from Elbe River (location 20), which also indicates a similarly high value (68) for the  $^{127}\text{I}^-/^{127}\text{IO}_3^-$ .

## Discussion

**Sources of  $^{129}\text{I}$  in the North Sea.** The  $^{129}\text{I}$  concentration in the English Channel and North Sea is 2–4 orders of magnitude higher than the environmental level of the post-nuclear era ( $10^{-10}$  for  $^{129}\text{I}/^{127}\text{I}$  ratio). The distribution of  $^{129}\text{I}$  (Figure 2a and b) indicates that the marine discharges of the La Hague nuclear reprocessing facility are the main source to the surface water of the North Sea and English Channel. Discharges of  $^{129}\text{I}$  from the Sellafield nuclear reprocessing facility may also contribute to the measured values in the North Sea, particularly the eastern and northern parts. Several investigations (14, 16, 21, 23–25) have shown that the plume of marine discharges from Sellafield into the Irish Sea moves northward along the British coast and converges into the



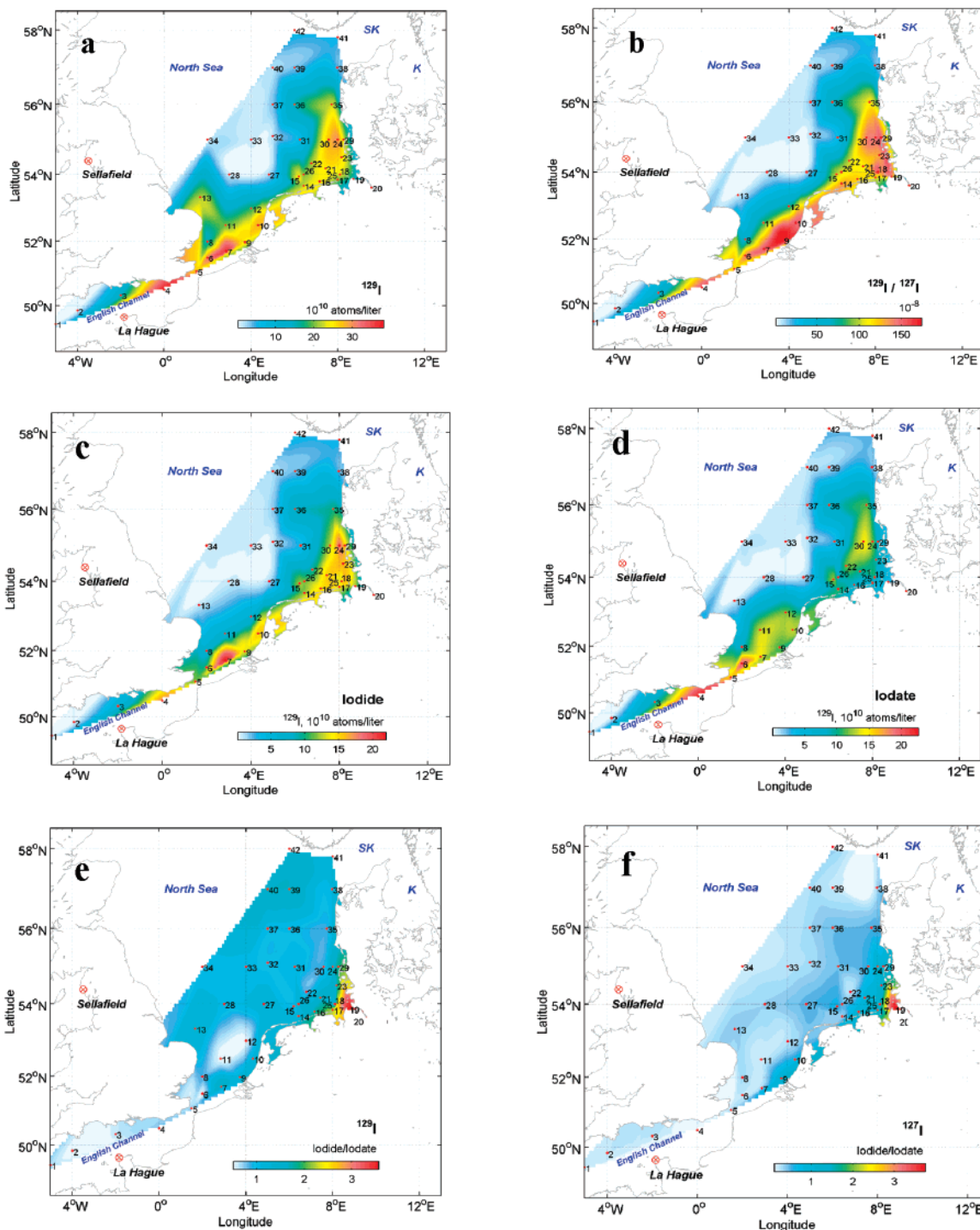


**FIGURE 2.** Distribution of total  $^{129}\text{I}$  (a),  $^{129}\text{I}/^{127}\text{I}$  atomic ratios (b),  $^{129}\text{I}^-$  (c),  $^{129}\text{IO}_3^-$  (d),  $^{129}\text{I}^-/^{129}\text{IO}_3^-$  (e), and  $^{127}\text{I}^-/^{127}\text{IO}_3^-$  molecular ratio (f) in the English Channel and the North Sea.

North Sea. Within the North Sea, the plume moves southward along the British east coast and further into the southern North Sea and then northward again along the European continental coast or moves across the North Sea from the west to east. Thus, it is expected that the  $^{129}\text{I}$  pool in the northern and western North Sea can receive contribution from the Sellafield discharges. Schnabel et al. (25) reported  $^{129}\text{I}/^{127}\text{I}$  values as high as  $3.4 \times 10^{-6}$  atom/atom in the Irish Sea and  $7 \times 10^{-8}$  on the British east coast in 2005. Their values on the British east coast are comparable with the values measured in this work ( $5.0\text{--}5.2 \times 10^{-8}$ ). However, the value is more than 20 times lower than that in the Northeastern English Channel and European continental coastal area. This

information indicates that the contribution of the Sellafield marine discharges to the total  $^{129}\text{I}$  inventory in the surface water of the North Sea is insignificant when compared with the contribution from the La Hague marine discharges.

The low salt content (0.45 g/L) and low stable iodine concentration ( $0.091 \mu\text{M}$ ) in sample from location 20 indicate insignificant incursion of the North Sea water into the Elbe River. Szidat et al. (26) reported an  $^{129}\text{I}$  concentration of  $0.4 \times 10^{10}$  atoms/L (with a ratio of  $^{129}\text{I}/^{127}\text{I} = 3.75 \times 10^{-8}$ ) in rainwater from northern Germany in 1997–1998, which is comparable with our value observed in the Elbe river. Apparently, the  $^{129}\text{I}$  in the Elbe River water strongly reflects precipitation input, while the contribution by inflow of the

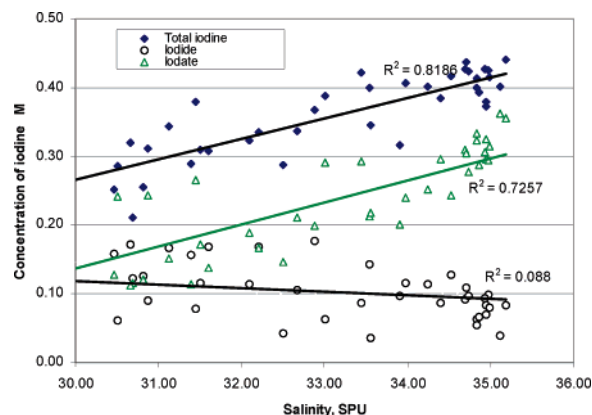


**FIGURE 3. Scatter plot of concentrations of iodide, iodate, and total iodine in seawater versus salinity**

North Sea water is limited. The slightly low  $^{129}\text{I}$  concentration in the seawater from location 19 might be attributed to dilution by the Elbe River, which is also confirmed by the relative lower salinity (20.9 S, Figure S-3) and total  $^{127}\text{I}$  concentration ( $0.185\ \mu\text{M}$ ), but a similar  $^{129}\text{I}/^{127}\text{I}$  ratio ( $1.39 \times 10^{-6}$ ) to the surrounding coastal water at this region.

The significant decrease in  $^{129}\text{I}$  concentration of samples from the northern North Sea and Skagerrak likely reflects dilution by relatively  $^{129}\text{I}$  poor source water from the North Atlantic and the Baltic Sea. Such waters contain orders of magnitude less  $^{129}\text{I}$  compared to the North Sea  $^{129}\text{I}$ -rich plume (13–14, Figure 2a and b). Alfimov et al. (14) reported  $^{129}\text{I}$  concentration similar to ours for samples collected in the same area.

**Transport Pathways of  $^{129}\text{I}$ .** The distribution pattern of  $^{129}\text{I}$  in the English Channel (Figure 2a and b) indicates a major transport direction from the English Channel northeastward to the North Sea. The dramatically decreased  $^{129}\text{I}$  level away from Cap de La Hague across the English Channel southwestward, but still higher  $^{129}\text{I}$  level in the southwest English Channel than the level in the Atlantic water ( $10^{-10}$  for  $^{129}\text{I}/^{127}\text{I}$  ratio), suggests very limited, but detectable, transport of  $^{129}\text{I}$  southwestward in the English Channel.

Within the North Sea, the pattern of  $^{129}\text{I}$  distribution indicates a northward transport mainly along the European continental coast, which is associated with apparently limited transport in the east–west direction.  $^{129}\text{I}$  transport in the southern North Sea is partly northward, also along the British coast, but for only a short distance. This pattern strongly coincides with the major surface water current from the English Channel northward along the European continental coast and into the North Sea (Figure S-5 shows two occasional circulations of surface water in the North Sea, which follow major transport pathways).

**$^{127}\text{I}$  and  $^{129}\text{I}$  Speciation.** Except along the Dutch coastal area and the German Bight,  $^{127}\text{I}$  mainly exists as iodate with a ratio of iodide to iodate of 0.11–0.48, especially in the open sea area, where this ratio is lower than 0.30. (Figure 2 and, Table S-2). A range of  $^{127}\text{I}^-/^{127}\text{IO}_3^-$  values similar to ours were reported by Truesdale and Upstill-Goddard (4) for seawater collected from the English Channel (with a ratio of 0.15) and offshore of the British east coast (with a ratio of 0.33) in 1999. A high iodide level with an  $^{127}\text{I}^-/^{127}\text{IO}_3^-$  range of 0.9–3.8 was observed in the seawater from the Dutch coast and German Bight (Figure 2 and Table S-2). Truesdale et al. (27) have reported high  $^{127}\text{I}^-/^{127}\text{IO}_3^-$  values for surface (0.6–1.0) water in a transect in the Skagerrak basin. In this work, one sample (location 43) collected from the Skagerrak shows a ratio of 1.15, which apparently agrees with the data of Truesdale et al. (27). Hou et al. (20) have also shown  $^{127}\text{I}^-/^{127}\text{IO}_3^-$  values of 1.75–1.92 in surface water from the Kattegat basin.

The  $^{129}\text{I}^-/^{129}\text{IO}_3^-$  values in all seawater investigated here are normally higher than the  $^{127}\text{I}^-/^{127}\text{IO}_3^-$  values, especially for the water from the English Channel. This behavior is mainly attributed to the different source of  $^{127}\text{I}$  and  $^{129}\text{I}$ . Because the source of  $^{129}\text{I}$  is anthropogenic, information on chemical speciation of  $^{129}\text{I}$  in the discharged liquid waste from the La Hague facility plays a main role. Presently, we have no data about this issue. We have not analyzed seawater from or in the vicinity of the discharge outlet tube from La Hague facility. The insignificant change in the  $^{129}\text{I}^-/^{129}\text{IO}_3^-$  values (0.51–0.77) in the English Channel and offshore the southern North Sea (Table S-2, Figure 2), however, implies that imprints of original  $^{129}\text{I}$  species in the discharged liquid waste from the La Hague facility are strongly reflected in these waters, and the value may represent the speciation of  $^{129}\text{I}$  in the source water. The  $^{127}\text{I}^-/^{127}\text{IO}_3^-$  ratios in the source water (the English Channel) are, on the other hand, low (0.1–0.2). Although the magnitude of iodide to iodate ratios are different for  $^{127}\text{I}$  and  $^{129}\text{I}$ , the  $^{127}\text{I}^-/^{127}\text{IO}_3^-$  ratio is correlated with  $^{129}\text{I}^-/^{129}\text{IO}_3^-$  ( $R^2 = 0.5$ , Figure S-7) in all seawater samples investigated here.

Similar to  $^{127}\text{I}$ , a significant increase of  $^{129}\text{I}^-/^{129}\text{IO}_3^-$  values was observed in the water from the Dutch coast and German Bight. However, the  $^{129}\text{I}^-/^{129}\text{IO}_3^-$  values (0.9–1.6) in the offshore waters and central North Sea are similar to that of the coastal waters in northern North Sea. The  $^{127}\text{I}^-/^{127}\text{IO}_3^-$  values in these waters are much lower than those in the coastal waters and even similar to those from the English Channel and southern North Sea. We relate this feature to preferential increase in  $^{129}\text{I}^-$  because of iodate reduction in coastal areas and subsequent penetration of such water into the offshore northern North Sea region, which is otherwise characterized by relatively low  $^{127}\text{I}^-/^{127}\text{IO}_3^-$  and total  $^{129}\text{I}$  concentration.

**Sources of Iodine in the North Sea.** As mentioned above, the distribution of  $^{129}\text{I}$  in the North Sea, especially coastal water along the European continental coast, suggests a main transport pathway via the English Channel. The relatively higher iodide level in the Dutch coast and German Bight compared to that in the English Channel indicates that the iodide in this area is produced locally. A significantly positive correlation between salinity and the total iodine ( $R^2 = 0.82$ ) and iodate ( $R^2 = 0.73$ ) concentrations in the investigated waters was obtained (Figure 3). These results suggest that dilution of the high salinity (>35S) and iodate-rich Atlantic Ocean water by fresh water input from European continent has contributed to the relatively low iodate and total iodine, as well as to the salinity in the North Sea, particularly along coastal areas. An insignificant correlation between iodide concentration and salinity was observed (Figure 3), which confirms that the iodide in the coastal waters was produced locally by a likely reduction of iodate.

Relatively high  $^{129}\text{I}^-/^{127}\text{I}^-$  values compared to the  $^{129}\text{IO}_3^-/^{127}\text{IO}_3^-$  values were found in all the investigated samples (Table 1, Figure S-4). The differences between the  $^{129}\text{I}^-/^{127}\text{I}^-$  and  $^{129}\text{IO}_3^-/^{127}\text{IO}_3^-$  values are significantly larger in the English Channel than those in the North Sea, especially in the coastal waters. This observation also suggests that part of the  $^{129}\text{IO}_3^-$  in the source water from the English Channel was reduced in the North Sea, particularly in the coastal areas.

**Conversion of Iodine Species in the North Sea Water.** Some processes, such as biological activity involving bacteria and enzyme and photochemical and chemical interactions, have been suggested to control the conversion of iodine species. However, it is still unclear which process or which type of organism controls the reduction of iodate in surface seawater and how fast the conversion process proceeds (1–4). Insignificant changes of  $^{127}\text{I}$  and  $^{129}\text{I}$  speciation in water from the English Channel to the southern North Sea were found here. The transit times of the water from La Hague to



Borkumriff on the Dutch coast and to the German Bight were estimated to be 11 and 14 months, respectively (24). It can be assumed that the water transited to the southern North Sea during 6–8 months, thus implying a rather sluggish change of  $^{129}\text{I}$  speciation from La Hague in the English Channel to the southern North Sea. The observation suggests that reduction of iodate and oxidation of iodide in open sea surface water is a relatively slow process. However,  $^{129}\text{IO}_3^-$  is rapidly reduced to  $^{129}\text{I}^-$  when it reaches the Dutch coast. This significant and rapid increase of  $^{129}\text{I}^-/^{129}\text{IO}_3^-$  values in the Dutch coastal seawater indicates that the reduction of iodate to iodide is a fast process in the coastal area. A relatively low oxidation–reduction potential ( $\text{ORP} = 60\text{--}90\text{ meV}$ ) observed in the Dutch coastal water (locations 7, 9, and 10) imply that chemical process is an important factor, in addition to biological activity, that participates in the reduction of  $^{129}\text{I}$ .

The significantly high iodide to iodate ratios for both  $^{129}\text{I}$  and  $^{127}\text{I}$  found in the water from German Bight (Figure 2 and Table S-2) might be attributed to local reduction of iodate in the area or that a transport of reduced  $^{129}\text{I}$  occurred in the Dutch coast. Absence of published reports on the chemical speciation of iodine in water from the European continental coast of the North Sea or the German Bight hinders temporal comparison. Therefore, it is difficult to establish whether anoxic conditions were recently developed or have existed for long time in these regions. However, Truesdale and Upstill-Goddard (4) have foreseen an exceptionally low iodate concentration in the Dutch and German coastal waters and in the Jutland coast current based on a modeling approach. The existence of anoxic conditions in the sediment of the German Bight (27–28) associated with shallow depths (14–29 m) may cause reduction of iodate in the area. In addition, the effect of exceptionally high anoxic conditions is illustrated by a iodide to iodate ratio of 68–70 in sample 20 collected in the Elbe River, which also shows a low oxidation–reduction potential ( $\text{ORP} = 22\text{ mV}$ ; Table S-1 and Figure S-3), indicating reductive water. Such reductive waters can be also the cause of the low  $\text{ORP}$  (52–56 mV) observed in the estuary of the Elbe River (locations 19 and 25) and contribute to the anoxic condition in the German Bight. A much higher  $^{129}\text{I}^-/^{129}\text{IO}_3^-$  and  $^{127}\text{I}^-/^{127}\text{IO}_3^-$  values observed in the water from the estuary of Elbe River suggests a rapid reduction of iodate in the Elbe River estuary, which could be mainly a locally controlled chemical process. Accordingly, some of the iodide was produced locally in the German Bight. However, local chemical process cannot fully explain the high iodide to iodate ratios in most surface water along the European continental coast of the North Sea. These waters have relatively high  $\text{ORP}$  (Table S-1 and Figure S-3) and oxygen concentration (29) and do not show significant correlation between  $\text{ORP}$  and the  $^{127}\text{I}^-/^{127}\text{IO}_3^-$  values (Figure S-6). Biological activity and the concentration of bacteria, which may affect the reduction of iodate, were not monitored, which make establishing a dominant mechanism for the reduction of iodate in the coast water difficult.

As one moves away from the German Bight to the west coast of Jutland, the iodide to iodate ratios become higher than those in the English Channel and similar to those along the Dutch coast, without significant change northwards along the European continental coast. Such a trend can be explained either by negligible reduction of iodate with time spent in the coastal area or by establishment of a dynamic equilibrium in the iodate–iodide redox pair in the coastal water of the northern North Sea.

The  $^{129}\text{I}$  concentrations in the central North Sea ( $1.1\text{--}3.5 \times 10^8\text{ atoms/L}$ ) are one order of magnitude lower than that in the coastal and offshore waters. As discussed above,  $^{129}\text{I}$  in the west and central North Sea may partly originate from the Sellafield marine discharges. However, the gradually east

to west decrease in  $^{129}\text{I}$  concentration and  $^{129}\text{I}/^{127}\text{I}$  value in the central North Sea surface water analyzed here suggests strong imprints of contribution from the La Hague facility. Regardless of the source, the much higher  $^{129}\text{I}^-/^{129}\text{IO}_3^-$  (0.9–2.7) compared to the  $^{127}\text{I}^-/^{127}\text{IO}_3^-$  (0.17–0.45) values in the central North Sea surface water indicate that iodide oxidation is a slow process in open waters of the North Sea. The similar high  $^{129}\text{I}^-/^{129}\text{IO}_3^-$  and low  $^{127}\text{I}^-/^{127}\text{IO}_3^-$  (0.17–0.45) behavior in the open water of the northern North Sea suggest insignificant oxidation of newly produced  $^{129}\text{I}^-$  during transport after production in the European continental coast. This pattern again confirms the slow oxidation of iodide in the open waters of the North Sea. These observations also support insignificant reduction of iodate during transit along the coastal areas and further oxidation of iodide to iodate in the coastal water, which might explain the insignificant correlation between  $\text{ORP}$  and the  $^{127}\text{I}^-/^{127}\text{IO}_3^-$  and  $^{129}\text{I}^-/^{129}\text{IO}_3^-$  observed in the North Sea water (Figure S-6).

The distribution of chemical species of  $^{129}\text{I}$  and  $^{127}\text{I}$  in the surface water investigated in this work shows that (1) a rapid reduction of iodate to iodide occurs in the coastal area, (2) the oxidation of the new produced iodide to iodate does not occur during its transit along the coast, and to the open sea, and (3) reduction of iodate or oxidation of iodide in the open sea seems to be a slow process. The difference between  $^{129}\text{I}$  and  $^{127}\text{I}$  species in seawater represents a potential tracer of iodide sources and conversion of iodine species in marine system, as well as in studying details of spatial and temporal evolution of ocean water. A future study of depth-related chemical speciation of  $^{129}\text{I}$  and  $^{127}\text{I}$  in the North Sea will shed more light on the conversion rates of iodine species, geochemical cycle of iodine in various reservoirs of marine system, and the magnitude and transport pathways of the Sellafield plume.

## Acknowledgments

The authors wish to thank the Villum Kann Rasmussen Foundation for financial support.

## Supporting Information Available

Discussions of analytical accuracy and stability of iodine species during storage, two tables, and seven figures as noted in the text. This material is available free of charge via the Internet at <http://pubs.acs.org>.

## Literature Cited

- Wong, G. T. F. The marine geochemistry of iodine. *Rev. Aquat. Sci.* **1991**, 4 (1), 45–73.
- Wong, G. T. F.; Cheng, X. H. The formation of iodide in inshore waters from the photochemical decomposition of dissolved organic iodine. *Mar. Chem.* **2001**, 74, 53–64.
- Truesdale, V. W.; Nausch, G.; Bale, A. J. The distribution of iodine in the Baltic Sea during summer. *Mar. Chem.* **2001**, 74, 87–98.
- Truesdale, V. W.; Upstill-Goddard, R. Dissolved iodate and total iodine along the British east coast. *Estuarine, Coastal Shelf Sci.* **2003**, 56, 261–270.
- Hirano, S.; Ishii, T.; Nakamura, R.; Matasuba, M.; Koyanagi, T. Chemical forms of radioactive iodine in seawater and its effects upon marine organisms. *Radioisotopes* **1983**, 32, 319–322.
- Amachi, S.; Kasahara, M.; Fujii, T.; Shinoyama, H.; Hanada, S.; Kamagata, Y.; Ban-nai, T.; Muramatsu, Y. Radiotracer experiments on biological volatilization of organic iodine from coastal seawaters. *Geomicrobiol. J.* **2004**, 21, 481–488.
- Fehn, U.; Snyder, G.; Egeberg, P. K. Dating of pore water with  $^{129}\text{I}$ : Relevance for the origin of marine gas hydrates. *Science* **2000**, 289, 2332–2335.
- Santschi, P. H.; Schwehr, K. A. I-129/I-127 as a new environmental tracer or geochronometer for biogeochemical or hydrodynamic processes in the hydrosphere and geosphere: the central role of organo-iodine. *Sci. Total Environ.* **2004**, 321, 257–271.

- (9) Hou, X. L.; Dahlgaard, H.; Nielsen, S. P. Iodine-129 time series in Danish, Norwegian and northwest Greenland coast and the Baltic Sea by seaweed. *Estuarine, Coastal Shelf Sci.* **2000**, *51*, 571–584.
- (10) Aldahan, A.; Alfimov, V.; Possnert, G.  $^{129}\text{I}$  anthropogenic budget: Major sources and sinks. *Appl. Geochem.* **2007**, *22* (3), 606–618.
- (11) Snyder, G.; Fehn, U. Global distribution of I-129 in rivers and lakes: implications for iodine cycling in surface reservoirs. *Nucl. Instrum. Methods* **2004**, *B223*, 579–586.
- (12) Reithmeier, H.; Lazarev, V.; Rühm, W.; Schwikowski, M.; Gäggeler, H.; Nolte, E. Estimate of European  $^{129}\text{I}$  releases supported by  $^{129}\text{I}$  analysis in an Alpine ice core. *Environ. Sci. Technol.* **2006**, *40*, 5891–5896.
- (13) Hou, X. L.; Dahlgaard, H.; Nielsen, S. P. Level and origin of iodine-129 in the Baltic Sea. *J. Environ. Radioact.* **2002**, *61*, 331–343.
- (14) Alfimov, V.; Aldahan, A.; Possnert, G.; Kekli, A.; Meili, M. Concentrations of  $^{129}\text{I}$  along a transect from the North Atlantic to the Baltic Sea. *Nucl. Instrum. Methods* **2004**, *B223–224*, 446–450.
- (15) Buraglio, N.; Aldahan, A. A.; Possnert, G. Distribution and inventory of  $^{129}\text{I}$  in the central Arctic Ocean. *Geophys. Res. Lett.* **1999**, *26* (8), 1011–1014.
- (16) Raisbeck, G. M.; Yiou, F.; Zhou, Z. Q.; Kilius, L. R.  $^{129}\text{I}$  from nuclear fuel reprocessing facilities at Sellafield (U.K.) and La Hague (France); potential as an oceanographic tracer. *J. Mar. Syst.* **1995**, *61*, 561–570.
- (17) Raisbeck, G. M.; Yiou, F.  $^{129}\text{I}$  in the ocean, origins and applications. *Sci. Total Environ.* **2000**, *237/238*, 31–41.
- (18) Schwehr, K. A.; Santschi, P. H.; Elmore, D. The dissolved organic iodine species of the isotopic ratio of I-129/I-127: A novel tool for tracing terrestrial organic carbon in the estuarine surface waters of Galveston Bay, Texas. *Limnol. Oceanogr.* **2005**, *3*, 326–337.
- (19) Hou, X. L.; Dahlgaard, H.; Rietz, B.; Jacobsen, U.; Nielsen, S. P.; Aarkrog, A. Determination of  $^{129}\text{I}$  in seawater and some environmental materials by neutron activation analysis. *Analyst* **1999**, *124*, 1109–1114.
- (20) Hou, X. L.; Dahlgaard, H.; Nielsen, S. P. Chemical speciation analysis of  $^{129}\text{I}$  in seawater and a preliminary investigation to use it as a tracer for geo-chemical cycle study of stable iodine. *Mar. Chem.* **2001**, *74*, 145–155.
- (21) Herrmann, J.; Kershaw, P. J.; Bailly du Bois, P.; Guegueniat, P. The distribution of artificial radionuclides in the English Channel, southern North Sea, Skagerrak and Kattegat, 1990–1993. *J. Mar. Syst.* **1995**, *6*, 427–456.
- (22) Nies, H.; Obrikat, D.; Herrmann, J. Recent radionuclide concentrations in the North Sea as a result of discharge from nuclear installations. *Kerntechnik* **2000**, *65*, 195–200.
- (23) Dahlgaard, H.; Aarkrog, A.; Hallstadius, L.; Holm, E.; Rioseco, J. Radiocaesium transport from the Irish Sea via the North Sea and the Norwegian Coastal Current to East Greenland. *Rapp. P.-V. Réun.-Cons. Int. Expl. Mer* **1986**, *186*, 70–79.
- (24) Dahlgaard, H.; Herrmann, J.; Salomn, J. C. A tracer study of the transport of coastal water from the English Channel through the German Bight to the Kattegat. *J. Mar. Syst.* **1995**, *6*, 415–425.
- (25) Schnabel, C.; Olive, V.; Atarashi-Andoh, M.; Dougans, A.; Ellam, R. M.; Freeman, S.; Maden, C.; Stocker, M.; Synal, H.-A.; Wacker, L.; Xu, S.  $^{129}\text{I}/^{127}\text{I}$  ratios in Scottish coastal surface sea water: geographical and temporal responses to changing emissions. *Appl. Geochem.* **2007**, *22* (3), 619–627.
- (26) Szidat, S.; Schmidt, A.; Handl, J.; Jakob, D.; Botsch, W.; Michel, R.; Synal, H. A.; Schnabel, C.; Suter, M.; Lopez-Gutierrez, J. M.; Städe, W. Iodine-129: Sample preparation, quality control and analyses of pre-nuclear materials and of natural waters from Lower Saxony Germany. *Nucl. Instrum. Methods* **2000**, *B172*, 699–710.
- (27) Truesdale, V. W.; Danielssen, D. S.; Waite, T. J. Summer and winter distributions of dissolved iodine in the Skagerrak. *Estuarine, Coastal Shelf Sci.* **2003**, *57*, 701–713.
- (28) Gerlach, S. A. Nitrogen, phosphorus, plankton and oxygen deficiency in the German Bight and in Kiel Bay. *Kiel. Meeresforsch. Sonderh.* **1990**, *7*, 1–341.
- (29) BSH, Sauerstoffgehalte in der Deutschen Bucht, September, 2005; [http://www.bsh.de/de/Meeresdaten/Beobachtungen/MURSYS-Umweltreportsystem/Mursys\\_031/seiten/noo25\\_01.jsp](http://www.bsh.de/de/Meeresdaten/Beobachtungen/MURSYS-Umweltreportsystem/Mursys_031/seiten/noo25_01.jsp).

Received for review March 7, 2007. Revised manuscript received June 26, 2007. Accepted June 27, 2007.

ES070575X

# Evaluation of the readsorption of plutonium and americium in dynamic fractionations of environmental solid samples

Roongrat Petersen<sup>a,\*</sup>, Xiaolin Hou<sup>b</sup>, Elo Harald Hansen<sup>a</sup>

<sup>a</sup> Department of Chemistry, Technical University of Denmark, Kemitorvet, Building 207, 2800 Kgs. Lyngby, Denmark

<sup>b</sup> Radiation Research Department, Risø National Laboratory for Sustainable Energy, NUK-202, Technical University of Denmark, DK-4000 Roskilde, Denmark

Received 9 May 2007; received in revised form 5 December 2007; accepted 30 January 2008

Available online 21 March 2008

## Abstract

A dynamic extraction system exploiting sequential injection (SI) for sequential extractions incorporating a specially designed extraction column is developed to fractionate radionuclides in environmental solid samples such as soils and sediments. The extraction column can contain up to 5 g of a soil sample, and under optimal operational conditions it does not give rise to creation of back pressure. Attention has been placed on studies of the readsorption problems during sequential extraction using a modified Standards, Measurements and Testing (SM&T) scheme with four-step sequential extractions. The degree of readsorption in dynamic and conventional batch extraction systems is compared and evaluated by using a double-spiking technique. A high degree of readsorption of plutonium and americium (>75%) was observed in both systems, and they also exhibited similar distribution patterns of the two radionuclides. However, the dynamic system is fully automated, eliminates manual separations, significantly reduces the operational time required, and offers detailed kinetic information.

© 2008 Elsevier Ltd. All rights reserved.

**Keywords:** Sequential extraction; Fractionation; Readsorption; Plutonium; Americium; Soil; Dynamic fractionation system

## 1. Introduction

Anthropogenic radionuclides have entered the environment from various sources including nuclear weapon testing, operation of nuclear power plants, production and reprocessing of nuclear fuel, nuclear accidents, and disposal of radioactive waste (Komosa, 2002). Sanderson et al. (1997) reported 150 accidents that have released radionuclides to the environment between 1945 and 1996. These accidents involve reactors and other nuclear facilities, satellites, nuclear weapons and large radiation sources. Plutonium (Pu) is one of the most important and most toxic radioactive elements. The concern of Pu contamination arises from the very long half-life of most of its isotopes, their accumulation in the human skeleton and their high radio- and bio-toxicities. Of major concern is that the deposited Pu in sediments might be re-dissolved and released to

the water (McDonald et al., 2001). Additionally,  $^{241}\text{Am}$  ( $T_{1/2} = 432.2$  years) is a decay product of  $^{241}\text{Pu}$  ( $T_{1/2} = 14.35$  years). The concentration of  $^{241}\text{Am}$  is increasing with the decay of  $^{241}\text{Pu}$  in the environment, and its maximum activity will occur in the middle of the 21st century as a consequence of its release to the environment in 1960–1970s. Due to its high specific activity and dose contribution, measurement and monitoring of its concentration are of high importance (Lloyd et al., 1997; Perma et al., 2003).

To evaluate the environmental impact of contaminated soils, knowledge of the total amount of radionuclides in soils without considering their speciation is not sufficient (Miró et al., 2005; Desideri et al., 2001). Because the radionuclides are present in many forms in soils, and since the fate of the radionuclides is controlled by the chemical forms in which they exist in the soils, it is important to have an understanding of the distribution of the radionuclides in each soil fraction. They may be contained in cation exchange sites, more tightly bound to adsorption sites, occluded into oxide, incorporated

\* Corresponding author. Tel.: +45 45252357; fax: +45 45883136.

E-mail address: [toey@kemi.dtu.dk](mailto:toey@kemi.dtu.dk) (R. Petersen).

into organic plant litter, included within soil micro-organisms and/or soil animals or integrated into the lattice structure of primary or secondary minerals. Radionuclides bound to the solid phase can be mobilised to the environment by changes in soil pH, temperature, redox potential, organic matter decomposition, leaching and ion exchange processes and by microbial activity (Kennedy et al., 1997).

Sequential extraction schemes to fractionate and determine metals and radionuclides in solid samples (soils, sediments, solid wastes, etc.) have been widely employed since the early 1970s (Tessier et al., 1979; Das et al., 1995; Kennedy et al., 1997). These operationally defined procedures are commonly performed by batch methods, being based on the successive use of a series of chemical reagents that sequentially extract various targeted phases in the sample due to their leachability. Radionuclides which are bound to, for example, carbonate minerals, oxides of Mn and Fe and organic matter phases will be released during the dissolution reactions. The results are useful for obtaining information about the origin, the mode of occurrence, the bioavailability, the potential mobility, and the transport of the elements in the natural environment. However, the techniques suffer from problems with the non-selectivity of the extractants used, the dependency of results on operating conditions, and readsorption (Lucey et al., 2007; Schultz et al., 1998a).

Readsorption happens when a targeted ion is released during an extraction and is readsorbed onto the remaining solid particles before the separation of the aqueous and the solid phases is effected. This phenomenon gives rise to unrepresentative results and leads to a significant underestimation within the dissolving phase and an overestimation in the receiving phase. Many authors have verified the readsorption problem and the inaccuracy deriving from it. Shan and Bin (1993) used model soils prepared by mixing a doped phase with other non-doped phases to evaluate the extent of the readsorption. They concluded that various proportions of metals released in the earlier fractionations are readsorbed onto other remaining phases. Kheboian and Bauer (1987) found that the recovery of spiked metals (Pb, Zn, Cu, and Ni) was less for model mixed-phase sediments than for single-phase materials. Gómez-Ariza et al. used the standard addition approach to assess the readsorption problem. They reported that readsorption occurs, and its extent depends on the characteristics of the sediment. Schultz et al. (1998a) used a double-spiking technique to examine readsorption of actinide elements (Am (Cm), Pu, and U). The results showed that actinide readsorption was very apparent in the first two fractions, the exchangeable and oxidizable ones, which were run at relatively high pH. Readsorption was less important under low pH conditions for the subsequent fractions. Lucey et al. (2007) used sodium citrate to inhibit the readsorption problems on a selected model phase and natural materials. It was found that in the absence of sodium citrate, very significant readsorption of Pu occurred during the extraction of the exchangeable fraction, which, in turn, redistributed among the remaining phases.

During the past decade, trends have been focused on the development of dynamic sequential extraction systems for

fractionation of heavy metals in soils and sediments in order to eliminate the drawbacks of the batch procedures, which are tedious, time consuming, labor intensive, subject to several potential errors, might cause sample contamination and imply high readsorption problems (Shiowatana et al., 2001a,b; Chomchoei et al., 2004, 2005a,b; Beauchemin et al., 2002; Fedotov et al., 2002; Jimoh et al., 2004). Since the naturally leaching processes occur under dynamic conditions, a dynamic extraction procedure should, therefore, mimic the environmental events more correctly than the batch system (Miró et al., 2005). The reduction of the readsorption problem during dynamic sequential extraction was investigated for the first time by Chomchoei et al. (2002) by exploiting a continuous-flow sequential extraction system, based on the Flow Injection Analysis (FIA) principle, furnished with an enclosed extraction chamber. However, the system had a problem of exhibiting decreasing flow rate with time due to gradual blockage of the membrane filter by fine particles.

A fully automated dynamic sequential extraction system with on-line detection has been developed in our group for fractionation of stable elements in soils and sediments by incorporation of a sample-packed microcolumn into the conduits of a sequential injection (SI) system (Chomchoei et al., 2004, 2005a,b). The system offers great advantages over the commonly used batch systems such as giving detailed kinetic data of the leaching processes, and providing a more realistic insight into the lability of metals from different soil fractions. Moreover, the system is fully automated, rapid, easy to operate, and less prone to risks of contamination and personal error. Especially, the system shows less problem of readsorption during extraction in comparison with the batch techniques, which should provide more accurate fractionation results (Petersen, 2005).

In this work, we aim to develop a dynamic extraction system for fractionation of radionuclides, Pu and Am, in soils exploiting the sequential injection (SI) system incorporating a specially designed extraction column which can contain a large amount of sample due to very low concentrations of Pu and Am in the environment. The readsorption problem of these radionuclides during dynamic sequential extraction was investigated and the results were compared with the batch extraction systems. According to the result from our previous work with stable elements, it was thought that dynamic extraction systems for fractionation of Pu and Am would show less readsorption problems due to short contact time between the extractant and the remaining solid phases. To the best of our knowledge, there is no study on development of dynamic extraction systems for fractionation of radionuclides in soils and sediments and, hence, no reports on investigation of the readsorption problem during such fractionations.

## 2. Experimental

### 2.1. Instrumentation

A FIALab-3500 flow injection/sequential injection system (FIALab, USA) equipped with an internally incorporated six port selection valve (SV), and



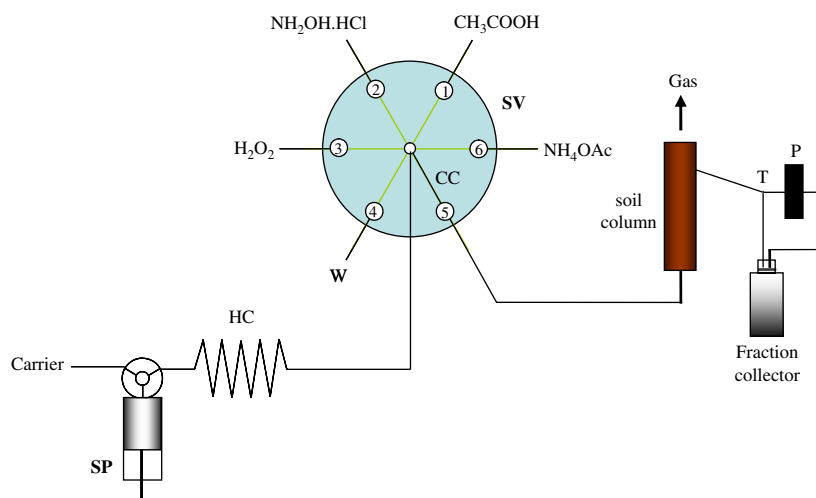


Fig. 1. Schematic diagram of the dynamic sequential extraction system. SP, syringe pump; HC, holding coil; SV, selection valve; CC, central communication channel; W, waste; Carrier, Milli-Q water; T, three-way valve; P, peristaltic pump.

a syringe pump (SP, Cavo, Sunnyvale, USA) with a capacity of 5 mL was used. The SI-system was computer-controlled by the associated FIALab software. The extraction column was connected within the SI-system as shown in Fig. 1. All the outlets of the SV were connected through PEEK ferrules with rigid PTFE tubing (0.5 mm i.d./1.60 mm o.d.). The central port of the SV was connected to the holding coil (HC), which consisted of PTFE tubing volume 1.8 mL (1.32 mm i.d./1.93 mm o.d.). The volume of the PTFE tubing (1.32 mm i.d./1.93 mm o.d.) connecting port 5 of the SV to the extraction column was 0.4 mL. In the oxidizable step (step IV), an auxiliary peristaltic pump was connected to the outlet line from the column in order to increase the out-flow rate and thus reduce excessive pressure in the system.

## 2.2. Extraction column

As mentioned, a new extraction column was designed and constructed in order to be able to contain larger amount of sample (up to 5 g). At the same time, the newly designed column should produce less back pressure in the SI-system. The extraction column designed for this work is shown in Fig. 2 with the critical dimensional details given in the figure. The column was machined from polysulphone (PSU) to tolerate the strong acid and high temperatures used. The sample container (cylindrical shape) and caps were screwed tightly in position. The o-rings and silicone gaskets were used to avoid leaking problems. The outlets of the sample container were furnished with membrane filters (Millipore, Fluoropore™ membrane filter, 25 mm diameter, 1.0 µm particle retention), which were laid on perforated filter supports to allow dissolved matter to flow through. Both ends of the outlet of the caps were connected through PEEK ferrules with rigid PTFE tubing and incorporated into the SI-system. The volume of the extraction column is ~3 mL, which can contain soil samples up to 5 g. The extraction column was placed vertically by using a clamp (Fig. 1). The top cap was specially designed to be able to release gas generated in the oxidizable step (step IV) by opening a PTFE ferrule, while the extract was guided quickly out of the column by means of the peristaltic pump, as facilitated by opening the three-way valve, T.

## 2.3. Modified SM&T sequential extraction scheme

A modified sequential extraction scheme of the Standards, Measurements and Testing (SM&T) program of the European Commission (formerly BCR) (Rauret et al., 1999; Mossop and Davidson, 2003) was employed using the following solutions:

Step I: 1 mol L<sup>-1</sup> NH<sub>4</sub>OAc (i.e. for radionuclides weakly bound to soil surfaces by electrostatic interactions, or readily released by ion exchange processes, or the so-called exchangeable fraction).

Step II: 0.11 mol L<sup>-1</sup> CH<sub>3</sub>COOH (i.e. for radionuclides bound to carbonates, or the so-called acid soluble fraction).

Step III: 0.1 mol L<sup>-1</sup> NH<sub>2</sub>OH·HCl (radionuclides bound to Fe–Mn oxides, or the so-called reducible fraction).

Step IV: 8.8 mol L<sup>-1</sup> H<sub>2</sub>O<sub>2</sub> (radionuclides bound to organic matter, or the so-called oxidizable fraction).

## 2.4. Procedure for readsorption study

Readsorption of Pu and Am was examined by a double-spiking technique which was proposed by Schultz et al. (1998a) for both dynamic and batch extraction systems. The experiments were designed to evaluate the readsorption of Pu and Am at each step of the sequential extraction procedure. Due to the similar chemical properties of curium and americium and absence of suitable alpha emitting isotopes of americium except <sup>243</sup>Am, <sup>244</sup>Cm and <sup>243</sup>Am were used as double-spiking tracers for the investigation of readsorption of Am. The very low concentration of <sup>238</sup>Pu in the environmental samples allows to use <sup>238</sup>Pu and <sup>242</sup>Pu as double-spiking tracers for the investigation of readsorption of Pu. In addition, <sup>242</sup>Pu and <sup>238</sup>Pu, <sup>243</sup>Am and <sup>244</sup>Cm can be easily resolved by alpha-spectrometry. Thus, the extraction reagent used in step I was preliminarily spiked with known activities of <sup>242</sup>Pu and <sup>243</sup>Am tracers, which in turn allowed to measure the level of readsorption during step I and to follow the redistribution of readsorbed <sup>242</sup>Pu and <sup>243</sup>Am among the remaining solid phases (steps II, III, IV and V (residue)). After the extraction period, the second set of isotopic tracers, <sup>238</sup>Pu and <sup>244</sup>Cm, was added to the extract prior to chemical separations in order to use them as chemical yield monitors throughout the separation procedures. A new set of extraction experiments was implemented for step II and afterwards for step III. Because of the length and cost of the post-extraction readsorption experiment, only two replicates on one soil sample were thoroughly analysed.

To preserve the conditions of normal extractions, the additions of tracers for readsorption study should ideally be infinitely small quantities that will not change the natural concentrations and also they should be easily detected (Belzile et al., 1989). However, the concentrations of Pu and Am in the selected environmental soil samples are relatively low (0.2 Bq kg<sup>-1</sup> of <sup>239/240</sup>Pu and 0.1 Bq kg<sup>-1</sup> of <sup>241</sup>Am). When spiking with small amounts of between 50% and 100% of the amount present in the control subsamples, the Pu and Am concentrations in each fraction will still be lower than the detection limit. Therefore, ~0.2 Bq of <sup>242</sup>Pu and <sup>243</sup>Am (10<sup>-10</sup> to 10<sup>-12</sup> mol L<sup>-1</sup> in extractants) were used in this work. At this concentration level, <sup>242</sup>Pu and <sup>243</sup>Am can be easily detected in each fraction when readsorption occurs. This concentration level is slightly higher than what have been reported elsewhere, that is, <sup>236</sup>Pu 10<sup>-15</sup> mol L<sup>-1</sup> and <sup>244</sup>Cm 10<sup>-14</sup> mol L<sup>-1</sup> (Schultz et al., 1998a). After addition, the extractant was readjusted to its original pH-value.

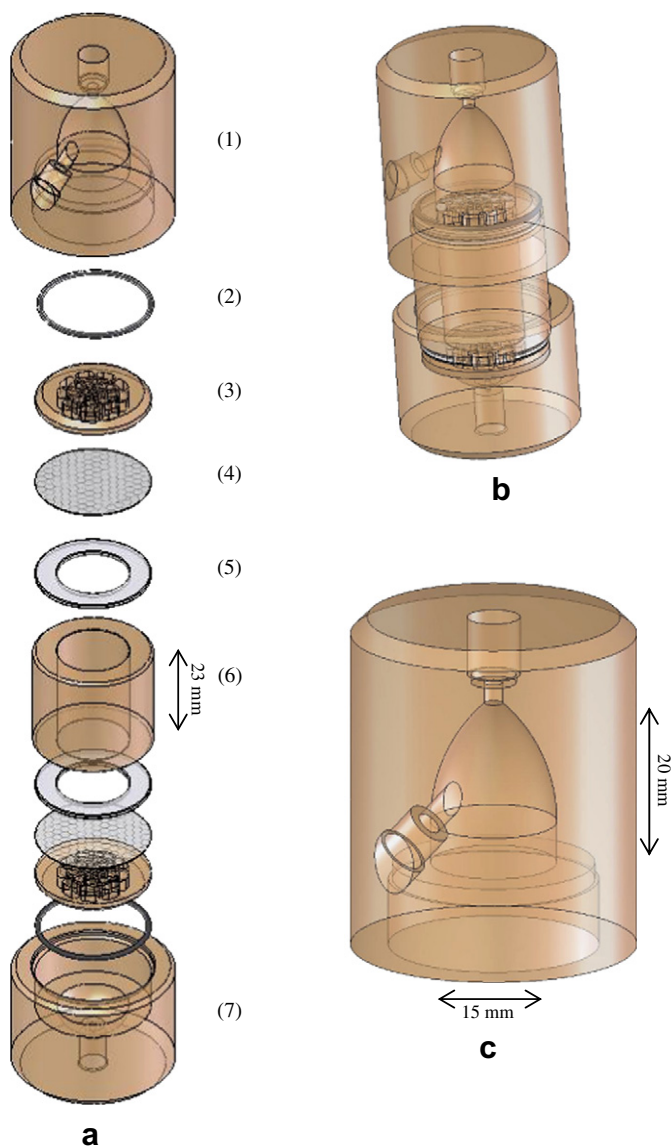


Fig. 2. Illustration of the extraction column used in this work: (a) schematic diagram of all components, that is, (1) top cap, (2) o-ring, (3) filter support, (4) membrane filter, (5) silicone gasket, (6) sample container, (7) lower cap; (b) sketch of the column; (c) detailed picture of the top cap.

The degree of readsorption can be calculated by the recovery of spiked radionuclide as follows:

$$\% \text{of recovery} = ((m_s - m_u)/m_a) \times 100$$

where  $m_u$  is the amount (mg) of metal extracted with unspiked extractant,  $m_s$  is the amount (mg) of metal extracted with spiked extractant and  $m_a$  is the amount (mg) of metal added to the extractant. The loss of spiked metal indicated evidence of readsorption and percent readsorption was evaluated from

$$\% \text{of readsorption} = 100 - \% \text{recovery}$$

## 2.5. Batch extraction

The batch extraction was carried out with the following procedure:

Step I: A 30 mL of 1 mol L<sup>-1</sup> NH<sub>4</sub>OAc was added to 3 g of dry soil in a 250 mL centrifuge tube. The tube was shaken for 2 h at ambient

temperature. The soil suspension was centrifuged at 2100 rpm for 10 min and filtered through a filter paper (0.45 µm Cellulose Nitrate Filter; Sartorius AG, Germany). The residue was washed twice with 20 mL distilled water by shaking for 15 min, centrifuged and filtered, the filtrates are collected.

Step II: A 120 mL of 0.11 mol L<sup>-1</sup> CH<sub>3</sub>COOH was added to the residue from step I. The soil suspension was shaken for 16 h (overnight) at ambient temperature. The sample was centrifuged, filtered and the residue was washed as described above.

Step III: A 120 mL of 0.1 mol L<sup>-1</sup> NH<sub>2</sub>OH·HCl was added to the residue from step II. The extraction procedure was repeated as described in step II.

Step IV: A 30 mL of H<sub>2</sub>O<sub>2</sub> (8.8 mol L<sup>-1</sup>) was added to the residue from step III and digested at room temperature for 1 h with occasional manual shaking. The suspension was then heated at 85 °C on a hotplate for 1 h and a second aliquot of 30 mL of extractant was added and heating at 85 °C continued for 1 h. The sample was then filtered and the extract separated as described in step I.

## 2.6. General procedure for dynamic extraction

The procedure for dynamic sequential extraction has been described in detail elsewhere (Chomchoei et al., 2004). In this work, totals of 30, 120, 120 and 60 mL of NH<sub>4</sub>OAc, CH<sub>3</sub>COOH, NH<sub>2</sub>OH·HCl, and H<sub>2</sub>O<sub>2</sub>, respectively, were used. Thus, the volumes of the extractants used in the dynamic extraction procedures are equal to that employed in the batch methods. Only 1.5 mL aliquots were manipulated at a time in the system to avoid problems of back pressure. The complete sequential extraction procedure runs through the following sequences. Syringe pump (SP) was set to aspirate 1.5 mL of extractant (at a rate of 6 mL min<sup>-1</sup>) from port 1 to the holding coil (HC). The extractant was then dispensed (1.8 mL min<sup>-1</sup>, except in step IV performed at 0.3 mL min<sup>-1</sup>) from HC directly to port 5 and then passed through the extraction column, allowing extraction to take place. The extract from the extraction column from each fraction was collected in a fraction collector. However, after the step of tracer addition for readsorption study, distilled water (~20 mL) was passed through the soil column to completely remove the remaining extractant before the next step was carried out. A washing step is required between the reducible fraction (step III) and the oxidizable fraction (step IV) due to rigorous reaction from these two extractants.

An aliquot of 5 mL of concentrated nitric acid was added to all extracts and the extracts were then evaporated until dryness. The dried extracts were digested using aqua regia solution before performing the analysis of the Pu and Am contents (see Section 2.8).

## 2.7. Soil samples

Environmental soil samples from different places around Denmark (Årslev, Borris, Kalø and Tystofte) were collected at the depth of 0–5 cm. The soil samples were dried at 100 °C. Big stones and roots were removed. Then the samples were ground using a hammermill. Afterward the samples were sieved, thus removing stones larger than 1.5 mm. Each soil sample was well mixed before subsamples were taken for analysis. The compositions and major element contents of all soil samples are given in Table 1. Calcium is operationally defined as indicator element for partitioning to the carbonate phase and Fe/Mn as indicators for extraction from the Fe–Mn oxide phase. Percentages of relative standard deviation (RSD) of all Fe, Mn, and Ca analysis were less than 8. This indicated good homogeneity of all the soil samples. The concentrations of <sup>238</sup>Pu, <sup>242</sup>Pu, <sup>243</sup>Am and <sup>244</sup>Cm are lower than the detection limit (DL). The method of Currie (1968) was used to calculate detection limit. This method defines the detection limit as:  $DL = (2.71 + 4.65(N_b)^{1/2})/t\eta/m$ ; here  $N_b$  is the blank counts,  $t$  is the counting time (s),  $\eta$  is the counting efficiency and  $m$  is the sample weight (g). Detection limits of <sup>238</sup>Pu, <sup>239/240</sup>Pu, <sup>242</sup>Pu, <sup>241</sup>Am, <sup>243</sup>Am and <sup>244</sup>Cm in this work are 0.021, 0.023, 0.019, 0.015 and 0.017 Bq kg<sup>-1</sup>, respectively.

A contaminated soil sample from Thule and one Irish Sea sediment was used for single extraction studies (Section 3.2). The Irish Sea sediment was collected 15 km north of Sellafield at 0–20 cm depth in 1999. After freeze

Table 1  
The compositions and major element contents of the soil samples investigated<sup>d</sup>

Sample	LOI <sup>c</sup> (%)	Total Fe <sup>a</sup>	Total Mn <sup>a</sup>	Total Ca <sup>a</sup>	Total <sup>239/240</sup> Pu <sup>b</sup>	Total <sup>241</sup> Am <sup>b</sup>
Årslev	9.3	7263 ± 490	192 ± 2.7	1005 ± 44.1	ND	ND
Borris	6.9	6597 ± 132	322 ± 1.5	32 ± 1	ND	ND
Kalø	10	3965 ± 212	327 ± 2.0	2852 ± 122	ND	ND
Tystofte	2.5	9736 ± 21.8	206 ± 16	216 ± 1.0	0.18 ± 0.03	0.11 ± 0.01

ND for not detected.

<sup>a</sup>  $n = 3$ ; mg kg<sup>-1</sup> soil.

<sup>b</sup>  $n = 2$ ; Bq kg<sup>-1</sup> soil.

<sup>c</sup> Using loss on ignition technique (Heiri et al., 2001).

<sup>d</sup> Average and one standard deviation are given.

drying, the whole sediment sample was ground, sieved to <1.5 mm and thoroughly mixed. The Thule soil sample at 0–3 cm depth was collected from Narssarsuk, Greenland, at position 76°26.959'N 69°19.200'W, in the year 2003. After freeze drying and ashing at 450 °C, the sample was sieved by removing stones larger than 1.5 mm. All subsamples were measured for <sup>241</sup>Am concentration by gamma spectrometry in order to avoid any hot particles in the bulk samples.

### 2.8. Dissolution of residues and determination of total concentrations of radionuclides and metals

The aqua regia procedure was used to dissolve the residues and to determine the total concentrations of radionuclides and metals. About 3.0 g solid sample or residues from the extraction column was placed into a 250 mL-beaker, 28 mL of aqua regia solution was added and a watch disk was put on the beaker. The sample was heated on a hotplate for 30 min on 150 °C and 2 h on 200 °C under reflux condition (Chen et al., 2001). For the determination of metals, the digested solution was filtered through a GF/A filter, and made up to 50.00 mL with 0.2 M HNO<sub>3</sub> and stored at 4 °C before analysis by flame atomic absorption spectrometry (F-AAS) using the matrix matching method. For the determination of radionuclides, the digested solution was diluted to 120 mL with distilled water, and then filtered through a GF/A filter. The residue was washed three times with 10 mL of 0.5 mol L<sup>-1</sup> HCl, the washes are combined with the filtrate for the analysis of Pu and Am contents using Risø standard radiochemical techniques (Chen et al., 2001). The sample solution was coprecipitated as hydroxide by adding ammonia solution to pH 8–9 and the precipitate was washed with NaOH to remove amphoteric elements. The Pu and Am were reduced to Pu(III) and Am(III) by adding K<sub>2</sub>S<sub>2</sub>O<sub>5</sub> and were coprecipitated as hydroxides at pH > 10, achieved by adding sufficient NaOH to the sample. The precipitate was dissolved by 8 mol L<sup>-1</sup> HNO<sub>3</sub> and retained on an anion exchange column while Am, U, and Th are eluted with 8 mol L<sup>-1</sup> HNO<sub>3</sub> and 12 mol L<sup>-1</sup> HCl, respectively. The Pu was stripped with 2 g NH<sub>4</sub>OH·HCl in 2 mol L<sup>-1</sup> HCl. The Am was isolated by series of calcium–oxalate coprecipitations, liquid–liquid extraction using 10% tri-*iso*-octyl-amine (TIOA)/xylene to remove U, Po, Pu and Fe<sup>3+</sup>, and followed by anion exchange chromatography.

## 3. Results and discussion

### 3.1. Dynamic sequential extractions

When employing flow injection (FI) or sequential injection (SI) for soil extraction, occurrence of high pressure in the system is the biggest concern. In recent years, the implementation of sample-packed microcolumn incorporated into the conduits of flow injection set-ups has attracted special interest for metal fractionation (Beauchemin et al., 2002; Jimoh et al., 2004). The systems are normally conducted by filling a cylindrical microcolumn with a low amount of the sample (typically 5–80 mg),

which provides a uniform extraction flow rate. Using a small amount of sample is not suitable for the extraction of a non-homogeneous soil sample because it may not be representative of the bulk of the sample (Chomchoei et al., 2005a). On the other hand, using higher amounts of soil sample can generate high pressure in the system. Shiowatana et al. (2001a) suggested that a high-pressure pump can be used in order to give a constant flow rate. However, this kind of pump cannot tolerate strong chemical reagents and heat.

In this respect, the sequential injection (SI) system with a dual-conical microextraction column for metal fractionation in soils and sediments was developed in our research group (Chomchoei et al., 2004, 2005a,b). The system was successfully applied to non-homogeneous samples by using 300 mg of soil sample. By means of a syringe pump, the reagents can be sequentially aspirated from the individual ports and then the solutions are placed into a holding coil. Therefore, a strong chemical reagent will not directly touch the surface of the plunger and cylinder of the syringe pump. The syringe pump can provide various and precise flow rates. Moreover, the system is fully automated, robust and easy to operate. However, to employ the SI-system for radionuclide fractionation, the design of a new extraction unit was imperative. The main goal of developing the new extraction system was to design a suitable sample container/column. The column should create less pressure during extraction and it should be able to contain a large amount of the soil sample because of the very low concentrations of radionuclides in the environmental samples.

In the preliminary study, different shapes of microcolumns were designed and tested by incorporating them in the SI-system, namely cylindrical column, wide-surface disc, and the cylindrical with wide-outlet. A cylindrical microcolumn was initially tested because it was simple and easy to construct. Filter supports at both ends were specially made in order to provide a large porous area. The top cap of the column with a releasing point can reduce pressure in the system during the extraction in the oxidizable step (step IV), see Fig. 2. Several different sizes of cylindrical column were made by the workshop at the Department of Chemistry (Technical University of Denmark) with different inner diameters (10 and 15 mm) and with different lengths (1.5–10 cm). The columns were filled with different amounts of sample (1–10 g). The extraction column was incorporated within the SI-system as shown in Fig. 1. It was found that high back pressure in the

system occurred when a long column with a small outlet and a large sample size were employed. The column with i.d. 15 mm and 1.5 cm long was selected, which can contain up to 5 g soil sample. There were no problems with back pressure at the flow rate used. However, a slight back pressure was encountered with larger amounts of soil sample and at higher flow rates. In the present system, the extractants, and their sequence, were automatically aspirated and propelled from different positions of the selection valve to leach metals in different targeted phases. The extracts in each fraction were collected in fraction collectors.

It should be emphasised that the procedure used in the standard scheme for the oxidizable fraction (step IV) as performed at high temperature is useful to estimate the metal content associated with oxidizable soil phases. It can be said that the digestion of the organic matter at high temperature evaluates the potential risk of the metals in soil samples, but a similar procedure at room temperature gives the current risk of the metal ions releasing to the environment. The oxidation of organic matter at room temperature should mimic the chemical condition, which is closer to the environmental situation (Chomchoei et al., 2005a; Fedotov et al., 2002). Therefore, in this work, the fourth step of the procedure was performed at the room temperature. Moreover, the flow rate for this step was set down to  $0.3 \text{ mL min}^{-1}$  in order to increase the contact time of the oxidizable sample and reagent.

### 3.2. Choice of extractant for the exchangeable fraction

In this work, the SM&T scheme was modified by including an exchangeable step. Radionuclides associated with this phase, as measured in the extractant, are assumed to be easily mobilised by the soil/soil solution ion exchange reactions and are therefore available for root uptake (Kennedy et al., 1997). Thus, the experiment was aimed of finding a suitable extractant for this phase, in order to be used in the readsorption evaluation. A number of extractants have been employed and investigated for assessing the availability of radionuclides in this phase (Das et al., 1995; Kennedy et al., 1997). The most commonly used mild extractants, namely  $0.01 \text{ mol L}^{-1} \text{ CaCl}_2$ ,  $1 \text{ mol L}^{-1} \text{ MgCl}_2$  and  $1 \text{ mol L}^{-1} \text{ NH}_4\text{OAc}$ , were selected to perform single extraction by the batch procedure.

Normally, the extractable amount of radionuclides from this phase is very low in comparison with the total concentration. Therefore, the highly contaminated samples, Irish Sea sediment and Thule soil, were chosen in order to be able to detect the released radionuclides from this fraction.

The results in Table 2 show that low extractable amounts of Pu and Am ( $<1\%$  of the total content) were observed for both samples. All extractants provided similar information about leachability of radionuclides. Notably, the  $\text{CaCl}_2$  extraction for the Thule soil sample indicated a significant lower extractable amount of  $^{239/240}\text{Pu}$ . High standard deviation of the extracted  $^{241}\text{Am}$  in the  $\text{NH}_4\text{OAc}$  extraction was observed due to a very low concentration of  $^{241}\text{Am}$  in this fraction. In a number of papers,  $\text{NH}_4\text{OAc}$  has been found to constitute a robust medium for extraction of radionuclides in the exchangeable phase (Kennedy et al., 1997; Grimshaw, 1989). Gleyzes et al. (2002) reported that metal complexes formed with acetate ions are slightly more stable than chloro-complexes. This favours the exchange and reduces readsorption or precipitation of the extracted metals. On the other hand, when the extraction is performed by using mild extractants, such as  $\text{CaCl}_2$ , readsorption can easily take place because of the low ionic strength of the extractant and the lack of a strong counter ion in the extractant (Litaor and Ibrahim, 1996). Therefore,  $\text{NH}_4\text{OAc}$  was chosen for the readsorption experiment in this work.

### 3.3. Comparison of the degree of readsorption for dynamic and batch systems

One of the most important problems with sequential extraction techniques is redistribution as a result of readsorption of dissolved metals onto the remaining solid phases during extraction. It has been recommended that the extraction time or contact time between the solid phase and the extracting reagent of the earlier steps of sequential extractions should be kept as short as possible to minimize the risk of readsorption to take place (Hirner, 1992; Belzile et al., 1989).

Our previous work with dynamic extraction system incorporating the microextraction column to fractionate stable metals in soils and sediments has shown many advantages over the batch system, and one of the major ones is less readsorption (Petersen, 2005). It was expected that the dynamic

Table 2  
Percent leachability of Pu and Am from the Irish Sea sediment and the Thule soil using batch single extraction procedures ( $n = 2$ )

Irish Sea sediment	Extractable amount ( $\text{Bq kg}^{-1}$ ) <sup>a</sup>			Total <sup>a</sup> ( $\text{Bq kg}^{-1}$ )	%Leachability (from $\text{NH}_4\text{OAc}$ )
	$\text{CaCl}_2$	$\text{MgCl}_2$	$\text{NH}_4\text{OAc}$		
$^{239/240}\text{Pu}$	$0.706 \pm 0.023$	$0.798 \pm 0.051$	$0.742 \pm 0.045$	$334 \pm 7.5$	0.2
$^{238}\text{Pu}$	$0.143 \pm 0.005$	$0.165 \pm 0.022$	$0.146 \pm 0.001$	$68.5 \pm 0.7$	0.2
$^{241}\text{Am}$	$0.746 \pm 0.197$	$0.526 \pm 0.013$	$0.706 \pm 0.108$	$469 \pm 80$	0.1
Thule soil				Total <sup>b</sup> ( $\text{Bq kg}^{-1}$ )	
$^{239/240}\text{Pu}$	$0.045 \pm 0.002$	$0.416 \pm 0.063$	$0.410 \pm 0.049$	54.3	0.7
$^{238}\text{Pu}$	$<0.021$	$<0.021$	$<0.021$	0.90	NC
$^{241}\text{Am}$	$<0.015$	$<0.015$	$0.077 \pm 0.036$	14.9	0.5

NC means not calculated.

<sup>a</sup> Average and one standard deviation are given.

<sup>b</sup> The analytical uncertainties are 5.5%, 11%, and 6% for  $^{239/240}\text{Pu}$ ,  $^{238}\text{Pu}$ , and  $^{241}\text{Am}$ , respectively.



Table 3  
Recoveries of spiked  $^{242}\text{Pu}$  in each extraction step when comparing the dynamic and the batch extraction systems<sup>b</sup>

Step $^{242}\text{Pu}$ Spiked	System	Replicate	Spiked $^{242}\text{Pu}$ (Bq)	Recovery, %					
				Step I <sup>a</sup> (exchangeable)	Step II <sup>a</sup> (acid soluble)	Step III <sup>a</sup> (reducible)	Step IV <sup>a</sup> (oxidizable)	Step V <sup>a</sup> (residue)	Total (I + II + III + IV + V)
I	Batch	1	0.2015	24 (0.0469)	0.1 (0.0023)	0.3 (0.0006)	37 (0.0740)	0.6 (0.0012)	62 (0.1250)
		2	0.2008	21 (0.0430)	0.5 (0.0010)	0.3 (0.0007)	46 (0.0930)	0.2 (0.0005)	68 (0.1382)
	Dynamic	1	0.2005	29 (0.0580)	1.0 (0.0016)	0.5 (0.0006)	60 (0.1170)	6.0 (0.0117)	96 (0.1889)
		2	0.2064	23 (0.0472)	1.0 (0.0021)	0.4 (0.0008)	52 (0.1077)	24 (0.0491)	100 (0.2069)
II	Batch	1	0.2017	(<0.000057)	3.7 (0.0075)	0.3 (0.0007)	70 (0.1419)	0.3 (0.0007)	74 (0.1508)
		2	0.2021	(<0.000057)	2.8 (0.0056)	0.2 (0.0005)	65 (0.1321)	0.3 (0.0007)	68 (0.1389)
	Dynamic	1	0.2054	(<0.000057)	3.9 (0.0080)	0.5 (0.0010)	65 (0.1340)	3.7 (0.0076)	73 (0.1506)
		2	0.2064	(<0.000057)	1.9 (0.0040)	0.4 (0.0009)	76 (0.1559)	10 (0.0207)	88 (0.1815)
III	Batch	1	0.1999	(<0.000057)	(<0.000057)	0.6 (0.0013)	66 (0.1342)	0.4 (0.0008)	67 (0.1363)
		2	0.1993	(<0.000057)	(<0.000057)	0.8 (0.0017)	62 (0.1256)	1.1 (0.0022)	64 (0.1295)
	Dynamic	1	0.1997	(<0.000057)	(<0.000057)	1.7 (0.0033)	45 (0.0912)	40 (0.0831)	87 (0.1776)
		2	0.2016	(<0.000057)	(<0.000057)	1.1 (0.0023)	63 (0.1276)	20 (0.0414)	84 (0.1713)

In parenthesis indicates activity in Bq unit.

Sample: soil from Tystofte 3 g in all cases.

<sup>a</sup> Originally,  $^{242}\text{Pu}$  concentrations in each step are less than detection limit (0.019 Bq kg<sup>-1</sup>).

<sup>b</sup> The analytical uncertainty is less than 12%.

extraction system developed in this work would also reduce readsorption of radionuclides (Pu and Am) during fractionation in comparison with the conventional batch methods.

In order to select a soil sample for readsorption study, parameters such as content of organic matter and Fe-oxide have been taken into consideration. This is because of the high affinity of Pu and Am for organic matter and for oxides (Komosa, 2002). The soil sample from Tystofte was selected for this study. It had the lowest organic matter and the highest Fe content. We expected that a large amount of the spiked Pu and Am would readsorb and redistribute to a larger extent to the Fe-oxide phase rather than to the organic matter phase. The double-spiking technique proposed by Schultz et al. (1998a) was used to determine the extent of Pu and Am readsorption during sequential extraction. Known activities of

$^{242}\text{Pu}$  and  $^{243}\text{Am}$  tracers were spiked to the extractant in order to measure the degree of readsorption. Recoveries and the distributions of  $^{242}\text{Pu}$  and  $^{243}\text{Am}$  among different fractions are shown in Tables 3 and 4, respectively.

The results showed that recoveries of  $^{242}\text{Pu}$  and  $^{243}\text{Am}$  in different spiked steps in the batch and dynamic extraction systems were similar, except recovery of  $^{243}\text{Am}$  at step I for dynamic system showed lower percentage (~2%) in comparison with the batch system (~9%). It was found that a very significant readsorption occurred in all steps. For example, recovery of spiked  $^{242}\text{Pu}$  in the exchangeable step was 24% in average and less than 10% for  $^{243}\text{Am}$ . In the acid soluble and the reducible fractions, recoveries of  $^{242}\text{Pu}$  and  $^{243}\text{Am}$  were less than 4% and 8%, respectively. A relatively low degree of readsorption in comparison with other steps was observed in the

Table 4  
Recoveries of spiked  $^{243}\text{Am}$  in each extraction step when comparing the dynamic and the batch extraction systems<sup>b</sup>

Step $^{243}\text{Am}$ spiked	System	Replicate	Spiked $^{243}\text{Am}$ (Bq)	%Recovery					
				Step I <sup>a</sup> (exchangeable)	Step II <sup>a</sup> (acid soluble)	Step III <sup>a</sup> (reducible)	Step IV <sup>a</sup> (oxidizable)	Step V <sup>a</sup> (residue)	Total (I + II + III + IV + V)
I	Batch	1	0.2006	7.8 (0.0156)	0.9 (0.0018)	0.4 (0.0008)	53 (0.1071)	1.5 (0.0031)	64 (0.1284)
		2	0.2011	10 (0.0195)	1.2 (0.0024)	0.5 (0.0011)	54 (0.1097)	1.5 (0.0030)	67 (0.1357)
	Dynamic	1	0.2006	2.4 (0.0049)	15 (0.0292)	(<0.000045)	63 (0.1272)	15 (0.0300)	95 (0.1913)
		2	0.2011	1.9 (0.0038)	12 (0.0242)	(<0.000045)	66 (0.1331)	11 (0.0229)	91 (0.1840)
II	Batch	1	0.1994	(<0.000045)	1.6 (0.0031)	0.4 (0.0009)	61 (0.1223)	2.0 (0.0039)	65 (0.1302)
		2	0.2023	(<0.000045)	1.3 (0.0026)	0.4 (0.0008)	65 (0.1312)	1.1 (0.0023)	68 (0.1369)
	Dynamic	1	0.1991	(<0.000045)	0.8 (0.0016)	1.9 (0.0037)	79 (0.1581)	7.6 (0.0153)	89 (0.1787)
		2	0.2006	(<0.000045)	0.5 (0.0011)	0.9 (0.0018)	70 (0.1408)	23 (0.0455)	94 (0.1892)
III	Batch	1	0.2010	(<0.000045)	(<0.000045)	7.4 (0.0148)	56 (0.1134)	2.0 (0.0040)	66 (0.1322)
		2	0.2003	(<0.000045)	(<0.000045)	0.9 (0.0018)	64 (0.1282)	2.5 (0.0050)	67 (0.1350)
	Dynamic	1	0.1990	(<0.000045)	(<0.000045)	3.0 (0.0060)	74 (0.1478)	14 (0.0273)	91 (0.1811)
		2	0.1991	(<0.000045)	(<0.000045)	1.4 (0.0028)	66 (0.1321)	14 (0.0289)	81 (0.1638)

In parenthesis indicates activity in Bq unit.

Sample: soil from Tystofte 3 g in all cases.

<sup>a</sup> Originally,  $^{243}\text{Am}$  concentrations in each step are less than detection limit (0.015 Bq kg<sup>-1</sup>).

<sup>b</sup> The analytical uncertainty is less than 11%.

exchangeable fraction for Pu ( $\sim 76\%$ , both methods) and for Am ( $\sim 90\%$ , batch method). The main reason for these is probably because ammonium acetate entails a high complexing capacity due to the acetate ion which may prevent readsorption or precipitation of the released ions from the soil sample (Gómez-Ariza et al., 2000).

In this study, both dynamic and batch extraction systems showed a high degree of readsorption. These unexpected results for the dynamic extraction system can be firstly explained by the relatively high pH of the extractants used in step I (pH in the individual steps: step I,  $\text{NH}_4\text{OAc}/\text{pH} = 7$ ; step II,  $\text{CH}_3\text{COOH}/\text{pH} = 3$ ; and step III,  $\text{NH}_2\text{OH}\cdot\text{HCl}/\text{pH} = 1.5$ ). Schultz et al. (1998a,b) reported that Pu and Am readsorption was very significant in the exchangeable phase ( $\text{MgCl}_2/\text{pH} = 5$ ) and the oxidizable phase ( $\text{NaOCl}/\text{pH} = 7.5$ ) due to a high pH of the extractant used. Lucey et al. (2007) found that very significant readsorption of Pu (87%) occurred in the exchangeable step ( $\text{H}_2\text{O}/\text{NH}_4\text{OH}$  with  $\text{pH} = 8$ ), which redistributed to the remaining phases. In contrast, readsorption during acid soluble ( $\text{NH}_4\text{OAc}$  with  $\text{HOAc}/\text{pH} = 5$ ), reducible ( $\text{NH}_2\text{OH}\cdot\text{HCl}$  in 25%  $\text{HOAc}/\text{pH} = 5$ ) and oxidizable ( $\text{H}_2\text{O}_2/\text{pH} = 2$ ) extractions was insignificant. Litaor and Ibrahim (1996) found that moderate amounts of the  $^{237}\text{Np}$ , used for a Pu readsorption study, were immediately lost from the extractant following the soluble ( $\text{H}_2\text{O}/\text{no}$  reported pH), exchangeable ( $0.01 \text{ mol L}^{-1} \text{ CaCl}_2/\text{no}$  reported pH) and oxidizable ( $\text{NaOCl}/\text{pH} = 9.5$ ) extractions and these losses increased significantly with time. There were no significant losses of the tracer following the removal of the acid soluble and reducible fractions. Their interpretation was that the extractants used, namely a mixture of acetate and citrate–bicarbonate–dithionite, are strong complexing ions, which successfully prevented readsorption. The results from a literature survey of Pu and Am readsorption studies and the results obtained in the present work show variability. This is probably due to inconsistency in the application of the sequential extraction procedure and the highly variable nature of the different soils.

Another explanation can be made considering the relatively large amount (3 g) of soil sample used in this work. The readsorption results from our previous work (Petersen, 2005; Chomchoei et al., 2002) showed less degree of metal readsorption. The spiked amount of radionuclide in this study was less than  $10^{-4} \text{ mg kg}^{-1}$  soil, which was much lower than those present in the abovementioned sources ( $\sim 1400 \text{ mg kg}^{-1}$  soil). It should be noted that the addition of a high concentration of metal could be used in the abovementioned reports because of high concentration of metals in the selected sample (SRM2710). However, an added amount of a similar magnitude cannot be applied in our case because of very high radioactivity (610 kBq for  $^{242}\text{Pu}$ ) which is more than five orders of magnitude higher than the activity of Pu in the environmental samples. Moreover, additions of very high concentration of radionuclides can disturb the original systems (Belzile et al., 1989).

The extent of redistribution depends on both the affinity of the remaining undissolved phases for the metal involved, and the ability of the used extractant to inhibit the readsorption. Several researchers have attempted to inhibit or counteract

radionuclides' readsorption problems using chelating agents (for example EDTA and sodium citrate) by stabilizing the radionuclides in solution by limiting precipitation and sorption (Lucey et al., 2007; Schultz et al., 1998a; Howard and Shu, 1996; Howard and Vandenbrink, 1999; Raksataya et al., 1997). Although, a chelating agent theoretically may be utilized to prevent or minimize readsorption and thereby improve the accuracy of the sequential extraction procedure, the amount added has to be adjusted according to soil properties to be effective. In fact, readsorption phenomena in the environmental processes would help toxic elements to remain in the soil fractions for longer period of time. According to the results from this work, radionuclides tend to be adsorbed to the organic matter phase and then assumed to be difficult to be released to the environment, yet might be mobilised by decomposition processes (e.g., weathering and microbial activity).

### 3.4. Distribution of Pu and Am and method validation

From the results (Tables 3 and 4), it was found that  $^{242}\text{Pu}$  and  $^{243}\text{Am}$  were redistributed among the remaining phases, especially to the oxidizable and residual fractions. The distribution of spiked Pu and Am showed similar patterns for both the dynamic and the batch procedures. Major amounts of spiked  $^{242}\text{Pu}$  ( $\sim 59\%$ ) and  $^{243}\text{Am}$  ( $\sim 64\%$ ) were mainly redistributed to the oxidizable fraction (organic matter phase, step IV). Several studies have demonstrated that organic matter plays a role in determining the form and behavior of trace metals and radionuclides in soils and sediments (Szabó et al., 1997). Gómez-Ariza et al. (1999) reported that the readsorption of metals was strongly dependent on the Fe–Mn oxide and organic matter content. Organic matter contains many functional groups such as carboxyl, carbonyl and phenylhydroxyl groups. These can preferably combine with metals and radionuclides (Sparks, 1995). Even though the selected soil sample contained low organic matter (2% loss on ignition) with high concentration of Fe, the obvious amount of spiked  $^{242}\text{Pu}$  and  $^{243}\text{Am}$  was redistributed to the organic matter phase instead of to the Fe/Mn oxide phase (reducible fraction, step III). About 13% of the spiked  $^{243}\text{Am}$  was distributed to the carbonate phase (acid soluble fraction, step II). These results agree with those previously reported (Desideri et al., 2001; Schultz et al., 1998b), where it was concluded that high affinity of Am was found in the carbonate and the organic matter phases.

It should be borne in mind that in the oxidizable phase (step IV), the proposed dynamic extraction system was operated at room temperature by passing the extractant slowly through the soil column, which provided 4 h extraction time. The batch extraction was performed at room temperature (1 h) and at  $85^\circ\text{C}$  (2 h). Therefore, the results from the dynamic system indicated that the percentages of leachability of radionuclides in this step were slightly lower than the batch system. However, the extractable amounts of Pu and Am in this step were higher than our expectation. It might be because the newly readsorbed radionuclides were loosely bound to the organic matter. Recoveries of the extractable amount of radionuclides in the

residual fraction (step V) using the dynamic extraction procedure were, of course, slightly higher than the batch procedure.

Validation of the proposed system can be performed by applying a mass balance. From the results, mass balance calculations showed that the Pu and Am activities derived from the dynamic sequential extraction experiments (Tables 3 and 4) agreed well with the spiked amounts of Pu and Am. The results indicate that the percentage recoveries of the spiked radionuclides exploiting the dynamic extraction system were better ( $\sim 89\%$ ) than that of the batch procedure ( $\sim 67\%$ ). Because the dynamic extraction procedure was performed in a closed and automatic system, it resulted in improved mass balance. In contrast, with the batch system, lower recoveries of Pu and Am were observed due to loss of Pu and Am during washing and filtration steps.

The precision of the results using the dynamic extraction system was relatively poorer than those of the batch procedure. For example the average of total recovery of  $^{242}\text{Pu}$ , spiked in step I, from batch and dynamic extractions was  $0.1316 \pm 0.0137$  and  $0.1979 \pm 0.0283$ , respectively. However, here it should be kept in mind that the dynamic extraction procedure is performed under non-equilibrium condition. The radionuclides were slowly dissolved from the targeted phase, resulting in incomplete leachability of targeted phases. However, longer extraction time with larger amount of extractant used would complete the dissolution and provide higher precision of the extraction (Shiowatana et al., 2001a).

#### 4. Conclusion

A dynamic extraction approach exploiting the SI-system with a newly designed extraction column was developed in this work to fractionate radionuclides (Pu and Am) in soils. This work is focused on investigating one of the biggest problems with sequential extraction techniques, namely readsorption and redistribution, by comparing the performance of the dynamic extraction with that of the batch extraction mode. The results showed high readsorption/redistribution problems in both systems. This indicates that the readsorption of Pu and Am occurs in a very short time scale. Even though extracts are rapidly removed from contact with the remaining solid phase in the dynamic system, the degree of readsorption is still high. However, based on the experimental results, it can be concluded that extractions performed by the dynamic approach are still preferable to those obtained with the batch procedures. The dynamic extraction system is a closed system providing no sample loss, less risk of personal errors, and eliminates external contamination. Therefore, it gives higher recoveries of the spiked radionuclides ( $\sim 89\%$  as compared to  $\sim 67\%$  recovery with the batch procedure). Besides, the continuous extraction approach mimics much better the real environmental conditions. The system is fully automated and computer-controlled. Uniform flow rates are obtained under the optimal operational conditions. Tedious procedures such as solid–liquid phase separation by centrifugation and manual filtration are completely eliminated. Washing between steps can be implemented simply by dispensing deionized water to the

column between extraction steps. The extraction time for the four steps comprises totally  $\sim 8$  h as compared to  $\sim 50$  h in the batch systems (even without considering the separation procedure by centrifuge and filtration). Furthermore, it is possible to obtain more detailed knowledge of the leaching kinetics when highly contaminated samples are applied (Chomchoei et al., 2004, 2005a).

Further studies are required to understand more about the readsorption events themselves, including factors affecting the degree of readsorption such as soil properties and how to solve or reduce this problem when performing dynamic sequential extraction procedures.

#### Acknowledgements

Roongrat Petersen is grateful to the Hans Christian Ørsted Postdoc Programme, Technical University of Denmark (DTU) for the postdoctoral stipend and to the Radioecology and Tracers Programme (headed by Sven P. Nielsen), Radiation Research Department, Risø National Laboratory, DTU for all support during her postdoc research. Special thanks are due to the mechanical workshop of the Department of Chemistry at DTU (headed by John Madsen), and especially to Anders Sølby, for constructing the extraction column. This work was partly financially supported by The Villum Kann Rasmussen Foundation.

#### References

- Beauchemin, D., Kyser, K., Chipley, D., 2002. Inductively coupled plasma mass spectrometry with on-line leaching: a method to assess the mobility and fractionation of elements. *Anal. Chem.* 74, 3924–3928.
- Belzile, N., Lecomle, P., Tessier, A., 1989. Testing readsorption of trace elements during partial chemical extractions of bottom sediments. *Environ. Sci. Technol.* 23, 1015–1020.
- Chen, Q., Aarkrog, A., Nielsen, S.P., Dahlgaard, H., Kolstad, A.K., Yu, Y., 2001. Procedures for determination of  $^{239,240}\text{Pu}$ ,  $^{241}\text{Am}$ ,  $^{237}\text{Np}$ ,  $^{234,238}\text{U}$ ,  $^{228,230,232}\text{Th}$ ,  $^{99}\text{Tc}$  and  $^{210}\text{Pb}$ – $^{210}\text{Po}$  in environmental materials. Risø-R-1263(EN), Risø National Laboratory, Denmark.
- Chomchoei, R., Hansen, E.H., Shiowatana, J., 2004. Utilizing a sequential injection system furnished with an extraction microcolumn as a novel approach for executing sequential extractions of metal species in solid samples. *Anal. Chim. Acta* 526, 177–184.
- Chomchoei, R., Miró, M., Hansen, E.H., Shiowatana, J., 2005a. Automated sequential injection-microcolumn approach with on-line flame atomic absorption spectrometric detection for implementing metal fractionation schemes of homogeneous and nonhomogeneous solid samples of environmental interest. *Anal. Chem.* 77, 2720–2726.
- Chomchoei, R., Miró, M., Hansen, E.H., Shiowatana, J., 2005b. Sequential injection system incorporating a micro-extraction column for automatic fractionation of metal ions in solid samples. Comparison of the extraction profiles when employing uni-, bi-, and multi-bi-directional flow plus stopped-flow sequential extraction modes. *Anal. Chim. Acta* 536, 183–190.
- Chomchoei, R., Shiowatana, J., Pongsakul, P., 2002. Continuous-flow system for reduction of metal readsorption during sequential extraction of soil. *Anal. Chim. Acta* 472, 147–159.
- Currie, L.A., 1968. Limits for qualitative detection and quantitative determination – application to radiochemistry. *Anal. Chem.* 40, 586–591.
- Das, A.K., Chakraborty, R., Cervera, M.L., de la Guardia, M., 1995. Review: metal speciation in solid matrices. *Talanta* 42, 1007–1030.

- Desideri, D., Meli, M.A., Roselli, C., Testa, C., Degetto, S., 2001. Speciation of natural and anthropogenic radionuclides in different sea sediment samples. *J. Radioanal. Nucl. Chem.* 248, 727–733.
- Fedotov, P.S., Zavarzina, A.G., Spivakov, B. Ya, Wennrich, R., Mattusch, J., Titze, K. de P.C., Demin, V.V., 2002. Accelerated fractionation of heavy metals in contaminated soils and sediments using rotating soiled columns. *J. Environ. Monitor.* 4, 318–324.
- Gleyzes, C., Tellier, S., Astruc, M., 2002. Fractionation studies of trace elements in contaminated soils and sediments: a review of sequential extraction procedures. *Trends Anal. Chem.* 21, 451–467.
- Grimshaw, H.M., 1989. In: Allen, S.E. (Ed.), *Chemical Analysis of Ecological Materials*. Blackwell Scientific Publications, Oxford, pp. 7–45.
- Gómez-Ariza, J.L., Giráldez, I., Sánchez-Rodas, D., Morales, E., 1999. Metal readsorption and redistribution during the analytical fractionation of trace elements in oxic estuarine sediments. *Anal. Chim. Acta* 399, 295–307.
- Gómez-Ariza, J.L., Giráldez, I., Sánchez-Rodas, D., Morales, E., 2000. Metal sequential extraction procedure optimized for heavily polluted and iron oxide rich sediments. *Anal. Chim. Acta* 414, 151–164.
- Heiri, O., Lotter, A.F., Lemcke, G., 2001. Loss on ignition as a method for estimating organic and carbonate content in sediment: reproducibility and comparability of results. *J. Paleolimnol.* 25, 101–110.
- Hirner, A.V., 1992. Trace element speciation in soils and sediments using sequential chemical extraction methods. *Int. J. Environ. Anal. Chem.* 46, 77–85.
- Howard, J.L., Shu, J., 1996. Sequential extraction analysis of heavy metals using a chelating agent (NTA) to counteract resorption. *Environ. Pollut.* 91, 89–96.
- Howard, J.L., Vandenbrink, W.J., 1999. Sequential extraction analysis of heavy metals in sediments of variable composition using nitrilotriacetic acid to counteract resorption. *Environ. Pollut.* 106, 285–292.
- Jimoh, M., Frenzel, W., Müller, V., Stephanowitz, H., Hoffmann, E., 2004. Development of a hyphenated microanalytical system for the investigation of leaching kinetics of heavy metals in environmental samples. *Anal. Chem.* 76, 1197–1203.
- Kennedy, V.H., Sanchez, A.L., Oughton, D.H., Rowland, A.P., 1997. Critical review: use of single and sequential chemical extractants to assess radionuclide and heavy metal availability from soils for root uptake. *Analyst* 122, 89R–100R.
- Kheboian, C., Bauer, C.F., 1987. Accuracy of selective extraction procedures for metal speciation in model aquatic sediments. *Anal. Chem.* 59, 1417–1423.
- Komosa, A., 2002. Study on geochemical association of plutonium in soil using sequential extraction procedure. *J. Radioanal. Nucl. Chem.* 252, 121–128.
- Litaor, M.I., Ibrahim, S.A., 1996. Plutonium association with selected solid phases in soils of Rocky Flats, Colorado, using sequential extraction technique. *J. Environ. Qual.* 25, 1144–1152.
- Lloyd, R.D., Miller, S.C., Taylor, G.N., Bruenger, F.W., Angus, W., Jee, W.S.S., 1997. Comparison of internal emitter radiobiology in animals and humans. *Health Phys.* 72, 100–110.
- Lucey, J.A., Vintró, L.L., Boust, D., Mitchell, P.I., Gouzy, A., Bowden, L., 2007. A novel approach to the sequential extraction of plutonium from oxic and anoxic sediment using sodium citrate to inhibit post-extraction resorption. *J. Environ. Radioact.* 93, 63–73.
- McDonald, P., Vives i Batlle, J., Bousher, A., Whittall, A., Chambers, N., 2001. The availability of plutonium and americium in Irish Sea sediments for re-dissolution. *Sci. Total Environ.* 267, 109–123.
- Miró, M., Hansen, E.H., Chomchoei, R., Frenzel, W., 2005. Dynamic flow-through approaches for metal fractionation in environmentally relevant solid samples. *Trends Anal. Chem.* 24, 759–771.
- Mossop, K.F., Davidson, C.M., 2003. Comparison of original and modified BCR sequential extraction procedures for the fractionation of copper, iron, lead, manganese and zinc in soils and sediments. *Anal. Chim. Acta* 478, 111–118.
- Perma, L., Jernstrom, J., Aldave de las Heras, L., de Pablo, J., Betti, M., 2003. Sample cleanup by on-line chromatography for the determination of Am in sediments and soils by  $\alpha$ -spectrometry. *Anal. Chem.* 75, 2292–2298.
- Petersen, R., 2005. Development of Methods for Single and Sequential Extractions of Metals in Soil Samples Exploiting Sequential Injection Analysis. PhD thesis, Department of Chemistry, Mahidol University, Thailand.
- Raksasataya, M., Langdon, A.G., Kim, N.D., 1997. Inhibition of Pb redistribution by two complexing agents (cryptand and NTA) during a sequential extraction of soil models. *Anal. Chim. Acta* 347, 313–323.
- Rauret, G., López-Sánchez, J.F., Sahuquillo, A., Rubio, R., Davidson, C.M., Ure, A.M., Quevauviller, Ph., 1999. Improvement of the BCR three-step sequential extraction procedure prior to the certification of new sediment and soil reference materials. *J. Environ. Monitor.* 1, 57–61.
- Sanderson, D.C.W., Cresswell, A.J., Allyson, J.D., McConville, P., 1997. Review of past nuclear accidents: source terms and recorded gamma ray spectra. UK Department of the Environment. Report Number DOE/RAS/97.001, London, UK.
- Schultz, M.K., Burnett, W.C., Inn, K.G.W., 1998a. Evaluation of a sequential extraction method for determining actinide fractionation in soils and sediments. *J. Environ. Radioact.* 40, 155–174.
- Schultz, M.K., Burnett, W.C., Inn, K.G.W., Smith, G., 1998b. Geochemical partitioning of actinides using sequential chemical extractions: comparison to stable elements. *J. Radioanal. Nucl. Chem.* 234, 251–256.
- Shan, X.-Q., Bin, C., 1993. Evaluation of sequential extraction for speciation of trace metals in model soil containing natural minerals and humic acid. *Anal. Chem.* 65, 802–807.
- Shiowatana, J., Tantidanai, N., Nookabkaew, S., Nacapricha, D., 2001a. A flow system for the determination of metal speciation in soil by sequential extraction. *Environ. Int.* 26, 381–387.
- Shiowatana, J., Tantidanai, N., Nookabkaew, S., Nacapricha, D., 2001b. A novel continuous-flow sequential extraction procedure for metal speciation in solids. *J. Environ. Qual.* 30, 1195–1205.
- Sparks, D.L., 1995. *Environmental Soil Chemistry*. Academic Press.
- Szabó, G., Gucci, J., Nisbet, A., 1997. Investigation of the solid phase speciation of Sr, Cs, Pu and Am in soils determined by extraction and ultra-filtration methods. *J. Radioanal. Nucl. Chem.* 226, 255–259.
- Tessier, A., Campbell, P.G.C., Bisson, M., 1979. Sequential extraction procedure for the speciation of particulate trace metals. *Anal. Chem.* 51, 844–851.



## Review

## A review on speciation of iodine-129 in the environmental and biological samples

Xiaolin Hou<sup>a,\*</sup>, Violeta Hansen<sup>a</sup>, Ala Aldahan<sup>b</sup>, Göran Possnert<sup>c</sup>, Ole Christian Lind<sup>d</sup>, Galina Lujanienė<sup>e</sup><sup>a</sup> Risø National Laboratory for Sustainable Energy, NUK-202, Technical University of Denmark, DK-4000 Roskilde, Denmark<sup>b</sup> Department of Earth Science, Uppsala University, SE-758 36 Uppsala, Sweden<sup>c</sup> Tandem Laboratory, Uppsala University, SE-751 21 Uppsala, Sweden<sup>d</sup> Norwegian University of Life Science, N-1432, Ås, Norway<sup>e</sup> Institute of Physics, Savanoriu 231, LT-0230 Vilnius, Lithuania

## ARTICLE INFO

## Article history:

Received 25 August 2008

Received in revised form 2 November 2008

Accepted 6 November 2008

Available online 17 November 2008

## Keywords:

Iodine-129

Speciation analysis

Tracer

Bioavailability

Environmental sample

## ABSTRACT

As a long-lived beta-emitting radioisotope of iodine,  $^{129}\text{I}$  is produced both naturally and as a result of human nuclear activities. At present time, the main part of  $^{129}\text{I}$  in the environment originates from the human nuclear activity, especially the releases from the spent nuclear fuel reprocessing plants, the  $^{129}\text{I}/^{127}\text{I}$  ratios have been reached to values of  $10^{-10}$  to  $10^{-4}$  in the environment from  $10^{-12}$  in the pre-nuclear era. In this article, we review the occurrence, sources, inventory, and concentration level of  $^{129}\text{I}$  in environment and the method for speciation analysis of  $^{129}\text{I}$  in the environment. Measurement techniques for the determination of  $^{129}\text{I}$  are presented and compared. An overview of applications of  $^{129}\text{I}$  speciation in various scientific disciplines such as radiation protection, waste depository, and environmental sciences is given. In addition, the bioavailability and radiation toxicity (dose to thyroid) of  $^{129}\text{I}$  are discussed.

© 2008 Elsevier B.V. All rights reserved.

## Contents

1. Introduction .....	182
2. Iodine in the nature and its speciation .....	182
2.1. Speciation of iodine in water .....	182
2.2. Speciation of iodine in biological and environmental samples .....	183
2.3. Speciation of iodine in atmosphere .....	184
2.4. Speciation of iodine in soil and sediment .....	184
3. Sources, inventory, and concentration level of $^{129}\text{I}$ in the environment .....	184
4. Measurement of $^{129}\text{I}$ .....	185
4.1. Gamma and X-ray spectrometry .....	185
4.2. Liquid scintillation counting (LSC) .....	185
4.3. Neutron activation analysis .....	185
4.4. Accelerator mass spectrometry (AMS) .....	187
4.5. Inductively coupled plasma mass spectrometry (ICP-MS) .....	188
5. Speciation analysis of $^{129}\text{I}$ in environmental and biological samples and its application .....	188
5.1. Speciation of $^{129}\text{I}$ in water .....	188
5.2. Speciation of $^{129}\text{I}$ in atmosphere .....	190

**Abbreviations:** AMS, accelerator mass spectrometry; AmAD, activity median aerodynamic diameter; DIT, diiodotyrosine; DRC, dynamic collision/reaction cell; EXAFS, extended X-ray absorption fine structure spectra; HpGe, high purity germanium; HPLC, high performance liquid chromatography; ICP-MS, inductively coupled plasma mass spectrometry; LSC, liquid scintillation counter; MIT, monoiodothyronine; NAA, neutron activation analysis; SIMS, secondary ion mass spectrometry;  $\text{T}_3$ , triiodothyronine;  $\text{rT}_3$ , reverse-triiodothyronine;  $\text{T}_4$ , thyroxine; TBAH, tetrabutylammoniumhydroxide; TEDA, triethylenediamine; TBP/OK, tri-*n*-butyl phosphate in odourless kerosene; XANES, X-ray absorption near-edge structure.

\* Corresponding author. Tel.: +45 4677 5357; fax: +45 4677 5347.

E-mail address: [xiaolin.hou@risoe.dk](mailto:xiaolin.hou@risoe.dk) (X. Hou).



5.3.	$^{129}\text{I}$ speciation in soil and sediment .....	192
5.4.	$^{129}\text{I}$ speciation in biological samples .....	193
6.	Bioavailability and radiation toxicity of $^{129}\text{I}$ .....	194
7.	Summary and perspectives .....	194
	Acknowledgements .....	195
	References .....	195

## 1. Introduction

Iodine occurs as a trace element in the Earth's crust, with an average abundance of  $0.45 \text{ mg kg}^{-1}$ . Most of iodine (>70%) in the Earth's surface environment exists in the oceans with a concentration range between 45 and  $60 \text{ ng mL}^{-1}$  [1,2]. The only stable isotope of iodine is  $^{127}\text{I}$  and the most long-lived radioisotope (15.7 My) is  $^{129}\text{I}$ , which is also the only naturally occurring radioisotope of iodine (Table 1). Human nuclear activity has produced and released a large amount of  $^{129}\text{I}$  to the environment thus elevating the  $^{129}\text{I}/^{127}\text{I}$  ratio by at least 2 orders of magnitude compared with the natural values. Due to the long half-life and high mobility with its near conservative behavior in stored radioactive waste,  $^{129}\text{I}$  is an important radionuclide in the waste management.

In order to assess short- and long-term consequences of radioactive contamination in the environment, information on the distribution of radionuclide species influencing mobility and biological uptake is needed [3]. Such information can be obtained by means of radionuclide speciation analysis, which can be defined as the identification and quantification of a radionuclide species in a sample. Information on total concentration (without speciation) alone is not sufficient to evaluate the potential impact of radioactive pollutants in the environment and consequently their bioavailability. Speciation analysis thus provides realistic picture about the radionuclide transport mechanisms in the environment and to the human body, as well as accurate risk assessments. Despite the significance of elemental speciation analysis, there are many difficulties associated with achieving universally accepted analytical methods as well as problems related to sampling and storage.

$^{129}\text{I}$  is one of key radionuclides in the nuclear waste depository,  $^{129}\text{I}$  has also been shown a very useful isotope for the age dating [4,5], a suitable oceanographic tracer for studying transport and exchange of water mass [6–15], as well as a useful environmental tracer for investigating geochemical cycle of stable iodine [16–19]. Knowledge on the speciation of  $^{129}\text{I}$  is a key issue for safety assessment of radioactive waste repositories, for estimation of human exposure through multiple pathways, as well as its application as an environmental and oceanographic tracer. In this article, we present a review on the state-of-the-art speciation analysis methods available for  $^{129}\text{I}$ .

Empirical data have shown different ratios of  $^{129}\text{I}/^{127}\text{I}$  for the different chemical species of iodine in water, soil, sediment [20–23], implying that the speciation of anthropogenic  $^{129}\text{I}$  in the environment is different compared with the speciation of stable iodine. The concentration of  $^{129}\text{I}$  in the environmental samples is normally 4–12 orders of magnitude lower than that of stable iodine, for this reason the analytical methods, including the species separation and analytical techniques for the stable iodine ( $^{127}\text{I}$ ) cannot be directly used for  $^{129}\text{I}$ . The speciation of stable  $^{127}\text{I}$  has been widely investigated in the environmental and biological samples; a few review articles related to the speciation of stable iodine are available [1,24–30]. However, the investigation of  $^{129}\text{I}$  speciation in the environmental, especially biological samples is still very limited. To our best knowledge, a comprehensive review article on speciation of  $^{129}\text{I}$  has not been published. This article aims to review the

occurrence, sources, environmental inventory, distribution, analytical method and speciation analysis of  $^{129}\text{I}$  in environmental and biological samples. The bioavailability of  $^{129}\text{I}$  and its radiation toxicity are also discussed.

## 2. Iodine in the nature and its speciation

Iodine is widespread trace element in the hydrosphere, lithosphere, atmosphere and biosphere. Oceans are considered the main source of iodine (concentration at  $45\text{--}60 \text{ ng mL}^{-1}$ ) to the continental environments, which is back ventilated to the oceans by runoff at concentration of about  $1\text{--}3 \text{ ng mL}^{-1}$  in fresh water. The lowest iodine concentration was observed in atmosphere ( $1\text{--}100 \text{ ng m}^{-3}$  total concentration) [20,31], while the iodine concentration in precipitation ( $1\text{--}6 \text{ ng mL}^{-1}$ ), which is removed from the atmosphere, is relatively higher [16,31]. In the continental environments, the oceanic iodine is commonly trapped by soils, sediments and biota, whereas another source of iodine is supplied by erosion of bedrock. Iodine concentration in soil ranges from  $0.5$  to  $40 \text{ } \mu\text{g g}^{-1}$  with common concentration of  $1\text{--}3 \text{ } \mu\text{g g}^{-1}$ , and the organic soils normally has a higher iodine concentration [32,33]. Generally, sedimentary rocks, especially surface sea sediments contain comparatively high concentrations of iodine ( $1\text{--}2000 \text{ } \mu\text{g g}^{-1}$ ) compared to metamorphic and magmatic rocks ( $<0.1 \text{ } \mu\text{g g}^{-1}$ ) [2]. In the biosphere, iodine concentrations depend on its availability and concentration in the surrounding environment. High concentration of iodine was observed in seaweeds ( $10\text{--}6000 \text{ } \mu\text{g g}^{-1}$  dry weight), of which brown algae shows the highest values ( $100\text{--}6000 \text{ } \mu\text{g g}^{-1}$ ) [34]. Terrestrial plants normally have lower iodine concentrations ( $<1 \text{ } \mu\text{g g}^{-1}$ ) than the marine ones. In mammals, iodine is mainly concentrated to thyroid, with concentration of  $0.5\text{--}5 \text{ mg g}^{-1}$  dry weight) [35,36], while iodine concentration in other tissues is normally much lower ( $<1 \text{ } \mu\text{g g}^{-1}$  dry weight) [37].

Iodine is an electronegative element with oxidation states of  $-1$ ,  $0$ ,  $+1$ ,  $+3$ ,  $+5$ , and  $+7$  and exists in multiform in aqueous solution. Iodine is a redox sensitive element forming a wide variety of organic and inorganic compounds and the most common inorganic forms of iodine are  $\text{I}^-$  (iodide),  $\text{HOI}$  (hypoiodous acid),  $\text{I}_2$  (elemental iodine), and  $\text{IO}_3^-$  (iodate) in natural environmental Eh–pH conditions (Fig. 1) [38,39]. As a biophilic element, iodine occurs in many organic compounds in nature such as alkyl iodide and is incorporated in organic matters such as proteins, polyphenols and humic substances [40–43].

### 2.1. Speciation of iodine in water

Speciation of iodine in natural water depends on several parameters including water chemistry, pH, Eh, temperature and organic productivity. In seawater, iodine mainly exists as iodate, iodide and minor organic iodine [1]. Distribution of iodine species in seawater varies with depth and geographic location. In anoxic water, most of iodine exists as iodide, e.g. in the Baltic Sea and the Black Sea [23,44,45], while in oxygenated/oxic water, such as ocean water, the dominant species of iodine is iodate. The concentration in the ocean ranges at  $<1\text{--}25 \text{ ng mL}^{-1}$  for iodide and  $25\text{--}60 \text{ ng mL}^{-1}$  for iodate. Iodide maximum is often found in surface water while

**Table 1**

Nuclear properties and production model of iodine isotopes with half-life more than 10 min.

Isotope	Half-life	Decay mode	$E_{\max}$ (keV)	Main $\gamma$ -X-ray energy (keV) (abundance)
$^{123}\text{I}$	13.27 h	EC + $\beta^+$	1074.9 (97%, EC)	159 (83%)
$^{124}\text{I}$	4.18 d	EC + $\beta^+$	2557 (25%, EC), 3160 (24%, EC), 1535 (12%, $\beta^+$ ), 2138 (11%, $\beta^+$ )	602.7 (63%), 723 (10%), 1691 (11%)
$^{125}\text{I}$	59.41 d	EC	150.6 (100%)	35.5 (6.68%), 27.2 (40%), 27.5 (76%)
$^{126}\text{I}$	13.11 d	EC + $\beta^+$ , $\beta^-$	869.4 (32%, $\beta^-$ ), 1489 (29%, EC), 2155 (23%, EC)	338.6 (34%), 666.3 (33%)
$^{127}\text{I}$	Stable			
$^{128}\text{I}$	24.99 m	$\beta^-$ , EC + $\beta^+$	2119 (80%, $\beta^-$ )	442.9 (17%)
$^{129}\text{I}$	$1.57 \times 10^7$ y	$\beta^-$	154.4 (100%)	39.6 (7.5%), 29.5 (20%), 29.8(38%)
$^{130}\text{I}$	12.36 h	$\beta^-$	587(47%), 1005 (48%)	536 (99%), 668.5 (96%), 739.5 (82%)
$^{131}\text{I}$	8.02 d	$\beta^-$	606 (90%)	364.5 (82%)
$^{132}\text{I}$	2.30 h	$\beta^-$	738 (13%), 1182 (19%), 2136 (19%)	667.7 (99%), 772.6 (76%)
$^{132\text{m}}\text{I}$	1.39 h	IT, $\beta^-$	1483 (8.6%, $\beta^-$ )	600 (14%), 173.7 (8.8%)
$^{133}\text{I}$	20.8 h	$\beta^-$	1240 (83%)	529.9 (87%)
$^{134}\text{I}$	52.5 m	$\beta^-$	1307 (30%)	847 (95%), 884 (65%)
$^{135}\text{I}$	6.57 h	$\beta^-$	970 (22%), 1388 (24%)	1260 (29%)

Half-lives of the isotopes are given as m: minutes; h: hours; d: days; and y: years. The decay model: EC for electron capture;  $\beta^+$  for positron emission;  $\beta^-$  for beta emission; IT for internal transfer. An isotope may decay by more than one model.

iodide decreases to  $<1 \text{ ng mL}^{-1}$  below the euphotic zone. Relatively high iodide concentration is normally found in coastal and estuary areas [15,46].

Organic iodine was reported in coastal and estuary area, corresponding to 5–40% of total dissolved iodine [47,48]. Some specific organic iodine compounds have been identified, including mainly volatile compounds, such as  $\text{CH}_3\text{I}$ ,  $\text{CH}_2\text{ClI}$ ,  $\text{CH}_2\text{I}_2$  and  $\text{CH}_3\text{CH}_2\text{CH}_2\text{I}$  [42,43]. Although the concentration of organic iodine in seawater is low, it plays a very important role in the global geochemical cycle of iodine. The transfer of iodine from the oceans to the atmosphere, and further to the terrestrial environment, is thought to occur primarily through the emission of organic iodine hydrocarbon from the seawater [49,140]. These volatile organic iodine species were also suggested to contribute to ozone depletions in the lower stratosphere, particularly the marine boundary layer [50,51] and cloud condensation in the lower troposphere [52]. In fresh water, such as rivers, lakes and rain, iodine exists also as iodide, iodate and organic iodine, but the relative concentration of organic iodine is higher compared to seawater [53,56].

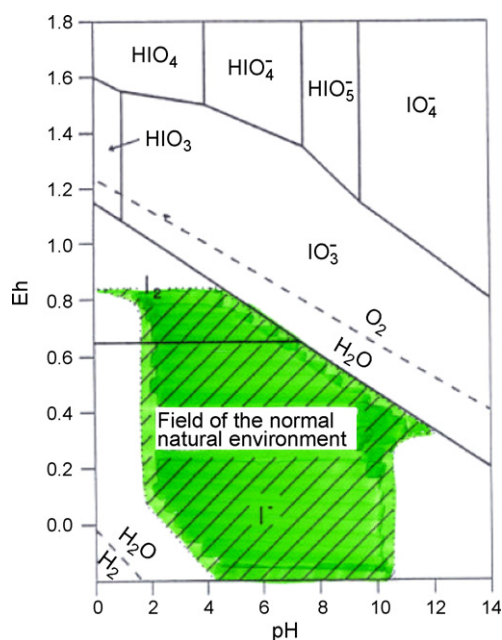


**Fig. 1.** Eh–pH diagram for iodine in water at 25 °C [38–39].

## 2.2. Speciation of iodine in biological and environmental samples

Iodine comprises a vital ingredient by the thyroid gland in mammals for the biosynthesis of the thyroid hormones triiodothyronine ( $\text{T}_3$ ) and thyroxine ( $\text{T}_4$ ). These hormones have an important influence on an extended range of biochemical reactions. Besides  $\text{T}_3$  and  $\text{T}_4$ , iodine also occurs as monoiodotyrosin (MIT), diiodotyrosine (DIT), and reverse-triiodothyronine ( $\text{rT}_3$ ), which are mainly bound with proteins in thyroid as well as blood, but they function as free  $\text{T}_3$  and  $\text{T}_4$ . In addition to thyroid, iodine is also distributed in many other tissues, mainly bound with proteins [57]. In urine, iodine mainly exists as iodide, with small amount of organic iodine. The element was also found as iodide, MIT, DIT,  $\text{T}_4$ ,  $\text{T}_3$ ,  $\text{rT}_3$  and other unknown species in fish flesh [58].

Breast milk samples taken from a selected group of European women contain  $95 \pm 60 \text{ ng iodine mL}^{-1}$  milk in average. In addition, total iodine varies according to lactation state, beginning at  $60 \text{ ng mL}^{-1}$  at 2nd day (postpartum), reaching  $100 \text{ ng mL}^{-1}$  at 3rd day, and decreasing to  $80 \text{ ng mL}^{-1}$  (6th day) or  $60 \text{ ng mL}^{-1}$  constantly from 9th to 60th day. More than 80% of iodine in human milk presents as iodide, and the rest occurs as organic iodine [59–61].

In seaweed, 9–99% of iodine is water-soluble depending on the seaweed species, the highest water-soluble iodine was observed in brown algae and lowest in green algae. In the water leachate of seaweed, iodine exists mainly as iodide, the percentage of organic iodine ranges in 5–40% and the iodate is less than 5%. In biological macromolecules, iodine is mainly bound with proteins, polyphenol and pigments [42,43], and iodine in the enzymatic hydrolyzed protein exists as MIT and DIT [62]. Recently, Küpper et al. [63] directly analyzed a brown seaweed (*Laminaria digitata*) using X-ray absorption spectroscopy (iodine K-edge), and confirmed that mainly accumulated iodine exists as iodide. Their experiments also showed that iodide in seaweed readily scavenges a variety of reactive oxygen species; it is therefore proposed that the biological role of iodide in the seaweed is as an inorganic antioxidant. It was also observed that on thallus surface and in apoplast of the seaweed, iodide detoxifies both aqueous oxidants and ozone, the latter resulting in the release of high level of molecular iodine ( $\text{I}_2$ ) and consequent formation of hygroscopic iodine oxides ( $\text{IO}_x$ ) leading to particle formation, which are precursor to cloud condensation nuclei. Some experiments have showed a significantly increasing  $\text{I}_2$  and particle concentrations in a culture chamber of brown seaweed, the released  $\text{I}_2$  from the brown seaweed is therefore linked with the for-

mation of coastal new particles and cloud condensation nuclei [64–67].

### 2.3. Speciation of iodine in atmosphere

Total concentration of iodine in the atmosphere ranges from 1 to  $100 \text{ ng m}^{-3}$  where a high iodine concentration was observed in urban area due to the combustion of oil and coal, as well as coastal area due to emission of gaseous iodine from algae, seawater, as well as sea spray [58,63–65,68,69,165]. In the atmosphere, iodine exists as particle associated iodine (particulate iodine), inorganic gaseous iodine ( $\text{I}_2$ , HI, HOI) and organic gaseous iodine ( $\text{CHI}_3$ ,  $\text{CH}_2\text{I}_2$ ,  $\text{CH}_3\text{CH}_2\text{CH}_2\text{I}$ , etc.); their concentrations vary with various parameters, such as location, season and climate [31,70–72]. Soluble species of iodine in the aerosol exist as iodide, iodate and organic iodine [54,73–75]. The photolysis of volatile gaseous iodine could generate active I which would interact with atmospheric species such as  $\text{O}_3$ ,  $\text{H}_x\text{O}_y$ , and  $\text{NO}_x$  to produce IO, HOI,  $\text{ION}_2$  and  $\text{I}_2$ . Production and cycling back to I could cause catalytic removal of troposphere  $\text{O}_3$ . A mixing ratio of IO up to 6.6 ppt has been measured at mace Head, Ireland [76]. A relative large amount of molecular iodine ( $\text{I}_2$ ) may be emitted from seaweed, the released  $\text{I}_2$  could be converted to active I, and then react with  $\text{O}_3$  to form IO, which was supposed to be a key route to produce new particles [63].

### 2.4. Speciation of iodine in soil and sediment

Iodine speciation in soil and sediment is normally investigated by sequential extraction, where results showed that most of iodine in soil and sediment is associated to organic matters, mainly humic substances. Part of iodine is also adsorbed on oxides and hydroxides of iron and manganese. The fraction of soluble iodine in soil and sediment comprises minor part of soil iodine and varies with the soil chemistry [21,22,77]. Iodine in soil solution exists as iodide, iodate, and humic substance (humic acid, and fulvic acid) depending upon the soil condition. It was reported that iodate is the dominant specie of iodine in soil solution under non-flooded oxidizing soil condition (85%), while under the flooded condition (anoxic) the dominant specie is iodide [78].

## 3. Sources, inventory, and concentration level of $^{129}\text{I}$ in the environment

Although all  $^{129}\text{I}$  formed in the primordial nucleosynthesis has decayed to  $^{129}\text{Xe}$  (stable), natural processes including the reactions of high-energy particles (cosmic rays) with xenon in the upper atmosphere, spontaneous fission of  $^{238}\text{U}$ , thermal neutron-induced fission of  $^{235}\text{U}$  and to a lesser extent the neutron activation reactions,  $^{128}\text{Te}(\text{n}, \gamma)^{129}\text{I}$  and  $^{130}\text{Te}(\text{n}, 2\text{n})^{129}\text{I}$ , contribute to a steady state concentration of  $^{129}\text{I}$ . The estimated atom ratios of  $^{129}\text{I}/^{127}\text{I}$  in the marine environment are  $3 \times 10^{-13}$  to  $3 \times 10^{-12}$  and even lower ratio of  $10^{-15}$  to  $10^{-14}$  in the lithosphere [79,80]. These ranges correspond to a steady state inventory of about 180 kg  $^{129}\text{I}$  in the hydrosphere and about 60 kg in lithosphere (total at about 250 kg). A representative ratio of  $^{129}\text{I}/^{127}\text{I}$  at  $1.5 \times 10^{-12}$  is commonly considered in the hydrosphere which has been based on measurement of marine sediment samples [81–83].

Since 1945, large amounts of  $^{129}\text{I}$  have been produced and released to the environment by human nuclear activities.  $^{129}\text{I}$  is mainly produced by neutron-induced fission of  $^{235}\text{U}$  and  $^{239}\text{Pu}$  in the explosion of nuclear devices, as well as in the operation of nuclear reactors for research and power production. An approximate rate of 0.17 and 0.28 g of  $^{129}\text{I}$  per kiloton TNT equivalent is produced from fission of  $^{235}\text{U}$  and  $^{239}\text{Pu}$ , respectively in a nuclear

explosion. Total yield of about 540 megatons TNT equivalent was produced from nuclear weapons testing in the atmosphere or at ground level during the period from 1945 to 1975. These tests have released about 57 kg of  $^{129}\text{I}$  to the environment [80]. The  $^{129}\text{I}$  injected to the atmosphere, especially into the stratosphere, has a relatively long residence time, which implies mixing and fallout over a large area. A globally elevated  $^{129}\text{I}$  level has been observed in the environment [26] resulting in a high ratio of  $^{129}\text{I}/^{127}\text{I}$ , particularly in the northern hemisphere. A relatively lower  $^{129}\text{I}/^{127}\text{I}$  value was observed in the southern hemisphere ( $10^{-11}$  to  $10^{-9}$ ) with the lowest ratio in the equatorial regions ( $10^{-11}$  to  $10^{-10}$ ). In general, the  $^{129}\text{I}/^{127}\text{I}$  ratio has been increased to  $10^{-11}$  to  $10^{-10}$  in the marine environment and  $10^{-11}$  to  $10^{-9}$  in terrestrial environment due to the nuclear weapons testing [26,35,77,84–91].

Routine operation of the nuclear reactors, for power production and research, may release  $^{129}\text{I}$  to the environment, but no significantly increased concentration was observed in the surrounding area of nuclear power plants [14]. Records of  $^{129}\text{I}$  releases from nuclear accidents are difficult to establish, mainly due to lack of contemporaneous measurement. The Windscale (10 October 1957) and Three Mile Island (28 March 1979) accidents may have released some amount of  $^{129}\text{I}$  to the environment, but it was not possible to be isolated from other signals [92]. A relatively better defined  $^{129}\text{I}$  signal is documented from the Chernobyl accident in 1986 [93]. A high  $^{129}\text{I}$  level ( $^{129}\text{I}/^{127}\text{I}$  ratio of  $10^{-6}$ ) was measured in environmental samples collected from the Chernobyl accident contaminated area [22,36,88,93–95]. A total release of  $^{129}\text{I}$  from the Chernobyl accident was estimated to be 1.3–6 kg [93,96].

Commonly a large amount of  $^{129}\text{I}$  is produced during the operation of a nuclear power reactor. The production efficiency of  $^{129}\text{I}$  in the reactor depends on burn-up of the uranium fuel, which is corresponding to the power production of the reactor. It was estimated that about 7.3 mg  $^{129}\text{I}$  is produced per MWd (megawatt day) [80]. About  $9.3 \times 10^9$  MWd of nuclear power has been produced in the world from 1980 to 2005, with a production of 368 GWe in 2005 [97], it can be estimated that about 68,000 kg  $^{129}\text{I}$  has been produced in the nuclear power reactors up to 2005. However, most of  $^{129}\text{I}$  generated in the nuclear power production was kept in the spent fuel. The fuel elements were encased in cladding that prevented the release of gaseous radioiodine to the atmosphere, and only a small part of them was released to the environment by the reprocessing of the spent fuel.

During reprocessing of nuclear fuel (mainly by PUREX process), the fuel is first dissolved with acid ( $\text{HNO}_3$ ). In this step, most of iodine is oxidized to volatile  $\text{I}_2$  and released from the fuel solution, which may be trapped and collected, while some part may be released from the reprocessing plant to the atmosphere [98,99]. The trapped  $^{129}\text{I}$  in solution may be stored or discharged to the environment. The  $^{129}\text{I}$  remained in the solution is extracted into the organic solvents during following extraction process using tri-*n*-butyl phosphate (TBP), where  $^{129}\text{I}$  may react with TBP and thus occurs in organic forms [100]. Many reprocessing plants have been operated since 1940s, and some of them are still in operation. The reprocessing plants at La Hague (France) and Sellafield (UK) are the largest. Until 2007, the La Hague reprocessing plant has discharged around 3800 kg  $^{129}\text{I}$  to the English Channel, and the Sellafield reprocessing plant has discharged 1400 kg  $^{129}\text{I}$  to the Irish Sea. Meanwhile these two reprocessing plants have also released 75 and 180 kg of  $^{129}\text{I}$  to the atmosphere, respectively. Another European spent fuel reprocessing plant was located at Marcoule (France) which has also released comparable amount of  $^{129}\text{I}$  (145 kg) to the atmosphere, but relatively small amount of liquid  $^{129}\text{I}$  (45 kg) to the Rhone river. Annual discharges of  $^{129}\text{I}$  from these three reprocessing plants are shown in Fig. 2 (liquid discharges) and Fig. 3 (atmosphere releases) [7,15,89,101,102]. It can be seen that a similar amount of



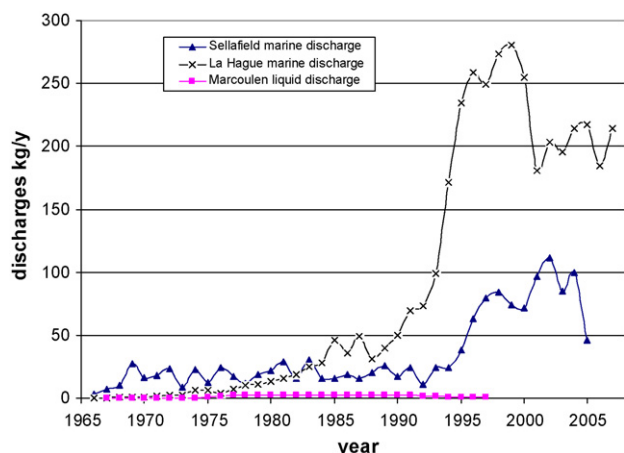


Fig. 2. Liquid discharges of  $^{129}\text{I}$  from spent nuclear fuel reprocessing plants at La Hague (France), Marcoule (France) and Sellafield (UK) (literature refers to the text).

$^{129}\text{I}$  has been released to the atmosphere from the three reprocessing plants with a relative constant rate of each ( $2\text{--}10\text{ kg y}^{-1}$ ). The marine discharges of  $^{129}\text{I}$  from La Hague and Sellafield is smaller and relatively constant before 1990 ( $<50\text{ kg y}^{-1}$ ), later on the discharge of  $^{129}\text{I}$  increased significantly to about  $250\text{ kg y}^{-1}$  for La Hague and  $80\text{ kg y}^{-1}$  for Sellafield. As a consequence, the  $^{129}\text{I}$  concentration in the Irish Sea, English Channel, North Sea, and Nordic Seas has significantly increased and the  $^{129}\text{I}/^{127}\text{I}$  ratio in these seawater has elevated to values of  $10^{-8}$  to  $10^{-5}$  [6,7,11–15,23,103–108]. Even high level of  $^{129}\text{I}$  concentration with a ratio of  $^{129}\text{I}/^{127}\text{I}$  at  $10^{-6}$  to  $10^{-4}$  has been measured in the terrestrial samples collected near the reprocessing plants at La Hague, Marcoule and Sellafield [77,105,109]. These high ratios are attributed to local deposition of atmospheric releases of  $^{129}\text{I}$  from the reprocessing plants.  $^{129}\text{I}$  has also been released from other reprocessing plants mainly to atmosphere, in which Hanford reprocessing plant (USA) released about  $260\text{ kg }^{129}\text{I}$  during its operation (1944–1972) [110] and about  $14\text{ kg}$  during its resumed operation (1983–1988) [82]; reprocessing plant at Tokai, Japan released about  $1.0\text{ kg }^{129}\text{I}$  since its operation from 1997 until 2005 [111,112]; about  $1.1\text{ kg}$  of  $^{129}\text{I}$  was released from the Karlsruhe reprocessing plant (WAK, Germany) during its operation (1971–1987) [113], and unknown amount of  $^{129}\text{I}$  from reprocessing plants in Russia, China and India. An elevated  $^{129}\text{I}$  levels with  $^{129}\text{I}/^{127}\text{I}$  ratio of  $10^{-6}$  to  $10^{-4}$  have been also reported in samples col-

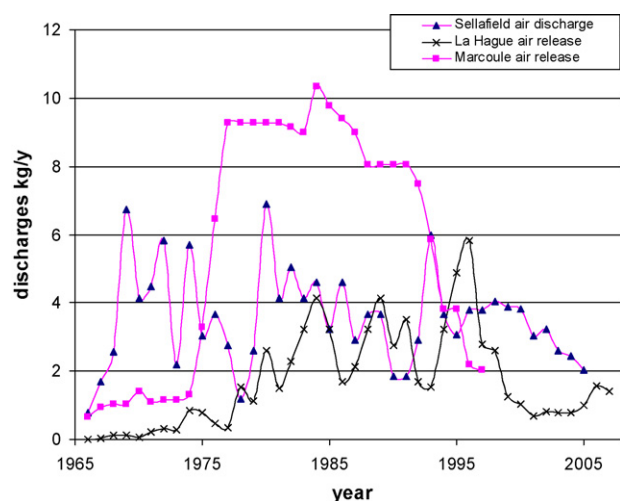


Fig. 3. Atmospheric releases of  $^{129}\text{I}$  from spent nuclear fuel reprocessing plants at La Hague (France), Marcoule (France) and Sellafield (UK).

lected in the regions near the reprocessing plants at WAK, Germany, Hanford, USA, Tokai, Japan, and India [98,13–116].

Table 2 summarizes the sources, inventory and environmental level of  $^{129}\text{I}$ . It is clear that presently the main source of  $^{129}\text{I}$  is the reprocessing plants at La Hague and Sellafield. However, the major part of  $^{129}\text{I}$  produced in reactors around the world, mainly power reactor ( $>90\%$ ), is still stored and pending for future reprocessing. At present, the different levels of  $^{129}\text{I}/^{127}\text{I}$  in the environment are envisaged as  $10^{-12}$  for the pre-nuclear era,  $10^{-9}$  in slightly contaminated regions and  $10^{-9}$  to  $10^{-6}$  in regions affected by the releases from the reprocessing plants. The highest ratio of  $^{129}\text{I}/^{127}\text{I}$  at  $10^{-6}$  to  $10^{-3}$  was found in regions locating at the vicinity ( $<50\text{ km}$ ) of the reprocessing plants.

#### 4. Measurement of $^{129}\text{I}$

$^{129}\text{I}$  decays by emitting  $\beta$ -particle with a maximum energy of  $154.4\text{ keV}$  and  $\gamma$ -ray of  $39.6\text{ keV}$  as well as X-rays ( $29\text{--}30\text{ keV}$ ) (Table 1). It can therefore be measured by  $\gamma$ -X-spectrometry and  $\beta$ -counting using liquid scintillation counters (LSC). Neutron activation analysis (NAA) is another radiometric method for the determination of  $^{129}\text{I}$ . The method is based on neutron activation of  $^{129}\text{I}$  to  $^{130}\text{I}$ , a short-lived radionuclide, emitting high-energy  $\gamma$ -rays ( $536\text{ keV}$  (99%),  $668.5\text{ keV}$  (96%), and  $739.5\text{ keV}$  (82%)), which is easily and efficiently measured by  $\gamma$ -spectrometry. Mass spectrometry, such as accelerator mass spectrometry (AMS) and inductively coupled plasma mass spectrometry (ICP-MS) has also been used for the determination of  $^{129}\text{I}$ . A summary of the most common used methods is presented below.

##### 4.1. Gamma and X-ray spectrometry

Gamma and X-ray spectrometry have been used to measure  $^{129}\text{I}$  in thyroid, urine, seaweed, and nuclear waste by using HpGe or plenary Si detector [104–106,117,118]. This is based on the counting the  $39.6\text{ keV } \gamma$ -ray or  $29.46 + 29.48\text{ keV}$  (58.1%) X-rays. Due to the low counting efficiency of gamma detector ( $<2\%$ ), low  $\gamma$ -ray abundance (7.5%), and high background, a detection limit of  $20\text{--}200\text{ mBq}$  was obtained [104,117,118] depending on the level of interfering radionuclides. In addition, due to the low energy of X- $\gamma$  rays ( $29\text{--}40\text{ keV}$ ) and normally big sample used ( $50\text{--}500\text{ g}$ ), elaborate self-absorption correction has to be carried out in order to obtain accurate results. A chemical separation of iodine from the matrix and interfering radionuclides can improve the detection limit to around  $20\text{ mBq}$  when using gamma spectrometry. In addition, due to small size of the separated sample ( $<20\text{ mg}$ ), the self-absorption correction can be neglected.

##### 4.2. Liquid scintillation counting (LSC)

Due to high beta energy of  $^{129}\text{I}$  ( $154\text{ keV}$ ), a better counting efficiency of LSC for  $^{129}\text{I}$  ( $60\text{--}95\%$ ) compared with X- $\gamma$ -spectrometry ( $<5\%$ ) can be obtained depending on the quench level. In this method, iodine has to be separated from the sample matrix as well as other radionuclides before counting. A detection limit of  $10\text{ mBq}$  has been reported [117].

##### 4.3. Neutron activation analysis

Neutron activation analysis was firstly proposed and applied in 1962 [79,119] for the determination of  $^{129}\text{I}$ , which based on the following nuclear reaction:

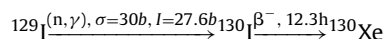


**Table 2**Sources, inventory/releases and environmental level of  $^{129}\text{I}$ .

Source	Inventory/release (kg) <sup>a</sup>	$^{129}\text{I}/^{127}\text{I}$ ratio in the environment	Reference <sup>b</sup>
Nature	250	$\sim 1 \times 10^{-12}$	[81–83]
Nuclear weapons testing	57	$1 \times 10^{-11}$ to $1 \times 10^{-9}$	[26,35,83–89]
Chernobyl accident	1.3–6	$10^{-8}$ to $10^{-6}$ (in contaminated area)	[22,36,89,94–96,127]
Marine discharge from European NFRP by 2007	5200	$10^{-8}$ to $10^{-6}$ (North Sea and Nordic Sea water)	[6,7,11,13–15,23,103,104,106–108]
Atmospheric release from European NFRP by 2007	440	$10^{-8}$ to $10^{-6}$ (in rain, lake and river water in west Europe)	[16,125,126,128]
		$10^{-6}$ to $10^{-3}$ (in soil, grass near NFRP)	[77,105,109,113]
Atmospheric release from Hanford NFRP	275	$10^{-6}$ to $10^{-3}$ (in air near NFRP)	[98,115]

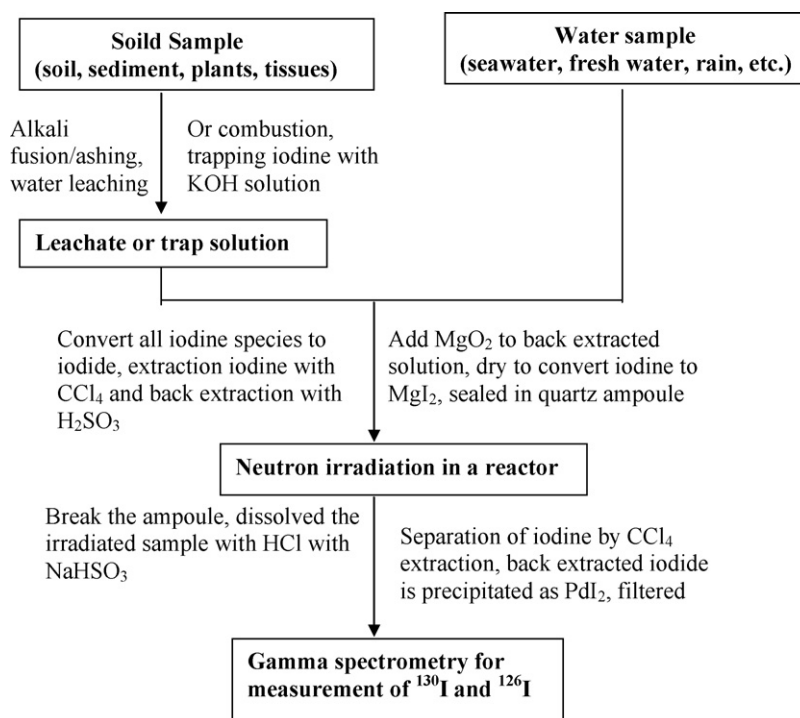
<sup>a</sup> Marine discharge refers to the sum discharges from La Hague and Sellafield reprocessing plants; the atmospheric release from European reprocessing plant refers to a sum of those from La Hague, Sellafield, Marcoule and WAK. The source of the data refers to the literatures cited in the text.

<sup>b</sup> The references for the environmental level of  $^{129}\text{I}$ ; NFRP: nuclear fuel reprocessing plant.

By measurement of activation product,  $^{130}\text{I}$  (12.3 h), decaying by emitting beta particles and gamma rays (Table 1),  $^{129}\text{I}$  is determined. Using NAA,  $^{129}\text{I}$  can be determined with a better sensitivity compared with the direct measurement due to the high specific radioactivity of  $^{130}\text{I}$  and suitable gamma energies (418 keV (34%), 536.1 keV (99%), 668.5 keV (96%), and 739.5 keV (82%)). However, interfering nuclear reactions from some nuclides other than iodine isotopes may occur during production of  $^{130}\text{I}$  in the samples. These nuclides include  $^{235}\text{U}$ ,  $^{128}\text{Te}$ , and  $^{133}\text{Cs}$ . Because of the extremely low concentration of  $^{129}\text{I}$  in environmental samples ( $10^{-17}$  to  $10^{-11} \text{ g g}^{-1}$ ), these interfering nuclides have to be removed from the sample before irradiation to avoid nuclear interference that will generate spurious results. The radioactivity produced from the activation products of the sample matrix elements, such as  $^{24}\text{Na}$  and  $^{82}\text{Br}$ , is more than 10 orders of magnitude higher than that of  $^{130}\text{I}$ , which hinders the direct measurement of  $^{130}\text{I}$  after irradiation. Bromine in particular, produces  $\gamma$ -rays of  $^{82}\text{Br}$  that interferes with the measurement of  $^{130}\text{I}$ , which necessities a post-irradiation chemical purification to provide a necessary decontamination with respect to this nuclide. Besides  $^{129}\text{I}$ , stable iodine ( $^{127}\text{I}$ ) can be simul-

taneously determined by fast neutron reaction  $^{127}\text{I}(n, 2n)^{126}\text{I}$ . A typical analytical procedure for the determination of  $^{129}\text{I}$  by radiochemical NAA [120] is shown in Fig. 4.

For solid sample, such as soil, sediment, vegetations and tissues, alkali fusion/ashing method can be used for decomposition of sample, in which the sample is first mixed with alkali solution, and then ashed or fused at  $600^\circ\text{C}$ . Iodine is then leached from the decomposed sample using water. The experimental results have showed that the recovery of iodine in ashing or fusion procedure is higher than 80% [121]. A combustion method has also widely been used for the separation of iodine from solid samples [121,122]. In this method, sample is combusted at higher temperature ( $>800^\circ\text{C}$ ), the released iodine, mainly as  $\text{I}_2$ , is trapped with alkali solution (KOH) or active charcoal. Iodine in the leachate or trapping solution is extracted with  $\text{CCl}_4$  (or  $\text{CHCl}_3$ ) after acidified and oxidized to  $\text{I}_2$ , and then back extracted with  $\text{H}_2\text{SO}_3$ . After conversion of separated iodine to  $\text{MgI}_2$ , it is applied for neutron irradiation. Fig. 5 shows a commercial combustion facility, which can be used for separation of iodine from solid sample. For water sample including milk and urine, iodine can be separated by anion exchange method. In

**Fig. 4.** Diagram of analytical procedure for the determination of  $^{129}\text{I}$  by radiochemical NAA.

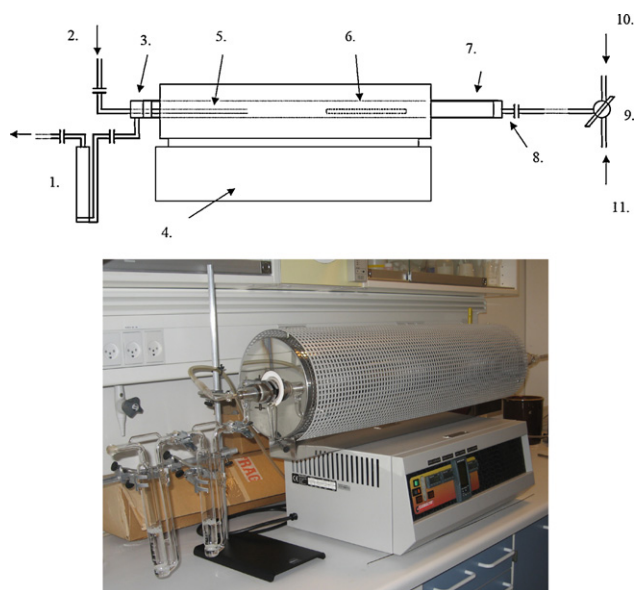


**Fig. 5.** Schematic diagram and picture of combustion facility (Carbolite, UK) for the separation of iodine from solid sample. (1) Gas bubbler (filling with NaOH solution for trapping iodine); (2) oxygen supply; (3) exhaust gas manifold; (4) temperature controller of combustion furnace; (5) second furnace (for complete combustion of residue from first furnace); (6) sample boat in the first furnace; (7) quartz working tube; (8) gas inlet adaptor; (9) three ways valve; (10) main oxygen supply; (11) compressed air supply (in the beginning of combustion, air is supplied to avoid a violet combustion under pure oxygen condition).

which, iodine is first converted to iodide and then absorbed by anion exchange resin (AG1) and separated from matrix elements. The iodide absorbed on resin is eluted by nitrate solution, and concentrated by extraction with  $\text{CCl}_4$  from the eluate [16,23,36,123]. The separated iodine in small volume of water sample is converted to  $\text{MgI}_2$  similar to solid samples.

The pre-separated iodine as  $\text{MgI}_2$  or adsorbed in active charcoal is irradiated in a nuclear reactor for 2–12 h and the irradiated samples is further purified by dissolution with acid and then extracted with  $\text{CCl}_4$ . Iodide is then precipitated as  $\text{PdI}_2$  for gamma counting. The  $^{130}\text{I}$  (from  $^{129}\text{I}$ ) and  $^{126}\text{I}$  (from  $^{127}\text{I}$ ) are counted using an HpGe detector. By comparison with standard and correction for chemical yield during the chemical separation, the absolute contents of  $^{129}\text{I}$  and  $^{127}\text{I}$  in the samples are calculated.

$^{127}\text{I}$  can also cause interference during the determination of  $^{129}\text{I}$  by three continuous neutron capture reactions,  $^{127}\text{I}(3n, \gamma)^{130}\text{I}$ . This interference varies as the square root of the neutron flux and increases with the length of the irradiation time. For irradiation of 10 h in a thermal neutron flux of  $4 \times 10^{13} \text{ n cm}^{-2} \text{ s}^{-1}$ , 1 g of  $^{127}\text{I}$  can produce  $^{130}\text{I}$  equivalent to  $7.7 \times 10^{-12} \text{ g}$  of  $^{129}\text{I}$ . For a sample with  $^{129}\text{I}/^{127}\text{I}$  ratio higher than  $10^{-11}$ , this interference can be corrected by simultaneous determination of  $^{127}\text{I}$  concentration via a fast neutron reaction of  $^{127}\text{I}(n, 2n)^{126}\text{I}$ . But, this interference limits the analysis of sample with  $^{129}\text{I}/^{127}\text{I}$  ratio lower than  $10^{-11}$ .

A large number of samples have been analyzed for  $^{129}\text{I}$  using NAA [13,14,16,22,23,35,36,77,85,86,113–116,118–121], and NAA is also a main method used for the determination of  $^{129}\text{I}$  in environmental samples besides AMS. A detection limit of  $1 \mu\text{Bq}$  (or  $2 \times 10^{-13} \text{ g}$ , or  $10^9$  atoms, or  $^{129}\text{I}/^{127}\text{I}$  ratio of  $10^{-10}$ ) has been reported [120].

#### 4.4. Accelerator mass spectrometry (AMS)

Mass spectrometric techniques, including AMS, SIMS and ICP-MS, have also been used for  $^{129}\text{I}$  determination. Almost all AMS

facilities can be understood as two mass spectrometers (called “injector” and “analyzer”) linked with a tandem accelerator. Before measurement, iodine needs to be separated from the sample and prepared as  $\text{AgI}$  precipitate. The separation procedure used in the NAA can be also used for AMS. The separated iodine as iodide is then precipitated as  $\text{AgI}$ , which is dried and then mixed with Ag or Nb powder for AMS measurement. The iodine in  $\text{AgI}$  target is injected to the system as a negative ion by ion sputtering (e.g. using a  $\text{Cs}^+$  primary ion source),  $\text{I}^-$  ions are easily formed in the sputter source, while  $^{129}\text{Xe}^-$ , the main isobaric interference, is unstable and decomposed rapidly thus having insignificant interference. The formed  $^{129}\text{I}^-$  and  $^{127}\text{I}^-$  negative ions are then accelerated to positive high-voltage terminal of a tandem accelerator where several electrons may be stripped off, converting negative ions to  $\text{I}^{3+}$ ,  $\text{I}^{5+}$  or  $\text{I}^{7+}$ . The stripping process has the advantage that it dissociates molecular ions if enough electrons are stripped off which results in a further elimination of interferences from  $^{128}\text{TeH}^-$  and  $^{127}\text{IH}_2^-$ . The positively charged ions from the accelerator then pass through a magnetic analyzer, where the ions of  $^{129}\text{I}$  and  $^{127}\text{I}$  with a well defined combination of charge state and energy are selected, and directed to a detector. Furthermore, the higher energies of the ions after acceleration allow an additional separation of the wanted ions from possible background ions at the particle detector. The separated  $^{129}\text{I}$  is detected by a combination of time-of-flight and silicon charged particle detectors or gas ionization energy detector. The instrumental background of  $^{129}\text{I}/^{127}\text{I}$  down to  $10^{-14}$  has been obtained [124]. The detection limit of  $^{129}\text{I}$  depends on the chemical separation procedure and iodine carrier. Commonly a blank  $^{129}\text{I}/^{127}\text{I}$  ratio of  $1 \times 10^{-13}$  was reported, which corresponds to  $10^{-9} \text{ Bq}$  (or  $10^{-16} \text{ g}$  or  $10^5$  atoms)  $^{129}\text{I}$  for 1 mg  $^{127}\text{I}$  carrier, and the analytical uncertainty is lower than 10% for a  $^{129}\text{I}/^{127}\text{I}$  ratio of  $10^{-12}$  [124]. Due to the very high sensitivity, most of determinations of  $^{129}\text{I}$  in environmental samples, especially low level geological samples, are now carried out by AMS. Actually, AMS is the only method for the determination of  $^{129}\text{I}$  in the pre-nuclear age samples ( $^{129}\text{I}/^{127}\text{I} < 10^{-10}$ ) [4,6–12,15,17,18,26,52,39,45,56,82–84,89,90,94,103,108,126–128]. AMS is a relative analytical method,  $^{129}\text{I}/^{127}\text{I}$  ratio is normally measured, and the  $^{129}\text{I}$  absolute concentration is calculated by the  $^{127}\text{I}$  content in the samples. For the samples with a  $^{129}\text{I}/^{127}\text{I}$  ratio higher than  $10^{-10}$ , a large amount of  $^{127}\text{I}$  carrier (1–2 mg) comparing to the  $^{127}\text{I}$  content in the sample itself ( $< 10 \mu\text{g}$ ) is normally added to the sample before chemical separation, the  $^{129}\text{I}$  concentration is then calculated by the  $^{127}\text{I}$  added and the measured  $^{129}\text{I}/^{127}\text{I}$  ratio. While for the sample with a low  $^{129}\text{I}/^{127}\text{I}$  ratio ( $< 10^{-13}$  to  $10^{-10}$ , pre-nuclear age sample or less contaminated by human nuclear activity such as deep seawater, soil or sediment from deep layer), a carrier free iodine needs to be separated because of interference of  $^{129}\text{I}$  in the  $^{127}\text{I}$  carrier ( $10^{-13}$  for  $^{129}\text{I}/^{127}\text{I}$  ratio for low background iodine carrier, such as iodine supplied by Woodward Iodine Corp. USA). For the high iodine concentration samples, such as brine, seaweed and thyroid, the carrier free  $^{129}\text{I}$  may be easily separated, but for low iodine concentration sample, such as fresh water, terrestrial plant and animal sample ( $< 5 \text{ ng mL}^{-1}$  water or  $1 \mu\text{g g}^{-1}$  plant or animal sample), it is difficult to separate enough amount of carrier free iodine ( $150 \mu\text{g}$ ) [129]. Yiou et al. [130] reported a method for prepare carrier free iodine from seawater. In this method, silver powder is first added to the water, iodine species is then adjust to molecular iodine ( $\text{I}_2$ ) and the water is stirred for 10–20 h, iodine is consequently absorbed on silver powder and separated from the seawater. The method is very simple to operate and very useful for the separation of inorganic iodine from the seawater without carrier added. However, the volume of the sample is small (100–250 mL), it is therefore not sufficiency for the analysis of low level  $^{129}\text{I}$  sample, which

needs a large sample. In addition, the recovery of iodine is also lower (<50%).

#### 4.5. Inductively coupled plasma mass spectrometry (ICP-MS)

ICP-MS has also been used for the determination of  $^{129}\text{I}$  [131–136]. In this method, iodine separated from the samples is introduced to the machine as solution or gaseous iodine ( $\text{I}_2$ ). The separation method used in NAA (Section 4.3) can be also used for the separation of iodine from the samples.

In ICP-MS, iodine introduced to the plasma is decomposed into iodine atom and ionized to positive iodine ion at a temperature of approximately 6000–8000 K. Due to higher ionization potential (10.45 eV), ionization efficiency of iodine is normally lower comparing to metals, which results in a lower analytical sensitivity of iodine. The positively charged iodine is extracted from the plasma (at atmospheric pressure) into a high vacuum of the mass spectrometer via an interface. The extracted ions are then separated by mass filters of either quadrupole type time-of-flight or combination of magnetic and electrostatic sector, and finally measured by an ion detector.

Problems associated to the determination of  $^{129}\text{I}$  using ICP-MS is low sensitivity (low ionization efficiency), isobaric and molecular ions interferences ( $^{129}\text{Xe}$ ,  $^{127}\text{IH}_2$ ,  $^{89}\text{Y}^{40}\text{Ar}$ ,  $^{115}\text{In}^{14}\text{N}$ ,  $^{113}\text{Cd}^{16}\text{O}$ ), memory effects, low abundance sensitivity of ICP-MS (tailing from the  $^{127}\text{I}$  peak), especially isobaric  $^{129}\text{Xe}$  interference and tailing of  $^{127}\text{I}$ . A dynamic reaction cell (DRC) ICP-MS by using oxygen as reaction gas has been found to significantly reduce signals of xenon ions by charge transfer. It was also found that pressurizing the collision cell with helium the tailing of  $^{127}\text{I}$  or abundance sensitivity can be improved. By using helium and oxygen in the DRC, and directly introducing gaseous iodine to the ICP-MS system, the detection limit of ICP-MS could be significantly improved to  $10^{-6}$  for  $^{129}\text{I}/^{127}\text{I}$  ratio (or  $25 \mu\text{Bq g}^{-1}$  for  $^{129}\text{I}$  at a  $^{127}\text{I}$  concentration of  $4 \mu\text{g g}^{-1}$ ) [134]. By trapping gaseous iodine thermally released from samples, and then desorbing it into the ICP-MS system, detection limit could be further improved to  $2.5 \mu\text{Bq g}^{-1}$  (or  $10^{-7}$  for  $^{129}\text{I}/^{127}\text{I}$  ratio) [135]. By using a similar technique, but directly introducing water samples in 1% tertiary amine carrier solution, a detection limit of  $37 \mu\text{Bq mL}^{-1}$  was reported [136].

Table 3 compares various analytical methods for the determination of  $^{129}\text{I}$ . The X- $\gamma$ -spectrometry and LSC are the least sensitive and long counting time, while they are cheaper and good accessible. These methods are therefore only suitable for the analysis of nuclear waste and high level environmental samples ( $^{129}\text{I}/^{127}\text{I}$  higher than  $10^{-6}$ ). By using DRC techniques, ICP-MS can be used for the determination of  $^{129}\text{I}$ , but the detection limit for  $^{129}\text{I}/^{127}\text{I}$  is only  $10^{-7}$ , it may only be suitable for the analysis of high level environmental samples. Only NAA and AMS are sensitive enough for the analysis of environmental samples ( $^{129}\text{I}/^{127}\text{I}$  ratio of  $10^{-6} \sim 10^{-10}$ ),

in which AMS is the only method for analysis of per-nuclear age samples with  $^{129}\text{I}/^{127}\text{I}$  ratio lower than  $10^{-10}$ .

### 5. Speciation analysis of $^{129}\text{I}$ in environmental and biological samples and its application

In principle, method for speciation of  $^{129}\text{I}$  in the environment should be the same as for stable iodine considering the natural sources and assuming isotopic equilibrium. However, as described above, the naturally occurred  $^{129}\text{I}$  (generated from the uranium fission and cosmic ray reaction of Xe) is overwhelmed by the anthropogenic  $^{129}\text{I}$  from the human nuclear activity since 1945, especially the release from the reprocessing plants since 1990s. This situation has created isotopic disequilibrium between  $^{127}\text{I}$  and  $^{129}\text{I}$  in the environment, which may partly result from a different distribution of  $^{129}\text{I}$  species compared to stable iodine ( $^{127}\text{I}$ ). Although there are a number of reports on the speciation analysis of stable iodine, data on  $^{129}\text{I}$  speciation is still scarce. The extremely low concentration of  $^{129}\text{I}$  in the environment compared to stable  $^{127}\text{I}$  ( $^{129}\text{I}/^{127}\text{I}$  lower than  $10^{-6}$ ) requires a large sample for the analysis of  $^{129}\text{I}$  species, which makes application of the conventional method used for speciation analysis of stable iodine impractical for  $^{129}\text{I}$ . New separation procedures have to be developed for  $^{129}\text{I}$  speciation analysis, which is reviewed below with comments on their potential applications.

#### 5.1. Speciation of $^{129}\text{I}$ in water

In seawater, iodine exists mainly as iodide and iodate with a minor organic iodine and consequently speciation analysis of iodine in seawater commonly focus on iodide and iodate. Hou et al. [23] has developed a chemical procedure for the separation of iodide and iodate from large seawater samples (up to 50 L). The method is based on different affinities of iodide, iodate and other anions, such as  $\text{Cl}^-$  and  $\text{Br}^-$ , on anion exchange column. Iodide with a strong affinity is absorbed on the column, while iodate with a low affinity pass through the column or very weakly adsorbed on the column with  $\text{Br}^-$  and  $\text{Cl}^-$ . These anions can easily be removed from the column by using low concentration of nitrate ( $<0.5 \text{ mol L}^{-1}$ ). The adsorbed iodide on the column is eluted using high concentration of nitrate ( $1.5\text{--}2.0 \text{ mol L}^{-1}$ ). Converting the anion exchange resin to nitrate form instead of chloride form enhances the capacity of the anion exchange column for iodide by 5–10 times, which is a useful approach for analysis of large seawater sample. The iodate in the effluent and wash (with  $\text{Br}^-$  and  $\text{Cl}^-$ ) is then converted to iodide by addition of  $\text{NaHSO}_3$  and acidifying to pH 2–3 using HCl. The solution is then passed through another anion exchange column, where the iodide absorbed on the column is eluted using  $2.0 \text{ mol L}^{-1} \text{ NaNO}_3$  for the determination of iodate. The iodide in nitrate eluate is then concentrated using  $\text{CCl}_4$  or  $\text{CHCl}_3$  extraction following the same procedure for extraction of total  $^{129}\text{I}$  (Section 4.3). The separated

**Table 3**  
Comparison of measurement methods for the determination of  $^{129}\text{I}$ .

Detection method	Target preparation	Detection limit		Reference number
		Bq	$^{129}\text{I}/^{127}\text{I}$ ratio	
X- $\gamma$ spectrometry	Direct measurement	100–200 mBq	$10^{-4}$ to $10^{-5}$	[106]
X- $\gamma$ spectrometry	Separated iodine (AgI)	20 mBq	$10^{-5}$ to $10^{-6}$	[117]
LSC	Separated iodine	10 mBq	$10^{-5}$ to $10^{-6}$	[117]
RNAA	Separated $\text{MgI}_2/\text{I}_2$ absorbed on charcoal	1 $\mu\text{Bq}$	$10^{-10}$	[120]
AMS	AgI	$10^{-9}$ Bq	$10^{-13}$	[124]
ICP-MS	Direct water measurement	40–100 $\mu\text{Bq mL}^{-1}$	$10^{-5}$ to $10^{-6}$	[136]
ICP-MS	Gaseous iodine	2.5 $\mu\text{Bq g}^{-1}$	$10^{-7}$	[135]



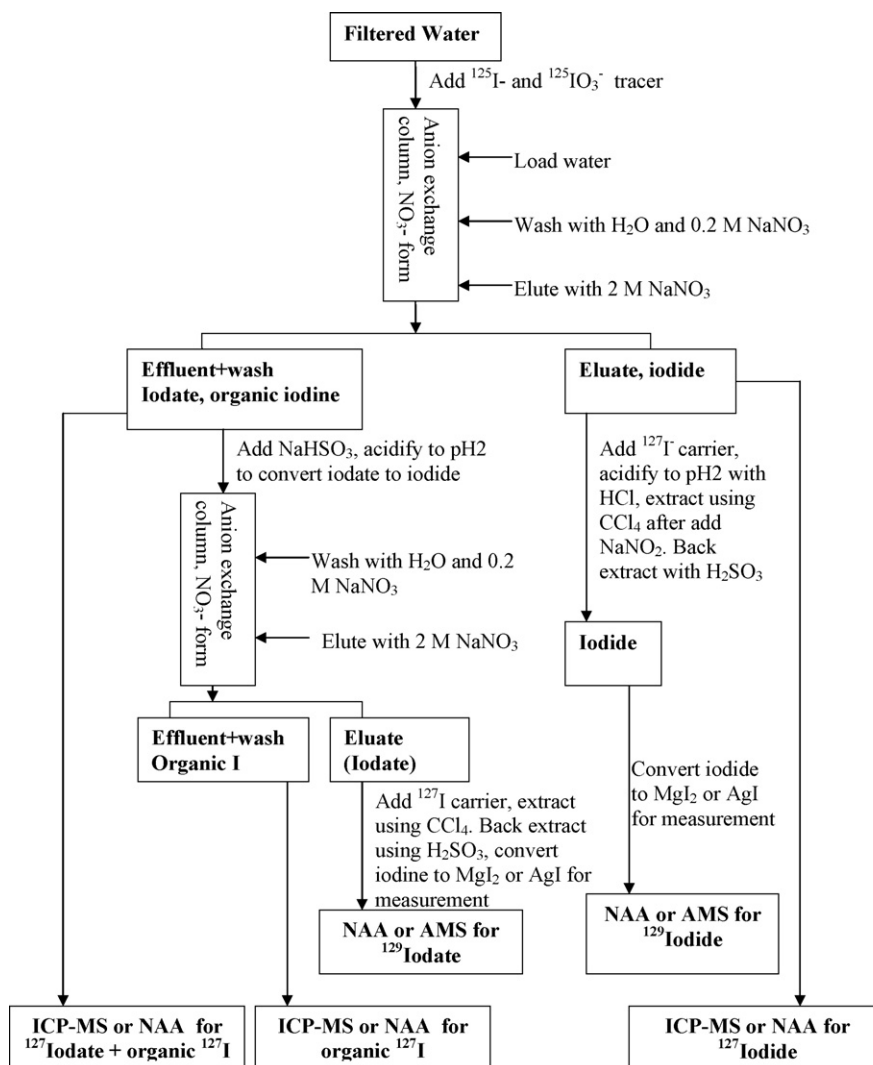


Fig. 6. Chemical procedure for speciation analysis of iodine in water sample.

$^{129}\text{I}$  in iodide and iodate is then measured using NAA or AMS [13,23]. A schematic flow chart of the analytical procedure is shown in Fig. 6. However, organic  $^{129}\text{I}$  cannot be determined in this procedure. Schwehr et al. [17] proposed a procedure for the determination of organic  $^{129}\text{I}$  where water sample is first digested by heating under ultrasonic condition in NaOH and ethanol medium. This step is supposed to decompose all organic matters and iodine in organic form would be released and converted to inorganic iodine. Later an anion exchange chromatography and  $\text{CCl}_4$  extraction are used to extract total  $^{129}\text{I}$ . The organic  $^{129}\text{I}$  in the sample is then calculated by the difference between total  $^{129}\text{I}$  and the sum of  $^{129}\text{I}^-$  and  $^{129}\text{IO}_3^-$ . For water from estuaries, rivers and lakes, the concentration of organic  $^{129}\text{I}$  may be significant comparing to iodide and iodate for which the procedure described above can be also used. In addition, the total  $^{129}\text{I}$  can also separated by evaporation of fresh water to dryness and decomposition of residue by digestion or combustion, following the extraction and precipitation as  $\text{MgI}_2$  or  $\text{AgI}$  [166].

Anion exchange chromatography is a good method for the separation of iodide and iodate, and has been successfully applied for the analysis of seawater and fresh water in the laboratory. However, the procedure is time consuming and not practically suitable for treatment of water samples in the field and on board sam-

pling vessels. It is recommended that speciation analysis, especially the separation part, to be carried out during a short time after the sampling. In addition *in situ* separation can meet the requirement of analysis of large number of samples without a problem of transport (shipping, etc.) to get the samples back to the laboratory. Accordingly, a new and simple speciation method has been developed using  $\text{AgCl}$  co-precipitation for the speciation analysis of  $^{129}\text{I}$  in seawater. In this method,  $^{125}\text{I}^-$  tracer and  $^{127}\text{I}^-$  carrier are first added to the seawater and the pH of sample is adjusted to 4–6 using  $\text{HCl}$ .  $\text{AgNO}_3$  is added with a ratio of  $\text{Ag}:\text{Cl}$  less than 100, and  $\text{Ag}:\text{I}$  higher than 5. After stirring for 0.5–1 h,  $\text{AgI}$  precipitated with  $\text{AgCl}$  is then separated by decanting the supernatant after settling down and centrifuging. The  $\text{AgI}$  is afterwards separated from  $\text{AgCl}$  by addition of  $\text{NH}_3$  to dissolve  $\text{AgCl}$ , and centrifuge. The separated  $\text{AgI}$  is used for AMS measurement of  $^{129}\text{I}^-$  after dryness [134]. For the determination of total inorganic  $^{129}\text{I}$ , the sample is acidified to pH 2 after addition of  $\text{NaHSO}_3$  and the iodate, which was converted to iodide, is then separated with iodide using the same method as for  $^{129}\text{I}^-$ . The concentration of  $^{129}\text{IO}_3^-$  is calculated by the difference between total inorganic  $^{129}\text{I}$  and  $^{129}\text{I}^-$ . The  $^{125}\text{I}$  tracer experiment showed that the recovery of iodine in this method is higher than 85%, and cross contamination of  $^{129}\text{I}^-$  and  $^{129}\text{IO}_3^-$  is less than 2% [137]. This separation

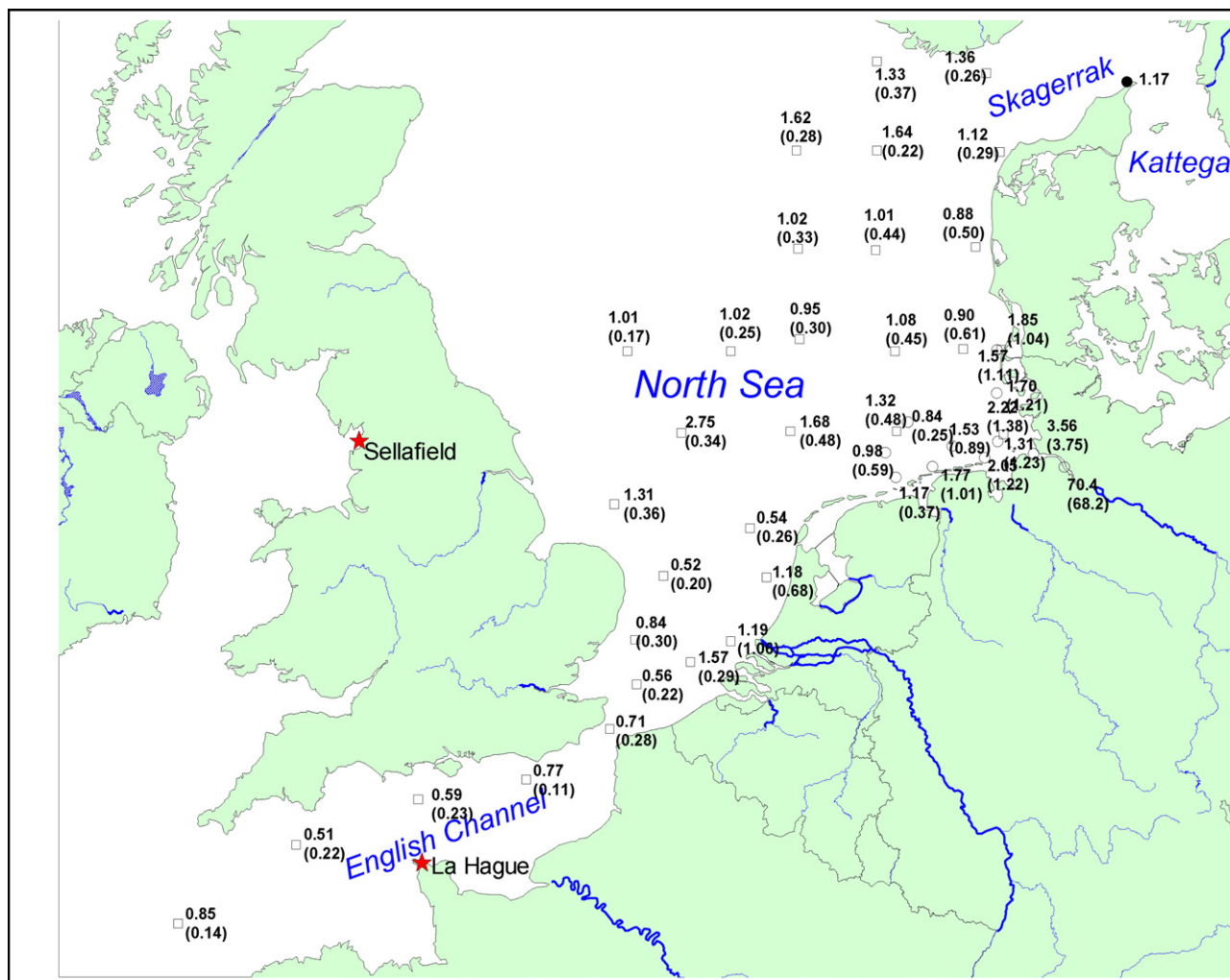


Fig. 7. Distribution of iodide/iodate ratios for  $^{129}\text{I}$  (upper number) and  $^{127}\text{I}$  (in parentheses) in Seawater from the English Channel and North Sea.

method is suitable for the *in situ* work in the field or on board of a ship.

$^{129}\text{I}$  discharged from reprocessing plants at La Hague and Sellafield has been used as a specific source of  $^{129}\text{I}$  in the Nordic seawater. The signal of  $^{129}\text{I}$  is used as a tracer to investigate marine geochemical cycle of stable iodine and in particular for conversion mechanisms of different chemical species of iodine as well as distinguishing newly produced from converted iodine species. Hou et al. [15,23] have measured iodide and iodate in seawater collected from the English Channel, North Sea, as well as Kattegat and Baltic Sea. The ratios of iodide/iodate for  $^{129}\text{I}$  and  $^{127}\text{I}$  in these waters are shown in Fig. 7, which indicates significantly different speciation distribution for  $^{129}\text{I}$  and stable iodine ( $^{127}\text{I}$ ). It was concluded that: (1) a rapid reduction of iodate to iodide occurs along the European continental coastal area, (2) oxidation of the new produced iodide to iodate does not occur during its transit along the European continental coast and (3) reduction of iodate or oxidation of iodide in the open sea seems to be a slow process [15]. The ratio of  $^{129}\text{I}/^{127}\text{I}$  for iodate in the Baltic seawater is much higher than that for iodide and close to the level in the Kattegat. This result suggests that  $^{129}\text{I}$  in the iodate form in Baltic Sea water seems originated from the Kattegat, and implies a slow reduction process of iodate in the Baltic Sea.

River flood can also provide  $^{129}\text{I}$  in the estuary areas as observed by speciation analysis of  $^{129}\text{I}$  and  $^{127}\text{I}$  in Galveston Bay, Texas, USA [17]. Organic  $^{129}\text{I}$  from the terrestrial source was observed in water with salinity up to about 20 within the Bay area, which agrees with the observation from stable isotopes, such as  $^{13}\text{C}$  and  $^{14}\text{N}$ , and suggested that organic  $^{129}\text{I}$  can be used as a tracer for the dissolved organic carbon in coastal zones.

## 5.2. Speciation of $^{129}\text{I}$ in atmosphere

As mentioned above, iodine in the atmosphere exists as particle associated, inorganic gaseous iodine (such as  $\text{I}_2$ ,  $\text{HI}$ ,  $\text{HIO}$ ) and organic gaseous iodine ( $\text{CH}_3\text{I}$ ,  $\text{CH}_2\text{I}_2$ ,  $\text{CH}_3\text{CH}_2\text{CH}_2\text{I}$ , etc.). Due to very low concentration of  $^{129}\text{I}$  in the atmosphere, the determination of individual species of  $^{129}\text{I}$  is difficult. The speciation analysis of  $^{129}\text{I}$  is mainly focused on the determination of three fractions of  $^{129}\text{I}$  (particle associated, inorganic and organic gaseous  $^{129}\text{I}$ ) [20,138], as well as the distribution of  $^{129}\text{I}$  in different size of particulates [139]. The main technique used for collection of three fractions of  $^{129}\text{I}$  is illustrated in Fig. 8 (Hou, unpublished). The sampler consists of multistage collector/trapper which is finally connected to a vacuum pump. Particle associated iodine is first collected by a membrane with small size pore ( $<0.45\ \mu\text{m}$ ), the

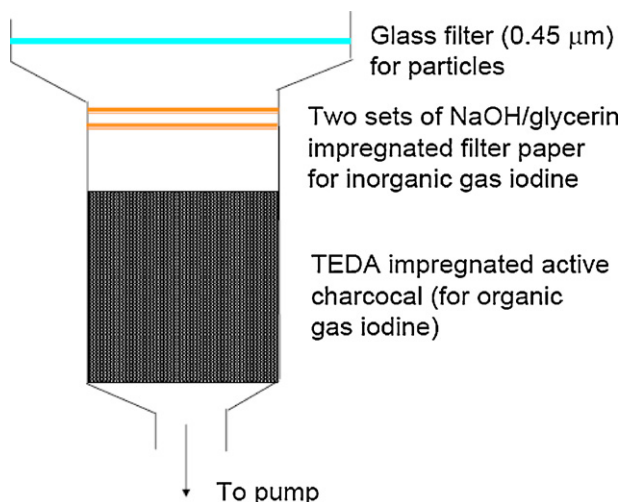


**Fig. 8.** Diagram of air sampler for collecting particle associated iodine, inorganic gaseous iodine and organic gaseous iodine.

gaseous iodine pass through the membrane, of which inorganic species, such as  $I_2$  and  $HI$ , is then trapped by cellulose filter papers previously impregnated with  $NaOH$ /glycerin. For completely trapping of the inorganic gaseous iodine, two cascade filter papers are used. Following the filter papers, an active charcoal column with length of 2.5 cm is used for trapping organic gaseous iodine. To obtain a sufficient trapping efficiency, the active charcoal was previously impregnated with tetrabutylammoniumhydroxide (TBAH) or triethylenediamine (TEDA) solution. Experiments have shown a satisfactory separation of three fractions of iodine [70,71]. Iodine in the collected fractions is then separated by combustion using a tube oven (Fig. 5), and trapped in  $NaOH$  solution, then extracted using  $CCl_4$  or  $CHCl_3$  and prepared as  $MgI_2$  or  $AgI$  for measurement. Besides  $^{129}I$ , stable iodine in the atmosphere is normally also required in order to obtain the  $^{129}I/^{127}I$  value, which is more useful instead of only  $^{129}I$  concentration. In this case, the stable iodine blank in collecting materials, such as filters, active charcoal, TBAH and/or TEDA is very important. A low iodine blank charcoal and chemical reagent have to be chosen. A low iodine content TEDA (Sigma, Germany) with iodine concentration of  $6.5 \text{ ng g}^{-1}$  was used in the author's laboratory, comparing with a similar reagent of TBAH (20% solution in water for synthesis, Merck, Germany) with an iodine concentration of  $164 \text{ ng mL}^{-1}$ . In addition, for reducing iodine blank in active charcoal,  $NaOH$  solution leaching and heating at high temperature ( $900\text{--}1000^\circ\text{C}$ ) under nitrogen condition have been used [71], however, our experiment showed that only less than half of iodine in the charcoal can be removed by these methods. It is therefore better to find a low iodine blank charcoal. A low iodine content active charcoal (for chromatography, Merck, Germany) was used in the author's laboratory, in this charcoal, the total iodine concentration of only  $40 \text{ ng g}^{-1}$  was measured, after washing with  $NaOH$  solution, the iodine concentration was reduced to  $30 \text{ ng g}^{-1}$ . The concentration of iodine in TEDA impregnated charcoal was measured to be only  $45 \text{ ng g}^{-1}$ , which is more than 30 times lower than the commercial TEDA impregnated charcoal specific designed for trapping radioactive iodine (TEDA Carbon Cartridge, The Staplex Company, Brooklyn, USA), we have measured iodine concentration in this charcoal to be  $1400 \text{ ng g}^{-1}$ .

Several investigations have been carried out to measure different species of  $^{129}I$  in atmosphere. Wershofen and Aumann [20] have measured  $^{129}I$  and  $^{127}I$  in three fractions in the atmosphere

collected from locations with varying distance (0–23 km) to the WAK reprocessing plant in Germany. They observed a different distribution of  $^{129}I$  and  $^{127}I$  in these three fractions. Particle associated  $^{129}I$  ranges at 2–30% of total  $^{129}I$ , while the corresponding  $^{127}I$  ranges at 12–28% of total iodine. The gaseous inorganic  $^{129}I$  fraction ranges at 17–35% while the  $^{127}I$  is 1.5–27%. Similarly large variation is found between gaseous organic  $^{129}I$  (34–98% of total  $^{129}I$ ), and  $^{127}I$  (46–74% of total iodine). It was also noticed that the closer the location to the reprocessing plant, the higher the percentage of gaseous organic  $^{129}I$ , while no such a trend was observed for  $^{127}I$ . This feature indicates that equilibrium between  $^{129}I$  and  $^{127}I$  in the atmosphere takes long time due to different sources and species.  $^{129}I$  species in the atmosphere near the Sellafield reprocessing plant (1.3 km northern northwest) was also measured. It was found that 63–100% of  $^{129}I$  was organic gaseous  $^{129}I$ , while inorganic gaseous and particle associated  $^{129}I$  compose less than 21% and 17% respectively (Ferozan, personal communication). Although direct measurement of  $^{129}I$  species in the atmosphere from the stack in reprocessing plants is not available, it was estimated that in one stack in Sellafield reprocessing plant, 70% iodine was released as inorganic  $^{129}I$  (mostly  $I_2$ ) and 30% of organic  $^{129}I$ . In another stack in the same reprocessing plant, 100%  $^{129}I$  is released as organic  $^{129}I$  (Ferozan, personal communication). However, the measured  $^{129}I$  in the environment was mainly organic gaseous  $^{129}I$  [20, Ferozan, personal communication].

Comparing with  $^{129}I$  released to the atmosphere from the stacks in reprocessing plants, a large amount of  $^{129}I$  has been discharged to the English Channel from La Hague reprocessing plant and to the Irish Sea from Sellafield reprocessing plant (Fig. 2). It is well known that iodine in the ocean is emitted to the atmosphere as methyl iodide and other gaseous forms, which may contribute to the  $^{129}I$  load in the atmosphere. It has been accepted for a long time that iodine in the ocean is the main source of iodine on land [137,140]. However, recent data suggest that releases from the terrestrial pool, vegetation and soil can add significant amounts to the atmosphere [141,142]. It was also argued that comparable iodine deposition in the coastal and the inland areas suggests that iodine flux to soil from terrestrial plant release is comparable to those from the ocean [141,142]. One measurement of  $^{129}I$  species in atmosphere over the North Sea has been carried out indicating that particle associated, inorganic and organic gaseous  $^{129}I$  were 18%, 43% and 40% respectively, with a similar distribution for  $^{127}I$ . The  $^{129}I/^{127}I$  values in different fractions were significantly different with the highest value ( $8.4 \times 10^{-7}$ ) in particle, lowest value in inorganic gas fraction ( $1.2 \times 10^{-7}$ ) and  $3.1 \times 10^{-7}$  in organic gas fraction [39]. This indicates different sources of  $^{129}I$  and  $^{127}I$  in the atmosphere and also shows that  $^{129}I$  can be used as a potential tracer for the geochemical cycle of stable iodine such as transfer of iodine from ocean to atmosphere, soil, plant and humans.

During the Chernobyl accident, a large amount of radioactivity was released to the atmosphere, including  $^{129}I$ ,  $^{131}I$ , and other iodine radioisotopes. Unfortunately, data on  $^{129}I$  speciation in the source plume from the accident is not available, but it was supposed that most of  $^{129}I$  and  $^{131}I$  have been released as  $I_2$ . Measurements carried out in Lithuanian and Japan for speciation of  $^{129}I$  and  $^{131}I$  during the Chernobyl accident [70,138] indicated that 60–80% was observed in organic gaseous form, whereas the inorganic gas composes less than 10%, and the particle associated form is less than 35%. The high fraction of organic form of  $^{129}I$  and  $^{131}I$  may be attributed to conversion during long distance (longer time) transport of the radioactive plume.

The availability of radionuclides in the atmosphere is not only related to their species, but also to the size of the particles. The size distributions of  $^{129}I$  and  $^{131}I$  associated particles in the

atmosphere have been investigated using cascade impactor air sampler [139,143,144]. It was observed that  $^{129}\text{I}$  and  $^{131}\text{I}$  are mainly associated with fine particles, with a  $^{129}\text{I}$  activity median aerodynamic diameter (AmAD) of  $0.4\text{ }\mu\text{m}$  [139]. A similar distribution pattern was also observed for  $^{131}\text{I}$  originated from the Chernobyl accident (with an AmAD of  $0.2\text{--}0.4\text{ }\mu\text{m}$ ) [143,144].

### 5.3. $^{129}\text{I}$ speciation in soil and sediment

Direct measurement of iodine speciation in soil and sediment is normally difficult, but techniques such as X-ray absorption near-edge structure (XANES) and extended X-ray absorption fine structure spectra (EXAFS) have been utilized. The relatively low concentration of  $^{129}\text{I}$  in the environment and the low sensitivity of XANES and EXAFS make direct measurement of  $^{129}\text{I}$  even more difficult. Therefore, sequential extraction or selective extraction is normally applied for separation of different components (speciation) of soil and sediment. A sequential extraction procedure that was proposed by Tessier et al. [145] has found wide applications. In this method the iodine was separated as water-soluble, exchangeable, carbonate, metal oxides (reducible), organic bound, and residue (mineral bound). Because iodine is easily volatile in acidic and oxidizing condition, modification of the original procedure has to be performed in order to avoid iodine loss during the extraction.

For the sequential extraction separation, the batch method is normally applied for easy operation and apparatus requirement. However, this method is time consuming, steady state leaching process and is associated with risk of cross contamination and re-adsorption. To overcome these shortages, a dynamically extraction method was therefore proposed for sequential extraction of some radionuclides [146], and has been applied for iodine fractionation/speciation in soil and sediment samples in the authors' lab.

In the batch sequential extraction procedure, the water-soluble iodine is first extracted using water and the leachate is separated by centrifuge. Remained solid is then treated with  $\text{CaCl}_2$ ,  $\text{MgCl}_2$  or  $\text{NH}_4\text{OAc}$  solution (pH 7–8) to recover exchangeable fraction. Remained residue from this treatment is extracted again using  $\text{NH}_4\text{OAc}$ , but at pH 5 for carbonate. All these steps are operated at room temperature. Afterward, the oxyhydroxides (or reducible) fraction is extracted using  $\text{NH}_2\text{OH}\cdot\text{HCl}\text{--HOAc}$  at pH 2 and the remained sample is finally extracted for organic fraction using  $\text{H}_2\text{O}_2\text{--HNO}_3$  at pH 2 or  $\text{NaOH}$  or  $\text{NH}_2\text{OH}\cdot\text{HCl}\text{--carbonate}$  (pH 8–9). These two steps are carried out at  $80\text{--}100\text{ }^\circ\text{C}$ . The remained fraction is treated as a residue. A schematic diagram of the whole procedure is shown in Fig. 9. Use of  $\text{H}_2\text{O}_2\text{--HNO}_3$  for the extraction of organic fraction means that the iodine will be oxidized to  $\text{I}_2$  and lost during the extraction. Therefore a use of  $\text{NaOH}$  ( $0.3\text{ mol L}^{-1}$ ) or  $\text{NH}_2\text{OH}\cdot\text{HCl}\text{--carbonate}$  is a recommended alternative method for extraction of iodine in organic fraction [21,77]. To completely destroying organic substances, treatment with  $\text{NaClO}$  decomposition is followed after the  $\text{NaOH}$  or  $\text{NH}_2\text{OH}\cdot\text{HCl}\text{--carbonate}$  extraction [147]. Another approach is to extract the organic fraction using  $\text{H}_2\text{O}_2\text{--HNO}_3$ , but both residues (before and after the extraction) are analyzed for iodine and the difference in iodine content of these two samples is calculated as the organic fraction [36].

For soil or sediment with high organic matter content, the order of sequential extraction may be partly modified due to the wrapping of grains by organic matters that may reduce the extraction efficiency during the different steps, especially for the oxides fraction step. Additionally, the released iodine from the sample may be easily re-adsorbed to organic matters during oxidizing and acid condition. For this purpose, iodine associated to organic fraction may be extracted before the oxides fraction and after the carbon-

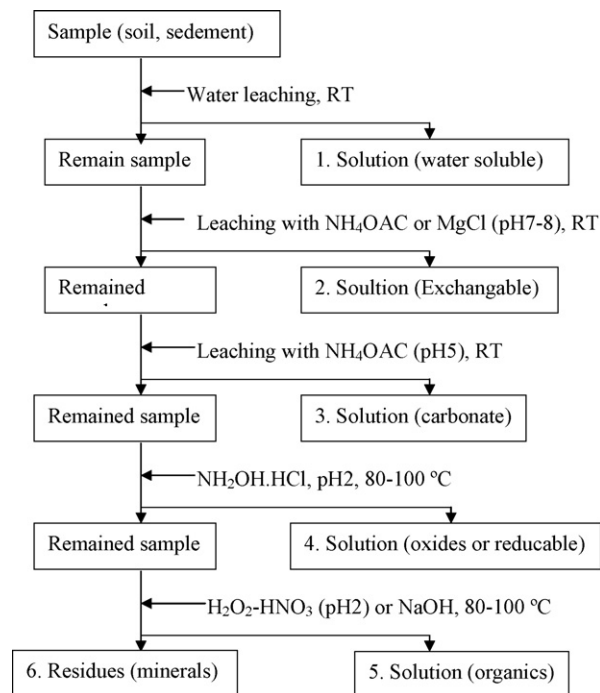


Fig. 9. Sequential extraction procedure for fractionation of iodine in soil and sediment samples.

ate fraction using  $\text{NaOH}$  or  $\text{NaOCl}$ . In this case, oxides component can be decomposed and iodine binding to this component can be completely released.

$^{129}\text{I}$  in the separated fractions is then further purified by  $\text{CCl}_4$  (or  $\text{CHCl}_3$ ) extraction after conversion of all iodine to iodide form. For the organic fraction, if  $\text{NH}_2\text{OH}\cdot\text{HCl}\text{--carbonate}$  or  $\text{NaOH}$  method is used, a further decomposition using  $\text{NaOCl}$  may be needed before the  $\text{CCl}_4$  extraction.  $^{129}\text{I}$  in the final residue can be separated using the same method as that for total  $^{129}\text{I}$  in soil and sediment sample, i.e. combustion or alkali fusion, described in the Section 4.3.

Schmitz and Aumann [21] have analyzed soils collected from a region closed to the WAK reprocessing plant in Germany and found a relatively higher percentage of  $^{129}\text{I}$  in water-soluble (39–49%), exchangeable (7–20%), and residue (25–70%) fractions compared to the organic (4–15%), oxides (7–13%) and carbonate (3–8%) fractions. However, a different distribution of stable iodine ( $^{127}\text{I}$ ) was observed where only <4% occurs in the water-soluble fraction. This difference between  $^{129}\text{I}$  and stable iodine may be attributed to the different sources of the two isotopes.  $^{129}\text{I}$  has mainly short period anthropogenic sources, while  $^{127}\text{I}$  has both natural and anthropogenic sources and resided in the soil for a relatively long time. This implies that chemical equilibrium between  $^{129}\text{I}$  and stable  $^{127}\text{I}$  within the soil environment may take a long time and resulting in different speciation patterns with respect to mobility and bioavailability of the two isotopes. Apparently, this result shows that  $^{129}\text{I}$  in the soil is more mobile and bioavailable than  $^{127}\text{I}$ .

Another distribution pattern of  $^{129}\text{I}$  is observed in the soil and sediment collected from coastal and estuarine area around the Sellafeld reprocessing plant [76] compared to that observed in the soil from near the WAK reprocessing plant [21]. Higher percentage of  $^{129}\text{I}$  was found in oxides (53–66%) and organic (23–43%) fractions, whereas only <7.5% was found in the other fractions (the residue was not included). A similar result was also obtained from soil sample (2–4 cm depth) collected from the Chernobyl accident contaminated area (10 km to Chernobyl power plant) and in sediment from the Irish Sea. In both materials,  $^{129}\text{I}$  in the oxides (30–40%) and



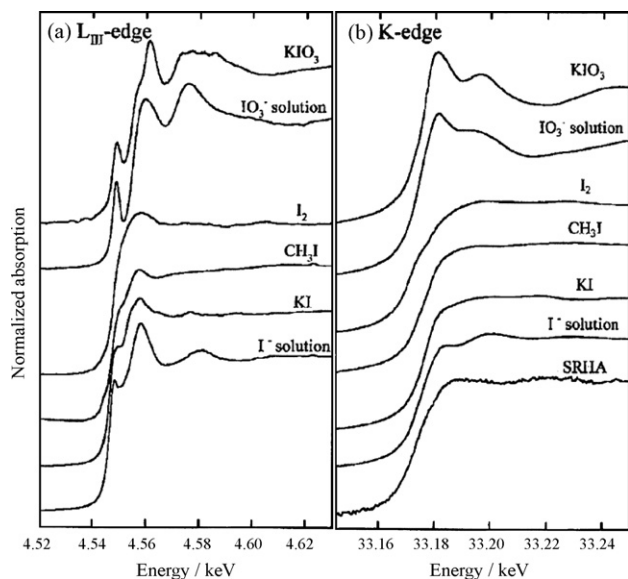


Fig. 10. Iodine L3-edge (a) and K-edge (b) XANES spectra of different iodine species reference materials [152].

organic (40–48%) fractions is higher than in the water-soluble fraction (6–13%) [22]. Results from sediment samples (organic content >50%) collected from a lake (in central Sweden) showed that most  $^{129}\text{I}$  is bound to the organic fraction (50–85%), whereas the water-soluble, exchangeable and carbonate fraction contain 5–8%, but relatively higher than  $^{127}\text{I}$  (2–4%). The oxides-related fraction contains <2% of  $^{129}\text{I}$  and  $^{127}\text{I}$  respective total content [147]. The different distribution of  $^{129}\text{I}$  in the near source area materials (Chernobyl, Sellafield and WAK) compared with far from source materials (central Sweden) may relate to conversion of  $^{129}\text{I}$  species upon transport as well as environmental conditions at the sampling site.

Besides fractionation, the chemical speciation of iodine in leachate, especially in water-soluble and exchangeable fraction can be carried out to investigate the chemical forms of iodine in soil and sediment sample. The method used for the speciation of iodine in water sample can be used for this purpose. Yuita [78] has investigated the chemical speciation of stable iodine in soil solution (water-soluble), high iodide percentage was observed in flood and anoxic condition, while iodate is the dominant species in non-flood and oxidizing condition. Data on the  $^{129}\text{I}$  speciation in soil solution are still lacking.

The direct measurement of *in situ* iodine speciation, especially in solid sample, is performed using XANES and EXAFS, which can be used to provide information on the local structure, coordination number and oxidation state of a range of elements in solution, solid form or at a solution–solid interface [147–149]. Using XANES a high intensity monochromatic X-ray beam (usually provided by a synchrotron source) is tuned through a range of energies from a few tens of eV below to about 100 eV above the binding energy of a core electron (e.g. iodine K-edge 33.17 keV and iodine L3-edge 4.557 keV) while keeping the beam on the same spot on the sample. The attenuation of the X-rays varies smoothly with incident energy until a critical energy is reached (i.e. core electron binding energy) and absorption (and fluorescence) abruptly increases. This discontinuity corresponds to the ejection of a core electron from an atom and is called the absorption edge, while the main absorption feature is referred to as the white line. The energy position of the white line is characteristic of the excited atom. The fine structure and position of the absorption edge can reveal information on the oxidation state of the element and its chemical surrounding (Fig. 10). This can readily

be utilized as a “fingerprinting” technique by comparing reference samples with unknown samples [100]. Further speciation information can be obtained at the same time by extending the energy range (~50–1000 eV above absorption edge) over which the data are collected, i.e. EXAFS (the entire structured absorption region (XANES + EXAFS) is also referred to as XAFS). EXAFS can give additional information on the coordination numbers and bond lengths to first, second and even more distant neighbor atoms [150]. However, EXAFS works best for ideal systems and information on the local structure is often needed before beginning an analysis [151].

Shimamoto and Takahashi [152] found that despite iodine K-edge XANES profiles are relatively featureless compared to those of  $\text{L}_{\text{III}}$  XANES, analysis of soil with iodine concentrations of  $55\text{ }\mu\text{g g}^{-1}$  and high Ca concentrations in particular, should preferably be carried out at the K-edge because of the lower detection limit (avoiding the interference of Ca K X-rays with  $\text{I L}\alpha$ ). They identified that the iodine in the soil is mainly as organic form. However, the detection limit of XANES is too high ( $>10\text{ }\mu\text{g g}^{-1}$  or  $>70\text{ Bq g}^{-1}$  for  $^{129}\text{I}$ ) to measure  $^{129}\text{I}$  in environmental samples. Reed et al. [100] utilized iodine K-edge XANES in an attempt to identify the speciation of 10–100 ppm concentrations of  $^{129}\text{I}$  ( $70\text{--}700\text{ Bq g}^{-1}$ ) in nuclear waste reprocessing solvent (tri-*n*-butyl phosphate in odourless kerosene (TBP/OK)) from Sellafield reprocessing plant. The XANES profile of the waste sample resembled those of organoiodide reference samples. However, the presence of some molecular iodine could not be excluded due to the similarities between organoiodide and  $\text{I}_2$  XANES spectra and poor statistics related to low concentrations. Other inorganic species of iodine appears to be relatively easy to deduce from organic species because they tend to have more structure in the post-edge region [100]. Employing  $\text{I L}_{\text{III}}$  XANES and EXAFS, Schlegel et al. [153] were able to show that iodine in naturally iodinated humic substances is aromatic-bound. XANES and EXAFS are qualitative analytical techniques, which means that information on distribution of different species of elements or radionuclides could not be supplied. Artifacts in XANES experiments due to radiation damage have been reported for several types of samples [154] and elements including iodine [152]. To monitor possible beam damage, energy scans repeated several times for each position of interest may be compared.

#### 5.4. $^{129}\text{I}$ speciation in biological samples

A large number of investigations have been carried out on the speciation of stable iodine, and on the determination of total  $^{129}\text{I}$  in biological samples including seaweed, grass, and thyroid. However, to our knowledge, published data on the speciation of  $^{129}\text{I}$  in biological samples are not available. The separation of different species of stable iodine in biological samples, such as blood, milk, urine, homogenate of tissues and extractions of plants is normally carried out by high performance liquid chromatography (HPLC), electrophoresis, and gel chromatography [57–60,62,155–157]. These methods are suitable for the species separation of stable iodine in biological samples, especially for organic species of iodine. However, the size of sample applied for the analysis is normally small (<1 mL), which is not suitable for  $^{129}\text{I}$  due to minute concentration compared to stable iodine in biological samples ( $^{129}\text{I}/^{127}\text{I} < 10^{-6}$ ).

The speciation analysis of  $^{129}\text{I}$  normally needs a large amount samples (>5 g) and the separation methods developed by Hou et al. [42,43,57] for seaweed and tissues are suitable for the speciation of  $^{129}\text{I}$ . For tissue samples, various sub-cellular fractions of tissue are separated using gradient centrifugation, these fractions include nuclei, cytosol, mitochondria, lysosome, and microsome. The iodine-bound proteins in cytosol of tissue are separated using gel chromatography (exclusion chromatography) for different molecular size. For the speciation analysis of  $^{129}\text{I}$  in

seaweed, various fractions such as water-soluble iodine, soluble organic iodine, iodide, iodate, and protein-, pigment-, polyphenol- or polysaccharide-bound iodine can be separated using the method developed by Hou et al. [42,43]. The soluble iodine was first separated from the seaweed by water leaching, iodide, iodate, and organic iodine in the leachate can be then separated by using the anion exchange method as that used for water samples (Fig. 4) [23]. To investigate combination of  $^{129}\text{I}$  in different components, such as protein, polyphenol, and pigment, several procedures can be used [43]. The separated organic binding  $^{129}\text{I}$  fractions needs to be decomposed to be converted into inorganic iodine, in which the ashing or combustion method described above can be used. The inorganic iodine is finally concentrated and purified by  $\text{CCl}_4$  extraction and precipitated as  $\text{AgI}$  for AMS measurement.

## 6. Bioavailability and radiation toxicity of $^{129}\text{I}$

The bioavailability of an element in the environment depends on its species. For  $^{129}\text{I}$ , there are practically scattered or almost lack of data about this issue. The various values of transfer factor (concentration of element in plant divided by that in the soil it grows on) of  $^{129}\text{I}$  from soil to the grass (from 0.07 to 2.9 dry/dry weight) may reflect the different species of  $^{129}\text{I}$  in the soil [158]. It is expected that the water-soluble and exchangeable  $^{129}\text{I}$  can easily be taken up by plants through root, while bound in other fractions, such as organic, oxides and minerals is more difficult to be taken up. However, uptake of iodine by leaves from atmosphere is also a main pathway of iodine in plants.

It was reported that the bioavailability of iodine through potassium iodide to human (or mammals) is 96.4%, while the bioavailability of iodine through organic forms such as moniodotyrosine is 80.0%. A high bioavailability of iodine in seaweed *Gracilaria verrucosa* and *Laminaria hyperborean* (80–99%) was also observed [159]. Jahreis et al. [160] investigated the uptake of iodine through diet in 12 women, and found that 89% of iodine was excreted in the urine, and 11% in the faeces. However, Wahl et al. [161] reported low uptake of iodine from normal diet where only 16–18% of the alimentary iodine was excreted in the urine. This may indicate that the type of diet and species of iodine in the foodstuff are factors affecting bioavailability of iodine to human. A relatively low water (or acid) leaching rate of iodine (28–40%) from vegetable (spinach and green seaweed) was reported by Hou et al. [43].

Iodine in food is digested and absorbed in stomach and small intestine and passes into blood. Inhaled iodine from the air is also transferred into blood. Most of iodine absorbed into the blood is concentrated in the thyroid, and small part of iodine is directly excreted to the urine depending on the total amount of iodine in the diet. Most of iodine (>80%) in the human body (or mammal) concentrated in the thyroid, which is therefore the target organ (to it a specific element or compound is concentrated) of iodine (including radioactive  $^{129}\text{I}$ ). An average iodine content in adult thyroid is 10–15 mg, essentially combined with thyroglobulin, which is breakdown to the hormones triiodothyronine ( $\text{T}_3$ ) and thyroxine ( $\text{T}_4$ ) and released to the blood and transferred to other body tissues. The thyroid takes up stable and radioactive iodine indiscriminately. Due to low beta and gamma energy of  $^{129}\text{I}$  (Table 1), radiation toxicity of  $^{129}\text{I}$  is therefore mainly related to internal exposure of the thyroid to the beta radiation of  $^{129}\text{I}$ . However, long half-life of  $^{129}\text{I}$  ( $1.57 \times 10^7$  years) means long-term and low dose exposure.  $^{129}\text{I}$  concentration (or  $^{129}\text{I}/^{127}\text{I}$  value) in thyroid can be supposed to be equilibrium with  $^{127}\text{I}$  the diet. It was reported that the equilibrium dose rate of  $^{129}\text{I}$  in the thyroid is  $0.151 \text{ mSv Bq}^{-1} \text{ y}^{-1}$  and  $0.0161 \text{ mSv Bq}^{-1} \text{ y}^{-1}$  for a 1-year-old child and an adult, respectively [162]. A value of  $10^{-6}$  for  $^{129}\text{I}/^{127}\text{I}$  ratio in thyroid means an amount of  $^{129}\text{I}$  at about  $10^{-9} \text{ g}$  (or  $6.55 \text{ mBq}$ ) and  $10^{-8} \text{ g}$  (or

$65.5 \text{ mBq}$ ) on the assumption of 1 and 10 mg stable iodine in thyroid for the 1-year-old child and adult respectively. The corresponding equilibrium annual dose equivalent to the thyroid can be therefore calculated to be about  $10^{-3} \text{ mSv y}^{-1}$  for both 1-year child and adult. In an environment without direct contamination from nuclear facilities,  $^{129}\text{I}/^{127}\text{I}$  ratio is much lower than  $10^{-6}$ , which implies an effective radiation dose to thyroid from the internal exposure of  $^{129}\text{I}$  is less than  $10^{-3} \text{ mSv y}^{-1}$ . This value is 40 times lower than the U.S. NRC regulation dose limit of  $0.04 \text{ mSv y}^{-1}$  for combined beta and photon emitting radionuclide to the whole body or any organ, and even 1000 times lower than the annual radiation dose of about  $1 \text{ mSv}$  from natural background radiation [163]. The highest  $^{129}\text{I}/^{127}\text{I}$  value reported is  $10^{-4}$ , in areas close to nuclear facility such as reprocessing plants [77,98,104,105,108,113], which corresponds to an annual radiation dose of  $0.1 \text{ mSv y}^{-1}$  to the thyroid. This value is only about 2.5 times higher than the regulation dose limit of  $0.04 \text{ mSv y}^{-1}$ . All these calculations don't consider the uptake of stable iodine from the diet with low  $^{129}\text{I}$  level. In order to prevent iodine deficiency disorder, iodine was supplied as iodinated salt or in other form to humans (and animals).  $^{129}\text{I}/^{127}\text{I}$  value in the iodinated food is much lower than the environmental level because stable iodine used for this purpose is normally produced from low  $^{129}\text{I}$  source ( $^{129}\text{I}/^{127}\text{I} < 10^{-9}$ ). In this case the  $^{129}\text{I}/^{127}\text{I}$  value in thyroid of humans or mammals will be significantly lower than the environmental level. This means a low radiation dose to the thyroid. Additionally, 10 times lower  $^{129}\text{I}/^{127}\text{I}$  value has been reported in the human (and animal) thyroid compared to the surrounding environment [36]. This feature implies that even in regions with high  $^{129}\text{I}/^{127}\text{I}$  value in the environment, the effective radiation dose of  $^{129}\text{I}$  to human thyroid is still lower than the regulation dose limit at present level. It has been mentioned above that there is about 68,000 kg of  $^{129}\text{I}$  stored in unprocessed spent fuel until 2005 which is 10 times more than the  $^{129}\text{I}$  released to the environment (<6000 kg). With the increasing number of nuclear power reactors, more  $^{129}\text{I}$  will be produced. If most of the spent fuel is going to be reprocessed, and  $^{129}\text{I}$  is released to the environment, it may increase the ratio of  $^{129}\text{I}/^{127}\text{I}$  to  $10^{-3}$ . In such a case, the annual dose to the thyroid may reach to  $1 \text{ mSv y}^{-1}$ , which excess the regulation radiation dose limit of  $^{129}\text{I}$  to thyroid ( $0.04 \text{ mSv y}^{-1}$ ) and comparable to the level of natural background radiation. Accordingly, from the view of radiation dose,  $^{129}\text{I}$  is less toxic at the present level or even higher level in the future. Le Guent et al. [164] estimated the radiation dose in a situation of high  $^{129}\text{I}$  exposure through diet and drinking water and found that the estimated effective dose is only 30 and  $60 \text{ mSv y}^{-1}$  at an uptake of  $153 \mu\text{g } ^{129}\text{I}$  per day for a 1-year child and an adult, respectively.

## 7. Summary and perspectives

The human nuclear activities, especially the releases from the spent nuclear fuel reprocessing plants, are presently the main source of  $^{129}\text{I}$  in the environment. The  $^{129}\text{I}$  concentration in environmental samples has increased 3–8 orders of magnitude compared with pre-nuclear era level, and reached to  $10^{-10}$  to  $10^{-4}$  for  $^{129}\text{I}/^{127}\text{I}$  ratio. Despite the importance of  $^{129}\text{I}$  speciation not only in radiation protection related to high mobility of iodine in nuclear waste depository and the environment and possible high bioavailability and concentration in human thyroid, but also in its application as an environmental tracer, the data are scarce. It is, therefore, the understanding of  $^{129}\text{I}$  speciation in the environment represents a vital tool for tracing transport mechanisms, distribution pathways and bioavailability in the environment. To achieve that, specific chemical extraction methods and high sensitivity analytical techniques have been developed recently. The reported works on  $^{129}\text{I}$  speciation mainly focus on water and atmosphere, and fractionation of  $^{129}\text{I}$  in soil and sediment. The methods used for speciation

analysis of  $^{129}\text{I}$  in water sample are based on anion exchange chromatography, and aimed for the determination of iodide, iodate and organically associated iodine.  $^{129}\text{I}$  speciation in seawater has shown potential tracer capability of sources. The method used for speciation of  $^{129}\text{I}$  in the atmosphere is based on trapping of different species by several filters, which separate  $^{129}\text{I}$  in three fractions, particle associated, inorganic gaseous and organic gaseous iodine. A few data have shown that speciation of  $^{129}\text{I}$  in atmosphere can supply useful information about the source and transfer pathway. The sequential extraction methods, normally used for various components of soil and sediment, have provided information about the water-soluble, exchangeable, carbonate, oxides, organic and mineral associated  $^{129}\text{I}$ . Some of the results have indicated different fractionation pathways for  $^{129}\text{I}$  and  $^{127}\text{I}$ . Until now there are no published data about the speciation of  $^{129}\text{I}$  in biological samples.

The bioavailability of  $^{129}\text{I}$  is expected to be strongly dependent on its speciation, where iodide and iodate have a higher bioavailability (uptake by plants and animals) than the fraction associated with organic matters. The radiation toxicity of  $^{129}\text{I}$  is relatively insignificant as the effective radiation dose to the thyroid is only about  $1\ \mu\text{Sv}\cdot\text{y}^{-1}$  at the present environmental level ( $^{129}\text{I}/^{127}\text{I}$  of  $10^{-6}$ ). This is 1000 times lower than the radiation dose from the natural background radiation ( $1\ \text{mSv}\cdot\text{y}^{-1}$ ). Even in the heavily contaminated areas ( $^{129}\text{I}/^{127}\text{I}$  of  $10^{-4}$ ), the radiation dose ( $0.1\ \text{mSv}\cdot\text{y}^{-1}$ ) is still 10 times lower than the dose from the nature background, and 2 times lower than the dose from natural  $^{40}\text{K}$  in human body.

## Acknowledgements

Authors (X.L. Hou and V. Hansen) thank Villum Kann Rasmussen Foundation for financial support. The authors also wish to thank the NKS-B programme for support of the SPECIATION project, which provided possibilities for cooperation of the authors from Nordic countries on this article.

## References

- [1] G.T.F. Wong, *Rev. Aquat. Sci.* 45 (1991) 45–73.
- [2] Y. Muramatsu, K.H. Wedepohl, *Chem. Geol.* 147 (1998) 201–216.
- [3] B. Salbu, *J. Environ. Radioact.* 96 (2007) 47–53.
- [4] U. Fehn, G. Snyder, P.K. Egeberg, *Science* 289 (2000) 2332–2335.
- [5] R.H. Nichols, G.M. Hohenberg, K. Kehm, Y. Kim, K. Marti, *Cosmochim. Acta* 58 (1994) 2553–2561.
- [6] G.M. Raisbeck, F. Yiou, Z.Q. Zhou, L.R. Kilian, *J. Mar. Syst.* 6 (1995) 561–570.
- [7] G.M. Raisbeck, F. Yiou, *Sci. Total Environ.* 238 (1999) 31–41.
- [8] J.C. Gascard, G. Raisbeck, S. Sequeira, F. Yiou, K.A. Mork, *Geophys. Res. Lett.* 31 (2004) 101308.
- [9] J.N. Smith, E.P. Jones, S.B. Moran, W.M. Smethie, W.E. Kieser, *J. Geophys. Res. Oceans* 111 (2005) C05006.
- [10] V. Alfimov, A. Aldahan, G. Possnert, *Geophys. Res. Lett.* 31 (2004) L19305.
- [11] V. Alfimov, A. Aldahan, G. Possnert, P. Winsor, *Mar. Pollut. Bull.* 49 (2004) 1097–1104.
- [12] N. Buraglio, A. Aldahan, G. Possnert, *Geophys. Res. Lett.* 26 (1999) 1011–1014.
- [13] X.L. Hou, H. Dahlgaard, S.P. Nielsen, *Estuar. Coast. Shelf Sci.* 51 (2000) 571–584.
- [14] X.L. Hou, H. Dahlgaard, S.P. Nielsen, J. Kucera, *J. Environ. Radiat.* 61 (2002) 331–343.
- [15] X.L. Hou, A. Aldahan, S.P. Nielsen, G. Possnert, H. Nies, J. Hedfors, *Environ. Sci. Technol.* 41 (2007) 5993–5999.
- [16] X.L. Hou, *J. Radioanal. Nucl. Chem.* 262 (2004) 67–75.
- [17] K.A. Schwehr, P.H. Santschi, D. Elmore, *Limnol. Oceanogr. Meth.* 3 (2005) 326–337.
- [18] P.H. Santschi, K.A. Schwehr, *Sci. Total Environ.* 321 (2004) 257–271.
- [19] J. Fabrykamartin, H. Bentley, D. Elmore, P.L. Airey, *Geochim. Cosmochim. Acta* 49 (1985) 337–346.
- [20] H. Wershofen, D.C. Aumann, *J. Environ. Radioact.* 10 (1989) 141–156.
- [21] K. Schmidt, D.C. Aumann, *J. Radioanal. Nucl. Chem.* 198 (1995) 229–236.
- [22] X.L. Hou, C.L. Fogh, J. Kucera, K.G. Andersson, H. Dahlgaard, S.P. Nielsen, *Sci. Total Environ.* 308 (2003) 97–109.
- [23] X.L. Hou, H. Dahlgaard, S.P. Nielsen, *Mar. Chem.* 74 (2001) 145–155.
- [24] J.S. Edmonds, M. Morita, *Pure Appl. Chem.* 70 (1998) 1567–1584.
- [25] J.V. Christensen, The behaviour of iodine in the terrestrial environment, Risø-M-2851, Risø National Laboratory, Denmark, 1990.
- [26] G. Snyder, U. Fehn, *Nucl. Instrum. Meth.* B223–224 (2004) 579–586.
- [27] Z.F. Chai, Z.Y. Zhang, W.Y. Feng, C.Y. Chen, D.D. Xu, X.L. Hou, *J. Anal. At. Spectrom.* 19 (2004) 26–33.
- [28] R.G. Wuilloud, J.C. Altamirano, *Curr. Anal. Chem.* 2 (2006) 353–377.
- [29] R.G. Wuilloud, J.C. Altamirano, Speciation of halogen compounds, in: E. Cornelis (Ed.), *Handbook of Elemental Speciation II*, John Wiley & Sons Ltd., 2003, pp. 564–620.
- [30] X.L. Hou, Iodine speciation in foodstuff, tissues and environmental samples, in: V.R. Preedy (Ed.), *The Comprehensive Handbook on Iodine*, Elsevier, 2009, Chapter 15.
- [31] S. Yoshida, Y. Muramatsu, *J. Radioanal. Nucl. Chem.* 196 (1995) 295–302.
- [32] Y. Muramatsu, S. Yoshida, *Geomicrobiol. J.* 16 (1999) 85–93.
- [33] M.H. Gerzabek, Y. Muramatsu, F. Strebl, S. Yoshida, *J. Plant Nutr. Soil Sci.* 162 (1999) 415–419.
- [34] X.L. Hou, X.J. Yan, *Sci. Total Environ.* 222 (1998) 141–156.
- [35] X.L. Hou, H. Dahlgaard, S.P. Nielsen, W.J. Ding, *Sci. Total Environ.* 246 (2000) 285–291.
- [36] X.L. Hou, H. Dahlgaard, S.P. Nielsen, A.F. Malencheko, J. Kucera, *Sci. Total Environ.* 302 (2003) 61–71.
- [37] X.L. Hou, C.F. Chai, Q.F. Qian, C.S. Li, Q. Chen, *Biol. Trace Elem. Res.* 56 (1997) 225–230.
- [38] Y. Liu, H.R. Gunten, Migration chemistry and behaviour of iodine relevant to geological disposal of radioactive wastes, A literature review with a compilation of sorption data, PSI-16, 1988, Paul Scherrer Institute, Switzerland.
- [39] R. Michel, K. Klipsch, Th. Ernst, M. Gorny, D. Jakob, J. Vahlbruch, H.-A. Synal, C. Schnabel, Ableitung von radioökologischen Parametern aus dem langfristigen Eintrag von Iod-129 (in German) Abschlussbericht zum Forschungsvorhaben StSch 4285, August 2004, in: Schriftenreihe Reaktorsicherheit und Strahlenschutz, BMU-2004-650, ISSN 1612-6386, <http://www.bmu.de/strahlenschutz/doc6872.php> und [www.zsr.uni-hannover.de](http://www.zsr.uni-hannover.de).
- [40] C. Schall, K.G. Heumann, G.O. Kirst, *Fresenius J. Anal. Chem.* 359 (1997) 298–305.
- [41] R.M. Moore, W. Graszko, *J. Geophys. Res.* 104 (1999) 11163–11171.
- [42] X.L. Hou, C.F. Chai, Q.F. Qian, X.J. Yan, X. Fan, *Sci. Total Environ.* 204 (1997) 215–221.
- [43] X.L. Hou, X.J. Yan, C.F. Chai, *J. Radioanal. Nucl. Chem.* 245 (2000) 461–467.
- [44] G.W. Luther, T. Ferdman, C.H. Culberson, J. Kostka, J.F. Wu, J.F. Estuar, *Coast. Shelf Sci.* 32 (1991) 267–279.
- [45] N.W. Truesdale, G. Nausch, A. Baker, *Mar. Chem.* 74 (2001) 87–98.
- [46] G.T.F. Wong, *Deep-Sea Res. Part 1* 42 (1995) 2005–2023.
- [47] S.D. Jones, V.W. Truesdale, *Limnol. Oceanogr.* 29 (1984) 1016–1028.
- [48] K.A. Schwehr, P.H. Santschi, *Anal. Chim. Acta* 482 (2003) 59–71.
- [49] M.L.A.M. Campos, P.D. Nightingale, T.D. Jickells, *Tellus* 48B (1996) 106–114.
- [50] S. Solomon, S.R. Garcia, A.R. Ravishankara, *J. Geophys. Res.* 99 (1994) 20491–20499.
- [51] J.P. Greeberg, A.B. Guenther, A. Turnipseed, *Environ. Chem.* 2 (2005) 291–294.
- [52] V.W. Truesdale, S.D. Jones, *J. Hydrol.* 179 (1996) 67–86.
- [53] P. Vaattovaara, P.E. Huttunen, Y.J. Yoon, J. Joutsensaari, K.E.J. Lehtinen, C.D. O'Dowd, A. Laaksonen, *Atmos. Chem. Phys.* 6 (2006) 4601–4616.
- [54] B.S. Gilfedder, M. Petri, H. Biester, *J. Geophys. Res. Atmos.* 112 (2007) D07301.
- [55] M.A.R. Abdel-Moati, *Mar. Chem.* 65 (1999) 211–225.
- [56] C. Reifenhäuser, K. Heumann, *Fresenius J. Anal. Chem.* 336 (1990) 559–563.
- [57] X.L. Hou, C.Y. Chen, W.J. Ding, C.F. Chai, *Biol. Trace Elem. Res.* 68 (1999) 69–76.
- [58] R. Simon, J.E. Tietge, B. Michalke, S. Degitz, K.W. Schramm, *Anal. Bioanal. Chem.* 372 (2000) 481–485.
- [59] P. Brätter, I.N. Blasco, V.E. Negretti de Brätter, A. Raab, *Analyst* 123 (1998) 821–826.
- [60] B. Michalke, *Pure Appl. Chem.* 78 (2006) 79–90.
- [61] M. Leiterer, D. Truckenbrodt, K. Franke, *Eur. Food Res. Technol.* 213 (2001) 150–153.
- [62] M. Shah, R.G. Wuilloud, S.S. Kannamkumaratha, J.A. Caruso, *J. Anal. At. Spectrom.* 20 (2005) 176–182.
- [63] F.C. Küpper, L.J. Carpenter, G.B. McFiggans, C.J. Palmer, T.J. Waite, E.M. Boneberg, S. Woitsch, M. Weiller, R. Abela, D. Grolimund, P. Potin, A. Butler, G.W. Luther III, P.M.H. Kroneck, W. Meyer-Klaucke, M.C. Feiters, *PNAS* 105 (2008) 6954–6958.
- [64] C.J. Palmer, T.L. Anders, L.J. Carpenter, F.C. Kupper, G.B. Mcfiggans, *Environ. Chem.* 2 (2005) 282–290.
- [65] R. von Glasow, *Environ. Chem.* 2 (2005) 243–244.
- [66] C.D. O'Dowd, J.L. Jimenez, R. Bahreini, R.C. Flagan, J.H. Seinfeld, K. Hameri, L. Pirjola, M. Kulmala, S.G. Jennings, T. Hoffmann, *Nature* 417 (2002) 632–636.
- [67] K. Sellegri, Y.J.Y. Loon, S.G. Jennings, C.D. O'Dowd, L. Pirjola, S. Cautenet, H.W. Chen, T. Hoffmann, *Environ. Chem.* 2 (2005) 260–270.
- [68] M.V. Frontasyeva, E. Steinnes, *J. Radioanal. Nucl. Chem.* 261 (2004) 101–106.
- [69] H.E. Gabler, K.G. Heumann, *Int. J. Environ. Anal. Chem.* 50 (1993) 129–146.
- [70] H. Noguchi, M. Murata, *J. Environ. Radiat.* 7 (1988) 65–74.
- [71] H.E. Gabler, K.G. Heumann, *Fresenius J. Anal. Chem.* 345 (1993) 53–59.
- [72] K.A. Rahn, R.D. Borys, R.A. Duce, *Science* 192 (1976) 549–550.
- [73] A.R. Baker, *Geophys. Res. Lett.* 31 (2004) L23S02.



- [74] A.R. Baker, C. Tunnicliffe, T.D. Jickells, J. Geophys. Res. Atmos. 106 (2001) 28743–28749.
- [75] A.R. Baker, Environ. Chem. 2 (2005) 295–298.
- [76] J. Stutz, K. Hebestreit, B. Alicke, U. Platt, J. Atmos. Chem. 34 (1999) 65–85.
- [77] B.T. Wilkins, Investigations of  $^{129}\text{I}$  in the Natural Environment: Results and Implications, NRPB-R225, National Radiological Protection Board, UK, 1989.
- [78] K. Yuita, Soil Sci. Plant Nutr. 38 (1992) 281–287.
- [79] R.R. Edwards, Science 137 (1962) 851.
- [80] NCRP, Iodine-129: evaluation of releases from nuclear power generation, NCRP Report no.75 (National Council on Radiation Protection and Measurements, Bethesda MD), 1983.
- [81] U. Fehn, G.R. Holdren, D. Elmore, T. Brunelle, R. Teng, P.W. Kubik, Geophys. Res. Lett. 13 (1986) 137–139.
- [82] J.E. Moran, U. Fehn, R.T.D. Teng, Chem. Geol. 152 (1998) 193–203.
- [83] L.R. Kilius, A.E. Litherland, J.C. Rucklidge, N. Baba, Appl. Radiat. Isot. 43 (1992) 279.
- [84] J.E. Moran, A. Oktay, P.H. Santschi, D.R. Schink, Environ. Sci. Technol. 33 (1999) 2536–2542.
- [85] J. Handl, E. Oliver, D. Jakob, K.J. Johanson, P. Schuller, Health Phys. 65 (1993) 265.
- [86] R. Seki, E. Kimura, T. Takahashi, N. Ikeda, J. Radioanal. Nucl. Chem. 138 (1990) 17–31.
- [87] L.W. Cooper, T.M. Beasley, X.L. Zhao, C. Soto, K.L. Vinogradova, K.H. Dunton, Mar. Biol. 131 (1998) 391.
- [88] U. Rao, U. Fehn, Cosmochim. Acta 163 (1999) 1927–1939.
- [89] H. Reithmeier, V. Lazarev, W. Rühm, M. Schwikowski, H. Gäggeler, E. Nolte, Environ. Sci. Technol. 40 (2006) 5891–5896.
- [90] D.R. Schink, P.-H. Santschi, O. Corapcioglu, P. Sharma, U. Fehn, Earth Planet. Sci. Lett. 135 (1995) 131–138.
- [91] T. Suzuki, S. Kabuto, H. Amano, O. Togawa, Quaternary Geochronol. 3 (2007) 268–275.
- [92] D. Gallagher, E.J. Mcgee, P.I. Mitchell, V. Alfimov, A. Aldahan, G. Possnert, Environ. Sci. Technol. 39 (2005) 2927–2935.
- [93] M. Paul, D. Fink, D.G. Hollos, A. Kaufman, W. Kutschera, M. Magaritz, Nucl. Instrum. Meth. B29 (1987) 341–345.
- [94] T. Straume, L.R. Anspaugh, A.A. Marchetti, G. Voigt, V. Minenko, F. Gu, P. Men, S. Trofimik, S. Tretyakevich, V. Drozdovitch, E. Shagalova, O. Zhukova, M. Germentchuk, S. Berlovich, Health Phys. 91 (2006) 7–19.
- [95] V. Mironov, V. Kudrjashov, F. Yiou, G.M. Raisbeck, J. Environ. Radioact. 59 (2002) 293–307.
- [96] A. Aldahan, V. Alfimov, G. Possnert, Appl. Geochem. 228 (2007) 606–618.
- [97] IAEA, Energy, electricity and nuclear power: developments and projections, International Atomic Energy Agency, STI/PUB/1304, 2007, [http://www-pub.iaea.org/MTCD/publications/PDF/Pub1304\\_web.pdf](http://www-pub.iaea.org/MTCD/publications/PDF/Pub1304_web.pdf).
- [98] B.G. Fritz, G.W. Patton, J. Environ. Radioact. 86 (2006) 64–77.
- [99] A.W. Castleman, I.N. Tang, H.R. Munkelwitz, J. Inorg. Nucl. Chem. 30 (1968) 5–13.
- [100] W.A. Reed, I. May, F.R. Livens, J.M. Charnock, A.P. Jeapes, M. Gresley, R.M. Mitchell, P. Knight, J. Anal. At. Spectrom. 17 (2002) 541–543.
- [101] J. Gray, S.R. Jones, A.D. Smith, J. Radiol. Prot. 15 (1995) 99–131.
- [102] IRRIN, Inventaire des rejets radioactifs des installations nucléaires, Groupe Radioécologie Bord Contentin, vol. 1, 1999.
- [103] F. Yiou, G.M. Raisbeck, G.C. Christensen, E. Holm, J. Environ. Radiat. 60 (2002) 61–71.
- [104] C. Frechou, D. Calmet, Czechoslovak J. Phys. 53 (2003) A83–A89.
- [105] C. Frechou, D. Calmet, J. Environ. Radiat. 70 (2003) 43–59.
- [106] D. Maro, D. Hebert, R. Gandon, L. Solier, Radioprotection 34 (1999) 13–24.
- [107] C. Schnabel, V. Olive, M. Atarashi-Andoh, A. Dougans, R.M. Ellam, S. Freeman, C. Maden, M. Stocker, H.A. Synal, L. Wacker, S. Xu, Appl. Geochem. 22 (2007) 619–627.
- [108] S.M. Keogh, A. Aldahan, G. Possnert, P. Finegan, L. Leon Vintro, P.I. Mitchell, J. Environ. Radioact. 95 (2007) 23–38.
- [109] C. Duffa, C. Frechou, Appl. Geochem. 18 (2003) 1867–1873.
- [110] HHIN, The Release of Radioactive Materials from Hanford: 1944–1972, The Hanford Health Information Network (HHIN), <http://www.doh.wa.gov/hanford/publications/history/release.html>.
- [111] K. Shinohara, J. Radioanal. Nucl. Chem. 260 (2004) 265–271.
- [112] JAEA, Annual report on the effluent control of low level liquid waste in nuclear fuel cycle engineering laboratories FY 2005, <http://jolissrch-inter.tokai-sc.jaea.go.jp/pdfdata/JAEA-Review-2006-024.pdf>.
- [113] E. Robens, D.C. Aumann, J. Environ. Radioact. 7 (1988) 159–175.
- [114] Y. Muramatsu, Y. Ohmomo, M. Sumiya, J. Radioanal. Nucl. Chem. Art. 123 (1988) 181–189.
- [115] R.E. Jaquish, K.R. Price, Iodine-129: Environmental Monitoring and Population Dose in the Hanford Environs PNL-SA-16066, Pacific Northwest Laboratory, Richland, Washington, 1988.
- [116] G.R. Doshi, S.N. Joshi, K.C. Pillai, J. Radioanal. Nucl. Chem. Lett. 155 (1991) 115–127.
- [117] J.A. Suarez, A.G. Espartero, M. Rodriguez, Nucl. Instrum. Meth. A369 (1996) 407–410.
- [118] P. Bouisset, O. Lefevre, X. Cagnat, G. Kerlau, A. Ugron, D. Calmet, Nucl. Instrum. Meth. A437 (1999) 114–127.
- [119] M.H. Studier, C. Postmus, J. Mech, R.R. Walters, E.N. Sloth, J. Inorg. Nucl. Chem. 24 (1962) 755–761.
- [120] X.L. Hou, H. Dalgaard, B. Rietz, U. Jacobsen, S.P. Nielsen, A. Aarkrog, Analyst 124 (1999) 1109–1114.
- [121] D.C. Auman, Radiochim. Acta 29 (1981) 209–215.
- [122] Y. Muramatsu, Y. Ohmomo, D.J. Christoffers, Radioanal. Nucl. Chem. Art. 83 (1984) 353–361.
- [123] S.J. Parry, B.A. Bennett, R. Benzing, A.E. Lally, C.P. Birch, M.J. Fulker, Sci. Total Environ. 173–174 (1995) 351–360.
- [124] N. Buraglio, A. Aldahan, G. Possnert, Nucl. Instrum. Meth. B161 (2000) 240–244.
- [125] A. Aldahan, A. Kekli, G. Possnert, J. Environ. Radioact. 88 (2006) 49–73.
- [126] N. Buraglio, A. Aldahan, G. Possnert, I. Vintersved, Environ. Sci. Technol. 35 (2001) 1579–1586.
- [127] R. Michel, J. Handl, T. Ernst, W. Botsch, S. Szidt, A. Schmidt, D. Jakob, D. Beltz, L.D. Romantschuk, H.A. Synal, C. Schnabel, J.M. Lopez-Gutierrez, Sci. Total Environ. 340 (2005) 35–55.
- [128] C. Schnabel, J.M. Lopez-Gutierrez, S. Szidt, M. Sprenger, H. Wernli, J. Beer, H.A. Synal, Radiochim. Acta 89 (2001) 815–822.
- [129] Z. Lu, U. Fehn, H. Tomaru, D. Elmore, X. Ma, Nucl. Instrum. Meth. B 259 (2007) 359–364.
- [130] F. Yiou, G. Raisbeck, H. Imbaud, Nucl. Instrum. Meth. B223 (2004) 412–415.
- [131] R.J. Cox, C.J. Picford, M. Thompson, J. Anal. Atom. Spectrom. 7 (1992) 635–640.
- [132] O.T. Farmer, C.J. Barinaga, D.W. Koppenaal, J. Radioanal. Nucl. Chem. 234 (1998) 153–157.
- [133] P. Biennu, E. Brochard, E. Excoffier, M. Piccione, Can. J. Anal. Sci. Spectrosc. 49 (2004) 423–429.
- [134] A.V. Izmer, S.F. Boulyga, J.S. Becker, J. Anal. At. Spectrom. 18 (2003) 1339–1345.
- [135] A.V. Izmer, S.F. Boulyga, M.V. Zoriy, J.S. Becker, J. Anal. At. Spectrom. 19 (2004) 1278–1280.
- [136] C.F. Brown, K.N. Geiszler, M.J. Lindberg, Appl. Geochem. 22 (2007) 648–655.
- [137] X.L. Hou, V. Hansen, A. Aldahan, G. Possnert, A simple Method for the Speciation Analysis of  $^{129}\text{I}$  in Seawater, Proceedings of 11th International Conference in Accelerator Mass Spectrometry, Rome, September 2008.
- [138] T. Nedveckaitė, W. Filistowicz, J. Radioanal. Nucl. Chem. Art. 174 (1993) 43–47.
- [139] H. Tsukada, J. Ishida, O. Narita, Atmos. Environ. 25A (1991) 905–908.
- [140] R. Fuge, C.C. Johnson, Geochem. Health 8 (1986) 31–54.
- [141] G. Krupp, D.C. Aumann, Chem. Erde 59 (1999) 57–67.
- [142] B.C. Sive, R.K. Varner, H. Mao, D.R. Blake, O.W. Wingenter, Geophys. Res. Lett. 34 (2007) L17808.
- [143] E.A. Bondietti, J.N. Brantley, Nature 322 (1986) 313–314.
- [144] R.H. Knuth, C.G. Sanderson, Particle size distribution of Chernobyl related aerosols in New York City, USDOE Report EML-460, 291–300, 1986.
- [145] A. Tessier, P.G.C. Campbell, M. Bisson, Anal. Chem. 51 (1971) 844–851.
- [146] R. Petersen, X.L. Hou, E.H. Hansen, J. Environ. Radioact. 99 (2008) 1165–1174.
- [147] E. Englund, X.L. Hou, A. Aldahan, G. Possnert, Sequential leaching of Iodine isotopes (127 and 129) in sediment, Proceedings of 11th International Conference in Accelerator Mass Spectrometry, Rome, September 2008.
- [148] D.G. Schulze, P.M. Bertsch, Synchrotron X-ray techniques in soil, plant, and environmental research Advances in Agronomy, vol. 55, Elsevier, 1995, pp. 1–66.
- [149] M.C. Feiters, F.C. Kupper, W. Meyer-Klaucke, J. Synchrotron Radiat. 12 (2005) 85–93.
- [150] R.J. Silva, H. Nitsche, Environmental actinide science, MRS Bull. 26 (2001) 707–713.
- [151] S.D. Conradson, XAFS—a technique to probe local structure, Los Alamos Sci. 26 (2000) 422–435.
- [152] Y.S. Shimamoto, Y. Takahashi, Anal. Sci. 24 (2008) 405–409.
- [153] M.L. Schlegel, P. Reiller, F. Mercier-Bion, N. Barré, V. Moulin, Geochim. Cosmochim. Acta 70 (2006) 5536–5551.
- [154] T. Bacquart, G. Deves, A. Carmona, R. Tucoulou, S. Bohic, R. Ortega, Anal. Chem. 79 (2007) 7353–7359.
- [155] B. Michalke, P. Schramel, Electrophoresis 20 (1999) 2547–2553.
- [156] B. Michalke, P. Schramel, H. Witte, Biol. Trace Elem. Res. 78 (2000) 67–79.
- [157] L.F. Sanchez, J. Szpunar, J. Anal. At. Spectrom. 14 (1999) 1697–1702.
- [158] E. Robens, J. Hauschild, D.C. Aumann, J. Environ. Radioact. 8 (1988) 37–52.
- [159] R. Aquaron, F. Delange, P. Marchal, V. Lognonne, L. Ninane, Cell. Mol. Biol. 48 (2002) 563–569.
- [160] G. Jahreis, W. Hausmann, G. Kiessling, K. Franke, M. Leitner, Exp. Clin. Endocrinol. Diab. 109 (2001) 163–167.
- [161] R. Wahl, K.W. Pilz-Mittenburg, W. Heer, E. Kallee, Zeitschrift Fur Ernährungswissenschaft 34 (1995) 269–276.
- [162] J.K. Soldat, Radiation doses from  $^{129}\text{I}$  in the environment, Health Phys. 30 (1976) 61–70.
- [163] D.W. Moeller, M.T. Ryan, Health Phys. 86 (2004) 586–589.
- [164] B. Le Gueff, J.L. Malarbet, M. Roy, A. Aurengo, C. Devillers, H. Metivier, Radiat. Protect. Dosim. 79 (1998) 211–214.
- [165] R.L. Vought, F.A. Brown, W.T. London, Archives of Environ. Health 20 (1970) 516–522.
- [166] G. Krupp, D.C. Aumann, J. Environ. Radiat. 46 (1999) 287–299.

available at [www.sciencedirect.com](http://www.sciencedirect.com)journal homepage: [www.elsevier.com/locate/aca](http://www.elsevier.com/locate/aca)

## Review article

# Critical comparison of radiometric and mass spectrometric methods for the determination of radionuclides in environmental, biological and nuclear waste samples

Xiaolin Hou\*, Per Roos

Radiation Research Department, Risø National Laboratory, NUK-202, Technical University of Denmark, DK-4000 Roskilde, Denmark

## ARTICLE INFO

## Article history:

Received 5 September 2007

Received in revised form

29 November 2007

Accepted 10 December 2007

Published on line 23 December 2007

## Keywords:

Review

Radionuclides

Radiometric methods

Mass spectrometric methods

Environmental radioactivity

Nuclear waste

Characterization of waste

Environmental samples

Alpha spectrometry

## ABSTRACT

The radiometric methods, alpha ( $\alpha$ )-, beta ( $\beta$ )-, gamma ( $\gamma$ )-spectrometry, and mass spectrometric methods, inductively coupled plasma mass spectrometry, accelerator mass spectrometry, thermal ionization mass spectrometry, resonance ionization mass spectrometry, secondary ion mass spectrometry, and glow discharge mass spectrometry are reviewed for the determination of radionuclides. These methods are critically compared for the determination of long-lived radionuclides important for radiation protection, decommissioning of nuclear facilities, repository of nuclear waste, tracer application in the environmental and biological researches, these radionuclides include  $^3\text{H}$ ,  $^{14}\text{C}$ ,  $^{36}\text{Cl}$ ,  $^{41}\text{Ca}$ ,  $^{59,63}\text{Ni}$ ,  $^{89,90}\text{Sr}$ ,  $^{99}\text{Tc}$ ,  $^{129}\text{I}$ ,  $^{135,137}\text{Cs}$ ,  $^{210}\text{Pb}$ ,  $^{226,228}\text{Ra}$ ,  $^{237}\text{Np}$ ,  $^{241}\text{Am}$ , and isotopes of thorium, uranium and plutonium. The application of on-line methods (flow injection/sequential injection) for separation of radionuclides and automated determination of radionuclides is also discussed.

© 2007 Elsevier B.V. All rights reserved.

\* Corresponding author. Tel.: +45 4677 5357; fax: +45 4677 5357.

E-mail address: [xiaolin.hou@risoe.dk](mailto:xiaolin.hou@risoe.dk) (X. Hou).

Abbreviations: AMS, accelerator mass spectrometry; CPM, counts per minute; DMG, dimethyl glyoxime; DRC, dynamic collision/reaction cell; EC, electron capture; ETV, electrothermal vaporization; FIA, flow-injection/sequential injection analysis; FWHM, full width at half maximum; GDMS, glow discharge mass spectrometry; GFM, gas-filled magnet; Ge(Li), lithium drift germanium; GM, Geiger-Müller; HDEHP, 2-ethylhexyl phosphoric acid; HpGe, high pure germanium; HPLC, high performance liquid chromatography; ICP-MS, inductively coupled plasma mass spectrometry; ICP-QMS, inductively coupled plasma quadrupole mass spectrometry; ICP-SFMS, inductively coupled plasma sector field mass spectrometry; IISD, ion implanted silicon detector; LSC, liquid scintillation counter; MS, mass spectrometry; My, million years; NAA, neutron activation analysis; REEs, rare earth elements; RIMS, resonance ionization mass spectrometry; SIMS, secondary ion mass spectrometry; TIMS, thermal ionization mass spectrometry; TIOA, tri-isooctylamine; TOF-MS, time of flight mass spectrometry; TOPO, tri-*n*-octylphosphine oxide; TTA, thenoyl trifluoroacetone.

0003-2670/\$ – see front matter © 2007 Elsevier B.V. All rights reserved.

doi:10.1016/j.aca.2007.12.012

Beta counting  
 Liquid scintillation counting  
 Gamma spectrometry  
 Inductively coupled plasma mass spectrometry  
 Accelerator mass spectrometry  
 Thermal ionization mass spectrometry  
 Secondary ion mass spectrometry  
 Glow discharge mass spectrometry  
 Neutron activation analysis

## Contents

1. Introduction .....	106
2. Radiometric methods .....	108
2.1. Alpha spectrometry .....	109
2.2. Gamma spectrometry .....	110
2.3. Beta counting .....	110
3. Mass spectrometry .....	111
3.1. Inductively coupled plasma mass spectrometry .....	112
3.2. Accelerator mass spectrometry .....	112
3.3. Thermal ionization mass spectrometry .....	113
3.4. Resonance ionization mass spectrometry .....	113
3.5. Secondary ion mass spectrometry .....	113
3.6. Glow discharge mass spectrometry .....	114
4. Comparison of radiometric and MS methods for the determination of radionuclides .....	114
4.1. Tritium .....	114
4.2. Carbon-14 .....	115
4.3. Chlorine-36 .....	115
4.4. Calcium-41 .....	116
4.5. Nickel-59, 63 .....	117
4.6. Strontium-89, 90 .....	118
4.7. Technitium-99 .....	120
4.8. Iodine-129 .....	122
4.9. Cesium-135, 137 .....	123
4.10. Lead-210 .....	124
4.11. Radium-226, 228 .....	125
4.12. Isotopes of thorium and uranium .....	127
4.13. Neptunium-237 .....	129
4.14. Plutonium isotopes .....	130
4.15. Amerium-241 .....	132
5. Application of on-line methods (flow injection/sequential injection) for separation of radionuclides .....	133
6. Conclusion .....	134
Acknowledgements .....	135
References .....	135

## 1. Introduction

There are many radionuclides naturally occurring in the environment, including the isotopes of uranium and thorium and their decay products,  $^{40}\text{K}$ , and those produced from the cosmic ray reactions, such as  $^3\text{H}$ ,  $^7\text{Be}$ ,  $^{10}\text{Be}$ ,  $^{14}\text{C}$ ,  $^{26}\text{Al}$ ,  $^{14}\text{C}$ , and  $^{129}\text{I}$ . The interest in the determination of these radionuclides mainly comes from the application of them

in geochronology ( $^{14}\text{C}$ ,  $^{10}\text{Be}$ ,  $^{210}\text{Pb}$ , etc.) and using them as environmental or paleoclimate tracers. In environmental samples with a high concentration of uranium and thorium, determination of radionuclides, such as  $^{222}\text{Rn}$ ,  $^{226}\text{Ra}$  in air and drinking water is important in the view of radiation protection. Besides the naturally occurring radionuclides, a large number of radionuclides have been produced and released to the environment by human nuclear activity, including nuclear weapons testing, operation of nuclear power plants, research

**Table 1 – Radionuclides interest in biological, environmental, and waste samples and their application**

Nuclides	Atom mass	Half-life	Decay mode	Specific activity (Bq g <sup>-1</sup> )	Application fields
<sup>3</sup> H	3.0161	12.3 y	β <sup>-</sup>	3.57 × 10 <sup>14</sup>	EM, DN, MT
<sup>14</sup> C	14.0032	5730 y	β <sup>-</sup>	1.65 × 10 <sup>11</sup>	Dating, DN, EM
<sup>36</sup> Cl	35.6983	0.301 My	β <sup>-</sup>	1.22 × 10 <sup>9</sup>	DN, WD, TE
<sup>41</sup> Ca	40.9623	0.103 My	EC	3.14 × 10 <sup>9</sup>	DN, WD, MT
<sup>55</sup> Fe	57.9383	2.73 y	EC	8.36 × 10 <sup>13</sup>	DT, MT
<sup>60</sup> Co	59.9338	5.27 y	β <sup>-</sup>	5.88 × 10 <sup>13</sup>	EM, DM, WD
<sup>59</sup> Ni	58.9343	76400 y	EC+β <sup>+</sup>	2.94 × 10 <sup>9</sup>	DT, WD
<sup>63</sup> Ni	62.9297	100.1 y	β <sup>-</sup>	2.10 × 10 <sup>12</sup>	DT, MT, WD, ET
<sup>79</sup> Se	78.9185	1.13 My	β <sup>-</sup>	2.08 × 10 <sup>8</sup>	DT, WD
<sup>89</sup> Sr	88.9075	50 d	β <sup>-</sup>	1.09 × 10 <sup>15</sup>	EM
<sup>90</sup> Sr	89.9077	29.1 y	β <sup>-</sup>	5.06 × 10 <sup>12</sup>	EM, DN, WD
<sup>99</sup> Tc	98.9063	0.211 My	β <sup>-</sup>	6.34 × 10 <sup>8</sup>	EM, ET, WD
<sup>129</sup> I	129.9050	15.7 My	β <sup>-</sup>	6.49 × 10 <sup>6</sup>	ET, MT, WD
<sup>135</sup> Cs	134.9060	2.3 My	β <sup>-</sup>	4.26 × 10 <sup>7</sup>	ET, WD
<sup>137</sup> Cs	136.9071	30.2 y	β <sup>-</sup>	3.20 × 10 <sup>12</sup>	EM, WD, DN
<sup>210</sup> Pb	209.9842	22.3 y	β <sup>-</sup>	2.83 × 10 <sup>12</sup>	Dating, EM
<sup>226</sup> Ra	226.0254	1600 y	α	3.66 × 10 <sup>10</sup>	EM, ET
<sup>228</sup> Ra	228.0311	5.75 y	β <sup>-</sup>	1.01 × 10 <sup>13</sup>	EM, ET
<sup>229</sup> Th	229.0318	7340 y	α	7.87 × 10 <sup>9</sup>	ET
<sup>230</sup> Th	230.0331	75380 y	α	7.63 × 10 <sup>8</sup>	EM
<sup>232</sup> Th	232.0381	14050 My	α	4.06 × 10 <sup>3</sup>	EM
<sup>234</sup> Th	234.0436	24.1 d	β <sup>-</sup>	8.56 × 10 <sup>14</sup>	ET, EM
<sup>233</sup> U	233.0396	0.1492 My	α	3.80 × 10 <sup>8</sup>	EM
<sup>234</sup> U	234.0410	0.2455 My	α	2.30 × 10 <sup>8</sup>	EM
<sup>235</sup> U	235.0439	703.8 My	α	8.00 × 10 <sup>4</sup>	EM, WD
<sup>236</sup> U	236.0456	23.4 My	α	2.40 × 10 <sup>6</sup>	EM
<sup>238</sup> U	238.0508	4468 My	α	1.24 × 10 <sup>4</sup>	EM, WD
<sup>237</sup> Np	237.0482	2.144 My	α	2.60 × 10 <sup>7</sup>	EM, ET
<sup>238</sup> Pu	238.0496	87.7 y	α	6.34 × 10 <sup>11</sup>	ET, EM
<sup>239</sup> Pu	239.0524	24110 y	α	2.30 × 10 <sup>9</sup>	EM, ET, DN, WD
<sup>240</sup> Pu	240.0538	6563 y	α	8.40 × 10 <sup>9</sup>	EM, ET, DN, WD
<sup>241</sup> Pu	241.0568	14.35 y	β <sup>-</sup>	3.82 × 10 <sup>12</sup>	EM, ET
<sup>242</sup> Pu	242.0587	0.3733 My	α	1.46 × 10 <sup>8</sup>	EM
<sup>244</sup> Pu	244.0640	80.8 My	α	6.71 × 10 <sup>5</sup>	EM
<sup>241</sup> Am	241.0568	432.2 y	α	1.27 × 10 <sup>11</sup>	EM, ET, DN, WD

My: million years; d: day; EC: electron capture, β<sup>+</sup>: positron emission; EM: environmental monitoring; DN: decommissioning of nuclear facilities; MT: medical tracer; ET: environmental tracer; WD, nuclear waste depository.

reactors, and nuclear fuel reprocessing. Nuclear accidents, such as the Chernobyl accident, have also released a large amount of radionuclides to environment [1]. Radionuclides applied in industry and hospital may also be released to environment, although most of them are short lived. For the radiation protection purpose, the level of these radionuclides in various environmental and biological samples needs to be determined. Meanwhile radionuclides released from the reprocessing plants can also be used as environmental tracer for the investigation of transport of water mass (<sup>134,137</sup>Cs, <sup>99</sup>Tc, <sup>129</sup>I) and atmospheric circulation (<sup>129</sup>I). In decommissioning of nuclear facilities and repository of nuclear waste, inventory of radioactivity or concentration of various radionuclides in the waste samples need to be determined. Table 1 lists radionuclides with a half-life longer than 10 years (except <sup>55</sup>Fe, <sup>60</sup>Co, <sup>234</sup>Th and <sup>89</sup>Sr) which are often required to be measured in environmental, biological and waste samples, the application fields of these radionuclides are also presented. Table 2 lists the sources and the production reactions of these radionuclides except the naturally occurred ones. For great number of radionuclides with half-life of less than 10 years, the radiometric methods are exclusively used for

their determination, which are therefore not discussed in this article.

Radionuclides are normally determined by their characteristic radiation, i.e. radiometric methods. In these methods, the decay rate (*A*, number of decays per unit of time) of the radionuclide of interest is measured, the atom number (*N*) of radionuclide of interest is calculated based on the statistical property of the decay of the radionuclide using its half-life (*T*<sub>1/2</sub>):  $N = A/\lambda = A/(\ln 2/T_{1/2})$ . Mass spectrometric methods, which are normally used for determination of isotopes of elements, can be also used for the determination of radionuclides (radioactive isotopes of elements). In these methods, the atom numbers of the radionuclide of interest are directly measured.

Fig. 1 plots the specific radioactivity (Bq g<sup>-1</sup>) vs. half-life of the radionuclide listed in Table 1. From this figure, it can be seen that the shorter the half-life of the radionuclide is, the higher the specific radioactivity of the radionuclides. It means that compared with the mass spectrometric method, the shorter the half-life of the radionuclide is, the more sensitive the radiometric method. In the other words, radiometric methods are generally sensitive for short-lived radionuclides,

**Table 2 – The sources and main production reactions of radionuclides interest in the biological, environmental, and waste samples**

Nuclides	Sources	Nuclear reactions for the production of radionuclide
$^3\text{H}$	NWT, ONF, RP	$^2\text{H}(\text{n}, \gamma)^3\text{H}$ ; $^3\text{He}(\text{n}, \text{p})^3\text{H}$ ; $^6\text{Li}(\text{n}, \alpha)^3\text{H}$
$^{14}\text{C}$	CRR, NWT, ONF, RP	$^{14}\text{N}(\text{n}, \text{p})^{14}\text{C}$ ; $^{13}\text{C}(\text{n}, \gamma)^{14}\text{C}$ ; $^{17}\text{O}(\text{n}, \alpha)^{14}\text{C}$
$^{36}\text{Cl}$	CRR, NWT, ONF, RP	$^{35}\text{Cl}(\text{n}, \gamma)^{36}\text{Cl}$ ; $^{40}\text{Ar}(\text{p}, \text{n}\alpha)^{36}\text{Cl}$ ; $^{36}\text{Ar}(\text{n}, \text{p})^{36}\text{Cl}$ ; $^{39}\text{K}(\text{n}, 2\text{n}2\text{p})^{36}\text{Cl}$ ; $^{40}\text{Ca}(\text{n}, 2\text{n}3\text{p})^{36}\text{Cl}$ ; $^{40}\text{Ca}(\mu^-, \alpha)^{36}\text{Cl}$ ; $^{39}\text{K}(\text{n}, \alpha)^{36}\text{Cl}$
$^{41}\text{Ca}$	NWT, ONF	$^{40}\text{Ca}(\text{n}, \gamma)^{41}\text{Ca}$
$^{59}\text{Ni}$	NET, ONF	$^{58}\text{Ni}(\text{n}, \gamma)^{59}\text{Ni}$
$^{63}\text{Ni}$	NET, ONF	$^{62}\text{Ni}(\text{n}, \gamma)^{63}\text{Ni}$ ; $^{63}\text{Cu}(\text{n}, \text{p})^{63}\text{Ni}$
$^{79}\text{Se}$	ONF, RP	$^{78}\text{Se}(\text{n}, \gamma)^{79}\text{Se}$ ; $^{235}\text{U}(\text{n}, \text{f})^{79}\text{Se}$
$^{89}\text{Sr}$	NWT, ONF, RP	$^{235}\text{U}(\text{n}, \text{f})^{89}\text{Sr}$ ; $^{88}\text{Sr}(\text{n}, \gamma)^{89}\text{Sr}$
$^{90}\text{Sr}$	NWT, ONF, RP	$^{235}\text{U}(\text{n}, \text{f})^{90}\text{Sr}$
$^{99}\text{Tc}$	ONF, RP, NOR	$^{235}\text{U}(\text{n}, \text{f})^{99}\text{Tc}$ ; $^{98}\text{Mo}(\text{n}, \gamma)^{99}\text{Mo}(\beta)^{99}\text{Tc}$
$^{129}\text{I}$	NWT, ONF, RP	$^{129}\text{Xe}(\text{n}, \text{p})^{129}\text{I}$ ; $^{235}\text{U}(\text{n}, \text{f})^{129}\text{I}$ ; $^{127}\text{I}(2\text{n}, \gamma)^{129}\text{I}$
$^{135}\text{Cs}$	NWT, ONF, RP	$^{235}\text{U}(\text{n}, \text{f})^{135}\text{Cs}$
$^{137}\text{Cs}$	NWT, ONF, RP	$^{235}\text{U}(\text{n}, \text{f})^{137}\text{Cs}$
$^{237}\text{Np}$	ONF, RP	$^{238}\text{U}(\text{n}, 2\text{n})^{237}\text{U} \rightarrow ^{237}\text{Np}$ ; $^{235}\text{U}(\text{n}, \gamma)^{236}\text{U}(\text{n}, \gamma)^{237}\text{U} \rightarrow ^{237}\text{Np}$
$^{238}\text{Pu}$	ONF, RP	$^{235}\text{U}(\text{n}, \gamma)^{236}\text{U}(\text{n}, \gamma)^{237}\text{U}(\beta^-)^{237}\text{Np}(\text{n}, \gamma)^{238}\text{Np}(\beta^-)^{238}\text{Pu}$ ; $^{238}\text{U}(\text{n}, 2\text{n})^{237}\text{U}(\beta^-)^{237}\text{Np}(\text{n}, \gamma)^{238}\text{Np}(\beta^-)^{238}\text{Pu}$
$^{239}\text{Pu}$	ONF, RP	$^{238}\text{U}(\text{n}, \gamma)^{239}\text{U}(\beta^-)^{239}\text{Np}(\beta^-)^{239}\text{Pu}$
$^{240}\text{Pu}$	ONF, RP	$^{238}\text{U}(\text{n}, \gamma)^{239}\text{U}(\beta^-)^{239}\text{Np}(\beta^-)^{239}\text{Pu}(\text{n}, \gamma)^{240}\text{Pu}$
$^{241}\text{Pu}$	ONF, RP	$^{238}\text{U}(\text{n}, \gamma)^{239}\text{U}(\beta^-)^{239}\text{Np}(\beta^-)^{239}\text{Pu}(\text{n}, \gamma)^{240}\text{Pu}(\text{n}, \gamma)^{241}\text{Pu}$
$^{242}\text{Pu}$	ONF	$^{238}\text{U}(\text{n}, \gamma)^{239}\text{U}(\beta^-)^{239}\text{Np}(\beta^-)^{239}\text{Pu}(\text{n}, \gamma)^{240}\text{Pu}(\text{n}, \gamma)^{241}\text{Pu}(\text{n}, \gamma)^{242}\text{Pu}$
$^{241}\text{Am}$	ONF, RP	$^{238}\text{U}(\text{n}, \gamma)^{239}\text{U}(\beta^-)^{239}\text{Np}(\beta^-)^{239}\text{Pu}(\text{n}, \gamma)^{240}\text{Pu}(\text{n}, \gamma)^{241}\text{Pu}(\beta^-)^{241}\text{Am}$

NWT: nuclear weapons testing; ONF: operation of nuclear facilities; CRR: Cosmic ray reaction; NOR: normal occurring radionuclide; RP, reprocessing plants.

while mass spectrometric methods are sensitive for long-lived radionuclides.

Several informative review articles on the mass spectrometric determination of long-lived radionuclides have been published in recent years [2–9], in which the performance, progress, and interferences of mass spectrometric methods have been discussed in detailed. A few review paper on brief evaluation of radiometric method and mass spectrometry is also available [10]. Rosenberg [11] reviewed the non-conventional measurement techniques for the determination of several long-lived radionuclides in nuclear fuel in 1993. In this article, the authors compared the radiometric methods and neutron activation analysis with mass spectrometric methods. With the significant progress of mass spectrometric techniques, especially inductively coupled plasma mass spectrometry (ICP-MS), the mass spectrometric techniques become more and more popular method for the determination of long-lived radionuclides. An overview review of traditional radiometric techniques with the recently improved mass

spectrometric methods can help the analysts and researchers to choose more suitable techniques and also improve the analytical capacity and analytical quality, while such a work is not available. This articles aims to compare the radiometric methods with various mass spectrometric methods for the determination of radionuclides in biological, environmental and waste samples. In which, different radiometric methods, such as gamma ( $\gamma$ )-spectrometry, alpha ( $\alpha$ )-spectrometry, and beta ( $\beta$ ) counting, and mass spectrometric methods, such as ICP-MS, accelerator mass spectrometry (AMS), thermal ionization mass spectrometry (TIMS), resonance ionization mass spectrometry (RIMS), secondary ion mass spectrometry (SIMS) and glow discharge mass spectrometry (GDMS) and their application for the determination of radionuclides are compared. Neutron activation analysis (NAA) method is discussed for the determination of some radionuclides. In addition, the application of on-line methods (flow injection/sequential injection) for separation of radionuclides and automated determination of radionuclides is also discussed.

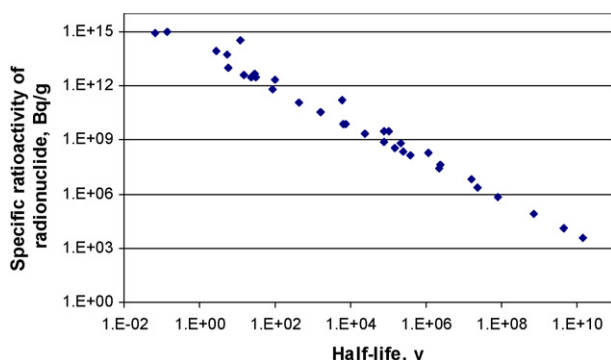


**Fig. 1 – Plot of the specific radioactivity ( $\text{Bq g}^{-1}$ ) vs. half-life of the radionuclides listed in Table 1.**

## 2. Radiometric methods

Radionuclides are unstable, they de-excite to stable state by radioactive decay with a specific rate (half-life,  $T_{1/2}$ ). The radioactivity of radionuclide ( $A$ ) can be expressed as:  $A = N \times (\ln 2/T_{1/2}) = N_0 \exp(-0.693 \times t/T_{1/2}) \times (\ln 2/T_{1/2})$ , here  $N$  is atoms number at time  $t$ ; and  $N_0$  is atoms number at beginning. There are several types of processes in the de-excitation of radionuclides, i.e.  $\alpha$  decay,  $\beta$  decay, electron capture, internal conversion,  $\gamma$ -ray emission, and spontaneous fission. In  $\alpha$  decay, the radionuclide is de-excited by emitting an  $\alpha$ -particle ( $^4\text{He}^{2+}$ ) with specific energy. The  $\alpha$  radionuclide (decay by emitting  $\alpha$ -particles) can be measured by  $\alpha$ -spectrometry.  $\beta$  decay is a de-excitation process of the radionuclide by emitting an



electron ( $\beta^-$ ) or a positron ( $\beta^+$ ), meanwhile, an antineutrino or neutrino is also emitted, they share the energy with the beta particle in the radioactive decay. Therefore, the resulting beta particles have a continuous distribution of energies from 0 to maximum decay energy. A beta emitter (emitting  $\beta^-$  particles) can be measured by beta counter, such as Geiger-Müller (GM) counter or a liquid scintillation counter (LSC). While radionuclides decay by  $\beta^+$  emission can be measured by  $\gamma$ -spectrometry, because  $\beta^+$  decay is followed by emitting two annihilation photons each having energy of 511 keV. Electron capture (EC) is a decay process where an atomic-shell electron is captured by the nucleus, this can be considered as an inverse of  $\beta^+$  decay, but the electron spectrum is discrete, because the energy of the captured electron has a well-defined value. EC is followed by X-ray and/or Auger electrons emission. The radionuclides with EC decay can therefore be determined by measuring their specific X-ray using X-ray spectrometry or by measuring Auger electrons using a liquid scintillation counter. The excited nucleus which formed as a consequence of  $\alpha$  or  $\beta$  decay of radionuclide can de-excite by emitting  $\gamma$ -rays with specific energy. The radionuclides with emission of  $\gamma$ -rays can be determined by  $\gamma$ -spectrometry. A radionuclide may have more than one decay process, in this case it can be measured by more radiometric methods, for example,  $^{129}\text{I}$  is a  $\beta$ -emitter, but also emitting  $\gamma$ -rays with a energy of 39.6 keV, which can be measured by both beta counting as well as  $\gamma$ -spectrometry. The advantages of three main radiometric methods are discussed below.

### 2.1. Alpha spectrometry

There are several types of detector that can be used for the measurement of alpha-emitting radionuclides; examples are Frisch grid ionization chambers, proportional counters, plastic- and liquid scintillation detectors and semiconductor detectors. Ionization chambers normally have a high counting efficiency, but have very poor energy resolution unless equipped with a shielding Frisch grid preventing induction from the positive ion-cloud and thereby enabling fast collection of the generated electrons. Frisch grid ionization chambers are therefore only used ionization chamber for total alpha activity measurements. Proportional counters as well as liquid scintillation counters both have the advantage that the alpha emitter can be placed inside the counter, thereby reaching  $4\pi$  counting efficiency. In both cases energy resolution is generally poor and for spectrometric use these detectors play only a minor role. Semiconductor detectors are normally used for the determination of  $\alpha$ -emitting radionuclides in the environmental and waste samples, especially when spectrometric information is needed. Both surface barrier and ion-implanted silicon semiconductor detectors are widely used in  $\alpha$  spectroscopy because of the relatively good counting efficiency and their superior energy resolution. The counting efficiency of this detector varies with size of the source and detector as well as with the source-detector distance, and is typically between 10% and 45%. The energy resolution presented as full width at half maximum (FWHM) of a peak ranges normally from 15 to 55 keV depending on the distance of source to detector, and the size and thickness of the source. The high charge (+2) and relatively low speed of alpha particles results

in significant energy losses even in very thin absorbers. The longer distance the source to the detector is, the better the resolution (the narrower the FWHM) due to a smaller space angle and therefore a shorter passage through the source of the alpha particles reaching the detector. Table 3 shows the energies of some interesting  $\alpha$  emitters in the analysis of environmental and waste samples. Although the resolution of semiconductors for  $\alpha$ -spectrometry is good, the relatively small difference in alpha particle energy between some alpha emitters makes it difficult to spectrometrically separate the peaks. This is usually the case with isotopes such as  $^{241}\text{Am}$  and  $^{238}\text{Pu}$ , and  $^{237}\text{Np}$ ,  $^{233}\text{U}$ ,  $^{234}\text{U}$  and  $^{230}\text{Th}$ . It is therefore that a good chemical separation of radionuclide of interest from the matrix and interfering radionuclides is required; otherwise, the self-absorption of  $\alpha$  particles in the source will not only reduce the counting efficiency, but also worsen the energy resolution of the  $\alpha$  spectrum. For this reason it is essential that a thin source is prepared in  $\alpha$ -spectrometry. This can be carried out by electro-deposition on stainless steel disks. Evaporation, co-precipitation, electrospraying, electrostatic precipitation, spontaneous deposition, molecular plating, and vacuum sublimation are also used to prepare  $\alpha$  source [12], but the energy resolution of  $\alpha$ -spectrum of the source prepared by many of these methods varies considerably because of the thickness of the source, especially, the evaporation and co-precipitation methods. A recently developed absorption method supplied a simple and thin alpha source, which is based on the sorption of some radionuclides such as radium onto a thin manganese oxide film [13].

The procedure blank contribution to the sample counts is a very important factor affecting the detection limit of any method. In  $\alpha$ -spectrometry, with a good chemical separation and source preparation, the blank contribution for artificial radionuclides can usually be kept low (<0.15 count per hour), while corresponding numbers for naturally occurring radioisotopes are somewhat higher but most of all have a much larger variability. In environmental samples, the concentration of radionuclides is normally very low; it requires a long counting time (1–10 days for the activity of radionuclide lower than 10 mBq) to acquire a low counting uncertainty. In the author's laboratory, the procedure blank count rate of  $\alpha$ -spectrometry is normally lower than 2 counts per day, the corresponding detection limit is less than 0.1 mBq for a counting efficiency of 30%. Table 3 lists the detection limits of radionuclides of interest in the environmental and waste samples in unit of nanogram. It can be seen that the detection limit of  $\alpha$ -spectrometry is very good. For the radionuclides with a half-life shorter than 1 million years (My), the detection limit by  $\alpha$ -spectrometry is lower than  $10^{-12}$  g.

The main disadvantage of  $\alpha$ -spectrometry is the long analysis time, which is a result of the long chemical separation procedure for the complete separation of the target radionuclide(s) from the matrix as well as from interfering radionuclides, and the very long counting time (1–30 days). This makes the analytical capacity low for this method. Due to the relatively low price of standard alpha spectrometry equipment, the radiochemistry- and environmental radioactivity laboratory is normally equipped with several detector units to meet the required analysis of large number of samples. In addition, it is also cheaper to run and maintain  $\alpha$ -spectrometry

**Table 3 – Energies of  $\alpha$  particles of radionuclides and detection limit of  $\alpha$ -spectrometry**

Radionuclide	$\gamma$ -Rays (abundance)	Energy of main $\alpha$ particles (MeV) (abundance)	Detection limits <sup>a</sup> (ng)
<sup>226</sup> Ra	186.2 (3.65%)	4.78 (94.5%), 4.60 (5.5%)	$1.95 \times 10^{-6}$
<sup>229</sup> Th	193.5 (4.5%), 86.4 (2.6%)	4.85 (56.2%), 4.90 (10.2%), 4.81 (9.3%), 5.05 (6.6%), 4.97 (6.0%), 4.84 (5.0%), 4.98 (3.2%)	$9.05 \times 10^{-6}$
<sup>230</sup> Th	67.7 (0.37%)	4.69 (76.3%), 4.62 (23.4%)	$9.34 \times 10^{-5}$
<sup>232</sup> Th	63.8 (0.26%)	4.01 (78.2%), 3.95 (21.7%)	17.55
<sup>233</sup> U	97.1 (0.02%)	4.82 (84.4%), 4.78 (13.2%),	$1.78 \times 10^{-4}$
<sup>234</sup> U	53.2 (0.12%)	4.77 (71.4%), 4.72 (28.4%)	$3.09 \times 10^{-4}$
<sup>235</sup> U	185.7 (57.2%), 143.8 (11.0%)	4.40 (55%), 4.37 (17.2%), 4.21 (5.7%), 4.60 (5.0%), 4.56 (4.2%)	0.89
<sup>236</sup> U	49.4 (0.078%)	4.49 (73.8%), 4.45 (25.9%)	$2.97 \times 10^{-2}$
<sup>238</sup> U	49.6 (0.064%)	4.20 (79.0%), 4.15 (20.9%)	5.73
<sup>237</sup> Np	29.4 (15.0%), 86.5 (12.4%),	4.79 (47.9%), 4.77 (33%), 4.64 (6.2%), 4.66 (3.3%)	$2.74 \times 10^{-3}$
<sup>238</sup> Pu	43.5 (0.039%)	5.50 (70.9%), 5.46 (29.0%)	$1.12 \times 10^{-7}$
<sup>239</sup> Pu	51.6 (0.027%)	5.16 (873.3%), 5.14 (15.1%)	$3.10 \times 10^{-5}$
<sup>240</sup> Pu	45.2 (0.045%)	5.17 (72.8%), 5.12 (27.1%)	$8.48 \times 10^{-6}$
<sup>242</sup> Pu	44.9 (0.036%)	4.90 (77.5%), 4.86 (22.4%)	$4.87 \times 10^{-4}$
<sup>244</sup> Pu		4.59 (80.6%), 4.55 (19.4%)	0.11
<sup>241</sup> Am	59.5 (35.9%)	5.49 (84.6%), 5.44 (13.0%)	$5.61 \times 10^{-7}$

<sup>a</sup> The detection limit of alpha spectrometry was supposed to be 0.1 mBq.

equipment, this makes this method low cost in the view of measurement. However, from the above it is obvious that normal separation procedures for  $\alpha$ -spectrometry is not suitable for fast analysis in emergency situations, which requires getting the analytical results in a shorter time (less than 1 day). A number of modified, rapid procedures have therefore been worked out to handle such situations for different radioisotopes in various matrixes.

## 2.2. Gamma spectrometry

Many  $\alpha$  and  $\beta$  decay radionuclides also emit  $\gamma$ -rays; they can therefore be determined by  $\gamma$ -spectrometry. A number of detectors can be used for the measurement of  $\gamma$ -rays, such as scintillation counter using NaI, CsF and ZnS as scintillator, gas filled counter, and semiconductor detectors based on lithium doped Si or high purity Ge, CdTe, and GaAs. However, since their introduction to the market in 1970s, mainly Si(Li) and Ge (lithium drift germanium Ge(Li)) semiconductor detector are widely used for the  $\gamma$ -spectrometry measurement of radionuclides in the biological, environmental and nuclear waste samples, because of their high energy resolution. The later development of Ge detector in 1980s by using high pure germanium detector makes the maintenance of the detector easy, because HpGe detector can be kept at room temperature without damage. It is therefore, more Ge(Li) detectors were replaced by HpGe detector in many radioanalytical laboratories, although the performance of both detectors are similar. The recent development in the  $\gamma$ -spectrometry is the introduction of large-volume Ge crystal, which significantly increases the counting efficiency to 100–150% (relative counting efficiency) [14], this is very useful for the analysis of environmental and waste samples.

Si(Li) detector or small planar Ge detector are normally used for the measurement of low energy  $\gamma$ -rays and X-rays (<100 keV) with an energy resolution of 0.15 keV at 5.9 keV, while larger Ge detector are better suited for high energy  $\gamma$ -rays (>25 keV) and normally have an energy resolution better

than 2 keV at 1332 keV. Due to the property of electromagnetic radiation,  $\gamma$ -ray can penetrate a long distance in the samples without significant absorption, especially high energy  $\gamma$ -rays. Sample usually does not need any treatment before counting, which makes the analysis quick and easy, and minimizes the risk of contamination during sample preparation. It is therefore that the radionuclides with emission of suitable energy  $\gamma$ -rays are normally measured by  $\gamma$ -spectrometry, such as <sup>60</sup>Co, <sup>65</sup>Zn, <sup>54</sup>Mn, <sup>94</sup>Nb, <sup>106</sup>Ru, <sup>133</sup>Ba, <sup>134</sup>Cs, <sup>137</sup>Cs, <sup>144</sup>Ce, <sup>152</sup>Eu, <sup>154</sup>Eu, and <sup>241</sup>Am. However, the counting efficiency of  $\gamma$ -spectrometry is low (<10% for absolute counting efficiency) and varies with the  $\gamma$ -ray energy, distance of source to the detector and the size of the Ge or Si crystal. In addition, the background count rate of  $\gamma$ -spectrometry is normally high (>10 counts per hour for 661.7 keV  $\gamma$ -ray of <sup>137</sup>Cs and >25 counts per hour for 59.5 keV  $\gamma$ -ray of <sup>241</sup>Am) and varies with the total radioactivity of sample and the shielding of the detector. The detection limit of  $\gamma$ -spectrometry (>50 mBq) is typically a few orders of magnitude higher than  $\beta$  counting and  $\alpha$ -spectrometry, but depends on the detector shielding, radionuclide of interest and interfering radionuclides. Due to the often superior detection limits of alpha spectrometry, trace level of the alpha emitting radionuclides listed in Table 1 are determined exclusively by  $\alpha$ -spectrometry except <sup>241</sup>Am, which can be measured by  $\gamma$ -spectrometry when the concentration is not too low.

## 2.3. Beta counting

Beta- or electron emitting radionuclides are normally measured by gas ionization detector, such as ionization chamber, gas flow GM detector, or liquid scintillation counters (LSC). GM counter is normally used for radionuclides emitting higher energy electrons due to the absorption of low energy electrons in the thin window separating the sample and gas volume. LSC has an advantage in measuring low-energy electron emitters due to the absence of attenuation when the sample is immersed within the scintillator. LSC can thus be

used for the measurement of both high and low energy  $\beta$ -emitters. Due to the continuous energy distribution of the emitted electrons in the beta decay, beta particle spectrometry is a poor way for identifying individual contributions in the beta spectrum. Determination of beta particle emitters therefore requires chemical separation of the radionuclide of interest from all other radionuclides before counting. Even so, several radioisotopes may present of one element (e.g.  $^{89}\text{Sr}$  and  $^{90}\text{Sr}$ ) and even if the isotope emits electrons at discrete energies (e.g. from internal transition and/or electron capture decay with subsequent Auger electron emission) the electron cascade emitted due to the subsequent filling of electron shell vacancies still results in a complicated energy distribution which prevents accurate analysis of several electron emitters in parallel. In LSC, the relatively poor energy resolution still enables the identification of foreign activity while for the GM-counter, which lacks energy resolution, any foreign activity in the sample has to be determined by other means, e.g. by checking the half-life of the isotope by repeated counting or by its energy using absorbers of different thickness between sample and counter. The absorption of electrons in matter is less than for  $\alpha$ -particles, especially for high-energy electrons. However, in order to minimize self-absorption in the sample and maintain a high counting efficiency, samples for GM counting needs to be prepared as a thin solid source which can be carried out by the same method as used for the  $\alpha$ -spectrometry, the very often used method is electro-deposition and/or micro co-precipitation. The counting efficiency of a GM counter varies from 10% to 70% with the energy of the emitted electrons, thickness of the source, and counter properties. For the analysis of environmental and low-level waste samples, a low-level GM counter is required. This is mainly achieved by reducing the background count rate of the detector by using heavy lead shielding and a GM guard detector above the sample detectors, operating in anti-coincidence mode with the sample detector(s). A background count rate of 0.1 counts per minute (CPM) was reported for a commercial low-level GM counter produced at Risø National Laboratory, Denmark, and

the detection limit reported is less than 1.5 mBq for  $^{99}\text{Tc}$  and  $^{90}\text{Sr}$  [15–17].

Table 4 lists radionuclides typically measured by beta counting and their approximate detection limits. The GM counter cannot be used effectively for the determination of radionuclides emitting low energy electrons, such as  $^3\text{H}$ ,  $^{14}\text{C}$ ,  $^{129}\text{I}$ , and  $^{241}\text{Pu}$ , because of high absorption of these  $\beta$ -particles in the detector window, LSC has to be used in this case. Besides the capability of being able to measurement low energy  $\beta$ -emitters, LSC also has the advantage of none or minimal self-absorption, high counting efficiency, homogeneous distribution of the sample in the scintillation cocktail, relative simple sample preparation procedure, and easy standardization using internal or external standard. Another capability of LSC is the determination of isotopes decaying by emitting a high proportion of conversion electrons or by electron capture, such as  $^{41}\text{Ca}$  and  $^{55}\text{Fe}$ , which is carried out by the measurement of the Auger electrons produced during these decay processes. However, due to the low energy of the Auger electrons (<20 keV), the counting efficiency of LSC for radionuclides decaying by these processes is low (<30%) [18,19]. Comparing with the GM counter, the background count rate is higher in LSC, the lowest count rate measured using the commercial Quantulus<sup>TM</sup> Ultra low-level LSC produced by Wallac, Perkin-Elmer is around 0.5 CPM for the  $^3\text{H}$  window and 1.5 CPM for the  $^{99}\text{Tc}$  window while the background for the anticoincidence shielded GM counter may be as low as 0.1–0.2 CPM, this makes the detection limit of LSC is worse than using low-level GM counters (Table 4). In addition, the quench correction is another drawback of LSC, which requires an extra work for acquiring accurate results.

### 3. Mass spectrometry

Inorganic mass spectrometry is extensively used for the determination of element concentrations in the trace and ultra-trace range by measuring the number of atoms of isotopes of the element. It has therefore also been used for the

**Table 4 – Energies of  $\beta$  particles of the radionuclides and the detection limits of beta counting methods [15–19]**

Radionuclides	Decay	$E_{\text{max}}$ (keV) (abundance)	Ld of LSC		Ld of GM detector	
			mBq	ng	mBq	ng
$^3\text{H}$	$\beta^-$	18.6	12.50	$2.50 \times 10^{-8}$		
$^{14}\text{C}$	$\beta^-$	156.5	17.14	$7.41 \times 10^{-5}$		
$^{36}\text{Cl}$	$\beta^-$	708.6	14.0	$8.10 \times 10^{-3}$	4	$2.33 \times 10^{-3}$
$^{41}\text{Ca}$	EC		15.00	$3.41 \times 10^{-3}$		
$^{55}\text{Fe}$	EC		15.00	$1.28 \times 10^{-7}$		
$^{63}\text{Ni}$	$\beta^-$	66.9	20.00	$6.78 \times 10^{-6}$	10	$3.39 \times 10^{-6}$
$^{79}\text{Se}$	$\beta^-$	151.1	15.00	0.072	8	0.038
$^{89}\text{Sr}$	$\beta^-$	1459.1	22.45	$1.47 \times 10^{-8}$	4	$2.62 \times 10^{-9}$
$^{90}\text{Sr}$	$\beta^-$	546	18.89	$2.66 \times 10^{-6}$	4	$5.64 \times 10^{-7}$
$^{99}\text{Tc}$	$\beta^-$	293.7	18.75	0.021	5	$5.62 \times 10^{-3}$
$^{129}\text{I}$	$\beta^-$	154.2	17.14	1.88		
$^{135}\text{Cs}$	$\beta^-$	269.3	18.75	0.313	5	0.0835
$^{210}\text{Pb}$	$\beta^-$	17.0 (84%), 63.5 (16%)	33.33	$8.40 \times 10^{-6}$	15	$3.78 \times 10^{-6}$
$^{228}\text{Ra}$	$\beta^-$	39.4 (50%), 25.7 (20%), 12.8 (30%)	20.00	$1.41 \times 10^{-6}$		
$^{234}\text{Th}$	$\beta^-$	199.1 (70.3%), 106.5 (26.8%)	18.57	$1.55 \times 10^{-8}$		
$^{241}\text{Pu}$	$\beta^-$	20.8	30.00	$5.59 \times 10^{-6}$		

determination of radionuclides (radioisotopes of elements) for more than 25 years [20–22]. Solid-state mass spectrometric methods, such as laser ablation ICP-MS [23,24], GDMS [25–27], and SIMS [28], allow direct determination of radionuclides in solid samples without any chemical preparation. This makes the analysis very simple and minimizes the risk from the contamination due to the limited sample handling. However, the interpretation and quantification of analytical results in solid-state mass spectrometry is a problem due to the complex dependence on signal strength and abundance of polyatomic species on the sample composition and structure. Also lack of suitable (matrix-matched) standard reference materials frequently prevents the quantification of data. In addition, the detection limit for many radionuclides is not sufficient for the direct analysis of environmental samples; chemical separation of the elements of interest from the matrix is one way for increasing the signal strength and limiting interferences (but will increase the blank) but the essential point in techniques like LA-ICP-MS or SIMS is to obtain spatial information of isotopes or elements and chemical modification of the sample is in these cases of limited interest. ICP-MS, TIMS [29,30], AMS [31,32] and RIMS [33,34] are very sensitive mass spectrometric techniques for the determination of ultra trace levels of isotopes, and have been widely used for the determination of ultra-low levels of selected radionuclides and the precise determination of isotopic ratios. Several review articles have addressed the application of mass spectrometric techniques for the determination of radionuclides [2–9,35].

### 3.1. Inductively coupled plasma mass spectrometry

ICP-MS is the most frequently used mass spectrometric technique for the determination of elements and isotope ratios in the trace and ultratrace concentration range. In recent year, it has also increasingly been used for determination of radionuclides in environmental, biological and waste samples [2–7,24,35]. In contrast to conventional inorganic solid mass spectrometric techniques, ICP-MS allows a simple sample introduction in an ion source operating at atmospheric pressure and an easy quantification procedure using aqueous standard solutions [8]. With laser ablation system coupled to an ICP-MS, direct analysis of solid samples can be performed. In ICP-MS, the chemical compounds contained in the sample solution are decomposed into their atomic constituents in an inductively coupled argon plasma at a plasma temperature of approximately 6000–8000 K, and the high temperature ensures a high degree of ionization (>90% for most elements) with a low fraction of multiply charged ions (~1%). The positively charged ions are extracted from the inductively coupled plasma (at atmospheric pressure) into a high vacuum of the mass spectrometer via an interface. The extracted ions are then separated by mass filters of either quadrupole type time of flight or combination of magnetic and electrostatic sector, and finally measured by an ion detector. The detection limit of ICP-MS varies from  $10^{-15}$  to  $10^{-8}$  g depending on interferences and the sensitivity of the instrument. In low-resolution mode, the sensitivity of double-focusing sector field ICP-MS is generally higher than conventional quadrupole ICP-MS instruments. Similarly the precision for isotope ratio

measurements using double focusing sector field ICP-MS with single ion detection is somewhat better than quadrupole ICP-MS (around 0.1% or better vs. 0.1–0.5% for quadrupole). Better precision of isotope ratio measurements (one order of magnitude) can be achieved by use of multi-ion collector device in sector field ICP-MS.

The major problem in determination of radioisotopes using ICP-MS is the appearance of isobaric interferences of other elements at the same mass, such as  $^{129}\text{Xe}$  interfering with  $^{129}\text{I}$  and  $^{238}\text{U}$  with  $^{238}\text{Pu}$ . Another important interference is from polyatomic ions, such as  $^{238}\text{U}^1\text{H}$  and  $^{204}\text{Pb}^{35}\text{Cl}$  which interferes with  $^{239}\text{Pu}$ . Some of these polyatomic species may be resolved from the element of interest using double-focusing sector field ICP-MS at a required mass resolution, but in this case the sensitivity will be reduced due to the strong collimation of the ion-beam. In quadrupole ICP-MS, the application of a collision/reaction cell (DRC) can significantly suppress the interfering isobaric ions by choice of an appropriate reaction gas. The low abundance sensitivity (or tailing) of ICP-MS is another drawback which limits its application for the determination of radionuclides. Several review articles have addressed the applications and limitations of ICP-MS for the determination of radionuclides [2–9]. Because of the high sensitivity, short analysis time and relatively easy operation, ICP-MS has been widely used for the determination of isotopes of uranium, thorium, and plutonium,  $^{79}\text{Se}$ ,  $^{90}\text{Sr}$ ,  $^{99}\text{Tc}$ ,  $^{129}\text{I}$ ,  $^{135}\text{Cs}$ ,  $^{210}\text{Pb}$ ,  $^{226}\text{Ra}$ ,  $^{228}\text{Ra}$ ,  $^{231}\text{Pa}$ ,  $^{237}\text{Np}$ ,  $^{241}\text{Am}$ ,  $^{243}\text{Am}$ , and  $^{244}\text{Cm}$  in environmental and waste samples [36–70].

### 3.2. Accelerator mass spectrometry

AMS emerged in the late 1970s from nuclear physics laboratories and soon became used as an ultra-sensitive mass spectrometric technique for measuring isotopes of elements, and is now widely used for the determination of radionuclides, especially long-lived radionuclides, such as  $^3\text{H}$ ,  $^{10}\text{Be}$ ,  $^{14}\text{C}$ ,  $^{26}\text{Al}$ ,  $^{32}\text{Si}$ ,  $^{36}\text{Cl}$ ,  $^{41}\text{Ca}$ ,  $^{53}\text{Mn}$ ,  $^{59}\text{Ni}$ ,  $^{129}\text{I}$ ,  $^{182}\text{Hf}$ ,  $^{210}\text{Pb}$  and actinides [31,71,72]. Almost all AMS facilities can be understood as two mass spectrometers (called “injector” and “analyzer”) linked with a tandem accelerator. The radionuclide of interest is first prepared as a solid target, and then injected to the system as a negative ion by ion sputtering (e.g. using a  $\text{Cs}^+$  primary ion source). The sputtered negative ions from the sample is pre-accelerated and mass analyzed by a magnet. Since not all elements form negative ions, isobaric interferences can be effectively suppressed in some important cases. In the case of  $^{14}\text{C}$ ,  $^{41}\text{Ca}$  and  $^{129}\text{I}$ , isobaric interferences are eliminated because  $^{14}\text{N}$ ,  $^{41}\text{K}$ , and  $^{129}\text{Xe}$  respectively do not form stable negative ions. The mass analyzed negative ions are then accelerated to the positive high-voltage terminal of a tandem accelerator where they encounter either a thin carbon foil or low-pressure gas. Several electrons may be stripped off, converting negative ions to multiply charged positive ions (e.g.  $^{129}\text{I}^{7+}$ ). The stripping process has the advantage that it dissociates molecular ions if enough electrons are stripped off which results in a further elimination of interferences. The positively charged ions from the accelerator then pass through a magnetic analyzer, where the ions of interest with a well defined combination of charge state and energy are selected, and directed to a detector. Furthermore, the higher energies



of the ions after acceleration allow an additional separation of the wanted ions from possible background ions at the particle detector. A range of ion detectors have been employed in the AMS system, of them, charged particle semiconductor detectors are only used for the measurement of the energy of ion, ionization chambers can measure both total energy of an ion as well as its rate of energy loss in the detector, time of flight systems are normally used for the measurement of energy of heavy ions such as for  $^{129}\text{I}$ . In addition, gas filled magnets (GFM) and X-ray detector have also been used in AMS measurement. The above features make this method possible to measure isotopic ratios well below  $10^{-10}$ , where many interesting long-lived radionuclides in the environment are expected. This is one of the reasons why AMS is among the most sensitive measurement methods for many long-lived radionuclides, or even only method for measuring some specific long-lived radionuclides, such as  $^{10}\text{Be}$ ,  $^{26}\text{Al}$ , and  $^{32}\text{Si}$ . However, due to high price, there are less than 100 AMS facilities installed worldwide, in which most of them are mainly used for the routine analysis of  $^{14}\text{C}$  for dating purpose. Although many installed AMS have the capability for the analysis of many long-lived radionuclides mentioned above, but most of these AMS only determine very few of these radionuclides in routine. The main drawback with AMS is that it is only applicable to those elements that form negative ions during the sputtering process. A further drawback with AMS facilities is the lack of flexibility in changing from one element of interest to another. This usually may require changing sputtering conditions, beam-line set-up and detector configuration which may require several days of work. A comprehensive review of AMS analytical technique has been given by Fifield [31], Skipperud and Oughton [73] reviewed the main application of AMS in environmental research.

### 3.3. Thermal ionization mass spectrometry

TIMS has been used for the determination of isotopic composition and concentration of different elements including radioisotopes of some elements, such as uranium, thorium and plutonium since 1980s [5,29,74–83,22,84–88]. In TIMS a small volume (down to  $1\ \mu\text{L}$ ) of aqueous solution containing the target nuclides or element in the nanogram to microgram range is deposited on a cleaned filament surface (mostly high-purity Re) and evaporated to dryness. The most frequently applied technique in TIMS works with two heated filaments (one for evaporation of the sample and the other for ionization of evaporated atoms) which are arranged opposite to each another. Due to the low initial energies (0.1–0.2 eV) of the ions formed on the hot thermal surface, mostly single magnetic sector field mass spectrometers are sufficient for ion separation. The introduction of fully automated thermal ionization mass spectrometers with multi-detector system over the last two decades has enhanced the capabilities of TIMS in many aspects. These include the possibility of achieving high internal precisions (0.001% or better on isotope ratios) using internal normalization methodology to correct for the isotope fractionation during analysis, as well as applying interfering element correction methodology to correct for the isobaric interference. The limiting factors for the accuracy of measured isotopic ratios in TIMS are mass discrimination in the

TIMS instrument (e.g. ion optical system or ion detector) and mass fractionation effects (caused during the evaporation of sample, where the measured isotope ratio changes with time). These inherent effects limiting the capability of isotope ratio measurements by TIMS can be considered by different internal calibration techniques or by using isotopic standard reference materials with well-known isotopic ratios for an element. Besides, U, Th and Pu, TIMS has also been used for many other radionuclides, such as  $^{41}\text{Ca}$ ,  $^{241}\text{Am}$ ,  $^{242}\text{Cm}$ ,  $^{126}\text{Sn}$ ,  $^{226}\text{Ra}$ ,  $^{228}\text{Ra}$  [82,89–92].

### 3.4. Resonance ionization mass spectrometry

RIMS as a highly selective and sensitive mass spectrometric technique for ultratrace and isotope analysis has been used for the determination of many radionuclides such as  $^{41}\text{Ca}$ ,  $^{90}\text{Sr}$ ,  $^{99}\text{Tc}$ ,  $^{135}\text{Cs}$ ,  $^{210}\text{Pb}$ ,  $^{236}\text{U}$ ,  $^{238}\text{Pu}$ ,  $^{239}\text{Pu}$ ,  $^{240}\text{Pu}$ ,  $^{242}\text{Pu}$ , and  $^{244}\text{Pu}$  in environmental, biological and waste samples [33,34,93–104]. In RIMS the solid or liquid samples are vaporized and atomized by an atomic beam source (e.g. in an atomic beam oven by thermal vaporization on a hot Re filament or by evaporation of sample using an electron beam). One or in most cases more lasers are tuned precisely to the wavelength required for the excited states and ionization of evaporated atoms in order to obtain a highly selective resonance ionization of the element of interest. RIMS offers a number of outstanding properties comparing to other mass spectrometric techniques, such as nearly complete isobaric suppression demonstrated to be better than  $10^8$ , obtained by the uniqueness of optical transitions, especially in multi-step excitations; high overall sensitivity with detection limits in the  $10^{-15}$  to  $10^{-18}\ \text{g}$  range, enabled by the high ionization efficiency, high transmission mass spectrometers, and low background ion detection; high isotopic selectivity with values of  $10^{13}$  and higher, which is achieved by combining isotope abundance sensitivity of the mass spectrometer and optical isotope selectivity in the laser excitation process. Due to these advantages, RIMS has found broad acceptance in various analytical fields, particularly ultratrace determination of long-lived radioisotopes. At present there are no commercial RIMS-instruments available which makes the technique rather rare compared to the other mass spectrometric techniques described.

### 3.5. Secondary ion mass spectrometry

SIMS is a surface analytical technique, and mainly applied for surface mapping and depth profiling of elements and/or isotope ratios. A depth resolution in the low nanometer range depending on sputtering technique may be obtained. In the lateral plans, SIMS are able to perform a microlocal analysis in the sub-micrometer range (e.g. for analysis of local inclusion or impurities). It is quite often used for the characterization of small particles, aerosols, as well as liquid or solid inclusions. SIMS can be applied for the characterization of bulk material with detection limits down to the low nanogram per gram range. SIMS allows precise isotope ratio measurements with precisions between 0.01% and 1%, by the application of multiple ion collectors, a precision of 0.002% can be reached. However, the quantification of analytical

results in SIMS is very difficult due to large matrix effects. Nevertheless, if a matrix matched standard reference material is available for SIMS, accurate analytical data can be obtained.

In SIMS, solid sample surface is sputtered by bombardment with a focused primary ion beam ( $\text{Ga}^+$ ,  $\text{Cs}^+$ ,  $\text{O}_2^+$  or  $\text{O}^-$ ), the sputtered ions (secondary ions) are separated by mass spectrometer according to their mass-to-charge ratios, the separated secondary ions is then collected for pulse or current measurement, as quantifiable mass spectra, as in-depth or along-surface profiles, or as distribution images of the sputtered surface. SIMS has also been used for the determination of radionuclides, especially radionuclides in environmental “hot” particles and spatial distribution of radionuclides in materials [9,27,28,105–114].

### 3.6. Glow discharge mass spectrometry

GDMS was established as a powerful and efficient analytical method for direct trace element determination and depth profile analysis of solids [26,27,115–117]. In GDMS, an argon gas glow discharge at a pressure of 0.1–10 Torr is used as an ion source. The cathode surface consisting of the sample material is sputtered by  $\text{Ar}^+$  ions, which are formed in low-pressure argon plasma and accelerated towards the cathode. Sputtered neutral particles of the sample are ionized in the glow discharge plasma (‘negative glow’) by Penning and/or electron impact ionization and charge exchange processes. The ionized ions of interest are then detected by mass spectrometry. For the direct analysis of solid samples, the commercial direct current glow discharge mass spectrometer VG-9000 (VG-Elemental, Thermo Instruments, UK) – a double-focusing sector field mass spectrometer with inverse Nier–Johnson geometry – has been available on the analytical market for many years. The analysis of nonconducting materials by d.c. GDMS is difficult due to charge-up effects on the sample surface. Different techniques such as mixing nonconducting powdered samples with a high-purity metal powder (or high-purity graphite) or the use of a secondary cathode have, therefore, been applied for the analysis of electrically insulating samples by d.c. GDMS. Due to the capacity of isotopic analysis, GDMS can be used for the determination of radionuclides, such as uranium, plutonium,  $^{237}\text{Np}$ ,  $^{137}\text{Cs}$ , and  $^{90}\text{Sr}$  [115,116]. Since the sample is directly analyzed, the sample preparation is very simple, which minimize the risk of contamination. It is also suitable for fast analysis, where radiometric methods are normally time consuming. However, due to low sensitivity and less accessibility of GDMS, the application of GDMS in the determination of radionuclides is very limited.

## 4. Comparison of radiometric and MS methods for the determination of radionuclides

For the determination of many specific radionuclides, both radiometric and mass spectrometric method can be used, while their application is directly related with the detection limits, analytical accuracy and capacity, and accessibility of the equipments. In addition, the sample preparation proce-

dures in terms of duration, complexity, the counting time, interferences, the man power and cost are also parameters should be considered in the choice of the analytical method. Due to the high sensitivity and accuracy, and easy access of radioactive measurement equipments in normal radiochemical laboratories, the determination of short-lived radionuclides ( $T_{1/2} < 10$  years), especially those with emission of  $\gamma$ -rays is exclusively carried out by radiometric method. Here we focus on the comparison of these two techniques for the determination of some of important radionuclides in the environmental and waste samples, especially long-lived alpha and pure electron emitters.

### 4.1. Tritium

Radiometric methods are sensitive ways for the determination of tritium due to its short half-life (12.3 years), and therefore its high specific radioactivity ( $3.6 \times 10^{14} \text{ Bq g}^{-1}$ ). Tritium decays by pure beta particle emission with a low energy ( $E_{\text{max}} = 18.6 \text{ keV}$ ), it is therefore favorably measured by liquid scintillation counting (LSC), a detection limit of 50 mBq ( $1 \times 10^{-16} \text{ g}$ ) was reported for the determination of tritium in nuclear waste with low-level LSC for 50 min counting time [118]. In LSC, the sample is normally prepared in a small volume of liquid (<10 mL), which is mixed with a scintillator cocktail for counting. The tritium concentration in environmental samples is normally very low ( $<1 \text{ mBq mL}^{-1}$ ), the LSC is therefore not sensitive enough for the direct measurement, an electrolytic method is therefore often applied to enrich tritium from water [119], the enrichment factor of 30–100 can easily be obtained for 100–500 mL water. For the determination of tritium in solid samples, a combustion method is used to convert tritium to THO, which subsequently is measured by LSC [118–120].

Tritium can also be measured by  $^3\text{He}$  mass spectrometry and AMS. In  $^3\text{He}$  mass spectrometry, the sample is first degassed to remove  $^3\text{He}$  in the sample, and then kept for some period of time for the in-growth of  $^3\text{He}$  from the decay of tritium. The  $^3\text{He}$  built from tritium is then measured by the noble-gas mass spectrometer. The  $^3\text{He}$  mass spectrometry method is more sensitive than LSC, a detection limit of  $0.5 \text{ mBq mL}^{-1}$  was reported [121,122], the main drawback of the  $^3\text{He}$  method is its long analysis time, which results from the in-growth of  $^3\text{He}$  from the decay of tritium, in addition, the sample preparation is also a complicated and time consuming process in this method.

AMS is also a sensitive method for the determination of tritium, a detection limit of 1 mBq (or  $10^{-13}$  to  $10^{-15}$  for  $^3\text{H}/^1\text{H}$  ratio) has been reported [123]. The primary benefit of this method is the analysis of small sample (2 mg hydrogen), which is very suitable for the analysis of biological samples. In AMS method, the tritium is first released from the sample, and converted to hydrogen gas which is then absorbed on metal (i.e. Ti), and then measured by AMS. It is therefore the sample preparation of AMS is more complicated comparing to LSC. Combining with the less availability of AMS facility, the application of AMS for the determination of tritium is very limited. In the routine analysis, LSC is still the most often used method for tritium determination in environmental and waste samples.

#### 4.2. Carbon-14

Carbon-14 is a naturally occurring radionuclide produced in the upper atmosphere by reaction of cosmic ray produced neutrons via  $^{14}\text{N}(\text{n}, \text{p})^{14}\text{C}$ ,  $^{14}\text{C}$  level in the atmosphere was approximately constant before the human nuclear activity (equilibrium between new generated  $^{14}\text{C}$  and removal of  $^{14}\text{C}$  due to its radioactive decay). After being fixed in living materials (plants, animals), the  $^{14}\text{C}$  concentration will decreased due to its radioactive decay with a half-life of 5730 years,  $^{14}\text{C}$  is therefore widely used for dating (age determination) purpose. Actually, the most of  $^{14}\text{C}$  measurement is used for dating. However, human nuclear activity has released large amount of  $^{14}\text{C}$  to the environment. In the nuclear facilities,  $^{14}\text{C}$  is mainly produced by neutron capture reactions of  $^{14}\text{N}$ ,  $^{13}\text{C}$  and  $^{17}\text{O}$  (Table 2). Therefore,  $^{14}\text{C}$  exists in almost all materials exposed to neutron irradiation.  $^{14}\text{C}$  is an important radionuclide in the decommissioning of nuclear facilities and repositories of nuclear waste due to its high concentration, long half-life and most of all due to carbon being an essential element for plants and animals.

$^{14}\text{C}$  is a pure beta emitter which decays by emitting  $\beta$ -particles with the maximum energy of 156 keV; it can therefore be measured by beta counting, mainly liquid scintillation counting. In this method,  $^{14}\text{C}$  is prepared as a liquid sample and then measured. The very often used method for the analysis of waste sample is combustion, in this case all forms of carbon is converted to  $\text{CO}_2$  and absorbed in alkaline solution, which is mixed with scintillator cocktail for the LSC. The detection limit of LSC for  $^{14}\text{C}$  therefore depends on the count rate of blank, counting efficiency and counting time. A detection limit of 30 mBq was reported for the analysis of nuclear waste and environmental sample such as graphite, concrete, soil, and milk powder, using low-level Quantulus<sup>TM</sup> 1200 LSC [118]. This is sensitive enough for the waste samples and the present environmental samples [118,124–128]. The traditional sample preparation method for the analysis of solid sample using combustion [124–128] is very time consuming, this makes the analytical capacity of LSC very low (<3 sample per day per person). Hou [118] developed a rapid method for separation of C-14 from solid samples by using a sample oxidizer, using this method the sample preparation time was reduced to only 2–3 min per sample. For the analysis of environmental samples with a low concentration of  $^{14}\text{C}$ , such as old materials for dating, the carbon released from the sample is normally converted to benzene in order to get a better counting efficiency and therefore a better detection limit [129,130]. However, due to the high detection limit, the measurement of very low-level  $^{14}\text{C}$  for dating requires large samples (>2 g) to get a good analytical accuracy or precision. This feature limits the application of LSC in  $^{14}\text{C}$  dating.

Due to the long half-life of  $^{14}\text{C}$ , it can readily measured by mass spectrometry techniques. The most sensitive method for the determination of  $^{14}\text{C}$  is AMS, which can detect  $10^{-7}$  Bq of  $^{14}\text{C}$  (or a  $^{14}\text{C}/^{12}\text{C}$  ratio of  $10^{-15}$ ), and the samples up to 60,000 years old have been dated by  $^{14}\text{C}$  AMS. Due to the very high sensitivity of AMS, a very small sample (<1 mg carbon) is required for the measurement, which makes it possible to analyze samples with very low carbon content, such as ice, water, ceramics, and metals. Besides good sensitivity, the analytical

precision of AMS (<0.2%) is also much better than radiometric method, which is a very important factor in the dating. AMS is therefore very suitable for radiocarbon dating. A large number of papers on the  $^{14}\text{C}$  dating using AMS has been published, a journal “Radiocarbon” mainly focus on this field. A compact AMS facility specifically for the radiocarbon dating has been recently developed and introduced to the market [131]. This leads to smaller dimensions, drastically reduced investment and operating costs of AMS facility for radiocarbon dating. In the AMS analysis of  $^{14}\text{C}$ , carbon is first released from the samples, mainly by combustion at high temperature, the released  $^{14}\text{C}$  as  $^{14}\text{CO}_2$  is then normally converted to graphite, and used for AMS. But  $\text{CO}_2$  samples can also be directly introduced to the AMS for measurement [132,133]. Due to high cost, complicated sample preparation procedure, and less accessibility of AMS, the AMS is mainly used for radiocarbon dating, while the determination of  $^{14}\text{C}$  in waste and normal environmental samples is mainly carried by radiometric method.

The ambient levels of  $^{14}\text{N}$  in air and the fact that ICP-MS plasmas operate at atmospheric conditions prevent the determination of  $^{14}\text{C}$  by this technique. The small mass difference, relatively poor abundance sensitivity, poor ionization in the plasma and normally very large atom number differences  $^{14}\text{N}:^{14}\text{C}$  makes it impossible to determine  $^{14}\text{C}$  even by using sector field ICP-MS in high resolution mode. The presence of nitrogen in nearly all materials makes determination even in solids under vacuum by most of mass spectrometric techniques (e.g. SIMS) a challenge.

#### 4.3. Chlorine-36

In nature,  $^{36}\text{Cl}$  is produced mainly by the cosmic ray reactions and thermal neutron reaction of  $^{35}\text{Cl}$  in the hydrosphere (Table 2). However, most of  $^{36}\text{Cl}$  in the present environment has been produced by human nuclear activities since 1950s via the neutron activation reaction. The interest in the determination of  $^{36}\text{Cl}$  in nuclear waste results from the long half-life of  $^{36}\text{Cl}$  and its high mobility in the environment, while the purpose of determination of  $^{36}\text{Cl}$  in the environmental sample normally focus on the application of this radionuclide as a environmental tracer.

$^{36}\text{Cl}$  is a pure beta particle emitter with a high energy ( $E_{\text{max}} = 708.6$  keV, 98.1%), it is therefore mainly measured by beta counting such as LSC [127,128,134–139]. The reported detection limit of LSC for  $^{36}\text{Cl}$  is 14 mBq using Quantulus<sup>TM</sup> low-level LSC for 50 min counting time [134]. A complete separation of  $^{36}\text{Cl}$  from the matrix and other radionuclides is required in this method. Hou et al. [134] reported a method for the separation of  $^{36}\text{Cl}$  from different types of nuclear waste samples, such as graphite, concrete and metals. The  $^{36}\text{Cl}$  was first released from the sample by acid digestion or alkaline fusion followed by acid leaching. The chlorine in the decomposed sample was then separated from the matrix by  $\text{AgCl}$  precipitation. The separated  $^{36}\text{Cl}$  was further purified by anion exchange chromatography, and the  $^{36}\text{Cl}$  in the  $\text{NH}_4\text{NO}_3\text{--NH}_4\text{OH}$  eluate was concentrated by evaporation. The separated sample was mixed with scintillation cocktail and measured by LSC. Due to the long chemical separation (4–7 h) and counting time (>30 min), the determination of  $^{36}\text{Cl}$  is normally time consuming (one day chemical separation and 1–2 h of measurement).



The concentration of  $^{36}\text{Cl}$  in environmental samples is normally very low ( $<1\text{ mBq g}^{-1}$ , or a ratio of  $^{36}\text{Cl}/^{35}\text{Cl}$  less than  $10^{-9}$ ), it is impossible to determine it by using LSC method. Due to the long half-life of  $^{36}\text{Cl}$  (301,000 years), mass spectrometry is a suitable tool for its determination. However, the isobaric interference ( $^{36}\text{S}$ ,  $^{36}\text{Ar}$ ) and bad abundance sensitivity ( $>10^{-7}$ ) in the most mass spectrometric techniques limit their application. The only mass spectrometric technique useful for determination of  $^{36}\text{Cl}$  in low-level environmental sample is AMS. The reported detection limit of AMS is  $10^{-9}\text{ Bq}$  (or a  $^{36}\text{Cl}/^{35}\text{Cl}$  ratio of  $10^{-15}$ ) [140–142]. In AMS,  $^{36}\text{Cl}$  is normally prepared as  $\text{AgCl}$  target and the measurement is conducted using  $^{36}\text{Cl}^{7+}$  ions. The  $^{36}\text{S}$  isobar is the principal challenge in AMS measurement of  $^{36}\text{Cl}$ , because sulfur forms negative ions as readily as chlorine and the concentration of  $^{36}\text{S}$  is normally much higher in the environmental samples compared to  $^{36}\text{Cl}$ . By using a 48 MeV  $^{36}\text{Cl}^{7+}$  ion energy and a multi-anode ionization chamber as detector,  $^{36}\text{S}$  can be highly suppressed by a factor of  $10^4$  [141]. In addition, chemical separation of sulfur from chlorine has to be used in the sample preparation, which is achieved by precipitation of sulfur as  $\text{BaSO}_4$ . Remaining sulfur normally exists as sulfate, which can be co-precipitated together with the  $\text{AgCl}$  as  $\text{Ag}_2\text{SO}_4$ . But the solubility of  $\text{Ag}_2\text{SO}_4$  is much higher than that of  $\text{AgCl}$ , and can therefore be separated by washing the precipitate with acidic solution [134].

The separation procedures of  $^{36}\text{Cl}$  for both of LSC and AMS analytical methods are similar time consuming, while the detection limit of AMS is a few order of magnitude better than LSC. AMS is the only method for the determination of  $^{36}\text{Cl}$  in environmental level, while LSC is still widely used for the analysis of nuclear waste sample, in which the  $^{36}\text{Cl}$  concentration is high, because of less cost and easy accessibility of LSC in normal radiochemical laboratory.

#### 4.4. Calcium-41

$^{41}\text{Ca}$ , a long-lived radionuclide ( $T_{1/2} = 1.03 \times 10^5$  years), is produced by neutron activation reaction of  $^{40}\text{Ca}$  (Table 2).  $^{41}\text{Ca}$  is an important radionuclide in the disposal of radioactive waste, because of its long half-life, high mobility in the environment and high bioavailability.  $^{41}\text{Ca}$  is also used as a tracer in the biomedical research [143], which requires a very sensitive determination of  $^{41}\text{Ca}$  because of the small sample size normally available.

$^{41}\text{Ca}$  decays to the ground state of  $^{41}\text{K}$  by pure electron capture, emitting X-rays and Auger electrons of very low energy (3.3 keV, 11.7%), which makes it possible, although difficult, to be measured by X-ray spectrometry [144] and LSC [19,145,146]. X-ray spectrometry is a simple method, but it is insensitive due to the low counting efficiency ( $<0.08\%$ ) of X-ray spectrometry for  $^{41}\text{Ca}$  and the low abundance of X-rays from  $^{41}\text{Ca}$  (11.4% for 3.31 keV  $\text{K}\alpha$  X-ray). A detection limit of 8 Bq for  $^{41}\text{Ca}$  was reported by using X-ray counting after chemical separation [144].

The chemical separation is necessary due to possible presence of beta, gamma or X-ray emitters which may either increase the baseline background or directly interfere with the  $\text{Ca}$  ( $\text{K}$ ) X-rays. A chemical separation of  $^{41}\text{Ca}$  from the sample matrix is also needed in many cases due to the self-absorption of X-rays in the sample which varies significantly with sample

size and also in the chemically separated sample due to the amount of stable  $\text{Ca}$  presents in the samples. A self-absorption correction must, therefore, be carried out. The most advantage of this technique is its short sample preparation procedure and minimized risk of contamination in the direct measurement.

LSC has been used for the determination of  $^{41}\text{Ca}$  by measurement Auger electrons emitted from  $^{41}\text{Ca}$ . Due to the relative high counting efficiency compared to X-ray spectrometry, a better detection limit can be obtained. However, due to the poor energy resolution of LSC and the low energy Auger electron spectrum of  $^{41}\text{Ca}$ , calcium has to be completely separated from the matrix and all other radionuclides before counting. Hou [19] reported a chemical procedure for the separation of calcium from concrete based on the precipitation of  $\text{Ca}(\text{OH})_2$  in high concentration of  $\text{NaOH}$  ( $>0.5\text{ mol L}^{-1}$ ) with a decontamination factor higher than  $10^4$  for most interfering radionuclides, such as  $^{133}\text{Ba}$ ,  $^{90}\text{Sr}$ ,  $^{60}\text{Co}$ , and  $^{152}\text{Eu}$ . A detection limit of 0.1 Bq was reported using LSC [19]. The drawback of this method is the long chemical separation procedure, and long counting time ( $>1\text{ h}$ ).

Mass spectrometric techniques including AMS [147–150] and RIMS [93,151] have also been used for the determination of  $^{41}\text{Ca}$ . Of these methods, AMS is the most sensitive method. AMS of  $^{41}\text{Ca}$  requires the injection of a molecular ion of  $\text{Ca}$ , because the formation of the  $\text{Ca}^-$  ion is very low in a sputter source,  $\text{CaH}_3^-$  is normally the ion of choice to eliminate the  $^{41}\text{K}$  isobar because the  $\text{KH}_3^-$  ion is not stable [150].  $\text{CaF}_3^-$  has also been used to inject  $\text{Ca}$  to the AMS system, since  $\text{KF}_3^-$  ion is instable [149]. In principle, a  $^{41}\text{Ca}/^{40}\text{Ca}$  ratio as low as  $10^{-15}$  can be measured by AMS, while the detection limit of  $^{41}\text{Ca}$  is mainly effected by the procedure blank and  $^{41}\text{K}$  interference, the reported detection limit is  $10^{-12}$  to  $10^{-13}$  for  $\text{Ca}/^{40}\text{Ca}$  ratio or 0.1 mBq  $\text{g}^{-1}$  for  $^{41}\text{Ca}$  [147,148].

RIMS is also a sensitive method for the determination of  $^{41}\text{Ca}$ . A detection limit of  $1\text{--}5 \times 10^{-11}$  for  $^{41}\text{Ca}/^{40}\text{Ca}$  ratio has been reported [93,151,152]. The precision of the isotope ratio determination is dominated by isotope fractionation effects, which may result from small errors in laser spectral or spatial positioning. They limit the precision to about 5% for  $\text{Ca}$  isotope ratios above  $10^{-10}$  and increase up to 30% near the detection limit due to low counting statistics.

Table 5 compares all four methods for the determination of  $^{41}\text{Ca}$ , AMS and RIMS are the most sensitive methods for  $^{41}\text{Ca}$ , they can therefore be used for all types of samples, and the samples amount required is small ( $<2\text{ mg Ca}$ ). But both AMS and RIMS are expensive and not easily accessible. X-ray spectrometer is the least sensitive method, but is easy to operator and samples are easily prepared. Low energy Ge- or Si(Li) detectors used for X-ray spectrometry may therefore be a suitable method for the analysis of nuclear waste samples containing higher level activity. LSC is not as sensitive as AMS and RIMS, and sample preparation for LSC is also rather time consuming. But LSC equipment is usually accessible in radiochemical laboratories. Besides X-ray spectrometry, the other three methods require a thorough chemical separation of  $\text{Ca}$  from the sample matrix and interfering isotopes. In which, a complete separation of other radionuclides is required in LSC, the chemical procedure therefore takes a long time. For AMS



**Table 5 – Comparison of X-ray spectrometry, LSC, RIMS, TIMS and AMS for the determination of  $^{41}\text{Ca}$** 

Sample	Detection method	Target preparation	Detection limit		Sep. time (h)	Count time	Ref.
			Bq	$^{41}\text{Ca}/^{40}\text{Ca}$			
Concrete	X-ray	$\text{CaC}_2\text{O}_4$	8 Bq		0–6	40–70 h	[144]
Concrete	LSC	$\text{CaCl}_2$	0.1 Bq		4–6	1 h	[19]
Waste	LSC	$\text{CaCl}_2$	0.3 Bq		4–6	4 h	[146]
Concrete	RIMS	$\text{Ca}(\text{NO}_3)_2$	30 mBq	$10^{-10}$	2–4	10–20 min	[93]
Concrete	RIMS	$\text{Ca}(\text{NO}_3)_2$	20 mBq	$6 \times 10^{-11}$	2–4	~ 1 h	[152]
Iron	RIMS	$\text{CaO}$	1 mBq	$5 \times 10^{-11}$	2–4	10–60 min	[151]
Snow	AMS	$\text{CaH}_2$	0.1 mBq	$5 \times 10^{-12}$	4–8	20–60 min	[147]
Iron	AMS	$\text{CaH}_2$	0.1 mBq	$2 \times 10^{-13}$	4–8	20–60 min	[151]

and RIMS the chemical separation steps are relative simple, Ca is normally separated from the decomposed sample by a simply calcium oxalate precipitation.

#### 4.5. Nickel-59, 63

$^{63}\text{Ni}$  and  $^{59}\text{Ni}$  are produced by neutron activation reactions of Ni and Cu (Table 2), which are released to the environment from the human nuclear activity. The interest in the determination of  $^{63}\text{Ni}$  and  $^{59}\text{Ni}$  results from the characterization of radioactive wastes for the decommissioning and disposal of nuclear waste, and the use in a number of applications including cosmic radiation studies, biomedical tracing and neutron dosimetry (Table 1) [18,153–156].

$^{63}\text{Ni}$  is a pure beta emitting radionuclide (Table 4), the radiometric methods including windowless gas flow GM counters, beta-spectrometry with semiconductor detectors and LSC have been used for its determination.  $^{59}\text{Ni}$  decays by electron capture with emission of X-rays, it can therefore be determined by X-ray spectrometry. The AMS has also been used for the determination of these two radioisotopes of nickel [153,154,157–160].

In the determination of  $^{63}\text{Ni}$  by gas flow GM counter or semiconductor detector, the  $^{63}\text{Ni}$  has to be prepared as thin source to minimize self-adsorption. This is usually carried out by electrodeposited of Ni on a metal disk. Due to its low beta energy, the counting efficiencies of ion implanted silicon detector (IISD) (1–6%) and GM counter (8–40%) are low and varies with the thickness of the source (stable Ni). Detection limits of 1 and 8 mBq were reported for GM counter and silicon detector, respectively for 50 h counting [161,162]. LSC has a high counting efficiency for  $^{63}\text{Ni}$  (70%), it is therefore widely used for the determination of  $^{63}\text{Ni}$  [18,163–167], the reported detection limit of LSC is 14–37 mBq for 30–1000 min counting time [18,167]. A slightly higher detection limit of LSC results from the relatively high background count rate of LSC (3–10 CPM) compared to GM counting and silicon detector (0.2 CPM). Because of the difficulties in identifying radioisotopes from the continuous energy spectrum of pure beta-emitters, they have to completely be separated from the matrix and other radionuclides before counting. Chemical separation of  $^{63}\text{Ni}$  is usually carried out by precipitating nickel as a hydroxide and then extracting the Ni-DMG (dimethyl glyoxime) complex using either solvent extraction or extraction chromatography, sometimes combined with an anion exchange step. A decontamination factor of  $10^5$  or higher was

obtained using a combination of these methods [18]. Chemical separation does not separate  $^{63}\text{Ni}$  from  $^{59}\text{Ni}$ , but since both  $^{63}\text{Ni}$  and  $^{59}\text{Ni}$  are produced by thermal neutron reactions with stable nickel  $^{62}\text{Ni}$  (3.65%) and  $^{58}\text{Ni}$  (68.1%), the initial activity ratio of  $^{63}\text{Ni}/^{59}\text{Ni}$  is around 100 or higher, which means that only  $^{63}\text{Ni}$  is measured by LSC. In addition, the signal of  $^{59}\text{Ni}$  in LSC occurs in the low energy part of the spectrum, which makes the interference of  $^{59}\text{Ni}$  to the  $^{63}\text{Ni}$  spectrum very limited. The high radioactive ratio of  $^{63}\text{Ni}/^{59}\text{Ni}$  at the same time makes LSC determination of  $^{59}\text{Ni}$  impossible.

As all other low-energy X-ray emitters, the determination of  $^{59}\text{Ni}$  also requires a separation of Ni from the matrix and other radionuclides because of the low energy of the K-X-rays emitted from  $^{59}\text{Ni}$  (6.9 keV, 30.4%), the same separation procedure used for  $^{63}\text{Ni}$  can also be used for  $^{59}\text{Ni}$ . The separated Ni is normally electrodeposited onto a metal disk for the X-ray counting. Due to the low counting efficiency (<1%) and relatively high background counts in X-ray spectrometry, this method is insensitive. A reported detection limit of X-ray spectrometry for the determination of  $^{59}\text{Ni}$  is 1–2 Bq [168].

AMS is a sensitive method for the determination of  $^{63}\text{Ni}$  and  $^{59}\text{Ni}$ . In this method, isobaric interference from  $^{63}\text{Cu}$  and  $^{59}\text{Co}$  is the main challenge, because Cu, Co and Ni easily form anions in the ion sputtering source. To minimize these interferences, a combination of chemical separation methods and AMS instrumental settings are used. A characteristic X-ray detector is used for post-spectrometer ion detection and identification. After separation in the AMS spectrometer, the Ni-ions are detected via X-rays emitted when they pass through a thin foil close to the detector. This allows identifying the ions by atomic number and thereby separating the isobars. By this method, a suppress rate of  $10^7$  for  $^{59}\text{Co}$  was obtained [154,159]. Combined with the chemical separation using DMG extraction, a detection limit of  $4 \times 10^{-9}$  for the  $^{59}\text{Ni}/\text{Ni}$  ratio (or 20 mBq) was reported [154]. For improvement of the detection limit, the Ni in the sample should be further purified and the instrumental background should be reduced. McAninch et al. [153] reduced the instrumental background of  $^{63}\text{Cu}$  and  $^{59}\text{Co}$  in the ion source by fabrication of Cu and Co free target holders, thorough cleaning of the ion source and addition of a cryogenic pumping system to the ion source [153]. The same authors reported a chemical purification method by using volatile  $\text{Ni}(\text{CO})_4$ , the Ni in ammonium solution was mixed with  $\text{NaBH}_4$  solution in a flask, and a mixture of CO and  $\text{He}_2$  was bubbled through the Ni solution to

**Table 6 – Comparison of X-ray spectrometry, GM counter, ion implanted silicon detector, LSC, and AMS for the determination of  $^{63}\text{Ni}$  and  $^{59}\text{Ni}$  determination of  $^{59}\text{Ni}$  and  $^{63}\text{Ni}$** 

Sample	Nuclide	Method	Target preparation	Detection limit (Bq)	Sep. time (h)	Count time	Ref.
Waste	$^{59}\text{Ni}$	X-spectrometry	Deposited on disk	1–2 Bq	5–6	7 h	[168]
Biological sample	$^{59}\text{Ni}$	AMS	$\text{Ni}(\text{CO})_4$ -Ni	0.05 mBq	7–8	15 min	[153]
Waste	$^{63}\text{Ni}$	LSC	Ni-DMG	14 mBq	4–6	30 min	[18]
Sludge	$^{63}\text{Ni}$	LSC	$\text{NiCl}_2$	37 mBq	4–6	17 h	[167]
Lichens	$^{63}\text{Ni}$	GM counter	Deposited on disk	1 mBq	6–8	50 h	[162]
Fucus	$^{63}\text{Ni}$	IISD	Deposited on disk	8 mBq	4–8	50 h	[161]
Copper wires	$^{63}\text{Ni}$	AMS	$\text{Ni}(\text{CO})_4$ -Ni	45 mBq	7–8	15 min	[153]
Copper	$^{63}\text{Ni}$	AMS	$\text{Ni}(\text{CO})_4$ -Ni	0.12 mBq	7–8	10–30 min	[160]

produce volatile  $\text{Ni}(\text{CO})_4$ , which was collected in a cold trap. The collected  $\text{Ni}(\text{CO})_4$  was heated and transferred to the AMS holder by  $\text{He}_2$  flow, where it was thermally decomposed to Ni. By this process, a Cu/Ni ratio of less than  $2 \times 10^{-8}$  in the sample was obtained, corresponding to a detection limit of  $2 \times 10^{-11}$  for  $^{59}\text{Ni}/\text{Ni}$  ratio or 0.05 mBq of  $^{59}\text{Ni}$  and 45 mBq of  $^{63}\text{Ni}$  [153]. Rugel et al. [160,169] reported an AMS method by using a cesium sputter ion source dedicated exclusively to  $^{63}\text{Ni}$  AMS measurements, the isobaric  $^{63}\text{Cu}$  background from this ion source is a factor of 100 less than that from the ion source usually used for other AMS measurements. In addition, the gas-filled magnet (GFM) was chosen in a way that most of the  $^{63}\text{Ni}$  ions could still enter the detector (about 80%), but the  $^{63}\text{Cu}$  ions were blocked by the aperture due to their higher mean magnetic rigidity in the gas. This resulted in a reduction of the copper count rate in the detector by a factor of about 3000. The final detector was a Frisch-grid ionization chamber with five  $\Delta E$  sections, enabling independent total energy measurements, position sensitivity and angle sensitivity in the vertical and horizontal plane. This combination improved the detection limit for  $^{63}\text{Ni}/\text{Ni}$  ratios down to  $6 \times 10^{-14}$  (or 0.12 mBq of  $^{63}\text{Ni}$ ) and a total isobaric suppression of about  $5 \times 10^9$ .

Table 6 compares different methods for the determination of  $^{59}\text{Ni}$  and  $^{63}\text{Ni}$ , the detection limit of radiometric methods (LSC, GM counter and ion implanted silicon detector) for  $^{63}\text{Ni}$  is similar to the initial AMS technique because of the relatively high specific activity of  $^{63}\text{Ni}$  and the interference of  $^{63}\text{Cu}$ . But detection limit of later developed AMS technique is much better than the radiometric method. All methods require a long chemical separation procedure, the counting times for LSC and AMS are similar, while a longer counting time is used by GM counter and ion implanted silicon detector. The radiometric methods are easily accessible and cheaper than AMS. Activity levels of  $^{63}\text{Ni}$  in nuclear waste samples are often sufficiently high to be determined by radiometric methods, while environmental samples are better analyzed by the more sensitive AMS method. The detection limit of AMS for  $^{59}\text{Ni}$  is more than 4 orders of magnitude lower than the radiometric methods even with a simple purification procedure. Radiometric method (in principal only X-ray spectrometry) can only be used for the determination of  $^{59}\text{Ni}$  in nuclear waste samples with high level ( $>1 \text{ Bq g}^{-1}$ ). The detection of  $^{59}\text{Ni}$  in environmental and most nuclear waste samples has to be carried out by AMS.

#### 4.6. Strontium-89, 90

Both  $^{90}\text{Sr}$  and  $^{89}\text{Sr}$  can be produced by neutron fission in nuclear reactor and weapons testing and released to environment, while  $^{89}\text{Sr}$  can also be produced by neutron activation of stable strontium (Tables 1 and 2).  $^{90}\text{Sr}$  is one of important radionuclides in the views of radiation protection, environmental monitoring, radioecology, and radioactive waste management due to its relative high radioactive level in environmental and nuclear waste samples. The interest in the determination of  $^{90}\text{Sr}$  and  $^{89}\text{Sr}$  comes also from utilization of them as environmental tracers (Table 1).

Both  $^{90}\text{Sr}$  and  $^{89}\text{Sr}$  are pure  $\beta^-$  emitters, the radiometric methods, such as gas flow GM counting and liquid scintillation counting are normally used for direct measurement of  $^{90}\text{Sr}$  and  $^{89}\text{Sr}$  or alternatively via  $^{90}\text{Y}$  (also pure  $\beta^-$  emitter), a short-lived ( $T_{1/2} = 2.67$  days) daughter of  $^{90}\text{Sr}$ . All these radiometric methods require previous chemical separation and pre-concentration in order to avoid interference from other radionuclides and problems with self-absorption due to the presence of calcium or stable strontium in the sample. Several techniques for the separation of strontium from matrices have been reported, such as solvent extraction using crown ether [170,171], liquid membrane extraction [172], extraction chromatography [173] using Sr-Spec resin [174,175], ion-exchange [176,177] and strontium rhodizonate and  $\text{CaHPO}_4$  precipitation. One general method based on the insolubility of strontium nitrate in strong nitric acid is still widely used for separation of Sr from Ca [178]. Recently a simple method based on  $\text{Ca}(\text{OH})_2$  precipitation in alkaline solution and  $\text{Ba}(\text{Ra})\text{SO}_4$  precipitate was applied to the separation of Sr from sample matrices and interfering radionuclides [16,179]. A detection limit of 5 mBq for  $^{90}\text{Sr}$  was reported by using an anticoincidence shielded gas flow GM counter [16]. When using gas flow GM detector,  $^{90}\text{Sr}$  is normally measured through its daughter  $^{90}\text{Y}$ , because of the low beta energy of  $^{90}\text{Sr}$  ( $E_{\text{max}} = 546 \text{ keV}$ ) and a consequence of low counting efficiency. In order to reach secular equilibrium between  $^{90}\text{Sr}$  and  $^{90}\text{Y}$ , the separated Sr-samples need to be kept for more than 2 weeks for the in-growth of  $^{90}\text{Y}$  before counting. The generated  $^{90}\text{Y}$  is then separated from  $^{90}\text{Sr}$ , which also enables observing the  $^{90}\text{Y}$  decay ( $T_{1/2} = 2.67$  days) by using repeated counting. This increases the confidence of the radiochemical purity of the sample. A direct separation of  $^{90}\text{Y}$  from the samples has also

been reported for the determination of  $^{90}\text{Sr}$ , this method can significantly shorten the time used for sample preparation by avoiding the waiting for the in-growth of  $^{90}\text{Y}$  from the separated  $^{90}\text{Sr}$  [180]. However, the decontamination factors for many interfering radionuclides, especially the short-lived activation and fission products, are not good. A detection limit of 10–30 mBq for  $^{89}\text{Sr}$  and  $^{90}\text{Sr}$  was reported by using LSC [180,181]. Due to the different beta energy of  $^{90}\text{Sr}$  and  $^{89}\text{Sr}$  ( $E_{\text{max}} = 1495 \text{ keV}$ ), they can be simultaneously measured by LSC via measuring Cherenkov radiation. The energy threshold of the fast moving electrons to produce Cherenkov radiation in water is 256 keV. Cherenkov radiation is emitted in the optical and UV parts of the electromagnetic spectrum, which means that it can be detected by the photomultipliers of an ordinary LSC. Due to the relatively low beta energy of  $^{90}\text{Sr}$ , very small fraction of the emitted beta particles give rise to Cherenkov radiation. In a recently separated Sr-sample, the Cherenkov counts mainly originates from  $^{89}\text{Sr}$ , but with the in-growth of  $^{90}\text{Y}$  ( $E_{\text{max}} = 2280 \text{ keV}$ ) by decay of  $^{90}\text{Sr}$ , the contribution from the  $^{90}\text{Y}$  ( $^{90}\text{Sr}$ ) increases. By measuring the sample two times, shortly after Sr-separation and after 3 weeks (when  $^{90}\text{Sr}$  and  $^{90}\text{Y}$  have reached equilibrium), both  $^{89}\text{Sr}$  and  $^{90}\text{Sr}$  can be determined. The main drawback of the radiometric methods is a long analytical time (5–20 days) because of the long chemical separation procedure and the waiting time for in-growth of  $^{90}\text{Y}$  from  $^{90}\text{Sr}$ .

Mass spectrometric techniques such as AMS, RIMS, ICP-MS and GDMS have also been used for the determination of  $^{90}\text{Sr}$  in environmental and waste samples [26,36–40,94,95,102,103]. In AMS determination of  $^{90}\text{Sr}$ ,  $\text{SrH}_3^-$  molecular ion is chosen as injection ion because  $\text{Sr}^-$  ion formation in sputter source is extremely weak. A similar method described above for  $^{41}\text{Ca}$  can be used for the preparation of the  $\text{SrH}_2$  target. The principal difficulty in the AMS measurement of  $^{90}\text{Sr}$  arises from the stable isobaric interference of  $^{90}\text{Zr}$ . Higher energies are therefore required in order to be able to discriminate  $^{90}\text{Sr}$  from  $^{90}\text{Zr}$ . Paul et al. [182] using a energy of 131 MeV, reported a suppression ratio of  $1 \times 10^5$  for  $^{90}\text{Zr}$ , and a detection limit of  $3 \times 10^{-13}$  for  $^{90}\text{Sr}/\text{Sr}$  ratio or 40 mBq for  $^{90}\text{Sr}$ .

RIMS in collinear geometry has been used for the determination of  $^{90}\text{Sr}$  [94]. After chemical separation, the Sr sample is placed in a conventional ion source. The Sr-ions are accelerated to 10–60 keV beam energy, mass separated and then neutralized. In quasi-collinear geometry, the atoms in the metastable state are selectively excited with 363.8 nm light emitting from an Ar-ion laser in the  $5s^4d^3D_3 \rightarrow 5s^23f^3F_4$  transition and subsequently field ionized, selected in an energy filter, and counted. A selectivity of  $>10^{11}$  in suppression of  $^{88}\text{Sr}$  and a detection limit of  $2 \times 10^6$  atoms (or 1.5 mBq) have been reported. The high experimental expense is a main drawback of RIMS in collinear geometry. The coherent multi-step RIMS has also been applied for the determination of  $^{90}\text{Sr}$  by using a double resonance excitation  $5s^2\ ^1S_0 \rightarrow 5s5p^3P_1 \rightarrow 5s6s^3S_1$  with  $\lambda_1 = 689.5 \text{ nm}$ ,  $\lambda_2 = 688.0 \text{ nm}$ , and subsequent photo-ionization at 488 nm [90]. This method gives an isotopic selectivity of  $1.4 \times 10^{10}$  against stable strontium and a detection limit of 4 mBq.

$^{90}\text{Sr}$  has also been determined by ICP-MS [36–38,70]. The main interference in the measurements of  $^{90}\text{Sr}$  by ICP-MS is the isobar  $^{90}\text{Zr}$  which has a natural abundance of 51%. An ETV

system was investigated in order to discriminate against zirconium which has a very high boiling point [39]. By selecting an appropriate temperature, relative Sr/Zr ratio was improved by a factor of 50 as compared to the conventional liquid mobilization. In spite of the improvements, detection limit reported for  $^{90}\text{Sr}$  was still around  $10 \text{ Bq mL}^{-1}$  (equivalent to  $2 \text{ pg mL}^{-1}$ ). Sector field ICP-MS has also been used for the determination of  $^{90}\text{Sr}$  [37,38]. By using cold plasma and medium mass resolution, the Zr signal is significantly reduced, and a detection limit of  $10 \text{ mBq mL}^{-1}$  was achievable in a pure water sample. However, the detection limits in urine was increased to  $0.4 \text{ Bq mL}^{-1}$  due to the presence of stable strontium. Zoriy et al. [37] used a similar operation condition with further optimization, and determined  $^{90}\text{Sr}$  in ground water samples, a detection limit of  $55 \text{ mBq mL}^{-1}$  was obtained when low stable Sr concentration ( $<6 \text{ ppb}$ , or a  $^{90}\text{Sr}/^{88}\text{Sr}$  ratio  $>2 \times 10^{-6}$ ) presents. For suppression of the isobaric interference from  $^{90}\text{Zr}$ , a dynamic reaction cell technique by employing oxygen gas was used in a quadrupole ICP-MS. This resulted in a significant removal of  $^{90}\text{Zr}$ , in addition, this method also suppress the interference from other molecular ions such as  $^{50}\text{Ti}^{40}\text{Ar}^+$  and  $^{50}\text{Cr}^{40}\text{Ar}^+$ . Combined with a chemical separation, a detection limit of  $0.5 \text{ Bq mL}^{-1}$  was obtained for water sample [70]. Besides the isobaric interference, abundance sensitivity (tailing of stable  $^{88}\text{Sr}$ ) is another problem in the ICP-MS measurement of  $^{90}\text{Sr}$ . The abundance sensitivity of ICP-MS for  $^{90}\text{Sr}/^{88}\text{Sr}$  is normally about  $10^{-6}$ , which makes the detection of  $^{90}\text{Sr}/^{88}\text{Sr}$  ratios less than  $10^{-7}$  very difficult. While the concentration of Sr normally is high in the environmental samples ( $7\text{--}9 \text{ mg L}^{-1}$  for seawater,  $20\text{--}300 \text{ mg kg}^{-1}$  soil), the ICP-MS measurable  $^{90}\text{Sr}$  in seawater will be higher than  $450 \text{ Bq L}^{-1}$ , which is much higher than the present  $^{90}\text{Sr}$  level in the environmental seawater ( $<50 \text{ mBq L}^{-1}$ ). This makes ICP-MS difficult to be used for the determination  $^{90}\text{Sr}$  in environmental samples.

As a directly analytical method, GDMS is a very attractive method for rapid analysis of  $^{90}\text{Sr}$ . However, the isobaric interference of  $^{90}\text{Zr}$  has to be removed which requires a very high MS resolution of around  $2 \times 10^6$ . It is therefore very difficult to determine  $^{90}\text{Sr}$  in environmental samples by this technique. Betti et al. [26] investigated application of GDMS for the determination of  $^{90}\text{Sr}$  in soil and sediment. The sample was fist mixed with silver powder and then pressed in a disk for GDMS analysis. A detection limit of  $50 \text{ mBq g}^{-1}$  was reported when no Zr was detected in the sample. However, for real environmental samples, the  $^{90}\text{Zr}$  concentration is much higher than that of  $^{90}\text{Sr}$ , which makes it impossible to directly determine  $^{90}\text{Sr}$  by this technique.

Table 7 compares the radiometric and mass spectrometric methods for the determination of  $^{90}\text{Sr}$ . The reported detection limit of radiometric methods such as gas flow GM counting and LSC is similar to that of AMS and RIMS. The detection limit of ICP-MS for real samples is a few orders magnitude higher than radiometric method, while GDMS require a Zr free sample, which makes it unsuitable for the analysis of real environmental sample. Radiometric method normally requires a complete separation of Sr from the matrix and other radionuclides; a long and time consuming separation procedure is therefore needed. In addition, a very long in-growth time (2–3 weeks) is needed in the radiometric method by measuring  $^{90}\text{Y}$ . A simple separation method, mainly focused on the sep-

**Table 7 – Comparison of radiometric and mass spectrometric methods for the determination of  $^{90}\text{Sr}$** 

Sample	Detection method	Target preparation	Detection limit	Sep. time <sup>a</sup>	Count time	Ref.
Water	GM counter	$\text{Y}_2(\text{C}_2\text{O}_4)_3$ precipitation	5 mBq	1–2 days/20 days	3–5 h	[16]
Water, milk	LSC by Cerenkov	Sr solution	10 mBq	1–2 days/20 days	2.5–3 h	[180]
Environmental samples	LSC	Sr solution	10 mBq	1–2 days/20 days	3–4 h	[179]
Water	AMS	$\text{SrH}_2$	40 mBq	6–8 h	0.5–1 h	[184]
Water	DR-RIMS	$\text{Sr}(\text{NO}_3)_2$ (pure Sr)	4 mBq		0.5 h	[102]
Aerosol	Collinear RIMS	$\text{Sr}(\text{NO}_3)_2$	1.5 mBq	5–8 h	0.5 h	[94]
Environmental samples	DRC-ICP-MS	Sr solution	5 Bq or $0.5 \text{ Bq mL}^{-1}$	5–8 h	5–10 min	[70]
Urine	ICP-SFMS	Sr solution	$400 \text{ mBq mL}^{-1}$	2–4 h	5–10 min	[38]
Water	ICP-SFMS	Sr solution	$55 \text{ mBq mL}^{-1}$	1–3 h	5–10 min	[37]
Soil, sediment	GDMS	No sep./Zr free	$50 \text{ mBq g}^{-1}$	No	<30 min	[26]

<sup>a</sup> For the radiometric methods, if  $^{90}\text{Y}$  is measured, a 2–3 weeks in-growth time is needed to get generation of  $^{90}\text{Y}$  from the separated  $^{90}\text{Sr}$ .

aration of Sr from the matrix and Zr, is required for AMS and RIMS, which therefore makes them suitable for rapid analysis. However, the analytical expense is normally much higher than using radiometric methods, and the AMS and RIMS instrumentation set-up for Sr-analysis is very rare. Based on these considerations, radiometric methods is still the main approach for the routine analysis of  $^{90}\text{Sr}$ . While a rapid analysis is required, mass spectrometric method, such as AMS and RIMS is a potential choice.

Due to the short half-life of  $^{89}\text{Sr}$ , radiometric method is the only suitable method for its determination. In recent years, a big effort was given to develop a rapid analytical method for the determination of  $^{90}\text{Sr}$ , which is stimulated by the requirement for the emergency action of the accident and terrorist attack. By solvent extraction, extraction chromatography separation, flow injection technique for the separation of  $^{90}\text{Sr}$  from the matrix, and direct measurement of  $^{90}\text{Sr}$  by LSC,  $^{90}\text{Sr}$  can be determined in a short time (<1 day) [183].

#### 4.7. Technetium-99

$^{99}\text{Tc}$  in environment is dominated by the releases from the nuclear fuel cycle and nuclear bomb tests, of which the most of them (>90%) was discharged from reprocessing plants in Europe. The interest in determination of  $^{99}\text{Tc}$  results partly from the absence of any stable technetium isotope,  $^{99}\text{Tc}$  as the completely dominating isotope of Tc is thus the only isotope available for studying the unknown environmental and biological behaviors of this element. In addition, the application of  $^{99}\text{Tc}$  as an environmental tracer is also an interest in its determination.

$^{99}\text{Tc}$  is a pure beta emitter with maximum beta particle energy of 294 keV. Radiometric methods using beta counting by gas flow GM counters or liquid scintillation is therefore the main techniques used for its determination. The detection limit of these methods depend on the count rate of blank and the counting time, a value of 1.5 mBq was reported by using an anti-coincidence shielded gas flow GM counter for 4 h counting time [182,185], while a higher value of 17 mBq was reported using 2 h counting by LSC which normally have a higher background count rate [186]. Radiometric methods require a thorough chemical separation of Tc from the matrix and other radionuclides, because of the difficulties of spectrometric isotope identification for beta emitters. Due to the generally low concentrations of  $^{99}\text{Tc}$  in the environment, large

samples are normally required for the analysis. The method adapted for the chemical separation is thus not only important for obtaining a good decontamination from other radionuclides but also to obtain a high chemical recovery of  $^{99}\text{Tc}$ . Technetium exists as the conservatively behaving  $\text{TcO}_4^-$  ion in oxygenated water, while Tc is reduced to particle reactive  $\text{Tc(IV)}$  in anoxic conditions. Technetium in water or leachate from solid samples is normally pre-concentrated by anion exchange chromatography, which is based on that  $\text{TcO}_4^-$  have a very high affinity for the column in alkaline or neutral solutions. By passing the solution through the column and washing with different solvents, such as low concentration NaOH,  $\text{HNO}_3$ , EDTA and NaClO solutions, most of the matrix elements and other radionuclides can be removed. The absorbed  $\text{TcO}_4^-$  is then eluted using concentrated  $\text{HNO}_3$  ( $12 \text{ mol L}^{-1}$ ). For further purification, solvent extraction using tri-isooctylamine (TIOA) in xylene has been used to extract  $\text{TcO}_4^-$ , which can then be back-extracted using NaOH solution. By this procedure, a decontamination factor of more than  $10^5$  relative to most interfering radionuclides was obtained [184–187]. Based on the insolubility of the reduced Tc, co-precipitation method has also been used for pre-concentration of Tc from aqueous solutions. In this method, technetium is first reduced by  $\text{Na}_2\text{S}_2\text{O}_5$ , then co-precipitated with  $\text{Fe(OH)}_2$  to separate it from a large volume of water [188,189]. The precipitate needs to be dissolved in a short time after separation for further chemical separation, otherwise the dissolution will become more difficult and recovery of Tc will be low. The separated Tc is normally electrodeposited onto a stainless steel disk for the measurement using an anti-coincidence shielded gas-flow GM counter [15]. Alternatively, the extracted organic phase can be directly mixed with a scintillation cocktail for LSC measurement [186]. Extraction chromatography using Eichrom TEVA column has also been used for the separation of Tc from other radionuclides [49,189]. In this method,  $\text{TcO}_4^-$  is absorbed on the column by passing through the solution, and the interfering radionuclides are removed by washing with  $0.1 \text{ mol L}^{-1}$   $\text{HNO}_3$ , the  $\text{TcO}_4^-$  on the column is then eluted using  $4 \text{ mol L}^{-1}$   $\text{HNO}_3$ . This method was proved to be useful especially for removal of  $^{106}\text{Ru}$ .

The long half-life of  $^{99}\text{Tc}$  (0.211 My) and low specific activity ( $6.3 \times 10^8 \text{ Bq g}^{-1}$ ) makes mass spectrometry a sensitive method for the determination of  $^{99}\text{Tc}$ , AMS [190–192], TIMS [193,194] and ICP-MS [46–53,195] have been used for the determination of  $^{99}\text{Tc}$ . In AMS, the separated  $\text{TcO}_4^-$  is mixed with



**Table 8 – Potential interfering species on mass 99 in ICP-MS**

Isobar/tailing	Oxide	Hydride	Argide	Chloride
<sup>99</sup> Ru (12.7%)	<sup>83</sup> Kr <sup>16</sup> O (11.5%)	<sup>98</sup> MoH (23.8%)	<sup>59</sup> Co <sup>40</sup> Ar (100%)	<sup>62</sup> Ni <sup>37</sup> Cl (3.6%)
<sup>98</sup> Ru (1.1%)	<sup>81</sup> Br <sup>18</sup> O (49.5%)	<sup>98</sup> RuH (1.9%)	<sup>63</sup> Cu <sup>36</sup> Ar	<sup>64</sup> Zn <sup>35</sup> Cl (48.6%)
<sup>100</sup> Ru (12.6%)	<sup>67</sup> Zn <sup>16</sup> O <sub>2</sub> (4.1%)		<sup>43</sup> Ca <sup>16</sup> O <sup>40</sup> Ar	
<sup>98</sup> Mo (24.1%)	<sup>51</sup> V <sup>16</sup> O <sub>3</sub> (99.8%)		<sup>40</sup> Ca <sup>18</sup> OH <sup>40</sup> Ar	
<sup>100</sup> Mo (9.6%)				

Al or Nb to prepare a target, the sputtered TcO<sup>−</sup> ions is then stripped to TcO<sup>14+</sup>, separated in mass spectrometry, and measured by a gas ionization chamber. Stable isotope <sup>99</sup>Ru is the main isobaric interference, which is suppressed by using the different energy loss of <sup>99</sup>Tc and <sup>99</sup>Ru in the detector. By optimal settings, >90% of <sup>99</sup>Ru can be rejected. However, for environmental samples, <sup>99</sup>Ru concentration is normally some orders of magnitude higher than <sup>99</sup>Tc, the chemical separation is necessary before the AMS determination. The sensitivity of this method depends very much on the amounts of Ru in the target. A detection limit of 6–10 μBq for water and environmental samples has been reported [190,192]. In TIMS, the separated TcO<sub>4</sub><sup>−</sup> is transferred to filament and reduced to TcO<sub>2</sub> using HI, the iodine is removed by pre-heating to 930 °C and the Tc is then measured using magnetic sector thermal ionization mass spectrometers equipped with ion counter. A detection limit of 0.02 mBq (or 11 fg) has been reported for geological samples [194]. Due to isobaric interferences from Mo and Ru, which have to be completely removed, the detection limit for more realistic samples has been reported to be 65 fg (0.1 mBq) mainly because of interferences from Mo.

ICP-MS as a very convenient mass spectrometric technique has been widely used for the determination of <sup>99</sup>Tc [46–53,195,196]. The main challenge for ICP-MS determination is interferences of isobaric and molecular ions. The possible contributors to the 99 peak background are listed in Table 8. Isobaric interferences from the stable isotope <sup>99</sup>Ru, abundance sensitivity or tailing of <sup>98</sup>Mo and <sup>100</sup>Mo, and the <sup>98</sup>MoH<sup>+</sup> molecular ion are the main interferences in the analysis of environmental samples using ICP-MS [46]. Due to high concentration of Ru (0.7 ng L<sup>−1</sup> in seawater) compared to <sup>99</sup>Tc in environmental samples (<8–5000 × 10<sup>−6</sup> ng L<sup>−1</sup>) and a high isotopic abundance of <sup>99</sup>Ru (12.7%), a high decontamination factor (10<sup>6</sup>–10<sup>7</sup>) for Ru is required. A good chemical separation is normally needed to meet this requirement. Electrothermal vaporization (ETV) as a sample introduction has been used to remove ruthenium due to its lower boiling point [47,195]. The contribution from <sup>98</sup>Mo to mass 99 was mainly due to abundance sensitivity and in a less extent due to formation of the <sup>98</sup>MoH. The relative contributions from MoH and abundance sensitivity however depend on sample introduction methodology and instrument operation conditions. The high concentration of Mo in environmental samples (10 μg L<sup>−1</sup> in seawater), and low abundance sensitivity of ICP-MS (10<sup>−6</sup>) require a high decontamination factor of Mo in the chemical separation (>10<sup>6</sup>). Sample introduction techniques such as ETV have also been used to remove Mo and reduce the formation of MoH<sup>+</sup> ions. A detection limit of 0.18 mBq has been reported by using ETV and ICP-QMS [47]. Normally, both radiometric and mass spectrometric methods have difficulties in performing accurate measurements of <sup>99</sup>Tc close to

the detection limits, but the procedure blank in the radiometric measurements can easily be kept in the same as the instrument blank and thus the detection limit is governed by the instrumentation background. On the other hand, the detection limit of ICP-MS is often set by the blank contribution from the chemical processing rather than the instrument blank alone. In this respect radiometric techniques have a well-defined detection limit contrary to what is obtained by the ICP-MS technique.

The chemical separation techniques used in radiometric methods can also be used for the mass spectrometric determination of <sup>99</sup>Tc. The main difference is that the separation methods used for radiometric determination focuses on the removal of radionuclides, the stable elements in the reagents and apparatus are not of importance. Since the stable isotopes <sup>99</sup>Ru, <sup>98</sup>Ru, <sup>100</sup>Ru, <sup>98</sup>Mo, and <sup>100</sup>Mo are the main interferences in the mass spectrometric determination of <sup>99</sup>Tc, it is necessary to use high purity chemical reagents and operate under clean conditions. In addition, a separation procedure designed for ICP-MS also needs to focus on the removal of Mo and Ru.

Due to lack of stable isotope of Tc, other radioisotopes of Tc or other elements such as rhenium have to be used as yield tracer in both radiometric and mass spectrometric methods. The short-lived radioisotope, <sup>99m</sup>Tc, obtained from a <sup>99</sup>Mo–<sup>99m</sup>Tc generator has been widely used as yield tracer in the chemical separation step for determination by radiometric and mass spectrometric methods. The drawback of <sup>99m</sup>Tc as yield tracer is the risk of radioactive contaminants of <sup>99</sup>Tc. In the generator, <sup>99</sup>Mo decays to both <sup>99m</sup>Tc and <sup>99</sup>Tc, and finally all to <sup>99</sup>Tc. Therefore, the generator has to be extensively eluted before use and a short in-growth period for new <sup>99m</sup>Tc generation should be applied to reduce the <sup>99</sup>Tc in the tracer. However the <sup>99m</sup>Tc tracer is still not pure enough for low-level environmental samples [17,187]. Hou et al. [17] have investigated the <sup>99</sup>Tc impurity in <sup>99m</sup>Tc eluate from a hospital <sup>99</sup>Mo–<sup>99m</sup>Tc generator, and found that a relatively higher contribution to <sup>99</sup>Tc in the eluate comes from <sup>99</sup>Mo breakthrough and <sup>99</sup>Tc remained on the column as reduced form. They developed a simple method by passing the new <sup>99m</sup>Tc eluate through two sets of alumina columns to remove the reduced <sup>99</sup>Tc and <sup>99</sup>Mo in the <sup>99m</sup>Tc solution, this procedure produced a pure <sup>99m</sup>Tc solution which is good enough for the use as yield tracer for environmental sample. The long-lived <sup>97</sup>Tc (T<sub>1/2</sub> = 2.6 My) is an idea tracer for mass spectrometry, but it is very difficult to be obtained. In addition the <sup>99</sup>Tc impurity in <sup>97</sup>Tc has to be investigated before use. Rhenium has a similar chemical properties as technetium, it has therefore been used as tracer in mass spectrometric determination of <sup>99</sup>Tc. However, the behavior of Re in chemical separation has to be well investigated in order to be sure it behaves the same way as <sup>99</sup>Tc [46].

**Table 9 – Comparison of radiometric and mass spectrometric methods for the determination of  $^{99}\text{Tc}$** 

Sample	Detection method	Target preparation	Detection limit	Sep. time <sup>a</sup>	Count time	Ref.
Environmental sample	GM detector	Tc on disk	1.5 mBq	1–2 days/7 days	3–4 h	[15]
Environmental sample	LSC	Tc solution	17 mBq	1–2 days/7 days	2 h	[186]
Geological samples	RIMS	TcO <sub>2</sub>	20 $\mu\text{Bq}$	1–2 days	30–60 min	[194]
Water	AMS	Tc in Al <sub>2</sub> O <sub>3</sub> or Nb <sub>2</sub> O <sub>5</sub>	6–10 $\mu\text{Bq}$	1 days	20–40 min	[190,192]
Sediment, seawater	ICP-SFMS	Tc solution	0.16–0.29 mBq	1–2 days	10–20 min	[47]
Seawater	ICP-MS with ETV	Tc in solution	0.18 mBq	1–2 days	20–40 min	[47]
Environmental sample	ICP-QMS	Tc in solution	10 mBq	1–2 days	20–40 min	[49]
Environmental sample	ICP-SFMS on-line	Tc in solution	0.05 mBq mL <sup>-1</sup> or 0.2 mBq	1 h/4–5 h	10–20 min	[196]

<sup>a</sup> For the radiometric methods, if  $^{99\text{m}}\text{Tc}$  is used as yield tracer, further 5–7 days decay time is needed after separation to remove all  $^{99\text{m}}\text{Tc}$  which interferes the counting using GM counter or LSC. For on-line ICP-MS, the separation procedure take about 1 h, while the sample preparation takes about 5 h.

Neutron activation analysis can be also used for the determination of  $^{99}\text{Tc}$  [200], which based on two reactions,  $^{99}\text{Tc}(n, \gamma)^{100}\text{Tc} \xrightarrow{\beta^-, 15.8\text{s}} ^{100}\text{Ru}$  and  $^{99}\text{Tc}(n, n')^{99\text{m}}\text{Tc} \xrightarrow{\text{IT}, 6.0\text{h}} ^{99}\text{Tc}$ , when counting  $^{100}\text{Tc}$ , which has a very short half-life (15.8 s),  $^{99}\text{Tc}$  has to be separated from the sample prior to irradiation; in addition a fast sample transfer system has to be used to shorten the decay time. NAA is theoretically a more sensitive method for  $^{99}\text{Tc}$ , and a detection limit of 2.5 mBq has been obtained using pre-separation and radiochemical NAA [197,198]. Compared with  $^{100}\text{Tc}$ ,  $^{99\text{m}}\text{Tc}$ , a neutron activation product of  $^{99}\text{Tc}$  by (n, n') reaction, has a longer half-life, it makes the post-irradiation separation becomes easier. However, the low neutron activation cross section (0.24 b) of  $^{99}\text{Tc}(n, n')^{99\text{m}}\text{Tc}$  reaction limits its analytical sensitivity [199]. The reported detection limit of this method is more than 1 Bq. Up to date NAA was mainly used for the analysis of samples with a high  $^{99}\text{Tc}$  concentration, such as radioactivity waste.

Table 9 compares the radiometric and mass spectrometric methods for the determination of  $^{99}\text{Tc}$ . AMS and RIMS are the most sensitive methods, their detection limits are 2 orders of magnitude better than radiometric method. These two methods are also rapid due to short counting time. The ICP-MS is comparable to the beta counting using GM detector, by using ETV or ICP-SFMS, the detection limit of ICP-MS may reach 10 times better than radiometric method. Due to the rapid analytical capacity and the installation of more ICP-MS instruments in radiochemical laboratories, many measurements of  $^{99}\text{Tc}$  have being carried out by ICP-MS in recent years. However radiometric methods are still the dominating analytical technique for the analysis of environmental samples due to the well controlled blank counts, easy accessible measurement equipment and low cost.

#### 4.8. Iodine-129

Iodine-129, a naturally occurring long-lived radioisotope of iodine (15.7 My) formed by cosmic ray reaction with Xe and fission of uranium, exists in the environmental with a low concentration ( $^{129}\text{I}/^{127}\text{I}$  ratio of  $10^{-12}$ ). Releases from human nuclear activities dominates the present  $^{129}\text{I}$  level in environment ( $^{129}\text{I}/^{127}\text{I}$  ratio of  $10^{-10}$  to  $10^{-4}$ ), in which discharges from nuclear reprocessing facilities are responsible for about 90% of the  $^{129}\text{I}$  environmental inventory [201,202].

$^{129}\text{I}$  decays by emitting  $\beta$ -particle with a maximum energy of 154.4 keV and  $\gamma$ -rays of 39.6 keV as well as X-rays (29–30 keV). It can therefore be measured by  $\gamma$ -spectrometry and  $\beta$ -counting using LSC [203,204]. Gamma spectrometry has been used to measure  $^{129}\text{I}$  in thyroid, urine, seaweed, and waste by using HpGe detector [203,216]. Due to the low counting efficiency of gamma detector (<2%), low  $\gamma$ -ray abundance (7.5%), and high background, a high detection limit of 20–200 mBq was obtained [216] depending on the level of interfering radionuclide. The direct measurement is easy operation, but a high detection limit (100–200 mBq). A chemical separation of iodine from the matrix and interfering radionuclides can improve the detection limit to around 20 mBq when using gamma spectrometry. Using LSC and measuring  $^{129}\text{I}$  separated from the matrix and other radionuclides results in a slight better detection limit of about 10 mBq [216]. A more sensitive method for the determination of  $^{129}\text{I}$  is neutron activation analysis, in this method, the sample is irradiated with neutrons in a reactor to convert  $^{129}\text{I}$  to short-lived  $^{130}\text{I}$  ( $T_{1/2} = 12.36\text{ h}$ ) by reaction  $^{129}\text{I}(n, \gamma)^{130}\text{I}$ , which is then measured by  $\gamma$ -spectrometry. For removal of the interference, the iodine needs to be separated from the sample before the neutron irradiation; a detection limit of 1  $\mu\text{Bq}$  has been reported [201,205].

Mass spectrometric techniques, AMS, SIMS and ICP-MS have also been used for the  $^{129}\text{I}$  determination. In AMS, the iodine needs to be separated from the sample and prepared as AgI precipitate, which is then mixed with Ag or Nb powder.  $\text{I}^-$  ions are easily formed in the sputter source, which is then stripped to  $\text{I}^{5+}$  or  $\text{I}^{7+}$  in the stripper tank, and separated from the interferences such as  $^{128}\text{TeH}^-$  and  $^{127}\text{IH}_2^-$ . The isobaric interference from  $^{129}\text{Xe}$  in AMS is not a problem because the formation of the  $^{129}\text{Xe}^-$  ion is extremely low. The separated  $^{129}\text{I}$  is then detected by a combination of time-of-flight and a silicon charged particle detector. The instrumental background of  $^{129}\text{I}/^{127}\text{I}$  down to  $10^{-14}$  has been obtained [206–208]. The detection limit of  $^{129}\text{I}$  very much depends on the level of procedure blank, by using a low  $^{129}\text{I}$  iodine carrier, a  $^{129}\text{I}/^{127}\text{I}$  ratio of  $1 \times 10^{-13}$  was reported, it corresponds to  $10^{-9}\text{ Bq } ^{129}\text{I}$  for 1 mg  $^{127}\text{I}$  carrier, and the analytical uncertainty is lower than 10% for a  $^{129}\text{I}/^{127}\text{I}$  ratio of  $10^{-12}$  [208]. Due to the very high sensitive, most of determinations of  $^{129}\text{I}$  in environmental samples, especially low-level geological samples, is now carried out by AMS. Actually, AMS is the only method

**Table 10 – Comparison of radiometric and mass spectrometric methods for the determination of  $^{129}\text{I}$** 

Sample	Detection method	Target preparation	Detection limit	Sep. time	Count time	Ref.
Thyroid, seaweed	$\gamma$ -Spectrometry	Direct measurement	100 mBq or $0.5 \text{ Bq kg}^{-1}$	No	20–60 h	[202]
Waste	$\gamma$ -Spectrometry	Separated iodine (AgI)	20 mBq	3–4 h	60 h	[216]
Waste	$\gamma$ -Spectrometry	Direct measurement	200 mBq	No	20 h	[216]
Seaweed	LSC	Separated iodine	10 mBq	3–4 h	1.5 h	[203]
Environmental samples	RNAA	Separated LiI	$1 \mu\text{Bq}$ or a $^{129}\text{I}/^{127}\text{I}$ ratio of $10^{-10}$	4–7 h	1 h	[205]
Environmental samples	AMS	AgI	$10^{-9} \text{ Bq}$ or a $^{129}\text{I}/^{127}\text{I}$ ratio of $10^{-13}$	4–7 h	20–30 min	[208]
Thyroid	SIMS	Direct measurement	5 Bq	No	10–60 min	[214]
Water	DRC-ICP-MS	Direct water measurement	$37 \mu\text{Bq mL}^{-1}$	0.5–1 h	20–30 min	[42]
Sediment	DRC-ICP-MS	Gaseous iodine	$2.5 \mu\text{Bq g}^{-1}$ or a $^{129}\text{I}/^{127}\text{I}$ ratio of $10^{-7}$	2–3 h	10–20 min	[41]

for the determination of  $^{129}\text{I}$  in the pre-nuclear age samples ( $^{129}\text{I}/^{127}\text{I} < 10^{-10}$ ) [202,199–212].

ICP-MS has been investigated for the determination of  $^{129}\text{I}$ , but the problems associated is low sensitivity, isobaric and molecular ions interferences ( $^{129}\text{Xe}$ ,  $^{127}\text{IH}_2$ ,  $^{89}\text{Y}^{40}\text{Ar}$ ,  $^{115}\text{In}^{14}\text{N}$ ,  $^{113}\text{Cd}^{16}\text{O}$ ), memory effects, low abundance sensitivity of ICP-MS (tailing from the  $^{127}\text{I}$  peak), especially isobar  $^{129}\text{Xe}$  and tailing of  $^{127}\text{I}$ . A dynamic reaction cell (DRC) ICP-MS by using oxygen as reaction gas has been found to significantly reduce xenon ions by charge transfer. It was also found that pressurizing the collision cell with helium the tailing of  $^{127}\text{I}$  or abundance sensitivity can be improved. By using helium and oxygen in the DRC, and directly introducing gaseous iodine to the ICP-MS system, the detection limit of ICP-MS could be significantly improved to  $10^{-6}$  for  $^{129}\text{I}/^{127}\text{I}$  ratio ( $25 \mu\text{Bq g}^{-1}$  for  $^{129}\text{I}$  at a  $^{127}\text{I}$  concentration of  $4 \mu\text{g g}^{-1}$ ) [213]. By trapping gaseous iodine thermally released from samples, and then desorbing it to the ICP-MS system, detection limit could be further improved to  $2.5 \mu\text{Bq g}^{-1}$  (or  $10^{-7}$  for  $^{129}\text{I}/^{127}\text{I}$  ratio) [41]. By using a similar techniques, but directly introducing water samples in 1% tertiary amine carrier solution, a detection limit of  $37 \mu\text{Bq mL}^{-1}$  was reported [42].

SIMS has also been used for the determination of  $^{129}\text{I}$  in the thyroid. Due to the low sensitivity of this method, only high level sample can be measured. The animal and human thyroid sample, in which more than  $10 \mu\text{g } ^{129}\text{I}$  was administrated, have been directly *in vivo* analyzed by SIMS to map the distribution of  $^{129}\text{I}$  in the thyroid [214,215]. The major benefit of this technique is the direct and *in vivo* analysis as well as the  $^{129}\text{I}$  spatial information in the sample

Table 10 compares the radiometric and mass spectrometric methods for the determination of  $^{129}\text{I}$ . The  $\gamma$ -spectrometry and LSC are the least sensitive and long counting time, while it is cheaper and good accessible. These methods are therefore only suitable for the analysis of waste and high level environmental samples. The sensitivity of SIMS is very low, but it can provide spatial information of  $^{129}\text{I}$  and directly used for *in vivo* analysis of high  $^{129}\text{I}$  level samples, it is therefore only used in some special samples. By using DRC techniques, ICP-MS can be used for the determination of  $^{129}\text{I}$  in relatively low-level samples, but the detection limit for  $^{129}\text{I}/^{127}\text{I}$  is only  $10^{-7}$ , it may only be suitable for the analysis of waste and high level environmental samples. Only NAA and AMS are sensitive enough for the analysis of environmental samples, especially AMS, which is the only method for the analysis of sample with a very low  $^{129}\text{I}$  level ( $< 10^{-10}$  for  $^{129}\text{I}/^{127}\text{I}$  ratio).

#### 4.9. Cesium-135, 137

Both  $^{135}\text{Cs}$  and  $^{137}\text{Cs}$  are fission products of  $^{235}\text{U}$  with a similar fission yield to mass 135 and 137 (6–7%). Due to a very high neutron absorption cross section of  $^{135}\text{Xe}$  ( $3.6 \times 10^6 \text{ b}$ ), the ratios of  $^{135}\text{Cs}/^{137}\text{Cs}$  in irradiated nuclear fuel varies with time of neutron irradiation. Therefore, the  $^{135}\text{Cs}/^{137}\text{Cs}$  ratio may be used as a marker for the source identification.  $^{135}\text{Cs}$  and  $^{137}\text{Cs}$  in environmental samples may originate from the weapons testing, operation of nuclear faculties such as nuclear power plants and reprocessing plants, and nuclear accidents.  $^{137}\text{Cs}$  is one of important radionuclides in the views of radiation protection, environmental monitoring and waste disposal.

$^{137}\text{Cs}$ , a short-lived radionuclide (30.07 years), decays by emitting  $\beta$ -particles with maximum energies of 514 keV (94.4%) and 1175 keV (5.4%), it is accompanied by  $\gamma$ -ray emission of 661.7 keV (85.1%).  $^{137}\text{Cs}$  can thus be measured by  $\beta$ -counting and  $\gamma$ -spectrometry. The often common choice to use gamma-counting is a consequence of the high abundance of the 661.7 keV  $\gamma$ -ray from  $^{137}\text{Cs}$ , little self-adsorption in the sample due to high energy, possibility of direct measurement and a minimum of contamination during sample preparation. These factors together with easy operational instrumentation make  $\gamma$ -spectrometry using HpGe detector an excellent method for the determination of  $^{137}\text{Cs}$  in waste and environmental samples. A detection limit for  $\gamma$ -spectrometry of  $^{137}\text{Cs}$  can be less than 50 mBq (or  $1 \text{ mBq g}^{-1}$  for 50 g sample), which is less than present environmental levels in most samples.

$^{135}\text{Cs}$ , a long-lived radionuclide (2.3 My), is a pure  $\beta$ -particle emitter with a maximum beta particle energy of 269 keV.  $^{135}\text{Cs}$  is therefore suitable to be determined by using a beta counter, such as GM counter and LSC. However, both of  $^{135}\text{Cs}$  and  $^{137}\text{Cs}$  exist in the sample, and the radioactivity concentration of  $^{137}\text{Cs}$  is normally more than 5 orders of magnitude higher than  $^{135}\text{Cs}$  due to the significantly different half-life of these two isotopes. The presence of  $^{137}\text{Cs}$  makes the detection of  $^{135}\text{Cs}$  by beta counting impossible.

$^{135}\text{Cs}$  can be also measured by gamma spectrometry by counting its 268.2 keV  $\gamma$ -ray (15.5%). However, the low specific activity of  $^{135}\text{Cs}$  ( $43 \text{ mBq ng}^{-1}$ ) and low counting efficiency of gamma spectrometry for  $^{135}\text{Cs}$  makes its determination by radiometric methods very difficult.

NAA can be also used for the determination of  $^{135}\text{Cs}$  based on the reaction:  $^{135}\text{Cs} \xrightarrow{(n,\gamma)} ^{136}\text{Cs} \xrightarrow{\beta, 13.16 \text{ day}} ^{136}\text{Ba}$  [217,218].

Because of the very low concentration of  $^{135}\text{Cs}$  in the environmental samples, a pre-irradiation concentration has to be carried out to separate Cs from a large amount of sample. The most used method for the separation and concentration of Cs in water samples is based on its specific absorption on ammonium phosphomolybdate (AMP) and copper ferrocyanide (CFC). However, before irradiation, Cs has to be separated from AMP and CFC to reduce the radioactivity of  $^{32}\text{P}$ ,  $^{99}\text{Mo}$ ,  $^{59}\text{Fe}$ ,  $^{64}\text{Cu}$ . Cs concentrated in AMP can be released by dissolution of AMP with diluted KOH, and the released Cs is then absorbed on a cation exchange resin for neutron irradiation [217]. For improvement of the detection limit, a post-irradiation separation of Cs can be carried out, the Cs on the irradiated cation exchange resin can be eluted by  $5\text{--}8\text{ mol L}^{-1}\text{ HNO}_3$ , and the released Cs is then separated by AMP precipitation or cation exchange chromatography [217]. The separated Cs sample is measured by an HpGe detector; the content of  $^{135}\text{Cs}$  can be calculated by counting the radioactivity of  $^{136}\text{Cs}$  using its main gamma rays with energies of 818.5 keV (100%), and 1048.1 keV (80.3%). The detection limit of NAA for  $^{135}\text{Cs}$  depends on the concentration of other Cs isotopes, especially  $^{133}\text{Cs}$  and  $^{137}\text{Cs}$ . A detection limit of  $10^{-4}\text{ Bq}$  ( $10^{-12}\text{ g}$ ) of  $^{135}\text{Cs}$  has been reported for a sample with a ratio of  $^{133}\text{Cs}:^{135}\text{Cs}:^{137}\text{Cs} = 1:1:1$  [217].

Mass spectrometry is a good technique for the determination of  $^{135}\text{Cs}$ . TIMS, SIMS and ICP-MS have been used for the determination of  $^{135}\text{Cs}$  and  $^{137}\text{Cs}$ . In TIMS, Cs in the sample is separated from the matrix and interfering element, especially Ba, and the separated Cs is finally loaded onto a Re filament. The main problem in the mass spectrometric determination of  $^{135}\text{Cs}$  and  $^{137}\text{Cs}$  is the stable isobaric interference of  $^{135}\text{Ba}$  and  $^{137}\text{Ba}$ , and the tailing of stable  $^{133}\text{Cs}$ . By a combination of proper chemical separation and heating the filament to introduce Cs to the system at  $700^\circ\text{C}$ , the contribution of Ba to  $^{135}\text{Cs}$  can be removed. By using an additional electrostatic analyzer, the removal of the tailing of  $^{133}\text{Cs}$  to  $^{135}\text{Cs}$  could be significantly improved. Lee et al. [219] has used a TIMS equipped with a static retarding potential repeller and a static quadrupole lens to determine  $^{135}\text{Cs}$ ,  $^{137}\text{Cs}$  and  $^{133}\text{Cs}$  in sediment samples. The tailing of  $^{133}\text{Cs}$  at 135 amu was better than  $3 \times 10^{-10}$ , and a ratio of  $^{135}\text{Cs}/^{133}\text{Cs}$  of  $1 \times 10^{-9}$  was measured.

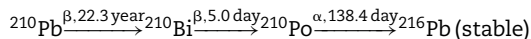
In RIMS, the separated Cs is loaded into a graphite tube, which is lined with titanium tubing, therefore resistively heated to atomize the sample, exciting using the  $6s\ ^2\text{S}_{1/2}$  ( $F=4$ )  $\rightarrow$   $6p\ ^2\text{P}_{3/2}$  ( $F'=5$ ) transition with an extended cavity diode laser followed by photoionization with the 488 nm line of an argon ion laser in order to obtain an optical selectivity for  $^{135}\text{Cs}$  against stable  $^{133}\text{Cs}$ . By this method, a  $^{135}\text{Cs}/^{133}\text{Cs}$  ratio of more than  $10^{-8}$  can be measured [97–99].

The main problem in determination of  $^{135}\text{Cs}$  by ICP-MS is the isobar  $^{135}\text{Ba}$  and the tailing from the  $^{133}\text{Cs}$ ,  $^{134}\text{Xe}$  and  $^{136}\text{Xe}$ . Chemical removal of barium has to be carried out before measurement. Further discrimination against barium may be done by using an ETV sample introduction system. By using different chemical modifiers in the ETV system, the detection limit of  $^{135}\text{Cs}$  can be significantly improved. Using KSCN as chemical modifier, the Cs signal was enhanced around 60 times without significantly enhancing the barium signal. By further using a vaporization temperature of  $1100^\circ\text{C}$  most of the cesium was vaporized while only some 0.03 ppm of the barium was vapor-

ized. An absolute detection limit of  $0.2\ \mu\text{Bq}$  ( $0.4\text{ fg}$ ) for  $^{135}\text{Cs}$  has been reported by using this method [220] in an artificial  $^{135}\text{Cs}$  solution. Considering the relatively poor abundance sensitivity of ICP-MS instrument, and the very low  $^{135}\text{Cs}/^{133}\text{Cs}$  ratio in real samples, the practical detection limit will be higher for environmental samples due mainly to the presence of stable  $^{133}\text{Cs}$  [221].

#### 4.10. Lead-210

$^{210}\text{Pb}$ , a short-lived beta emitter (22.3 years), is one of decay products in the  $^{238}\text{U}$  decay chain. The interest in the determination of  $^{210}\text{Pb}$  mainly comes from its application in geochronology, air flux of radon, and radiation protection in uranium mine.  $^{210}\text{Pb}$  decays by emitting soft  $\beta$ -particles of maximum energy of 17.0 keV (84%) and 63.5 keV (16%) accompanying by a 46.5 keV  $\gamma$ -rays (4.25%) to  $^{210}\text{Bi}$  (5 days) and then to  $^{210}\text{Po}$  (138 days) as shown below:



The determination of  $^{210}\text{Pb}$  can be carried out by  $\gamma$ -spectrometry, beta counting using GM counter through its daughter  $^{210}\text{Bi}$ , which emits a high energy beta particles ( $E_{\text{max}} = 1.2\text{ MeV}$ ), and by alpha spectrometry of its granddaughter  $^{210}\text{Po}$ .  $\gamma$ -Spectrometry is the easiest method, the sample can be directly measured using an HpGe detector. However, due to the low energy of its  $\gamma$ -ray, the self-absorption and interference from other  $\gamma$ -X rays have to be considered. A detection limit of 440 mBq was reported by using  $\gamma$ -spectrometry and a 1000 min counting time [222]. For beta counting, the sample needs to be decomposed and Pb needs to be separated from the matrix and other radionuclides. Solvent extraction, precipitation and ion exchange methods have been used to separate Pb. The separated Pb is kept for 8–9 days for the in-growth of  $^{210}\text{Bi}$ , which is then measured using GM detector or LSC [223,224]. A detection limit of 7 mBq was reported using this method [222]. For  $\alpha$ -spectrometry, the sample is first decomposed, after removal of the  $^{210}\text{Po}$  in the samples by solvent extraction or self-deposition on a silver disk [225], the sample is kept for more than 3 months for the in-growth of  $^{210}\text{Po}$ , the newly generated  $^{210}\text{Po}$  from  $^{210}\text{Pb}$  is then self-deposited onto a silver disk and measured by  $\alpha$ -spectrometry using semiconductor detector. Because of the very low background counts and the high counting efficiency (30–40%), detection limits of 0.1–1 mBq, depending on the in-growth time, have been obtained [222,226]. The drawback of  $\alpha$ -spectrometry is the long analytical time due to the waiting for in-growth of  $^{210}\text{Po}$ . The relatively higher detection limit of  $\gamma$ -spectrometry and the complicated separation procedure for beta counting make the  $\alpha$ -spectrometry an attractive technique, especially for the analysis of the very low-level samples [227].

ICP-MS has also been used for the determination of  $^{210}\text{Pb}$ , the main problem in this method results from the interference of molecular ions such as  $^{209}\text{Bi}^1\text{H}$ ,  $^{208}\text{Pb}^1\text{H}_2$ ,  $^{194}\text{Pt}^{16}\text{O}$ ,  $^{198}\text{Hg}^{12}\text{C}$ , and  $^{170}\text{Er}^{40}\text{Ar}$ , and the abundance sensitivity by the tailing of  $^{209}\text{Bi}$  and  $^{208}\text{Pb}$ . By converting lead into the volatile tetraethyl lead, and directly introducing this form of Pb to the plasma, most of molecular ions interferences can be sig-

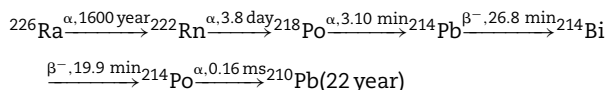


nificantly removed. Since the ethylated species of bismuth are also volatile, this element is a major problem, chemical removal of this element prior to analysis is therefore imperative. In spite of the improved sample introduction technique and a thorough chemical clean-up of the samples, the detection limits for water sample was not better than  $90 \text{ mBq L}^{-1}$  ( $10 \text{ pg L}^{-1}$ ) after pre-concentration, mainly because of the tailing from the stable lead isotopes [228]. This makes ICP-MS less attractive compared to radiometric methods, although a rapid analysis can be carried out by this technique.

#### 4.11. Radium-226, 228

$^{226}\text{Ra}$  and  $^{228}\text{Ra}$  originate from the naturally decay series of  $^{238}\text{U}$  and  $^{232}\text{Th}$ . Concentrations of  $^{226}\text{Ra}$  and  $^{228}\text{Ra}$  in typical soil samples are  $1000$  and  $5 \text{ fg g}^{-1}$  (or  $30$  and  $50 \text{ mBq g}^{-1}$ ), respectively. The interest in the determination of  $^{226}\text{Ra}$  and  $^{228}\text{Ra}$  comes not only from the radiation protection concern, but also from the application of them as environmental tracers.

$^{226}\text{Ra}$ , a long-lived radionuclide (1600 years), decays by emitting alpha particles with energies of  $4.60$  and  $4.78 \text{ MeV}$  to  $^{222}\text{Rn}$ , accompanied with an emission of  $186.2 \text{ keV}$  ( $3.59\%$ )  $\gamma$ -ray. This decay follows by a few short-lived decay daughters as shown below:



$^{226}\text{Ra}$  can thus be determined by  $\alpha$ -spectrometry and  $\gamma$ -spectrometry. The  $\gamma$ -rays from its granddaughters  $^{214}\text{Bi}$  ( $609.3 \text{ keV}$  ( $46.1\%$ ) and  $1120.3 \text{ keV}$  ( $15.1\%$ )) and  $^{214}\text{Pb}$  ( $295.2 \text{ keV}$  ( $19.3\%$ ) and  $351.9 \text{ keV}$  ( $37.6\%$ )) can also be used for the determination of  $^{226}\text{Ra}$ . In addition, LSC has been used for the determination of  $^{226}\text{Ra}$  by measuring alpha particles of  $^{226}\text{Ra}$ , its daughters or  $^{226}\text{Ra}$  plus its daughters ( $^{222}\text{Rn}$ ,  $^{218}\text{Po}$ ,  $^{214}\text{Po}$ ) by using alpha-beta discrimination mode in LSC equipment. In  $\gamma$ -spectrometric measurement of  $^{226}\text{Ra}$ , the interference with the  $185.7 \text{ keV}$   $\gamma$ -ray from  $^{235}\text{U}$  has to be subtracted because the two gamma lines cannot be resolved using gamma spectrometry. The low abundance of the  $186.2 \text{ keV}$   $\gamma$ -ray of  $^{226}\text{Ra}$  ( $3.6\%$ ), the interference from  $^{235}\text{U}$  and Compton background due to

the presence of other radionuclides make this method insensitive, the detection limit varies from  $0.1$  to  $1 \text{ Bq}$  depending on the background level [229]. Measurement via the  $\gamma$ -rays of  $^{214}\text{Bi}$  and  $^{214}\text{Pb}$  can improve the detection limit because of less interference and higher abundance of these  $\gamma$ -rays, however, the leaking of  $^{222}\text{Rn}$  gas, the daughter of  $^{226}\text{Ra}$  and the mother of  $^{214}\text{Bi}$  and  $^{214}\text{Pb}$ , is the main problem related to the reliability of analytical results.

LSC is a sensitive method for the determination of  $^{226}\text{Ra}$ , which can be carried out by measuring the  $\beta$ -emitting daughter isotopes  $^{214}\text{Bi}$  and  $^{214}\text{Pb}$ , or the  $\alpha$ -emitters  $^{226}\text{Ra}$ ,  $^{222}\text{Rn}$ ,  $^{218}\text{Po}$  and  $^{214}\text{Po}$ . The detection limit by measuring  $\alpha$ -emitters is much better than that of  $\beta$ -emitters, because of the low background in the alpha windows of LSC and the high counting efficiency of LSC for  $\alpha$ -emitters ( $>95\%$ ). If all four  $\alpha$ -emitters ( $^{226}\text{Ra}$ ,  $^{222}\text{Rn}$ ,  $^{218}\text{Po}$  and  $^{214}\text{Po}$ ) are measured, the counting efficiency will be higher than  $380\%$ , which is more than one order of magnitude higher than that of counting beta emitters. In addition only  $^{214}\text{Po}$  may be used alone for the determination of  $^{226}\text{Ra}$  in LSC, since it is completely separated from the peaks of  $^{226}\text{Ra}$  and other daughters (Fig. 2). A spectrum of  $^{226}\text{Ra}$  using  $^{133}\text{Ba}$  as chemical yield tracer is shown in Fig. 2, in the beta window, the  $^{133}\text{Ba}$  tracer,  $^{214}\text{Bi}$  and  $^{214}\text{Pb}$  are measured, while in the alpha windows,  $^{226}\text{Ra}$  and its daughters  $^{222}\text{Rn}$ ,  $^{218}\text{Po}$  and  $^{214}\text{Po}$  are measured. In this method, Ra has to be separated from the matrix and other radionuclides. In addition, the measurement of  $^{226}\text{Ra}$  can also be carried out by extracting  $^{222}\text{Rn}$  to the organic scintillation cocktail and the LSC counting of  $^{222}\text{Rn}$ ,  $^{218}\text{Po}$  and  $^{214}\text{Po}$  is thereby done. In this case, chemical separation of Ra from other radionuclides may not be so stringent, because most of radionuclides do not be extracted into the organic cocktail but rather in the aqueous phase. By using this method, a detection limit of  $0.3$ – $1.4 \text{ mBq}$  has been reported [230,231]. The main drawback of the LSC is the long analytical time which results from a long waiting time (3 weeks) for the in-growth of the  $^{226}\text{Ra}$  daughters.

The most sensitive radiometric method for  $^{226}\text{Ra}$  is  $\alpha$ -spectrometry due to the very low background counts. In this method, Ra has to be separated from the matrix and other radionuclides, and electrodeposited on a disk or precipitated and filtered on a filter. The main problem of electrodeposited

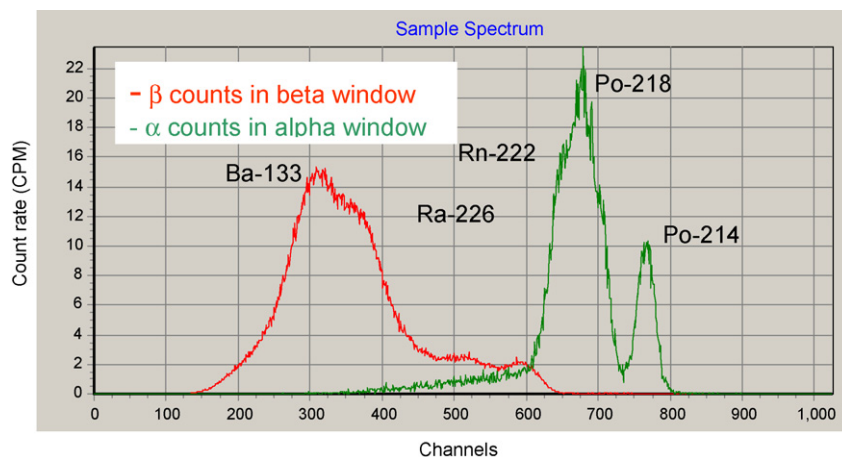
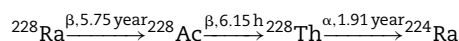


Fig. 2 – Beta spectroscopy of  $^{226}\text{Ra}$  measured by  $\alpha$ - $\beta$  separation in Quantulus™ 1220 LSC.

sources for alpha spectrometry of Ra is the interference of Ba, which exists in environmental samples with a much higher concentration than that of Ra. A high Ba concentration in the separated solution prepared for electrodeposition will significantly reduce the chemical yield of Ra in the electrodeposition process and worsen the resolution of  $\alpha$ -spectroscopy by increasing the thickness of the source, it is therefore Ba has to be completely separated from Ra before electrodeposition [232]. Co-precipitation of Ra and then filtered on a filter is an easy method for the preparation of the alpha source, but the self-absorption and thereby the reduced energy resolution is the main problem in this method because of the thickness of the source. A new development on the chemical separation and alpha spectrometric determination of Ra is the thin film absorption of Ra from the solution [13]. In this method, polyamide piece was immersed in  $\text{KMnO}_4$  solution at 60 °C under stirring, a manganese oxide layer was generated on the polyamide substrate. The prepared thin film was then suspended in the sample solution with pH of 4–8 for 40–50 h under stirring at room temperature. Following the sorption step, samples were washed and measured using alpha or gamma spectrometry. The absorption efficiency is higher than 99% for 1 L sample solution using a film of 2.5 cm<sup>2</sup>. With the increasing of the sample volume, the absorption efficiency decreases. This method is easy to operate, but not suitable for a large volume sample. Another drawback of the  $\alpha$ -spectrometry is the risk of the contamination of the detector, because the release of the  $^{222}\text{Rn}$  from the Ra source and deposition of its daughter on the detector, however, this risk is quite less due to shorter half-lives of most daughter radionuclides of  $^{226}\text{Ra}$ . A detection limit of 0.2–0.5 mBq has been reported for this method for 2 days counting time [13,233].

Radium-228, a short-lived radioisotope of Ra (5.75 years), decays by low energy  $\beta^-$  emission (12–40 keV) to  $^{228}\text{Ac}$ , with emission of 12–17 keV low energy gamma rays (3%) which are difficult to be detected. This decay follows by a few short-lived decay daughters as shown below:



$^{228}\text{Ac}$ , daughter of  $^{228}\text{Ra}$ , decays by emitting high energy beta particles (1.16 MeV), accompanying by  $\gamma$ -rays (911.2 keV (25.8%), 969.0 keV (15.8%)).  $^{228}\text{Ra}$  is therefore normally determined by  $\gamma$ -spectrometry and beta counting of its short-lived daughter  $^{228}\text{Ac}$  or by  $\alpha$ -spectrometry of its granddaughter  $^{228}\text{Th}$ . Direct  $\gamma$ -counting is the simplest method, but a high detection limit (100 mBq) is normally obtained [236]. In the beta counting method, Ra is first separated from the matrix and Ac, after in-growth of  $^{228}\text{Ac}$  from  $^{228}\text{Ra}$  for 3–24 h, the generated  $^{228}\text{Ac}$  is separated from Ra, which can be carried out by solvent extraction using 2-ethylhexyl phosphoric acid (HDEHP) or extraction chromatography. The separated  $^{228}\text{Ac}$  is prepared as a precipitate such as  $\text{Ac}_2(\text{C}_2\text{O}_4)_3$  for beta counting. A detection limit of 15 mBq has been reported by using this method and counting by a GM counter for 100 min [236]. The separated  $^{228}\text{Ac}$  can be also measured by LSC, in this case a slight higher detection limit of 25 mBq was reported [237]. In the  $\alpha$ -spectrometry, the Ra is separated from the matrix and other radionuclides, and prepared as a  $\alpha$  source by electrode-

positing on disc or precipitating/adsorbing on filter. The  $^{228}\text{Th}$  generated from  $^{228}\text{Ra}$  is then measured by  $\alpha$ -spectrometry. The advantage of this method is the simultaneous determination of  $^{224}\text{Ra}$ ,  $^{226}\text{Ra}$  and  $^{228}\text{Ra}$ , and a relatively low detection limit (0.2 mBq) [234]. The drawback is the very long analytical time (1–2 years) due to the long waiting time for the in-growth of the longer-lived  $^{228}\text{Th}$  (1.9 years).

Mass spectrometric methods, AMS, TIMS and ICP-MS have also been used for the determination of  $^{226}\text{Ra}$  and  $^{228}\text{Ra}$ . In AMS, the separated Ra is simply adsorbed in a carbon powder matrix,  $\text{RaC}_2^-$  is normally chosen as injection ion because of the low count rate of  $\text{Ra}^-$ . The mass separated Ra ions are measured by multi-anode gas ionization detector. A detection limit of  $10^7$  atoms or 0.1 mBq for  $^{226}\text{Ra}$  and 40 mBq for  $^{228}\text{Ra}$  has been reported [238], which is comparable to alpha spectrometric method for  $^{226}\text{Ra}$ , and beta counting method for  $^{228}\text{Ra}$ , but worse than alpha spectrometry for  $^{228}\text{Ra}$  ( $^{228}\text{Th}$ ). The major advantage of AMS for radium measurements is the ability to measure both isotopes within a short time. TIMS is a sensitive method for the determination of  $^{226}\text{Ra}$ , a detection limit of 37  $\mu\text{Bq}$  was reported. While, detection limit of 12 mBq for  $^{228}\text{Ra}$  is comparable to beta counting but worse than alpha counting using  $^{228}\text{Th}$  [239,92]. The drawback of this method is the interference from Ba, which has to be completely separated from Ra. In ICP-MS, there are no isobaric interferences to  $^{226}\text{Ra}$ , while  $^{228}\text{Th}$  is a potential isobaric interference to  $^{228}\text{Ra}$ . As a short-lived decay product of  $^{228}\text{Ra}$ , the mass concentration of  $^{228}\text{Th}$  in the samples is normally less than 30% of  $^{228}\text{Ra}$ . However, with fractionation in natural process, concentration of  $^{228}\text{Th}$  in some samples may be comparable or even higher than that of  $^{228}\text{Ra}$ . In addition the polyatomic interferences and signal suppression due to a high salt load to the plasma makes chemical separation of radium necessary before ICP-MS measurement. Since radium is an alkaline earth element, high concentrations of barium, strontium and calcium may be expected to follow in the separation and polyatomic species like  $^{88}\text{Sr}^{138}\text{Ba}$  may appear. Other potential interferences include  $^{208}\text{Pb}^{18}\text{O}$  and  $^{146}\text{Nd}^{40}\text{Ar}_2$  as well as several combinations of molybdenum isotopes with xenon isotopes. A detection limit of 0.1–0.5 mBq for  $^{226}\text{Ra}$  has been reported using a SF-ICP-MS combined with an APEX-Q nebuliser [59,240], which is comparable to radiometric method. The main advantage of mass spectrometric method is the short analytical time, normally only some minutes excluding sample preparation.

Table 11 compares the radiometric and mass spectrometric methods for the determination of  $^{226}\text{Ra}$  and  $^{228}\text{Ra}$ .  $\gamma$ -Spectrometry is the simplest, cheaper and rapid method, but the sensitivity is low, and can only be used for high level or large soil or sediment samples. Mass spectrometric methods including ICP-MS are sensitive for  $^{226}\text{Ra}$ , they are comparable to the LSC and alpha spectrometry, and the analytical time is much shorter than using radiometric methods. AMS and TIMS can be used for the determination of  $^{228}\text{Ra}$ , the sensitivity is comparable with beta counting, but lower than alpha spectrometry using the daughter isotope  $^{228}\text{Th}$ . Due to the restricted availability to AMS and TIMS instrumentation configured for such measurements, radiometric methods are still the most suitable method for the determination of  $^{228}\text{Ra}$ .

**Table 11 – Comparison of radiometric and mass spectrometric methods for determination of  $^{226}\text{Ra}$  and  $^{228}\text{Ra}$** 

Sample	Detection method	Nuclide	Detection limit	Sept. time	Count time	Ref.
Environmental samples	$\gamma$ -Spectrometry	$^{226}\text{Ra}$	0.1–1 Bq	No	5 h	[229]
Water	$\gamma$ -Spectrometry	$^{226}\text{Ra}$ (via $^{214}\text{Pb}$ )	80 mBq	No	40 h	[235]
Environmental samples	LSC	$^{226}\text{Ra}$ (via its daughters)	0.3–1.4 mBq	2 h/30days*	6 h	[230,231]
Environmental samples	$\alpha$ -Spectrometry	$^{226}\text{Ra}$	0.2–0.5 mBq	2–4 days	2 days	[13,233,234]
Environmental sample	TIMS	$^{226}\text{Ra}$	37 $\mu\text{Bq}$	4–5 h	20–30 min	[239,92]
water	ICP-MS	$^{226}\text{Ra}$	0.1–0.5 mBq	2–4 h	10 min	[240,252]
Water	ICP-MS/flow-injection separation	$^{226}\text{Ra}$	0.34 mBq	20–30 min	20 min	[59]
Water	AMS	$^{226}\text{Ra}$	0.1 mBq	3–5 h	30 min	[238]
Environmental samples	$\alpha$ -Spectrometry	$^{228}\text{Ra}$ (via $^{228}\text{Th}/^{224}\text{Ra}$ )	0.2 mBq	2–4 days/6–12 months*	2–3 days	[234]
Water	LSC	$^{228}\text{Ra}$	25 mBq	1–2 days	60 min	[237]
Water	GM counter	$^{228}\text{Ra}$ (via $^{228}\text{Ac}$ )	15 mBq	4–8 h	100 min	[236]
Water	$\gamma$ -Spectrometry	$^{228}\text{Ra}$ (via $^{228}\text{Ac}$ )	100 mBq	No	40 h	[235]
Environmental sample	TIMS	$^{228}\text{Ra}$	12 mBq	4–5 h	20–30 min	[239,92]
Water	AMS	$^{228}\text{Ra}$	40 mBq	3–5 h	30 min	[238]

\* Time of separation and in-growth of  $^{222}\text{Rn}$  from  $^{226}\text{Ra}$  or  $^{228}\text{Th}/^{224}\text{Ra}$  from  $^{228}\text{Ra}$ .

#### 4.12. Isotopes of thorium and uranium

The determination of uranium and thorium isotopes has historically been a subject mostly within the fields of geochronology and geochemistry. Within the fields of environmental sciences and health physics, interest has been widespread although to a lesser extent. In recent years uranium isotopes has also been of major interest within the field of nuclear forensic analysis. Among the naturally occurring uranium and thorium isotopes, there are some very long-lived ( $^{238}\text{U}$ ,  $^{235}\text{U}$  and  $^{232}\text{Th}$ ), some with intermediate half-lives ( $^{234}\text{U}$  and  $^{230}\text{Th}$ ) and some with a short half-life ( $^{228}\text{Th}$ ,  $^{234}\text{Th}$ ,  $^{231}\text{Th}$ ). When concerning nuclear materials, additional isotopes like  $^{236}\text{U}$  and occasionally  $^{233}\text{U}$  are of interest. The analytical methods used for these isotopes depends mainly on what isotopes are of interest, their half-lives, decay mode and risk of interferences in the various techniques. Due to the huge span in specific activity (from 19 TBq mg $^{-1}$  for  $^{231}\text{Th}$  to 4 Bq mg $^{-1}$  for  $^{232}\text{Th}$ ), both mass spectrometric and radiometric methods are required in order to be able to analyze all isotopes. In general, the long-lived radioisotopes are best determined by mass spectrometric methods, while the short-lived ones are preferably determined by radiometric methods.

The geochronology and the geochemistry societies mainly seek to obtain high precision isotope ratios ( $^{234}\text{U}/^{238}\text{U}$ ,  $^{230}\text{Th}/^{234}\text{U}$ ), while the health physics interest is mainly focused on concentrations. An exception is nuclear forensic groups requiring high precision  $^{235}\text{U}/^{238}\text{U}$  and  $^{236}\text{U}/^{238}\text{U}$  ratios. Achieving high precision means counting a sufficient number of events (radioactive decays or ions) which may be done by either a sensitive instrumentation or a large sample mass (activity). Lack of suitable, high abundance gamma lines emitted by the long-lived U and Th-isotopes means that the standard radiometric method is alpha spectrometry where the chemically separated U or Th-isotopes usually have been electrodeposited on stainless steel discs and measured using semiconductor detectors for charged particles [242]. From

spectroscopy point of view, alpha spectrometry of the natural composition of either the U or the Th-isotopes presents few problems. This technique has been used for more than 30 years and is well established and very reliable. It should be kept in mind that mass spectrometry often requires considerable skill of the operators to obtain reliable results. For both elements, tracer isotopes ( $^{232}\text{U}$  and  $^{229}\text{Th}$ ) are readily available for alpha spectrometry and do not disturb other peaks in the spectrum. In cases where the  $^{230}\text{Th}/^{229}\text{Th}$  is very low and/or the energy resolution is poor, a correction for  $^{229}\text{Th}$  in the  $^{230}\text{Th}$  peak must be performed. The major obstacle with alpha spectrometry of the U and Th-isotopes are long counting times (days–weeks) and a limited precision due to the counting statistics. The development of detector hardware for alpha spectrometry during the last 10 years has been very limited and in principle all measurements are being performed using ion implanted planar silicon detectors.

Due to the low specific activity of the long-lived  $^{238}\text{U}$  and  $^{232}\text{Th}$  isotopes (12.3 and 4 Bq mg $^{-1}$  respectively), there is an upper limit as to how much U or Th that can be accepted on the disc before severe degradation of the alpha spectrum starts due to self-absorption of the alpha particles in the source. This means that there is an upper limit of the count rate that can be achieved in alpha spectrometry for the alpha emitting  $^{238}\text{U}$ ,  $^{235}\text{U}$ ,  $^{234}\text{U}$ ,  $^{232}\text{Th}$  and  $^{230}\text{Th}$  isotopes. To compensate for the low count rates, long counting times have been necessary in order to obtain sufficiently good counting statistics. Even with counting times in the order of weeks to months, only a very tiny fraction of the U and Th isotopes are detected on the steel disc. The instrumental efficiency may be measured as the count rate relative to the amount of U or Th isotopes present on the disc and is thus extremely small. Although matrix suppression of the signal also occurs in mass spectrometry, counting of the ions instead of their emitted radiation makes mass spectrometric analysis of the long-lived  $^{238}\text{U}$  and  $^{232}\text{Th}$  around six orders of magnitude more sensitive than the radiometric methods. The development within high-

precision isotope ratio mass spectrometry has partly been driven by the geochemical/geochronological society and today multicollector systems both in TIMS and ICP-MS instruments has further manifested mass spectrometry as the main tool for high-precision measurements of the U-isotopes and long-lived Th-isotopes  $^{232}\text{Th}$  and  $^{230}\text{Th}$ .

At present both MC-ICP-MS and MC-TIMS instruments are considered the ultimate tools for isotope ratio measurement of the longer lived U and Th isotopes. TIMS instruments show the best ion beam stability and better abundance sensitivity due to the lower spread in ion energy than ICP-MS instruments. With the introduction of multi-collectors in ICP-MS instruments, the ion beam instability could be compensated for and the internal precision in TIMS and MC-ICP-MS instruments may typically reach 0.01 per mille [246]. The main factor limiting precision and accuracy in TIMS is the time dependent mass fractionation that arises from the evaporation process at the filament. This means that the isotope ratio changes with time during the analysis. In order to overcome this instrumental-induced mass fractionation, a double-spike technique is required. For uranium a  $^{236}\text{U}$ – $^{233}\text{U}$  mixture with known atom ratio may be applied or the natural  $^{238}\text{U}/^{235}\text{U}$  atom ratio of 137.88 may be used, but for thorium isotopes this technique is not possible due to lack of natural occurring isotopes of known ratios and due to lack of other isotopes than  $^{229}\text{Th}$  as spike. In order to correct for mass fractionation in Th-analysis by TIMS, external correction factors have to be applied by analyzing suitable thorium standards. An alternative to minimize the influence of the time dependent mass fractionation is to integrate the signal over the complete analysis time until the sample has been consumed. The main advantage with MC-ICP-MS over TIMS is the absence of any time dependence in mass fractionation (although mass-fractionation in ICP-MS typically is an order of magnitude larger than in TIMS) and the significantly less complicated sample preparation, which means a higher throughput of samples during any given time. For thorium in particular, ICP-MS is better than TIMS due to the low ionization efficiency at the TIMS filament. Another advantage with ICP-MS instruments is that other isotope systems than what is intended to be measured may be used to correct for the mass bias. A well-known uranium isotope mixture may thus be used to correct for mass fractionation acting on the  $^{230}\text{Th}/^{232}\text{Th}$  isotopes. A similar approach is not possible in TIMS due to the temperature dependent element evaporation from the filament. The temperature dependent evaporation is, on the other hand, one of the advantages in TIMS since it means a more element specific input to the instrument and thus a significantly reduced risk of isobaric and polyatomic interferences. Several review articles on radiometric and mass-spectrometric techniques for measuring U and Th isotopes are available [241–244].

Mass spectrometric techniques like MC-ICP-MS and TIMS are presently the standard accepted methods for determination of long- and intermediate half-life U and Th isotopes within the geological sciences, the requirements of high precision measurements are less in the health physics societies which means that alpha spectrometry and/or single collector ICP-MS is the standard techniques used. For ICP-MS instruments the most critical parameter is the abundance sensitivity

which determines whether the intermediate half-life isotopes  $^{234}\text{U}$  and  $^{230}\text{Th}$  can be measured without significant influence of tailing from the more abundant  $^{235}\text{U}$ ,  $^{238}\text{U}$  and  $^{232}\text{Th}$  isotopes. In alpha spectrometry this is never a problem. When faced with poor abundance sensitivity of ICP-MS instruments, alpha spectrometry is preferred. The better peak shape in quadrupole based instruments (better defined boundaries) means that despite the absence of flat topped peaks in Q-ICP-MS a more reliable  $^{230}\text{Th}/^{232}\text{Th}$  ratio may be obtained since no interference corrections needs to be applied for tailing.

Apart from the natural uranium isotopes,  $^{236}\text{U}$  (half-life:  $2.4 \times 10^7$  years) produced through neutron activation reaction of  $^{235}\text{U}$  in nuclear reactors, is of interest in nuclear forensic analysis. Due to the very low atom ratio of  $^{236}\text{U}/^{235}\text{U}$  (ppb–ppm levels) in samples of interest, ordinary ICP-MS is often not sufficient due to the poor abundance sensitivity and the hydride formation ( $^{235}\text{UH}$ ). Boulyga and Heumann [247], using a ELEMENT 2 SF-ICP-MS optimized for improved abundance sensitivity and minimized hydrides, have managed to measure  $^{236}\text{U}/^{238}\text{U}$  atom ratios down to  $10^{-7}$  which may be sufficient even at very low-levels of contamination of nuclear material. Alpha spectrometry proves difficult in analyzing  $^{236}\text{U}$  due to similar alpha particle energies as  $^{235}\text{U}$ . TIMS, and in particular AMS, is the best technique suited for this analysis. This is because of the excellent abundance sensitivity achieved by these techniques. A comparison between AMS and MC-ICP-MS for the measurement of  $^{236}\text{U}$  and the naturally occurring uranium isotopes was presented by Buchholz et al. [248]. With AMS, measurement of  $^{236}\text{U}/^{238}\text{U}$  atom ratios down to  $10^{-15}$  is possible using high energy filters, and a detection limits in the order of  $10^4$  atoms has been reported [245]. Due to the several other measurement techniques available for the analysis of naturally occurring U and Th isotopes these isotopes are rarely analyzed by AMS.

There may be a choice between mass-spectrometric and radiometric methods for U and Th isotopes with long and intermediate half-lives, while for the short-lived Th-isotopes,  $^{228}\text{Th}$  and  $^{234}\text{Th}$  (half-lives of 1.91 years and 24 days respectively), radiometric methods may be the only possible technique for their determination when present at environmental levels. The alpha-emitter  $^{228}\text{Th}$  is most conveniently determined by standard alpha spectrometry, it may also be determined by gamma spectrometry through one of its daughter isotopes when activity levels are sufficient. The beta emitter  $^{234}\text{Th}$  has played a major role as a particle tracer in the marine environment, especially a rate tracer for particulate organic carbon (POC) vertical fluxes [250]. Several techniques for direct measurement of  $^{234}\text{Th}$  onboard a ship or in the shore based laboratory have been developed. Being a fairly low-abundant gamma emitter (64 keV (4.8%) and 93 keV (5.6%)), a large sample volumes of sea-water is required for the analysis, but significantly smaller volumes, down to a few liters, is enough when using anti-coincidence shielded GM-counters and measuring the combined electron emission of both  $^{234}\text{Th}$  and  $^{234}\text{Pa}$  which reaches secular equilibrium within some tens of minutes after separation of Th. A recent review article on the methodology for analyzing  $^{234}\text{Th}$  in marine systems has been presented by Van der Loeff et al. [249].



#### 4.13. Neptunium-237

Neptunium-237 presenting in environment has been produced by  $^{238}\text{U}(n, 2n)^{237}\text{U} \rightarrow ^{237}\text{Np}$  reaction through fast neutrons in nuclear bomb testing and reactors and  $^{235}\text{U}(n, \gamma)^{236}\text{U}(n, \gamma)^{237}\text{U} \rightarrow ^{237}\text{Np}$  reaction in nuclear reactors followed by releases from spent fuel reprocessing. It is also produced as a consequence of the decay of  $^{241}\text{Am}$ . The interest in the determination of  $^{237}\text{Np}$  results from tracer applications and in connection to repositories of nuclear waste because of its relatively high mobility in the environment and as a consequence the most hazardous radioisotopes in spent nuclear fuel.

$^{237}\text{Np}$  is an  $\alpha$ -emitting long-lived radionuclide (2.144 My),  $\alpha$ -spectrometry has therefore traditionally been used for its measurement. Due to the low concentration encountered in environmental samples, a pre-concentration and completely separation from interfering radionuclides are necessary. Ion exchange, extraction chromatography and solvent extraction, are normally used for the separation of  $^{237}\text{Np}$  [251–259]. Control of the valence state of Np plays an important role in the chemical separation procedure. Neptunium can exist as  $\text{Np}^{3+}$ ,  $\text{Np}^{4+}$ ,  $\text{NpO}_2^+$ , and  $\text{NpO}_2^{2+}$ , among these,  $\text{NpO}_2^+$  is the most stable form in the environment. For pre-concentration of neptunium from the matrix, hydroxide co-precipitate method is widely used. However,  $\text{NpO}_2^+$  cannot be completely co-precipitated with  $\text{Fe}(\text{OH})_3$ , it has to be therefore reduced to  $\text{Np}^{4+}$  before hydroxide precipitation. Solvent extraction using tri-*n*-octylphosphine oxide (TOPO) in toluene or thenoyl trifluoroacetone (TTA) in oxylene has been used to separate Np from metals, uranium, thorium and other transuranics. In this step, Np is adjusted to  $\text{Np}^{4+}$  and extracted into organic phase in low concentration of  $\text{HNO}_3$  (1–2 mol L<sup>-1</sup>) or high concentration of  $\text{HCl}$  (8–12 mol L<sup>-1</sup>), and back-extracted using high concentration of  $\text{HNO}_3$  (8 mol L<sup>-1</sup>) [255,258]. However, due to the insufficient decontamination from some elements, an anion exchange method is normally followed after solvent extraction. Based on the formation of anionic complex of  $\text{Np}^{4+}$  with  $\text{NO}_3^-$  and  $\text{Cl}^-$  in high concentration of  $\text{HNO}_3$  and  $\text{HCl}$  media, Np is first adjusted to  $\text{Np}^{4+}$  and absorbed onto an anion exchange column, uranium, which do not form a stable complex anion in  $\text{HNO}_3$  solution, passes through the column and Th, which does not form complex anion in  $\text{HCl}$  solution, is removed from the column by washing with 12 mol L<sup>-1</sup>  $\text{HCl}$ . The Np remained on the column is finally eluted from the column by 4–6 mol L<sup>-1</sup>  $\text{HCl}$  with  $\text{NH}_2\text{OH}\cdot\text{HCl}$ , or 4 mol L<sup>-1</sup>  $\text{HCl}$ –0.1 mol L<sup>-1</sup>  $\text{HF}$ . By this method, decontamination factors of  $10^6$  for U and  $10^5$  for Th, and a detection limit of 0.1 mBq have been reported [254,255].

Due to the long half-life of  $^{237}\text{Np}$ , mass spectrometric methods are sensitive for its determination, AMS [256], ICP-MS [257], and GDMS [115] have been used for the determination of  $^{237}\text{Np}$ . In AMS, the separated Np is mixed with  $\text{Fe}_2\text{O}_3$  and used as a target;  $\text{NpO}^-$  ions are sputtered by ion source, separated in the mass spectrometer and counted by an ionization chamber. A sensitivity of 0.024  $\mu\text{Bq}$  was measured, considering the procedure blank count rate; a detection limit of 7  $\mu\text{Bq}$  was reported [256]. A GDMS method was reported for the direct determination of  $^{237}\text{Np}$  in sediment from the Irish Sea [115]. Since the sample was non-conducting, secondary cathode of

Ti was used. The main interference from the molecular ion  $^{181}\text{Ta}^{40}\text{Ar}^{16}\text{O}$  can be avoided by choosing a high resolution of 1700. A detection limit of 2.1–7.9 mBq g<sup>-1</sup> was reported [115]. ICP-MS is the most often used mass spectrometric method for the determination of  $^{237}\text{Np}$ , the main interference is the tailing of  $^{238}\text{U}$ . Due to the much higher concentration of uranium in almost any type sample compared to Np, a good chemical separation of Np from uranium is required. Several polyatomic interferences such as  $^{197}\text{Ag}^{40}\text{Ar}$ ,  $^{181}\text{Ta}^{40}\text{Ar}^{16}\text{O}$ ,  $^{183}\text{W}^{40}\text{Ar}^{14}\text{N}$ , combinations of thallium and mercury isotopes with sulfur and chlorine isotopes, and palladium isotopes with xenon as well as  $^{153}\text{Eu}^{84}\text{Kr}$  are possible interferences. With a through chemical separation, most of these interferences can be removed. Detection limit for  $^{237}\text{Np}$  is more dependent on procedure blank levels (uranium and polyatomic interferences) than on instrument sensitivity. Sector field instruments and quadrupole instruments equipped with guard electrode using high-efficiency nebuliser may be tuned to have signal intensities of 10–20 MHz ppb<sup>-1</sup> while still maintaining instrument background count rates at mass 237 below 1 cps. A detection limit of 1 nBq was reported by using SF-ICP-MS [159]. While, detection limits of 0.01–0.1  $\mu\text{Bq}$  of  $^{237}\text{Np}$  are easily obtained by present ICP-MS systems and a chemical removal of uranium, this level is impossible to be detected even with the best radiometric systems available. It is therefore ICP-MS is becoming more common used method for the determination of  $^{237}\text{Np}$  in the environmental samples. An inter-comparison of  $^{237}\text{Np}$  determination in artificial urine samples was carried out using alpha spectrometry and ICP-MS by Lee et al. [260], they concluded that based on the analytical accuracy, the best results obtained by ICP-MS were comparable with but not better than the most accurate results obtained by alpha-particle spectrometry. Alpha spectrometry measurements overall gave consistently better agreement with known values.

NAA can be also used for the determination of  $^{237}\text{Np}$  based on the reaction:  $^{237}\text{Np} \xrightarrow{(n, \gamma), \sigma=169\text{b}, I=600\text{b}} ^{238}\text{Np} \xrightarrow{\beta^-, 2.1\text{ day}} ^{238}\text{Pu}$ . Uranium may interfere with the analysis by the following reactions:  $^{238}\text{U}(n, 2n)^{237}\text{U} \xrightarrow{\beta^-} ^{237}\text{Np}(n, \gamma)^{238}\text{Np}$  and  $^{235}\text{U}(n, \gamma)^{236}\text{U}(n, \gamma)^{237}\text{U} \xrightarrow{\beta^-} ^{237}\text{Np}(n, \gamma)^{238}\text{Np}$ . Although these interferences are said to be small, uranium has to be separated from the sample prior to the neutron irradiation. In addition, the pre-irradiation separation can also be used to concentrate Np from a large sample, and to avoid working with high activity. The chemical procedure used for alpha spectrometry of  $^{237}\text{Np}$  can be also used for the pre-concentration of Np in NAA. A post-irradiation chemical separation is also necessary in order to achieve adequate decontamination from other gamma and beta emitters produced by activation of remaining impurity elements. A detection limit of  $^{237}\text{Np}$  as low as 0.01 mBq (0.5 fg) in environmental and biological samples has been reported [261], and NAA has been successfully used for the determination of  $^{237}\text{Np}$  in various environmental samples, such as soil, sediment, seawater, seaweed and fish [261,251,252,262].

One of the main problems in determination of  $^{237}\text{Np}$ , either by radiometric or mass spectrometric methods, is the lack of a suitable tracer. Both the gamma emitting short-lived  $^{239}\text{Np}$  ( $T_{1/2} = 2.35$  days) and  $^{235}\text{Np}$  (half-life of 396 days) may be used to trace the separation chemistry [258]. While  $^{242}\text{Pu}$  is mainly

used as tracer in many laboratories [255,259] because  $^{242}\text{Pu}$  isotope is relatively close to  $^{237}\text{Np}$  with respect to mass and ionization potential, can be obtained very pure (essentially free from  $^{237}\text{Np}$ ), and has a chemistry similar to that of plutonium.

#### 4.14. Plutonium isotopes

The interest in determining plutonium isotopes in environmental samples results from dosimetric reasons in the case of accidents or releases, interest in its biogeochemical behaviour in the environment, and tracing the source of the plutonium using the isotopic composition as a fingerprint. The most interest isotopes of Pu in environmental and waste sample are  $^{238}\text{Pu}$ ,  $^{239}\text{Pu}$ ,  $^{240}\text{Pu}$ , and  $^{241}\text{Pu}$ .  $^{241}\text{Pu}$  is a beta emitter with maximum energy of 20.8 keV, while the other isotopes are alpha emitters (Tables 1, 3 and 4). Alpha spectrometry is normally used for the determination of  $^{238}\text{Pu}$  and  $^{239+240}\text{Pu}$ . Due to the similar energies of alpha particles from  $^{239}\text{Pu}$  (5.16 MeV) and  $^{240}\text{Pu}$  (5.17 MeV),  $\alpha$ -spectrometry can only measured the sum activity of  $^{239}\text{Pu}$  and  $^{240}\text{Pu}$ . Spectrometric interferences for the  $\alpha$ -spectrometric determination of  $^{238}\text{Pu}$  and  $^{239+240}\text{Pu}$  are mainly from  $^{214}\text{Am}$  and  $^{210}\text{Po}$ ,  $^{224}\text{Ra}$ ,  $^{229}\text{Th}$ ,  $^{231}\text{Pa}$ ,  $^{232}\text{U}$ , and  $^{243}\text{Am}$ , respectively. In addition, the matrix elements have to also be removed to improve the resolution. It is therefore that plutonium has to be separated from the matrix and other interfering radionuclides before measurement. Co-precipitation, solvent extraction, ion exchange chromatography and extraction chromatography are often used for the separation of Pu. The separation of Pu by ion exchange chromatography is based on the formation of anionic complexes of Pu(IV) with  $\text{NO}_3^-$  or  $\text{Cl}^-$  in concentrated HCl or  $\text{HNO}_3$ . Pu is first adjusted to Pu(IV) by first reducing all Pu to Pu(III) using sulphite and then oxidized to Pu(IV) by nitrite. The Pu(IV) in  $8\text{ mol L}^{-1}$   $\text{HNO}_3$  is loaded onto an anion exchange column, which is then washed by  $8\text{ mol L}^{-1}$   $\text{HNO}_3$ , and  $12\text{ mol L}^{-1}$  HCl, so americium, uranium and thorium are moved. Pu remained on the column is finally eluted by reducing Pu to Pu(III) by using  $2\text{ mol L}^{-1}$   $\text{HCl-NH}_2\text{OH-HCl}$  solution [255]. In extraction chromatography, Eichrom UTEVA and TRU columns are used. Plutonium is first reduced to Pu(III) and then passed through an Eichrom UTEVA column, U and Th are absorbed onto the column, while Pu(III) and Am(III) are passed through. The effluents containing Pu is loaded to an Eichrom TRU column and converted to Pu(IV) using nitrite, the column is then washed with  $3\text{ mol L}^{-1}$   $\text{HNO}_3$  and  $9\text{ mol L}^{-1}$  HCl to remove Am, Pu remained on the column is finally eluted by  $0.1\text{ mol L}^{-1}$   $\text{NH}_4\text{HC}_2\text{O}_4$  solution [263]. Due to the very low concentration of Pu in environmental samples, pre-concentration of Pu from a large samples (such as 100–1000 L seawater) is necessary, which is normally carried out by  $\text{Fe}(\text{OH})_3$  or  $\text{CaC}_2\text{O}_4$  co-precipitation or absorption onto  $\text{MnO}_2$  impregnated fibers filter [255,263–265]. The separated Pu is normally electrodeposited onto a disk for  $\alpha$ -spectrometric measurement. Micro-precipitation using  $\text{LnF}_3$  has also been used to prepare the Pu source, but the resolution is not as good and electrodeposition. A detection limit of 0.05 mBq for  $^{238}\text{Pu}$  and  $^{239+240}\text{Pu}$  was obtained in the authors' laboratory by  $\alpha$ -spectrometry and counting for 3 days [265]. Besides  $\alpha$ -spectrometry, X-spectrometry has also

been used for the determination of  $^{239}\text{Pu}$  and  $^{240}\text{Pu}$ , which is based on the somewhat different intensities of the emitted  $\text{L}_x$ -rays from the  $^{239}\text{Pu}$  and  $^{240}\text{Pu}$  isotopes. A detection limit of 2–4 mBq for  $^{239}\text{Pu}$  and  $^{240}\text{Pu}$  has been reported by using  $\text{L}_x$  X-ray spectrometry and counting in underground laboratory [266].

The determination of  $^{241}\text{Pu}$  can be carried out by direct measurement of  $^{241}\text{Pu}$  using LSC or  $\alpha$ -spectrometry by measuring its decay daughter  $^{241}\text{Am}$ . In the direct LSC method, Pu has to be separated from the matrix and all other radionuclides, especially interfering beta emitters. The chemical procedure used for alpha isotopes of Pu can also be used for  $^{241}\text{Pu}$ . Actually, the separated Pu used for determination of  $^{238}\text{Pu}$  and  $^{239+240}\text{Pu}$  is normally used for LSC of  $^{241}\text{Pu}$  after the  $\alpha$ -spectrometric measurement. A detection limit of 11 mBq has been reported [267] using LSC. In the  $\alpha$ -spectrometry method, the separated plutonium have to be kept for more than half year for the in-growth of  $^{241}\text{Am}$ , the generated  $^{241}\text{Am}$  is then separated from plutonium and measured by  $\alpha$ -spectrometry, in this case, the detection limit varies with the in-growth time, a detection limit of 0.3 mBq can be obtained using  $\alpha$ -spectrometry and 13 years in-growth time [268].

Mass spectrometric techniques such as TIMS [269], AMS [270,271], RIMS [96,272], and ICP-MS [64,273,274,276,277] have also been used for the determination of Pu isotopes. During the last decade, the use of ICP-MS has gained a increased interest as an alternative to alpha spectrometry because of the good sensitivity, short analytical time and  $^{239}\text{Pu}$ – $^{240}\text{Pu}$ – $^{242}\text{Pu}$  isotopic information which are difficult to obtain through alpha spectrometry due either to overlapping peaks of  $^{239}\text{Pu}$  and  $^{240}\text{Pu}$  or to the low specific activity of  $^{242}\text{Pu}$  ( $1.4 \times 10^8 \text{ Bq g}^{-1}$ ). The mass spectrometric techniques should be seen as a complement rather than a replacement to ordinary alpha spectrometry since the latter technique is still very suitable for the analysis of  $^{238}\text{Pu}$  and the  $^{238}\text{Pu}/^{239+240}\text{Pu}$  ratio, which in some cases is more informative than the  $^{240}\text{Pu}/^{239}\text{Pu}$  ratio obtained by mass spectrometry. The  $^{238}\text{Pu}$  in environmental samples is very difficult to be determined by mass spectrometric techniques due to its low mass concentration and serious isobaric interference from  $^{238}\text{U}$  which is much more abundant in environmental samples. Furthermore, mass spectrometric techniques are also insufficient to accurately analyse the short-lived  $^{241}\text{Pu}$  (14.4 years) in normal environmental samples unless the  $^{241}\text{Pu}/^{239}\text{Pu}$  ratio is large like in samples contaminated by material from the Chernobyl accident. Measuring  $^{241}\text{Am}$  by solid-state alpha spectrometry or direct analysis of  $^{241}\text{Pu}$  by low-level liquid scintillation counting are more sensitive ways than using ICP-MS, but may necessarily not be more accurate due to problems with cross-calibration of tracers ( $^{242}\text{Pu}$ – $^{243}\text{Am}$ ), imprecise detector efficiency or unknown blank contribution and calibration problems (LSC). Due to the high sensitivity of many ICP-MS instruments, it is possible to determine Pu-isotopes at very lower level. There are however a number of problems that have to be addressed and dealt with before being able to trust the weak signals provided by the instrument when measuring Pu at low-levels (fg–pg range). Some of these are the relatively low abundance sensitivity, the risk of interferences from polyatomic species, blanks, background and sensitivity.

The most important problem when measuring low-level samples for Pu by ICP-MS is the interference from uranium, because the mass concentration of uranium is usually  $10^6$ – $10^9$  times higher than that of Pu. The tailing and formation of  $\text{UH}^+$  thus represent a major disturbance at mass 239 unless uranium is removed prior to analysis. This particular problem is seldom encountered in alpha spectrometry due to the low specific activity of uranium and that the alpha energies of U and Pu isotopes do not overlap. A partial overlap of  $^{234}\text{U}$  (4.77 MeV) and the  $^{242}\text{Pu}$  (4.90 MeV) tracer may occur at situations when the U concentration on the electrodeposited steel disc is high enough to affect the energy resolution. In this case, the low energy side of the  $^{242}\text{Pu}$  peak may tail into the  $^{234}\text{U}$  peak. However, problems with uranium are much less severe in alpha spectrometry which therefore sets much lesser demands on the degree of removal of uranium from the sample. While in the alpha spectrometric determination of  $^{238}\text{Pu}$  (5.50 MeV), the interference from the  $^{228}\text{Th}$  peak (5.42 MeV) may be a severe problem. A thorough removal of thorium prior to analysis is necessary to obtain a reliable result when analysing low-level samples. The contribution of  $^{228}\text{Th}$  to  $^{238}\text{Pu}$  can also be corrected for by measuring  $^{224}\text{Ra}$  (5.65 MeV), the decay daughter of  $^{228}\text{Th}$ . In this case, the sample after electrodeposition needs to be kept for about 3 week for the in-growth of  $^{224}\text{Ra}$  (5.65 MeV), so that the daughter product, to reach secular equilibrium with  $^{228}\text{Th}$ . Varga et al. [274] compared alpha spectrometry and ICP-SFMS, a comparable detection limits were obtained for  $^{239,240}\text{Pu}$  by two techniques (0.1–0.2 mBq).

In TIMS, problems with uranium are less severe since uranium and plutonium have different ionisation potentials and thus are emitted from the filament at different temperatures (plutonium leaves the filament before uranium). The dry sample introduction furthermore reduces  $\text{UH}^+$  species considerably and abundance sensitivity is generally orders of magnitude better in TIMS instruments than in ICP-MS. The stability of the ion beam also permits  $^{239}\text{Pu}/^{240}\text{Pu}$  ratios of a precision in ppm range rather than at percentage range typical for single detector ICP-MS. Recent multicollector ICP-MS instruments have however an isotope ratio precision and sensitivity that surpasses most commercial TIMS instrument. In ICP-MS, matrix suppression of the signal occurs when the sample introduced to the mass spectrometer is not pure enough. In TIMS this suppression is normally more severe than in ICP-MS and this therefore sets a higher demand on the chemical isolation of the Pu before loading onto the filament. Using ordinary commercial TIMS instruments (e.g. Finnigan MAT 262) a detection limit of around 1 fg ( $2\text{ }\mu\text{Bq}$ )  $^{239}\text{Pu}$  has been reached [30].

Alpha spectrometry is more straightforward than any of the mass spectrometric methods and the risk of interfering signals is less than ICP-MS. In alpha spectrometry there is no interference from the presence of microgram amounts of stable elements on the disc after separation and electrodeposition. While in ICP-MS, several polyatomic species may appear in the mass range 230–245 when micrograms of lead, mercury, thallium and REEs remain in the sample after separation. This makes the evaluation of mass spectra from samples weak in plutonium more critical than alpha spectrometry. It is possible to reach better detection limits by ICP-MS for  $^{239}\text{Pu}$  when a thorough quality control is followed. The main drawback of

alpha spectrometry is the very long counting times for low activity samples, weeks to months.

RIMS is a sensitive mass spectrometric method for determination of Pu-isotopes. The method also enables an ultrahigh selective determination of the element with almost completely elimination of interferences from other elements. These instruments are however not commercially available and are designed for one element due to the specific laser tuning used and adaptation to a new element requires elaborate development. This method had been used for the determination of Pu isotopes in environmental sample, a detection limit of  $10^6$ – $10^7$  atoms corresponding to 1–10  $\mu\text{Bq}$   $^{239}\text{Pu}$  has been reported. Comparing to radiometric method, a similar chemical separation is needed for RIMS, but the counting time (1–2 h) is remarkable shorter than alpha spectrometry [96]. AMS similarly offers a very good sensitivity and abundance sensitivity well suited for ultra trace detection of plutonium, a detection limit of 0.5–2  $\mu\text{Bq}$  for  $^{239}\text{Pu}$  has been reported by using AMS [270,275]. However, commercially available AMS instruments are expensive and normally not developed for heavy ion detection. Analysis of heavy elements like the actinides is still only performed at physics laboratories where larger instrument are available. Contrary to RIMS, which can be interfaced to a TOF-MS and therefore analyse the Pu-isotopes simultaneously, AMS needs to do peak hopping since only one ion mass can be transported through the analyser ion optics at any time. This results in less precise isotope ratios.

A new pre-concentration technique was recently developed to separate plutonium from as large as  $10\text{ m}^3$  of seawater sample by solid phase extraction using  $\text{MnO}_2$  impregnated fibres [264]. This is very useful for the determination of ultra low-level samples by alpha spectrometry or ICP-MS.

Table 12 compares the radiometric method and mass spectrometric methods for the determination of plutonium isotopes, AMS, TIMS and RIMS are more sensitive than alpha spectrometry method for the determination of  $^{239,240}\text{Pu}$ , ICP-MS is comparable with alpha spectrometry and LSC for  $^{239,240}\text{Pu}$  and  $^{241}\text{Pu}$ . All mass spectrometry methods are able to measure  $^{239}\text{Pu}$ ,  $^{240}\text{Pu}$  and  $^{241}\text{Pu}$ , but not  $^{238}\text{Pu}$  because of isobaric interference of  $^{238}\text{U}$ . While alpha spectrometry can measure  $^{239,240}\text{Pu}$  and  $^{238}\text{Pu}$ , but can not separate  $^{239}\text{Pu}$  and  $^{240}\text{Pu}$ . Mass spectrometric methods are comparable to LSC for the determination of  $^{141}\text{Pu}$  respect to the sensitivity. The chemical separation procedures are similar for both radiometric and mass spectrometric methods, while the counting time of mass spectrometric methods are much shorter than that of radiometric methods. Lee et al. [276] compared alpha spectrometry, LSC, AMS, ICP-MS and TIMS techniques by analysis some environmental reference materials, they concluded that the analytical results of  $^{239,240}\text{Pu}$  by alpha spectrometry are in general in good agreements with ICP-MS and AMS, and the results of  $^{241}\text{Pu}$  by LSC and ICP-MS are reasonable good agreement, radiometric methods are still a powerful techniques because of simplicity of measurement, good resolution and reasonable sensitivity, ICP-MS and AMS have proved to be high sensitive techniques which will be used more frequently in the future for the determination of Pu isotopes. However, mass spectrometry cannot replace radiometric methods, because mass spectrometry cannot supply a reliable measurement of



**Table 12 – Comparison of radiometric and mass spectrometric methods for the determination of isotopes of plutonium**

Sample	Detection method	Nuclide	Detection limit	Sept. time	Count time	Ref.
Environmental samples	X-spectrometry underground counting	$^{239}\text{Pu}$ , $^{240}\text{Pu}$	4.4 mBq, 2.0 mBq	3–5 days	57 days	[266]
Environmental sample	$\alpha$ -Spectrometry	$^{239+240}\text{Pu}$ , $^{238}\text{Pu}$	0.05 mBq	2–3 days	3 days	[265]
Environmental sample	$\alpha$ -Spectrometry	$^{239+240}\text{Pu}$ , $^{238}\text{Pu}$	0.02 mBq	3–4 days	5 days	[274]
Environmental sample	LSC	$^{241}\text{Pu}$	11 mBq	2–3 days	5 h	[267]
Environmental sample	$\alpha$ -Spectrometry	$^{241}\text{Pu}$ (via $^{241}\text{Am}$ )	0.5 mBq	3–5 days (13 year) <sup>a</sup>	3 h	[268]
Urine	TIMS	$^{239}\text{Pu}$ , $^{240}\text{Pu}$ $^{241}\text{Pu}$	1.4 $\mu\text{Bq}$ 0.9 $\mu\text{Bq}$ 0.4 mBq	2–3 days	20–30 min	[30]
Environmental sample	ICP-SFMS	$^{239}\text{Pu}$ $^{240}\text{Pu}$ $^{241}\text{Pu}$	0.021 mBq 0.014 mBq 11.9 mBq	3–4 days	20 min	[274]
Environmental sample	RIMS	$^{239}\text{Pu}$ $^{240}\text{Pu}$ $^{241}\text{Pu}$	10 $\mu\text{Bq}$ 30 $\mu\text{Bq}$ 20 mBq	2–4 days	1–2 h	[96]
Seawater	ICP-MS	$^{239}\text{Pu}$ $^{240}\text{Pu}$	0.78 mBq mL <sup>-1</sup> 3.6 mBq mL <sup>-1</sup>	3–4 days	20 min	[264]
Urine	AMS	$^{239}\text{Pu}$	0.5 $\mu\text{Bq}$	2–3 days	20–40 min	[275]

<sup>a</sup> In-growth time for the generation of  $^{241}\text{Am}$  from the decay of  $^{241}\text{Pu}$ .

$^{238}\text{Pu}$  and alpha spectrometry is still the most sensitive and reliable method for  $^{238}\text{Pu}$ .

#### 4.15. Amerium-241

$^{241}\text{Am}$  as an anthropogenic radionuclide has been released into environment from the weapons testing, reprocessing plants and nuclear accident. Since  $^{241}\text{Am}$  is a decay daughter of  $^{241}\text{Pu}$  ( $T_{1/2} = 14.35$  years), its concentration will increase in the future in the environment and it is estimated to reach its maximum activity in the middle of the 21st century [278]. The interest in the determination of  $^{241}\text{Am}$  results from its high specific activity and dose contribution, and application as a unique tracer in oceanographic and sedimentation studies.

$^{241}\text{Am}$  decays by emitting  $\alpha$ -particles of 5.44–5.49 MeV, accompanying by emission of 59.5 keV (35.9%)  $\gamma$ -ray.  $^{241}\text{Am}$  can therefore be measured by  $\gamma$ -spectrometry and  $\alpha$ -spectrometry. Gamma spectrometry is an easy and direct method for the determination of  $^{241}\text{Am}$ , but care must be taken to properly correct for the attenuation of  $\gamma$ -ray in the samples in order to obtain accurate results. In addition, the sensitivity of  $\gamma$ -spectrometry is also low because of the generally low counting efficiency of HpGe detector and the small (or thin layer) sample have to be used for reducing the self-adsorption of  $\gamma$ -ray in the sample. A detection limit of 0.1–1 Bq kg<sup>-1</sup> has been reported for the direct measurement of soil and biota (Byrne 1993) by  $\gamma$ -spectrometry using HpGe detector. Chemical separation before  $\gamma$ -counting can significantly improve the detection limit by using a large sample and reducing the self-absorption. In the author's laboratory, a detection limit of 50 mBq has been obtained for the direct  $\gamma$ -counting of solid sample, which is therefore suitable for the screen of the sample. Alpha spectrometry is a more sensitive method for the determination of  $^{241}\text{Am}$ . In this case,  $^{241}\text{Am}$  has to be separated from matrices and interfering radionuclides, especially

Pu, Th, Ra, and Po because of close  $\alpha$ -energies of  $^{210}\text{Po}$ ,  $^{238}\text{Pu}$ ,  $^{224}\text{Ra}$  and  $^{228}\text{Th}$  to  $^{241}\text{Am}$ . Co-precipitation of hydroxides or oxalate, solvent extraction using TIOA/xylene, anion exchange and extraction chromatography are used for the separation. The solvent extraction using TIOA/oxylene is based on the extraction of Pu, Po, U, and Fe to organic phase, while Am remain in the aqueous phase. The anion exchange chromatography is based on absorption of the Pu(IV) and U(IV) to the column in high concentration of HCl and Th(IV) and Pu (IV) in high concentration of HNO<sub>3</sub> medium, while Am does not form anionic complex in neither HNO<sub>3</sub> nor HCl and could not be absorbed on the column. For removal of most rare earth elements (REEs) which may interferes with the  $\alpha$ -spectrometric determination of  $^{241}\text{Am}$  due to increased self-absorption in the source and thus poor resolution, extraction chromatography using Eichrom TRU column and anion exchange chromatography have been used. In anion exchange chromatography, Am is prepared in a 1.0 mol L<sup>-1</sup> HNO<sub>3</sub>–93% CH<sub>3</sub>OH solution and loaded to the anion exchange column, the column is then washed with 0.1 mol L<sup>-1</sup> HNO<sub>3</sub>–0.5 mol L<sup>-1</sup> NH<sub>4</sub>SCN–80% CH<sub>3</sub>OH, in this case, REEs pass through the column, Am on the column is then eluted by 1.5 mol L<sup>-1</sup> HCl–83% CH<sub>3</sub>OH. The separated  $^{241}\text{Am}$  is normally electrodeposited on a disc for measurement using  $\alpha$ -spectrometry, a detection limit of 0.1–0.2 mBq has been reported depending on the counting time and count rate of the procedure blank [278–280].

ICP-MS has also been used for the determination of  $^{241}\text{Am}$  in environmental samples. In the ICP-MS, the main problem comes from the isobaric and molecular ions interferences, such as  $^{241}\text{Pu}^+$ ,  $^{240}\text{Pu}^1\text{H}^+$ ,  $^{209}\text{Bi}^{32}\text{S}^+$ ,  $^{209}\text{Bi}^{16}\text{O}_2^+$ ,  $^{206}\text{Pb}^{35}\text{Cl}^+$ ,  $^{205}\text{Ti}^{36}\text{Ar}^+$ ,  $^{204}\text{Pb}^{37}\text{Cl}^+$ ,  $^{207}\text{Pb}^{34}\text{S}^+$ , and  $^{201}\text{Hg}^{40}\text{Ar}^+$ . Using SF-ICP-MS in high resolution mode can solve some of these problems with molecular ions, while this will cost at a lower sensitivity. The  $^{241}\text{Pu}$  isobaric interference requires a very high resolution (10,800,000), which cannot be solved by SF-

ICP-MS. Since  $^{241}\text{Am}$  is a decay product of  $^{241}\text{Pu}$ , in some samples the mass concentration of  $^{241}\text{Am}$  is much lower than  $^{241}\text{Pu}$ , which therefore requires a thorough chemical separation of Am from Pu before measurement. In addition, chemical separation can also remove most of the stable elements, which forms the interfering molecular ions [281–283]. The chemical separation procedure used in the  $\alpha$ -spectrometry can also be used for the ICP-MS analysis of Am. Although less demand on removal alpha emitters, a relatively thorough removal of the stable matrix elements is required for low-level samples. A detection limit of 0.1 mBq has been reported by using SF-ICP-MS with chemical separation [278], which is comparable with  $\alpha$ -spectrometry, but the analytical time (1 days chemical separation and 2 h measurement) is much shorter than  $\alpha$ -spectrometry (3–4 days separation with 3–5 days measurement). The drawback of ICP-MS compared with  $\alpha$ -spectrometry is the analytical reliability of ultra-low-level of  $^{241}\text{Am}$  measurement, the contribution of noises and interfering ions to the small signal is difficult to identify. The rapid analytical capacity of ICP-MS makes it however an attractive method, especially for the emergency analysis.

## 5. Application of on-line methods (flow injection/sequential injection) for separation of radionuclides

In the traditional analytical procedure for radionuclides, the target radionuclides have to be pre-concentrated and separated before measurement because of their low activities in environmental samples and the presence of interfering elements and radionuclides. Co-precipitation, solvent extraction, ion exchange and extraction chromatography are commonly used techniques, of which ion exchange chromatography and extraction chromatography are the dominant techniques for the separation of target radionuclide from the interfering elements and radionuclides. These methods are tedious, time consuming, and labor-intensive. For example, the determination of plutonium and americium normally takes up to 3–4 days per sample. Moreover, the methods require large volumes of organic solvents or mineral acids, and embody the risk of cross-contamination.

Flow-injection (FI)/sequential injection analysis (FIA) has been widely used for the determination of trace elements since its introduction in 1975 [284] and made a significant progress not only in terms of efficiency, but also in reliability, rapidity and robustness [285]. However, this technique has not been applied for the determination of radionuclides until 1996 [183]. With the requirement of rapid analysis of radionuclides for emergency purpose and the increased application of ICP-MS, the automated analysis of radionuclides by hyphenation of flow injection/sequential injection for on-line separation with ICP-MS measurement has becoming more attractive for waste and environmental radioactivity analysis.

The automated analysis using FI on-line separation is normally composed of a multi-port valve, a solvent distributor which can divert solution to different direction, peristaltic pump, and chromatographic column (one or more). The operation of the system is controlled by a PC and automated

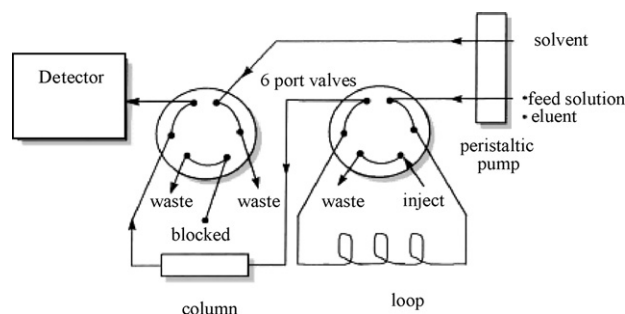


**Fig. 3 – Schematic diagram of the sequential injection manifold interface with the detector (modified from Truscott et al. [297]).**

running, Fig. 3 shows the schematic diagram of this system. The prepared sample in a suitable solution is first loaded to a loop, which is then loaded to the column. The column is then washed with different solvent to remove the interfering elements and radionuclides. The target radionuclide is finally eluted from the column, which can be directly introduced to the detector or collected by a fractionation collector for measurement later. The main advantages of the sequential injection system compared to the traditional separation method include: (1) rapid separation; (2) directly connection to the detector such as ICP-MS for the measurement; (3) automated operation, so less manpower and less cost; (4) less consumption of the chemical reagents; (5) less cross contamination; (6) less risk of exposure of chemicals to the laboratory staff because of less contact with the chemical reagents. In recent years, this method has been used for the determination of  $^{90}\text{Sr}$ ,  $^{99}\text{Tc}$ , and actinides, some examples are given below.

Grate et al. [183,286] described a automated method for the determinations of  $^{90}\text{Sr}$  in nuclear waste by using a sequential inject separation and a flow through liquid scintillation counter for on-line detection. In this method, an Eichrom Sr-Spec resin was used for the extraction chromatographic separation, which can efficiently separate the interfering radionuclides, such as  $^{137}\text{Cs}$  and  $^{90}\text{Y}$  from  $^{90}\text{Sr}$ . The analytical time can be reduced to 40 min, while the traditional method normally requires 1–3 days. A HPLC using ion chromatography was also used for the automated separation of  $^{90}\text{Sr}$  [287], with the on-line detection using LSC, and waste water sample can be rapid analysis.

In the determination of  $^{99}\text{Tc}$ , an anion exchange column was used for the separation of  $^{99}\text{Tc}$  from other radionuclides. In this method, all technetium in the sample has to be converted to  $\text{TcO}_4^-$  before the separation. Combined with an on-line flow through scintillation detector, the  $^{99}\text{Tc}$  in waste samples was determined. The analytical time was only less than 13 min per sample [288]. A method by using extraction chromatography (TEVA) in the sequential injection system and direct ICP-MS detection has been reported for the determination of  $^{99}\text{Tc}$  in environmental samples [196]. Due to the interference of  $^{99}\text{Ru}$  and  $^{98}\text{MoH}$  in the ICP-MS determination of  $^{99}\text{Tc}$ , the high concentrations of Mo and Ru in environmental samples have to be removed. For this purpose, two TEVA column was used, and a decontamination factor of  $10^4$  to  $10^5$

for Ru and Mo was obtained. An analytical time of 3–5 h for soil sample, and a detection limit of  $0.05 \text{ mBq mL}^{-1}$  was reported [196].

Benkhedda et al. [59] reported an automated analytical method for the determination of  $^{226}\text{Ra}$  by combining sequential injection and ICP-MS. In this method two extraction columns containing Eichrom Ln and Sr-Spec resin were used. The sample solution was first loaded on the Ln column, where Ra, Sr, and Ba were absorbed and separated from the matrix elements. Ra, Sr and Ba were then eluted from the Ln column and passed through Sr-Spec column, where, Sr and Ba are absorbed, while Ra was passed through the column and directly introduced to the plasma of the ICP-MS instrument. The entire analysis took only 20 min per sample, a detection limit of  $0.34 \text{ mBq}$  for a 20 mL water sample was obtained.

There are many works have been carried out on the development of an automated method for the determination of actinides [286,289–297]. An HPLC with mix bed ion exchange column has been used to separate actinides and employing ICP-MS for the detection. CS10 column was used for the separation of Pu, U and Am, but the separation of Pu from U was not sufficiently good. While, CS5A column gave a good separation of U, Pu, Am and Cm from each other. Neither column could separate Pu from Np, but it does not effect the ICP-MS detection of the isotopes of these two elements. The method has been successfully used for the analysis of spent nuclear fuel [294]. For the separation of Np from Pu, an extraction chromatographic column (UTEVA) was investigated. After adjusting Pu to Pu(IV) and Np to Np(V), these two elements can be completely separated by this method [295]. Extraction chromatographic resin TRU in the sequential injection system has been used for the separation of Am and Pu from the matrix and from each other. In this method, the Pu is adjusted to Pu(IV) before the loading to the column, in this case, Pu is absorbed on the column while Am pass through the column. The main problem is the decontamination of U from Pu which is not very good; the method has been used for the analysis of waste sample. For the analysis of environmental sample which contains high uranium and lead, two extraction chromatographic columns using Sr-Spec and TEVA resin in the sequential injection system has to be used [196,289,290]. In this method, the sample in  $5 \text{ mol L}^{-1} \text{ HNO}_3$  solution was loaded to the Sr-Spec column, Pu on the column is then eluted by  $0.8 \text{ mol L}^{-1} \text{ HNO}_3$  and loaded onto the TEVA column, while Pb is retained on the Sr-Spec column. The uranium absorbed on the TEVA column is washed out by  $1 \text{ mol L}^{-1} \text{ HNO}_3$ , the Pu retained on the column is then eluted by  $1 \text{ mol L}^{-1} \text{ HCl}$ , and injected to the detector for measurement. A decontamination factor of  $10^6$  for U and  $10^4$  for Pb and a detection limit of  $1.5 \mu\text{Bq mL}^{-1}$  for 5 L seawater have been obtained, an analytical time of 4 h per sample was reported [196]. The application of sequential injection systems can significantly shorten the analytical time. For waste water sample it is possible to complete a full automated analysis [286]. However for the analysis of environmental sample and solid waste sample, an off-line pre-concentration step is necessary. The solid sample has to be decomposed to release the target radionuclide from the sample to solution, the traditional co-precipitation can be used for pre-concentration of target radionuclide from

large volume of water sample or pre-separation of target radionuclide from a large amount of matrix elements which may worse the column separation. Although the SI system has been used for the automated determination of radionuclides for more than 10 years, the application is still limited to a few laboratories, most of radiochemical laboratories still use the traditional method. This may results from a few reasons: (1) a pre-concentration is still needed for the environmental samples; (2) the developed system are normally small scale, which is not enough for the analysis of the low-level environmental samples; (3) the decontamination factor is not high enough; (4) less robust of the SI system, especially the column part, which may cause a much longer time for reparation. However, the automated SI system is still very attractive for the determination of radionuclides because of its remarkable advantages. With the development of the extraction chromatographic techniques and new generation of flow inject technique; this technique will become more and more popular in radiochemical laboratories for the determination of radionuclides in environmental and waste samples.

## 6. Conclusion

Radiometric methods, as the traditional analytical methods, are still the unique techniques for the determination of short-lived radionuclides ( $T_{1/2} < 10$  year), and dominating analytical techniques for the determination of most long-lived radionuclides in waste and environmental samples. Mass spectrometric techniques such as AMS, TIMS and RIMS, especially AMS, are very sensitive techniques for the determination of many very long-lived radionuclides, such as  $^{14}\text{C}$ ,  $^{36}\text{Cl}$ ,  $^{41}\text{Ca}$ ,  $^{59}\text{Ni}$ ,  $^{129}\text{I}$ , and  $^{135}\text{Cs}$ , they can not only measure the very low-level of these radionuclides, but also significantly reduce the sample amount needed for the analysis, they are therefore better than radiometric techniques, especially for the biological and low-level environmental samples. SIMS and GDMS are not sensitive enough for the determination of radionuclides in low-level, however they are useful techniques for surface and profile analysis for some radionuclides, especially characterization of hot particles and spatial distribution analysis of radionuclides in the biological tissues. With the improvement and popularity of ICP-MS analytical techniques, it is becoming a competitive technique for the determination of many long-lived radionuclides, such as  $^{99}\text{Tc}$ ,  $^{237}\text{Np}$ , and isotopes of U, Th, and Pu because of its comparable detection limits to the radiometric methods and rapid analytical capacity. Regardless the application, it is desirable that the techniques for determination of a radionuclide are sensitive, accurate, rapid and low cost. Unfortunately no single analytical technique can meet all of these goals for all application. Each technique has its own strengths and weaknesses. In general, mass spectrometric techniques are good complementary to the radiometric techniques for the determination of most of long-lived radionuclides, which has been used for the investigation which previously required too large sample or were not possible due to lack of sensitivity of radiometric techniques. However, mass spectrometry cannot replace the radiometric techniques for the determination of many radionuclides

because of the isobaric interference, stability, less accessible, high cost and noise of equipment. In addition, radiometric methods do not require extensive equipments or infrastructure, and can be scaled down and even portable for field measurement.

## Acknowledgements

The authors wish to thank the Villum Kann Rasmussen Foundation for financial support. The comments from two referees are appreciated by authors, which significantly improved the quality of the paper.

## REFERENCES

- [1] M. Eisenbud, G. Thomas (Eds.), *Environmental Radioactivity*, fourth ed., Academic Press, CA, 1997.
- [2] J.S. Becker, H.-J. Dietze, *Adv. Mass Spectrom.* 14 (1998) 681–689.
- [3] J.S. Becker, H.-J. Dietze, *J. Anal. At. Spectrom.* 14 (1999) 1403–1500.
- [4] J.S. Becker, *Spectrosc. Eur.* 14 (6) (2002) 8–16.
- [5] J.S. Becker, *Spectrochim. Acta Part B* 58 (2003) 1757–1784.
- [6] J.S. Becker, *J. Anal. At. Spectrom.* 20 (2005) 1173–1184.
- [7] D. Lariviere, V.F. Taylor, R.D. Evans, R.J. Cornett, *Spectrochim. Acta B* 61 (2006) 877–904.
- [8] X.D. Hou, W. Chen, Y.H. He, B.T. Jones, *Appl. Spectrosc. Rev.* 40 (2005) 245–267.
- [9] M. Betti, A.D. Heras, G. Tamborini, *Appl. Spectrosc. Rev.* 41 (2006) 491–514.
- [10] E.R. Gonzales, S.R. Garcia, C. Mahan, W. Hang, *J. Radioanal. Nucl. Chem.* 263 (2005) 457–465.
- [11] R.J. Rosenberg, *J. Radioanal. Nucl. Chem. Art.* 171 (1993) 465–482.
- [12] E. Holm, *Source preparation for alpha and beta measurement*, NKS-40, 2001.  
<http://130.226.56.167/nordisk/publikationer/1994.2004/NKS-40.pdf>.
- [13] D. Karamanis, K.G. Ioannides, K.C. Stamoulis, *Anal. Chim. Acta* 573 (2006) 319–327.
- [14] P. Sangsingkeow, K.D. Berry, E.J. Dumas, T.W. Raudorf, T.A. Underwood, *Nucl. Instrum. Meth. A* 505 (2003) 183–186.
- [15] Q.J. Chen, H. Dahlgaard, S.P. Nielsen, *Anal. Chim. Acta* 285 (1994) 177–180.
- [16] Q.J. Chen, X.L. Hou, Y.X. Yu, H. Dahlgaard, S.P. Nielsen, *Anal. Chim. Acta* 466 (2002) 109–116.
- [17] X.L. Hou, M. Jensen, S.P. Nielsen, *Appl. Radiat. Isot.* 65 (2007) 610–618.
- [18] X.L. Hou, L.F. Østergaard, S.P. Nielsen, *Anal. Chim. Acta* 535 (2005) 297–307.
- [19] X.L. Hou, *Radiochim. Acta* 93 (2005) 611–617.
- [20] D.E. Nelson, R.G. Korteling, W.R. Stott, *Science* 198 (1977) 507.
- [21] S.W. Downey, N.S. Norgar, C.M. Miller, *Anal. Chem.* 56 (1984) 827.
- [22] D.J. Rokop, R.E. Perrin, G.W. Knobeloch, V.M. Armijo, W.R. Shields, *Anal. Chem.* 54 (1982) 957–960.
- [23] M. Gastel, J.S. Becker, H.-J. Dietze, *Spectrochim. Acta B* 52 (1997) 2051–2059.
- [24] J.S. Becker, C. Pickhardt, H.-J. Dietze, *Int. J. Mass Spectrom.* 203 (2000) 283–297.
- [25] L. Aldave de las Heras, E. Hmecek, O. Bildstein, M. Betti, *J. Anal. At. Spectrom.* 17 (2002) 1011–1014.
- [26] M. Betti, S. Giannarelli, T. Hiernaut, G. Rasmussen, L. Koch, *Fresenius J. Anal. Chem.* 355 (1996) 642–646.
- [27] M. Betti, *Int. J. Mass Spectrom.* 242 (2005) 169–182.
- [28] A.G. Adriaens, J.D. Fassett, W.R. Kelly, D.S. Simons, F.C. Adams, *Anal. Chem.* 64 (1992) 2945–2950.
- [29] K.L. Ramakumar, S. Jeyakumar, R.M. Rao, L. Gnanayyan, H.C. Jain, *J. Radioanal. Nucl. Chem. Articles* 190 (1995) 121–136.
- [30] N.L. Elliot, G.A. Bickel, S.H. Linauskas, L.M. Paterson, *J. Radioanal. Nucl. Chem.* 267 (2006) 637–650.
- [31] L.K. Fifield, *Rep. Prog. Phys.* 62 (1999) 1223–1274.
- [32] W. Kutschera, *Int. J. Mass Spectrom.* 242 (2005) 145–160.
- [33] K. Wendt, N. Trautmann, *Int. J. Mass Spectrom.* 242 (2005) 161–168.
- [34] C. Crüning, G. Huber, P. Klopp, J.V. Kratz, P. Kunz, G. Passler, N. Trautmann, A. Waldek, K. Wendt, *Int. J. Mass Spectrom.* 235 (2004) 171–178.
- [35] C.K. Kim, R. Seki, S. Morita, S. Yamasaki, A. Tsumura, Y. Igarashi, M. Yamamoto, *J. Anal. At. Spectrom.* 6 (1991) 205–209.
- [36] H. Isnard, M. Aubert, P. Blanchet, R. Brennetot, F. Chartier, V. Geertier, F. Manuguerra, *Spectrochim. Acta Part B At. Spectrosc.* 61 (2006) 150–156.
- [37] M.V. Zoriy, P. Ostapczuk, L. Halicz, R. Hille, J.S. Becker, *Int. J. Mass Spectrom.* 242 (2005) 203–209.
- [38] A.P. Vonderheide, M.V. Zoriy, A.V. Izmer, C. Pickhardt, J.A. Caruso, P. Ostapczuk, R. Hille, J.S. Becker, *J. Anal. At. Spectrom.* 19 (2004) 675–680.
- [39] N. Berryman, T. Probst, *Radiochim. Acta* 76 (1997) 191–195.
- [40] F. Baumgartner, M.A. Kim, T. Probst, *Radiochim. Acta* 61 (1993) 235–240.
- [41] A.V. Izmer, S.F. Boulyga, M.V. Zoriy, J.S. Becker, *J. Anal. At. Spectrom.* 19 (2004) 1278–1280.
- [42] C.F. Brown, K.N. Geiszler, M.J. Lindberg, *Appl. Geochem.* 22 (2007) 648–655.
- [43] O.T. Farmer, C.J. Barinaga, D.W. Koppenaal, *J. Radioanal. Nucl. Chem.* 234 (1998) 153–157.
- [44] R.J. Cox, C.J. Pickford, M. Thompson, *J. Anal. At. Spectrom.* 7 (1992) 635–640.
- [45] A. Bartosova, P. Rajec, A. Klimekova, *Chem. Pap.* 60 (2006) 125–131.
- [46] J.L. Mas, M. Garcia-Leon, J.P. Bolivar, *Radiochim. Acta* 92 (2004) 39–46.
- [47] M.J. Keith-Roach, S. Turup, D.H. Oughton, H.H. Dahlgaard, *Analyst* 127 (2002) 70–75.
- [48] K. Tagami, S. Uchida, T. Hamilton, W. Robison, *Appl. Radiat. Isot.* 53 (2000) 75–79.
- [49] M. McCartney, K. Rajendran, V. Olive, R.G. Busby, P. McDonald, *J. Anal. At. Spectrom.* 14 (1999) 1849–1852.
- [50] S. Morita, C.K. Kim, Y. Takaku, R. Seki, N. Ikeda, *Appl. Radiat. Isot.* 42 (1991) 531–534.
- [51] M. Hollenbach, J. Grohs, S. Mamich, M. Kroft, E.R. Denoyer, *J. Anal. At. Spectrom.* 9 (1994) 927–933.
- [52] R. Chiappini, J.M. Taillade, S. Brebion, *J. Anal. At. Spectrom.* 11 (1996) 497–503.
- [53] D.M. Beals, *J. Radioanal. Nucl. Chem. Articles* 201 (1996) 253–263.
- [54] V.F. Hodge, G.A. Laing, *Radiochim. Acta* 64 (1994) 211–215.
- [55] C.J. Park, P.J. Oh, H.Y. Kim, D.S. Lee, *J. Anal. At. Spectrom.* 14 (1999) 223–227.
- [56] Y.J. Kim, C.K. Kim, C.S. Kim, J.Y. Yun, B.H. Rho, *J. Radioanal. Nucl. Chem.* 240 (1999) 613–618.
- [57] S. Joannon, C. Pin, *J. Anal. At. Spectrom.* 16 (2001) 32–37.
- [58] M.V. Zoriy, Z. Varga, C. Pickhardt, P. Ostapczuk, R. Hille, L. Halicz, I. Segal, J.S. Becker, *J. Environ. Monit.* 7 (2005) 514–518.
- [59] K. Benkhedda, D. Lariviere, S. Scott, D. Evans, *J. Anal. At. Spectrom.* 20 (2005) 523–528.



- [60] M.S. Choi, R. Francois, K. Sims, M.P. Bacon, S. Brown-Leger, A.P. Fleer, L. Ball, D. Schneider, S. Pichat, *Mar. Chem.* 76 (2001) 99–112.
- [61] M. Ayranov, U. Krahenbuhl, H. Sahli, S. Rollin, M. Burger, *Radiochim. Acta* 93 (2005) 631–645.
- [62] D.E. Vance, V.F. Belt, T.J. Oatts, D.K. Mann, *J. Radioanal. Nucl. Chem.* 234 (1998) 143–146.
- [63] S. Sumiya, S. Morita, K. Tobita, M. Kurabayashi, *J. Radioanal. Nucl. Chem. Articles* 177 (1994) 149–159.
- [64] O.F.X. Donard, F. Bruneau, M. Moldovan, H. Garraud, V.N. Epov, D. Boust, *Anal. Chim. Acta* 587 (2007) 170–179.
- [65] T.C. Kenna, *J. Anal. At. Spectrom.* 17 (2002) 1471–1479.
- [66] S. Sturup, H. Dahlgaard, S.C. Nielsen, *J. Anal. At. Spectrom.* 13 (1998) 1321–1326.
- [67] S. Aguerre, C. Frechou, *Talanta* 69 (2006) 565–571.
- [68] K. Hoppstock, J.S. Becker, H.J. Dietze, *At. Spectrosc.* 18 (1997) 180–185.
- [69] V.N. Epov, V. Taylor, D. Lariviere, R.D. Evans, R.J. Cornett, *J. Radioanal. Nucl. Chem.* 258 (2003) 473–482.
- [70] V.F. Taylor, R.D. Evans, R.J. Cornett, *Anal. Bioanal. Chem.* 387 (2007) 343–350.
- [71] A.J.T. Jull, G.S. Burr, *Earth Planet. Sci. Lett.* 243 (2006) 305–325.
- [72] C. Vockenhuber, I. Ahmad, R. Golser, W. Kutschera, V. Liechtenstein, A. Priller, P. Steier, S. Winkler, *Int. J. Mass Spectrom.* 223–224 (2003) 713–732.
- [73] L. Skipperud, D.H. Oughton, *Environ. Int.* 30 (2004) 815–825.
- [74] C.C. Shen, H. Cheng, R.L. Edwards, S.B. Moran, H.N. Edmonds, J.A. Hoff, R.B. Thomas, *Anal. Chem.* 75 (2003) 1075–1079.
- [75] P. Goodall, C. Lythgoe, *Analyst* 124 (1999) 263–269.
- [76] A. Bollhofer, A. Eisenhauer, N. Frank, D. Pech, A. Mangini, *Geologische Rundschau* 85 (1996) 577–585.
- [77] S.K. Aggarwal, S. Kumar, M.K. Saxena, P.M. Shah, H.C. Jain, *Int. J. Mass Spectrom.* 151 (1995) 127–135.
- [78] S.K. Aggarwal, D. Alamelu, *Int. J. Mass Spectrom.* 241 (2005) 183–188.
- [79] S.K. Aggarwal, *Radiochem. Acta* 94 (2006) 397–401.
- [80] D.A. Pickett, M.T. Murrell, R.W. Williams, *Anal. Chem.* 66 (1994) 1044–1049.
- [81] F. Mcdermott, T.R. Elliott, P. Vancalsteren, C.J. Hawkesworth, *Chem. Geol.* 103 (1993) 283–292.
- [82] A.S. Cohen, N.S. Belshaw, R.K. Onions, *Int. J. Mass Spectrom. Process.* 116 (1992) 71–81.
- [83] W.R. Kelly, J.D. Fassett, *Anal. Chem.* 55 (1983) 1040–1044.
- [84] S. Richter, S.A. Goldberg, *Int. J. Mass Spectrom.* 229 (2003) 181–197.
- [85] S.K. Sahoo, Y. Nakamuran, K. Shiraishi, A. Masuda, *Int. J. Environ. Anal. Chem.* 84 (2004) 919–926.
- [86] D. Delanghe, E. Bard, B. Hamelin, *Mar. Chem.* 80 (2002) 79–93.
- [87] A. McCormick, *Appl. Radiat. Isot.* 43 (1992) 271–278.
- [88] T. Yokoyama, A. Makishima, E. Nakamura, *Chem. Geol.* 181 (2001) 1–12.
- [89] C. Hennessy, M. Berglund, M. Ostermann, T. Walczyk, H.A. Synal, C. Geppert, K. Wendt, P.D.P. Taylor, *Nucl. Instr. Meth. Phys. Res. B* 229 (2005) 281–292.
- [90] F. Chartier, M. Aubert, M. Pilier, *Fresenius J. Anal. Chem.* 364 (1999) 320–327.
- [91] S.K. Aggarwal, D. Alamelu, *Int. J. Mass spectrum.* 241 (2005) 83–84.
- [92] T. Yokoyama, E. Nakamura, *J. Anal. At. Spectrom.* 19 (2004) 717–727.
- [93] P. Müller, B.A. Bushaw, K. Blaum, S. Diel, Ch. Geppert, A. Nähler, N. Trautmann, W. Nörtershäuser, K. Wendt, *Fresenius J. Anal. Chem.* 370 (2001) 508–513.
- [94] K. Wendt, J.V. Kratz, J. Lantzsich, P. Müller, W. Nörtershäuser, A. Seibert, N. Trautmann, W. Waldek, K. Zimmer, *Kerntechnik* 62 (1997) 2–3.
- [95] K. Wendt, N. Trautmann, B.A. Bushaw, *Nucl. Inst. Meth. Phys. Rev. B* 172 (2000) 162–169.
- [96] M. Nunnemann, N. Erdmann, H.U. Hasse, G. Huber, J.V. Kratz, P. Kunz, A. Mansel, G. Passler, O. Stetzer, N. Trautmann, A. Waldek, *J. Alloys Compd.* 271 (1998) 45–48.
- [97] L. Pibida, W. Nörtershäuser, J.M.R. Hutchinson, B.A. Bushaw, *Radiochim. Acta* 89 (2001) 161–168.
- [98] L. Pibida, C.A. McMahon, B.A. Bushaw, *Appl. Radiat. Isot.* 60 (2004) 567–570.
- [99] L.R. Karam, L. Pibida, C.A. McMahon, *Appl. Radiat. Isot.* 56 (2002) 369–374.
- [100] N. Trautmann, *Ultratrace analysis of Tc*, *Radiochim. Acta* 63 (1993) 37–43.
- [101] A. Ofan, I. Ahmad, J.P. Greene, M. Paul, M.R. Savina, *New Astron. Rev.* 50 (2006) 640–643.
- [102] B.A. Bushaw, B.D. Cannon, *Spectrochim. Acta Part A* 52 (1997) 1839–1854.
- [103] B.A. Bushaw, W. Nörtershäuser, *Spectrochim. Acta Part B* 55 (2000) 1679–1692.
- [104] N. Erdmann, G. Herrmann, G. Huber, S. Köhler, J.V. Kratz, A. Mansel, M. Nunnemann, G. Passler, N. Trautmann, A. Turchin, A. Waldek, *Fresenius J. Anal. Chem.* 359 (1997) 378–381.
- [105] H.U. Zwick, E.T. Aerne, A. Hermann, H.A. Thomi, M. Lippens, *J. Nucl. Mater.* 202 (1993) 65–69.
- [106] A. Amaral, P. Galle, C. Cossonnet, D. Franck, P. Pihet, M. Carrier, O. Stephan, *J. Radioanal. Nucl. Chem.* 226 (1997) 41–45.
- [107] S. Portier, S. Bremier, C.T. Walker, *Int. J. Mass Spectrom.* 263 (2007) 113–126.
- [108] Y. Ranebo, M. Eriksson, G. Tamborini, N. Niagolova, O. Bildstein, M. Betti, *Microsc. Microanal.* 13 (2007) 179–190.
- [109] R. Kips, A. Leenaers, G. Tamborini, M. Betti, S. Van den Bergh, R. Wellum, P. Taylor, *Microsc. Microanal.* 13 (2007) 156–164.
- [110] G. Tamborini, M. Betti, V. Forcina, T. Hiernaut, B. Giovannone, L. Koch, *Spectrochim. Acta Part B* 53 (1998) 1289–1302.
- [111] G. Tamborini, M. Betti, *Mikrochim. Acta* 132 (2000) 411–417.
- [112] G. Tamborini, M. Wallenius, O. Bildstein, L. Pajo, M. Betti, *Mikrochim. Acta* 139 (2002) 185–188.
- [113] M. Betti, G. Tamborini, L. Koch, *Anal. Chem.* 71 (1999) 2616–2622.
- [114] N. Erdmann, M. Betti, O. Stetzer, G. Tamborini, J.V. Kratz, N. Trautmann, J. van Geel, *Spectrochim. Acta Part B* 55 (2000) 1565–1575.
- [115] L.A.D. Heras, E. Hmecek, O. Bildstein, M. Betti, *J. Anal. Atom. Spectrom.* 17 (2002) 1011–1014.
- [116] M. Betti, *J. Anal. Atom. Spectrom.* 11 (1996) 855–860.
- [117] M. Betti, G. Rasmussen, L. Koch, *Fresenius J. Anal. Chem.* 355 (1996) 808–812.
- [118] X.L. Hou, *Appl. Radiat. Isot.* 62 (2005) 871–882.
- [119] C.B. Taylor, Present status and trends in electrolytic enrichment of low-level tritium in water. In: *Methods of Low-level Counting and Spectrometry*. IAEA-SM-252/68, 1981, pp. 303–222.
- [120] F. Pointurier, N. Gaglian, G. Alanic, *Appl. Radiat. Isot.* 61 (2004) 293–298.
- [121] K.A. Surano, G.B. Hudson, R.A. Failor, J.M. Sims, R.C. Holland, S.C. MacLean, J.C. Garrison, *J. Radioanal. Nucl. Chem. Articles* 161 (1992) 443–453.
- [122] M.J. Wood, R.G.C. McElroy, R.A. Surette, R.A. Surette, R.M. Brown, *Health Phys.* 65 (1993) 610–627.
- [123] M.L. Chiarappa-Zucca, K.H. Dingley, M.L. Roberts, C.A. Velsko, A.H. Love, *Anal. Chem.* 74 (2002) 6285–6290.

- [124] U. Wenzel, D. Herz, P. Schmidt, J. Radioanal. Chem. 53 (1979) 7–15.
- [125] A.V. Bushuev, Yu.M. Verzhilov, V.M. Zubarev, A.E. Kachanovskii, O.V. Matveev, I.M. Proshin, L.V. Bidulya, A.A. Ivanov, A.K. Kalugin, Atomic Energy 73 (1992) 959–962.
- [126] A. Endo, Y. Harada, K. Kawasaki, M. Kikuchi, Appl. Radiat. Isot. 60 (2004) 955–958.
- [127] A. Raymond, Analyse des radioisotopes emetteurs beta purs ( $^3\text{H}$ ,  $^{14}\text{C}$ ,  $^{36}\text{Cl}$ ,  $^{63}\text{Ni}$ ) dans le graphite irradie, Rapport Techniques, CEA-RT-DSD-20, CEA, France, 1990.
- [128] H.Y. Yang, Z.H. Wang, W. Liu, X.L. Wen, H. Zheng, Chin. J. Atomic Energy Sci. Technol. 30 (1996) 509–515.
- [129] C.J. Passo, R. Anderson, D. Roberts, G.T. Cook, Radiocarbon 40 (1998) 193–200.
- [130] H. Sakurai, W. Kato, Y. Takahashi, K. Suzuki, Y. Takahashi, S. Gunji, F. Tokanai, Radiocarbon 48 (2006) 401–408.
- [131] H.-A. Synal, S. Jacob, M. Suter, Nucl. Instr. Meth. B 172 (2000) 1–7.
- [132] T. W. Stafford, P.E. Hare, L. Currie, A.J.T. Jull, D.J. Donahue, J. Archaeol. Sci. 18 (1991) 35–72.
- [133] D.J.W. Mous, W. Fokker, R. Van den Broek, R. Koopmans, Radiocarbon 40 (1998) 283–288.
- [134] X.L. Hou, L.F. Østergaard, S.P. Nielsen, Anal. Chem. 79 (2007) 3126–3134.
- [135] X.Q. Liu, H.W. Gaeggeler, D. Laske, F.C. Brandt, J.C. Alder, K. Kurtz K. Report, NAGRA-NTB-91-07, Switzerland, 1991.
- [136] D.L. Moir, A.W. Tarr, K.J. Ross, H.G. Delaney, J. Radioanal. Nucl. Chem. Lett. 200 (1995) 365–373.
- [137] M. Itoh, K. Watanabe, M. Hatakeyama, M. Tachibana, Analyst 127 (2002) 964–966.
- [138] L. Ashton, P. Warwick, D. Giddings, Analyst 124 (1999) 627–632.
- [139] C. Fréchou, J.P. Degros, J. Radioanal. Nucl. Chem. 263 (2005) 333–339.
- [140] R.J. Delmas, J. Beer, H.A. Synal, R. Muscheler, J.R. Petit, M. Pourchet, Tellus Ser. B—Chem. Phys. Meteorol. 56 (2004) 492–498.
- [141] H.A. Synal, J. Beer, G. Bonani, C. Lukaszczuk, M. Suter, Nucl. Instr. Meth. B 92 (1994) 79–84.
- [142] R. Seki, D. Arai, Y. Nagashima, T. Imanaka, T. Takahashi, T. Matsushiro, J. Radioanal. Nucl. Chem. 225 (2003) 245–247.
- [143] D. Elmore, M.H. Bhattacharyya, N. Saccogibson, D.P. Peterson, Nucl. Instr. Meth. B 52 (1990) 531–435.
- [144] M. Itoh, K. Watanabe, M. Hatakeyama, M. Tachibana, Anal. Bioanal. Chem. 372 (2002) 532–540.
- [145] R.L. Barquero, J.M. Los Arcos, Nucl. Instr. Meth. A 369 (1996) 353–358.
- [146] J.A. Suárez, M. Rodriguez, A.G. Espartero, G. Piña, Appl. Radiat. Isot. 52 (2000) 407–413.
- [147] L. Zerle, T. Faestermann, K. Knie, G. Korschinek, E. Nolte, J. Geophys. Res. 102 (1997) 19517–19527.
- [148] B. DittrichHannen, F. Ames, M. Suter, M.J.M. Wagner, C. Schnabel, R. Micheal, U. Herpers, E. Gunther, Nucl. Instr. Meth. B 113 (1996) 453–456.
- [149] P.W. Kubik, D. Elmore, Radiocarbon 31 (1989) 324–326.
- [150] P. Sharma, R. Middleton, Nucl. Instr. Meth. B 29 (1987) 63–66.
- [151] C. Geppert, P. Muller, K. Wendt, C. Schnabel, H.A. Synal, U. Herpers, S. Merchel, Nucl. Instr. Meth. B 229 (2005) 519–526.
- [152] N. Trautmann, G. Passler, K.D.A. Wendt, Anal. Bioanal. Chem. 378 (2004) 348–355.
- [153] J.E. McAninch, L.J. Hainsworth, A.A. Marchetti, M.R. Leivers, P.R. Jones, A.E. Dunlop, R. Mauthe, S. Vogel, I.D. Proctor, T. Straume, Nucl. Instr. Meth. B 123 (1997) 137–143.
- [154] P. Persson, B. Erlandsson, K. Freimann, R. Hellborg, R. Larsson, J. Persson, G. Skog, K. Stenström, Nucl. Instr. Meth. B 160 (2000) 510–514.
- [155] K.S. Kasprzak, F.W. Sunderman Jr., Pure Appl. Chem. 51 (1979) 1375–1389.
- [156] L. Hedouin, O. Pringault, M. Metian, P. Bustamante, M. Warnau, Chemosphere 66 (2007) 1449–1457.
- [157] A. Wiebert, P. Persson, M. Elfman, B. Erlandsson, R. Hellborg, P. Kristiansson, K. Stenström, G. Skog, Nucl. Instr. Meth. B 109/110 (1996) 175–178.
- [158] W. Kutschera, I. Ahmad, B.G. Glagola, R.C. Pardo, K.E. Rehm, D. Berkovits, M. Paul, J.R. Arnold, K. Nishiizumik, Nucl. Instr. Meth. B 73 (1993) 403–412.
- [159] P. Persson, M. Kiisk, B. Erlandsson, K. Freimann, R. Hellborg, G. Skog, K. Stenström, Nucl. Instr. Meth. B 172 (2000) 188–192.
- [160] G. Rugel, A. Arazi, K.L. Carroll, T. Faestermann, K. Knie, G. Korschinek, A.A. Marchetti, R.E. Martinelli, J.E. McAninch, W. Rühm, T. Straume, A. Wallner, C. Wallner, Nucl. Instr. Meth. B 223 (2004) 776–781.
- [161] E. Holm, B. Oregioni, D. Vas, H. Pettersson, J. Rioseco, U. Nilsson, J. Radioanal. Nucl. Chem. Articles 138 (1990) 111–118.
- [162] E. Holm, P. Roos, B. Skwarzec, Appl. Radiat. Isot. 43 (1992) 43–49.
- [163] P.E. Warwick, I.W. Croudace, Anal. Chim. Acta 567 (2006) 277–285.
- [164] C. Scheuerer, R. Schupfner, H. Schuttelkopf, J. Radioanal. Nucl. Chem. Articles 193 (1995) 127–131.
- [165] J.M. Jo, B.J. Cheng, C.L. Tseng, J.D. Lee, Anal. Chim. Acta 281 (1993) 429–433.
- [166] M. Numajiri, Y. Oki, T. Suzuki, T. Miura, M. Taira, Y. Kanda, Y. Kondo, Appl. Radiat. Isot. 45 (1994) 509–514.
- [167] J.H. Kaye, R.S. Strebin, A.E. Nevissi, J. Radioanal. Nucl. Chem. Articles 180 (1994) 197–200.
- [168] I. Gresits, S. Tolgyesi, J. Radioanal. Nucl. Chem. 258 (2003) 107–112.
- [169] G. Rugel, T. Faestermann, K. Knie, G. Korschinek, A.A. Marchetti, J.E. McAninch, W. Rühm, T. Straume, C. Wallner, Nucl. Instr. Meth. B 172 (2000) 934–938.
- [170] E.P. Horwitez, M.T. Dietz, D.E. Fisher, Solvent Extr. Ion Exch. 8 (1990) 557.
- [171] M. Pimpl, J. Radioanal. Nucl. Chem. 194 (1995) 311.
- [172] C.W. Lee, K.H. Hong, M.H. Lee, Y.H. Cho, G.S. Choi, Y.W. Choi, S.H. Moon, J. Radioanal. Nucl. Chem. 243 (2000) 767.
- [173] E.P. Horwitz, M.T. Dietz, D.E. Fisher, Anal. Chem. 63 (1991) 522.
- [174] M. Heilgeist, J. Radioanal. Nucl. Chem. 245 (2000) 249.
- [175] F. Gouteland, R. Nazard, C. Bocquet, N. Coquenlorge, P. Letessier, D. Calmet, Appl. Radiat. Isot. 53 (2000) 145.
- [176] J. Cobb, P. Warwick, R.C. Carpenter, R.T. Morrison, Sci. Total Environ. 173/174 (1995) 179.
- [177] R. Stella, T.G. Valentini, L. Maggi, J. Radioanal. Nucl. Chem. 161 (1992) 413.
- [178] IAEA, IAEA, Reference method for marine radioactivity studies, IAEA Technical Report Series No.-118. International Atomic Energy Agency, Vienna, 1970.
- [179] L. Popov, X.L. Hou, S.P. Nielsen, Y. Yu, J. Radioanal. Nucl. Chem. 269 (2006) 161–173.
- [180] J. Suomela, L. Wallberg, J. Melin, Method for determination of  $^{90}\text{Sr}$  in food and environmental samples by Cerenkov counting, Swedish Radiation Protection Institute, SSI-Rapport 93-1, 1993, p. 19.
- [181] K.C. Stamoulis, K.G. Ioannides, D.T. Karamanis, D.C. Patiris, J. Environ. Radioact. 93 (2007) 144–156.
- [182] Q.J. Chen, H. Dahlgaard, H.J.M. Hansen, A. Aarkrog, Anal. Chim. Acta 228 (1990) 163–167.
- [183] J.W. Grate, R. Strebin, J. Janate, Anal. Chem. 68 (1996) 333–340.
- [184] M. Paul, D. Berkovits, L.D. Cecil, H. Feldstein, A. Hershkowitz, Y. Kashiv, S. Vogt, Nucl. Inst. Meth. Phys. Rev. B 123 (2000) 162–169.



- [185] Q.J. Chen, A. Aarkrog, H. Dalhgaard, S.P. Nielsen, E. Holm, H. Dick, K. Mandrup, J. Radioanal. Nucl. Chem. Articles 131 (1989) 171–197.
- [186] F. Wigley, P.E. Warwick, I.W. Croudace, J. Caborn, A.L. Sanchez, Anal. Chim. Acta 380 (1999) 73–82.
- [187] M. Dowdall, Ø.G. Selnaes, J.P. Gwynn, B. Lind, Water, Air, Soil Pollut. 156 (2004) 287–297.
- [188] A. Aarkrog, L. Carlsson, Q.J. Chen, H. Dahlgaard, E. Holm, L. Huynh-Ngoc, L.H. Jensen, S.P. Nielsen, H. Nies, Nature 335 (1988) 338–340.
- [189] T.K. Ikaheimonen, V.P. Vartti, E. Ilus, J. Mattila, J. Radioanal. Nucl. Chem. 252 (2002) 309–313.
- [190] L. Wacker, L.K. Fifield, S.G. Tims, Nucl. Instr. Meth. B 223 (2004) 185–189.
- [191] L.K. Fifield, R.S. Carling, R.G. Cresswell, P.A. Hausladen, M.-L. di Tada, J.P. Day, Nucl. Instr. Meth. B 168 (2000) 427–436.
- [192] B.A. Bergquist, A.A. Marchetti, R.E. Martinelli, J.E. McAninch, G.J. Nimz, I.D. Proctor, J.R. Southon, J.S. Vogel, Nucl. Instr. Meth. B 172 (2000) 328–332.
- [193] D.J. Rokop, N.C. Rokop, K. Schroeder, Wolfsberg, Anal. Chem. 62 (1990) 1271.
- [194] P. Dixon, D.B. Curtis, J. Musgrave, F. Roensch, J. Roach, D. Rokop, Anal. Chem. 69 (1997) 1692–1699.
- [195] M. Song, T.U. Probst, Anal. Chim. Acta 413 (2000) 207–215.
- [196] C.K. Kim, C.S. Kim, B.H. Rho, J.I. Lee, J. Radioanal. Nucl. Chem. 252 (2002) 421–427.
- [197] S. Foti, E. Delucchi, V. Akamian, Anal. Chim. Acta 60 (1972) 261–268.
- [198] S. Foti, E. Delucchi, V. Akamian, Determination of picogram amounts of technetium in environmental samples by neutron activation analysis, Anal. Chim. Acta 60 (1972) 269–276.
- [199] N. Ikeda, R. Seki, M. Kamemoto, M. Otsuji, Activation analysis for technetium-99 by the use of a neutron excitation reaction, J. Radioanal. Nucl. Chem. Articles 131 (1989) 65–71.
- [200] X.L. Hou, Activation analysis for the determination of long-lived radionuclides, in: P.P. Povinec (Ed.), Analysis of Environmental Radionuclides, Elsevier, 2007, pp. 371–406.
- [201] X.L. Hou, H. Dahlgaard, S.P. Nielsen, Estuarine Coast. Shelf Sci. 51 (2000) 571–584.
- [202] X.L. Hou, A. Aldahan, S.P. Nielsen, G. Possnert, H. Nies, J. Hedfors, Environ. Sci. Technol. 41 (2007) 5993–5999.
- [203] C. Frechou, Optimisation of the measurement protocols of  $^{129}\text{I}$  and  $^{129}\text{I}/^{127}\text{I}$ , Ph.D. thesis, CEA/Saclay, 2000.
- [204] F. Verrezen, C. Hurtgen, Appl. Radiat. Isot. 43 (1992) 61–68.
- [205] X.L. Hou, H. Dahlgaard, B. Rietz, U. Jacobsen, S.P. Nielsen, A. Aarkrog, Analyst 124 (1999) 1109–1114.
- [206] J.M. Lopez-Gutierrez, H.A. Synal, M. Suter, C. Schnabel, M. Garcia-Leon, Appl. Radiat. Isot. 53 (2000) 81–85.
- [207] W.E. Kieser, X.L. Zhao, C.Y. Soto, B. Tracy, J. Radioanal. Nucl. Chem. 263 (2005) 375–379.
- [208] N. Buraglio, A. Aldahan, G. Possnert, Nucl. Instr. Meth. B 161 (2000) 240–244.
- [209] A. Aldahan, A. Kekli, G. Possnert, J. Environ. Radioact. 88 (2006) 49–73.
- [210] A. Aldahan, E. Englund, G. Possnert, I. Cato, X.L. Hou, Appl. Geochem. 22 (2007) 37–647.
- [211] U. Fehn, Science 289 (2000) 2332.
- [212] H. Tomaru, Z.L. Lu, G.T. Snyder, R. Matsumoto, Chem. Geol. 236 (2007) 350–366.
- [213] A.V. Izmer, S.F. Boulyga, J.S. Becker, J. Anal. At. Spectrom. 18 (2003) 1339–1345.
- [214] C. Briancon, J. Jeusset, C. Francese, F. Omri, S. Halpern, P. Fragu, Biol. Cell 74 (1992) 75–80.
- [215] E. Hindie, A. Petiet, K. Bourahla, N. Colas-Linhart, G. Slodzian, R. Dennebouy, P. Galle, Cell. Mol. Biol. 47 (2001) 403–410.
- [216] J.A. Suarez, A.G. Espartero, M. Rodriguez, Nucl. Instr. Meth. A 369 (1996) 407–410.
- [217] J.H. Chao, C.L. Tseng, Determination of  $^{135}\text{Cs}$  by neutron activation analysis, Nucl. Instr. Meth. Phys. Res. A272 (1996) 275–279.
- [218] H.H. Stamm, Determination of  $^{135}\text{Cs}$  in sodium from an in-pile loop by activation analysis, J. Radioanal. Chem. 14 (1973) 367–373.
- [219] T. Lee, T.L. Ku, H.-L. Lu, J.C. Chen, Geochim. Cosmochim. Acta 57 (1993) 3493–3497.
- [220] M. Song, T.U. Probst, N.G. Berryman, Fresenius J. Anal. Chem. 370 (2001) 744–751.
- [221] A.M. Meeks, J.M. Giaquinto, J.M. Keller, J. Radioanal. Nucl. Chem. 234 (1998) 131–135.
- [222] Y.Y. Ebaid, A.E.M. Khater, J. Radioanal. Nucl. Chem. 270 (2006) 609–619.
- [223] S.A. Brown, J. Radioanal. Nucl. Chem. 264 (2005) 505–509.
- [224] G.A. Peck, J.D. Smith, Anal. Chim. Acta 422 (2000) 113–120.
- [225] Q.J. Chen, X.L. Hou, H. Dahlgaard, S.P. Nielsen, A. Aarkrog, J. Radioanal. Nucl. Chem. 249 (2001) 587–593.
- [226] P. Vesterbacka, T.K. Ikaheimonen, Anal. Chim. Acta 545 (2005) 252–261.
- [227] A. Zaborska, J. Carroll, C. Papucci, P. Janusz, J. Environ. Radioact. 93 (2007) 38–50.
- [228] D. Larivière, K.M. Reiber, R.D. Evans, R.J. Cornett, Anal. Chim. Acta 549 (2005) 188–196.
- [229] H.F. Lucas, F. Markun, J. Environ. Radioact. 15 (1992) 1–18.
- [230] W.C. Burnett, W.C. Tai, Anal. Chem. 64 (1992) 1691–1697.
- [231] J.A. Sanchez-Cabeza, L. Pujol, Analyst 123 (1998) 399–403.
- [232] M.T. Crespo, A.S. Jimenez, J. Radioanal. Nucl. Chem. Articles 221 (1997) 149–152.
- [233] S. Purkl, A. Eisenhauer, Appl. Radiat. Isot. 59 (2003) 245–254.
- [234] G.G. Jia, G. Torri, P. Innocenzi, R. Ocone, A. Di Lullo, J. Radioanal. Nucl. Chem. 267 (2006) 505–514.
- [235] P. Parekh, D. Haines, A. Bari, M. Torres, Health Phys. 85 (2003) 613–620.
- [236] B. Parsa, A. Hoffman, J. Radioanal. Nucl. Chem. Articles 158 (1992) 53–63.
- [237] S. Nour, A. Ei-Sharkawy, W.C. Burnett, E.P. Horwitz, Appl. Radiat. Isot. 61 (2004) 1173–1178.
- [238] S.G. Tims, G.J. Hancock, L. Wacker, L.K. Fifield, Nucl. Instr. Meth. B 223 (2004) 796–801.
- [239] A.S. Cohen, Anal. Chem. 63 (1991) 2705–2708.
- [240] D. Larivière, V.N. Epov, K.M. Reiber, R.J. Cornett, R.D. Evans, Anal. Chim. Acta 528 (2005) 175–182.
- [241] A.O. Nier, J. Chem. Educ. 66 (1989) 385–388.
- [242] M. Ivanovich, A. Murray, Spectroscopic methods, in: M. Ivanovich, R.S. Harmon (Eds.), Uranium-Series Disequilibrium, Applications to Earth, Marine, and Environmental Sciences, Clarendon Press, Oxford, 1992.
- [243] J.H. Chen, R.L. Edwards, G.L. Wasserburg, Mass spectrometry and applications to uranium-series disequilibrium, in: M. Ivanovich, R.S. Harmon (Eds.), Uranium-Series Disequilibrium, Applications to Earth, Marine, and Environmental Sciences, Clarendon Press, Oxford, 1992.
- [244] S.J. Goldstein, C.H. Stirling, Techniques for measuring Uranium-series nuclides: 1992–2002, in: B. Bourdon, G.M. Henderson, C.C. Lundstrom, S.P. Turner (Eds.), Uranium-Series Geochemistry, Reviews in Mineralogy & Geochemistry, vol. 52, 2003.
- [245] C. Tuniz, J.R. Bird, D. Fink, G.F. Herzog, Accelerator Mass Spectrometry, CRC Press LLC, Boca Raton, 1998.
- [246] J.R. de Laeter, Mass Spectrom. Rev. 17 (1998) 97–125.

- [247] S.F. Boulyga, K.G. Heumann, *J. Environ. Radioact.* 88 (2006) 1–10.
- [248] B.A. Buchholz, T.A. Brown, T.F. Hamilton, I.D. Hutcheon, A.A. Marchetti, R.E. Martinelli, E.C. Ramon, S.J. Tumey, R.W. Williams, *Nucl. Instr. Meth. B* 259 (2007) 733–738.
- [249] M.R. Van der Loeff, M.M. Sarin, M. Baskaran, C. Benitez-Nelson, K.O. Buesseler, M. Charette, M. Dai, Ö. Gustafsson, P. Masque, P.J. Morris, K. Orlandini, A. Rodriguez y Baena, N. Savoye, S. Schmidt, R. Turnewitsch, I. Vöge, J.T. Waples, *Mar. Chem.* 100 (2006) 190–212.
- [250] P. Roos, J.R. Valeur, *Cont. Shelf Res.* 26 (2006) 474–487.
- [251] A.S. Hursthouse, M.S. Baxter, K. McKay, F.R. Livens, *J. Radioanal. Nucl. Chem. Articles* 157 (1992) 281–294.
- [252] S.K. Jha, I.S. Bhat, *J. Radioanal. Nucl. Chem. Articles* 182 (1994) 5–10.
- [253] N. Baglan, C. Bouvier-Capely, C. Cossonnet, *Radiochim. Acta* 90 (2002) 267–272.
- [254] Q.J. Chen, H. Dahlgaard, S.P. Nielsen, A. Aarkrog, I. Christensen, A. Jensen, *J. Radioanal. Nucl. Chem.* 249 (2001) 527–533.
- [255] Q.J. Chen, H. Dahlgaard, S.P. Nielsen, A. Aarkrog, *J. Radioanal. Nucl. Chem.* 253 (2002) 527–533.
- [256] M.J. Keith-Roach, J.P. Day, L.K. Fifield, F.R. Livens, *Analyst* 126 (2001) 58–61.
- [257] T.C. Kenna, *J. Anal. At. Spectrom.* 17 (2002) 1471–1479.
- [258] L. Patric, P. Roos, M. Eriksson, E. Holm, *J. Environ. Radioact.* 73 (2004) 73–84.
- [259] L. Patric, P. Roos, M. Eriksson, E. Holm, H. Dahlgaard, *J. Environ. Radioact.* 82 (2005) 285–301.
- [260] S.C. Lee, J.M. Hutchinson, K.G.W. Inn, M. Thein, *Health Phys.* 68 (1995) 350–358.
- [261] P. Germian, G. Pinte, *J. Radioanal. Nucl. Chem. Articles* 138 (1990) 49–61.
- [262] A.R. Byrne, *J. Environ. Radioact.* 4 (1986) 133–144.
- [263] R. Jakopic, P. Tavcar, L. Benedik, *Appl. Radiat. Isot.* 65 (2007) 504–511.
- [264] K. Norisuye, K. Okamura, Y. Sohrin, H. Hasegawa, T. Nakanishi, *J. Radioanal. Nucl. Chem.* 267 (2005) 183–193.
- [265] Q.J. Chen, A. Aarkrog, S.P. Nielsen, H. Dahlgaard, H. Nies, Y.X. Yu, K. Mandrup, *J. Radioanal. Nucl. Chem.* 172 (1993) 281–288.
- [266] D. Arnold, *Appl. Radiat. Isot.* 64 (8) (2006) 1137–1140.
- [267] L.L.W. Kwong, J. Gastaud, J. La Rosa, S.H. Lee, P.P. Povinec, E. Wyse, *J. Radioanal. Nucl. Chem.* 261 (2004) 283–289.
- [268] A.V. Muravitsky, V.F. Razbudey, V.V. Tokarevsky, P.N. Voron, *Appl. Radiat. Isot.* 63 (2005) 487–492.
- [269] K.O. Buesseler, J. Halversen, *J. Environ. Radioact.* 5 (1987) 425–444.
- [270] Y. Ohtsuka, Y. Takaku, J. Kimura, S. Hisamatsu, J. Inaba, *Anal. Sci.* 21 (2005) 205–208.
- [271] E. Hrnccek, P. Steier, A. Wallner, *Appl. Radiat. Isot.* 63 (2005) 633–638.
- [272] M. Sankari, P.V.K. Kumar, M.V. Suryanarayana, *Int. J. Mass Spectrom.* 254 (2006) 94–100.
- [273] C.S. Kim, C.K. Kim, P. Martin, U. Sansone, *J. Anal. At. Spectrom.* 22 (2007) 827–841.
- [274] Z. Varga, G. Surányi, N. Vajda, Z. Stefánka, *J. Radioanal. Nucl. Chem.* 274 (2007) 87–94.
- [275] N.D. Priest, G.D. Pich, L.K. Fifield, R.G. Cresswell, *Radiat. Res.* 152 (1999) S16–S18.
- [276] S.H. Lee, J. Gastaud, J.J. La Rosa, L.L.W. Kwong, P.P. Povinec, E. Wyse, L.K. Fifield, P.A. Hausladen, L.M. Di Tada, G.M. Santos, *J. Radioanal. Nucl. Chem.* 248 (2001) 757–764.
- [277] Z. Varga, G. Suranyi, N. Vajda, Z. Stefanka, *Radiochim. Acta* 95 (2007) 81–87.
- [278] Z. Varga, *Anal. Chim. Acta* 587 (2007) 165–169.
- [279] D. Arginelli, M. Montalto, S. Bortoluzzi, M. Nocente, M. Bonardi, F. Groppi, *J. Radioanal. Nucl. Chem.* 263 (2005) 275–279.
- [280] L. Perna, J. Jernstrom, L.A. de las Heras, J. de Palo, M. Betti, *Anal. Chem.* 75 (2003) 2292–2298.
- [281] P.E. Warwick, I.W. Croudace, S.S. Oh, *Anal. Chem.* 73 (2001) 3410.
- [282] S.H. Lee, J. La Rosa, J. Gastaud, P.P. Povinec, *J. Radioanal. Nucl. Chem.* 263 (2005) 419–425.
- [283] E.P. Horwitz, M. Dietz, R. Chiarizia, H. Diamond, S.L. Maxwell, M. Nelson, *Anal. Chim. Acta* 310 (1995) 63.
- [284] J. Ruzicka, E.H. Hansen, *Anal. Chim. Acta* 78 (1975) 145–157.
- [285] E.H. Hansen, M. Miro, *TRAC-Trends Anal. Chem.* 26 (2007) 18–26.
- [286] O. Egorov, J.W. Grate, J. Ruzicka, *J. Radioanal. Nucl. Chem.* 234 (1998) 231–235.
- [287] P. Desmartin, Z. Kopajtic, W. Haerdi, *Environ. Monit. Assess.* 44 (1997) 413–423.
- [288] V.N. Epov, K. Benkhedda, R.D. Evans, *J. Anal. At. Spectrom.* 20 (2005) 990–992.
- [289] C.S. Kim, C.H. Kim, J.I. Lee, K.J. Lee, *J. Anal. At. Spectrom.* 15 (2000) 247–255.
- [290] C.S. Kim, C.K. Kim, *Anal. Chem.* 74 (2002) 3824–3832.
- [291] C.S. Kim, C.K. Kim, K.J. Lee, *J. Anal. At. Spectrom.* 19 (2000) 743–750.
- [292] O. Egorov, M.J.O. Hara, O.T. Farmer III, J.W. Grate, *Analyst* 126 (2001) 1594–1601.
- [293] O.B. Egorov, M.J. O'Hara, J.W. Grate, *J. Radioanal. Nucl. Chem.* 263 (2005) 629–633.
- [294] L. Perna, F. Bocci, L. Aldave de lash eras, J. De Pablo, M. Betti, *J. Anal. At. Spectrom.* 17 (2002) 1166–1171.
- [295] L. Perna, M. Betti, J.M.B. Morrero, R. Fuoco, *J. Anal. At. Spectrom.* 16 (2001) 26–31.
- [296] J. Jerström, J. Lehto, M. Betti, *J. Radioanal. Nucl. Chem.* 274 (2007) 95–102.
- [297] J.B. Truscott, P. Jones, B.E. Fairman, E.H. Evans, *Anal. Chim. Acta* 433 (2001) 245–253.

# Iodine Speciation in Foodstuffs, Tissues, and Environmental Samples: Iodine Species and Analytical Method

**Xiaolin Hou** Risø National laboratory for Sustainable Energy, NUK-202, Technical University of Denmark, DK-4000 Roskilde, Denmark

## Abstract

Different species of iodine are involved in the transport of iodine from air, soil and water to food, and from food to the human body. In water, most iodine occurs as iodide and iodate while, in some cases, the concentration of organic iodine may be high. In the air, iodine exists as particle associated iodine, inorganic gaseous iodine ( $I_2$ , HIO), and organic gaseous iodine ( $CH_3I$ ,  $CH_2I_2$ , etc.). In the body of humans and other mammals, iodine is utilized by the thyroid gland for the biosynthesis of the thyroid hormones  $T_4$  and  $T_3$ . Besides  $T_3$  and  $T_4$ , iodine also exists as MIT, DIT,  $T_3$ , and  $rT_3$ , which are mainly bound with proteins in thyroid and other tissues, but function as free  $T_3$  and  $T_4$ . In milk and urine, most iodine occurs as iodide, but some species of organic iodine were also found. In seaweed, iodine species varies widely with the species of seaweed. In brown seaweed, most of iodine exists as iodide; while in green seaweed, iodine is mainly bound to organic molecules, such as protein and polyphenol. Iodine species in fish are similar to that in the human body. The most commonly used methods of assay are chromatographic techniques, such as anion exchange, size exclusion and reverse-phase chromatography, coupled with ICP-MS detection. This chapter presents the analytical methods for iodine species in water, air, tissues and biological samples, and also in foodstuffs and environmental samples. The bioavailability and toxicity of different iodine species are also discussed.

## Abbreviations

CE	Capillary electrophoresis
DIT	Diiodotyrosine
GC	Gas chromatography
HPLC	High-performance liquid chromatography

IC	Ion chromatography
ICP-MS	Inductively coupled plasma mass spectrometry
IIH	Iodine-induced hyperthyroidism
LC	Liquid chromatography
MIT	Monoiodotyrosine
NAA	Neutron activation analysis
RP-HPLC	Reverse-phase high-performance liquid chromatography
$rT_3$	Reverse triiodothyronine
SEC	Size exclusion chromatography
$T_3$	Triiodothyronine
$T_4$	Thyroxine

## Introduction

Iodine is an essential element in humans and other mammals, which is used for the synthesis of the thyroid hormones triiodothyronine ( $T_3$ ) and thyroxine ( $T_4$ ). These hormones play a prominent role in the metabolism of most cells of the organism and in the process of early growth and development of most organs, especially brain (Anderson *et al.*, 2000). Besides  $T_3$  and  $T_4$ , reverse  $T_3$  ( $rT_3$ ), monoiodotyrosine (MIT), and diiodotyrosine (DIT) are also synthesized and distributed in the body of humans and animals, but only  $T_3$  and  $T_4$  have a biological function. Iodine in the human body mainly comes through dietary and water intake, and inhalation of atmospheric iodine. Due to low concentrations of iodine in the air ( $10\text{--}20\text{ ng/m}^3$ ), food and water intake form the major source of iodine for adults, while for infants it is milk. The concentration of iodine in foodstuffs is directly related to that in the environment where the foods come from. Iodine deficiency disorders are mainly found in places where the concentration of iodine in the soil and drinking water is very low. In the water, foodstuffs, and

**Table 15.1** Iodine species in nature

Name	Chemical formula	Samples
Iodide	$I^-$	Water, plant, animal
Iodate	$IO_3^-$	Water
Elemental iodine	$I_2$	Air
Periodate	$IO_4^-$	Water
Hypoiodite	$IO^-$	Air, water
Methyl iodide	$CH_3I$	Air, water
Methyl di-iodide	$CH_2I_2$	Air, water
Ethyl iodide	$C_2H_5I$	Air, water
Propyl iodide	$C_3H_7I$	Air, water
Butyl iodide	$C_4H_9I$	Air, water
Methyl iodide bromide	$CH_2BrI$	Air, water
Triiodothyronine	$T_3$ (Figure 15.6)	Animal, plant, milk
Thyroxine	$T_4$ (Figure 15.6)	Animal, plant, milk
Monoiodotyrosine	MIT	Animal, plant, milk
Diiodotyrosine	DIT (Figure 15.6)	Animal, plant, milk
Reverse triiodothyronine	$rT_3$ (Figure 15.6)	Animal, plant, milk
Particle-associated iodine	–	Air, water

Note: The name and chemical formulas of the iodine species occurring in nature are shown; the possible sample types in which the species exist are also shown in the third column.

environmental samples, iodine exists in different species, such as iodide, iodate and in association with various organic compounds. Table 15.1 shows the various iodine species in nature. The species of iodine in the water and environmental samples is related to the level of iodine in plants and foodstuffs. The species of iodine in foodstuffs directly affects the bioavailability of iodine to humans and animals. This article reviews the speciation of iodine in water, air, foodstuffs and biological and environmental samples. In addition, the bioavailability and toxicity of iodine species are also discussed.

## Speciation of Iodine in Water

Interest in the species of iodine in water has increased in the past decades. Water is considered to be an important source of iodine for humans and animals (Rasmussen *et al.*, 2000); it also supplies iodine to plants.

## Distribution of iodine species

The iodine species present in water depend on the nature of the water. In seawater, iodine mainly exists as iodate, iodide, and minor organic iodine (Wong, 1991). The distribution of iodine species in seawater depends on the water chemistry, and varies with depth and geographic location. In anoxic water, most iodine exists as iodide, such as in the Baltic Sea and the Black Sea (Luther *et al.*, 1991; Truesdale *et al.*, 2001; Hou *et al.*, 2001). While in oxygenated/oxic

water the concentration of iodate is high, the concentration in the open sea is  $<0.01$ – $0.2 \mu M$  for iodide and  $0.2$ – $0.5 \mu M$  for iodate. Iodide maxima are often found in surface water. Below the euphotic zone, iodide decreases to below  $0.01 \mu M$ . Higher iodide concentrations are normally found in coastal and estuary areas; Figure 15.1 shows the distribution of iodide/iodate in the surface water of the North Sea (Hou *et al.*, 2007).

Organic iodine found in coastal and estuary areas corresponded to 5–40% of total dissolved iodine (Schwehr and Santschi, 2003; Jones and Truesdale, 1984; Cook *et al.*, 2000). A few specific organic iodine compounds, mainly volatile compounds, have been identified, such as  $CH_3I$ ,  $CH_2ClI$ ,  $CH_2I_2$ , and  $CH_3CH_2CH_2I$  (Schall *et al.*, 1997; Moore and Graszko, 1999). Although the concentration of organic iodine in seawater is low, it plays an important role in the global geochemical cycle of iodine, because the transfer of iodine from the iodine-rich ocean to the atmosphere, and then to the terrestrial environment, is thought to occur primarily through the volatilization of organic iodine hydrocarbon in seawater (Campos *et al.*, 1996). These volatile organic iodine species were also supposed to relate to the ozone depletion in the stratosphere (Solomon *et al.*, 1994). In freshwater, iodine also exists as iodide iodate and organic iodine, but the concentration of organic iodine is normally relatively high in freshwater, such as river water, lake water and rain (Gilfedder *et al.*, 2007; Abdel-Moati, 1999; Reifenhäuser and Heumann, 1990; Truesdale and Jones, 1996).

## Speciation analysis of inorganic iodine

A number of analytical methods have been reported for the speciation analysis of iodine in water. In seawater, iodate can be directly determined by titrimetry, colorimetry, and differential pulse polarography methods (Wong and Cheng, 1998; Luther *et al.*, 1991; Herring and Liss, 1974; Stipanicev and Branica, 1996), and iodide by cathodic stripping voltammetry, chromatography, and inductively coupled plasma atomic emission spectrometry or mass spectrometry (ICP-MS) (Tian and Nicolas, 1995; Brandao *et al.*, 1995; Anderson *et al.*, 1996; Radlinger and Heumann, 1997). Organic iodine was normally given as the difference between total iodine (sum of all forms of inorganic and organic iodine) and total inorganic iodine ( $IO_3^- + I^-$ ), in which the concentration of total iodine was determined as  $IO_3^-$  or  $I^-$  after organic iodine had been decomposed and converted into  $IO_3^-$  or  $I^-$  by UV irradiation or/and redox treatment (Luther *et al.*, 1991).

In addition, chromatographic separation combined with detection methods, such as neutron activation analysis (NAA) and ICP-MS, was also reported for chemical speciation analysis of iodine in water (Hou *et al.*, 1999b; Reifenhäuser and Heumann, 1990; Schwehr and Santschi, 2003). In

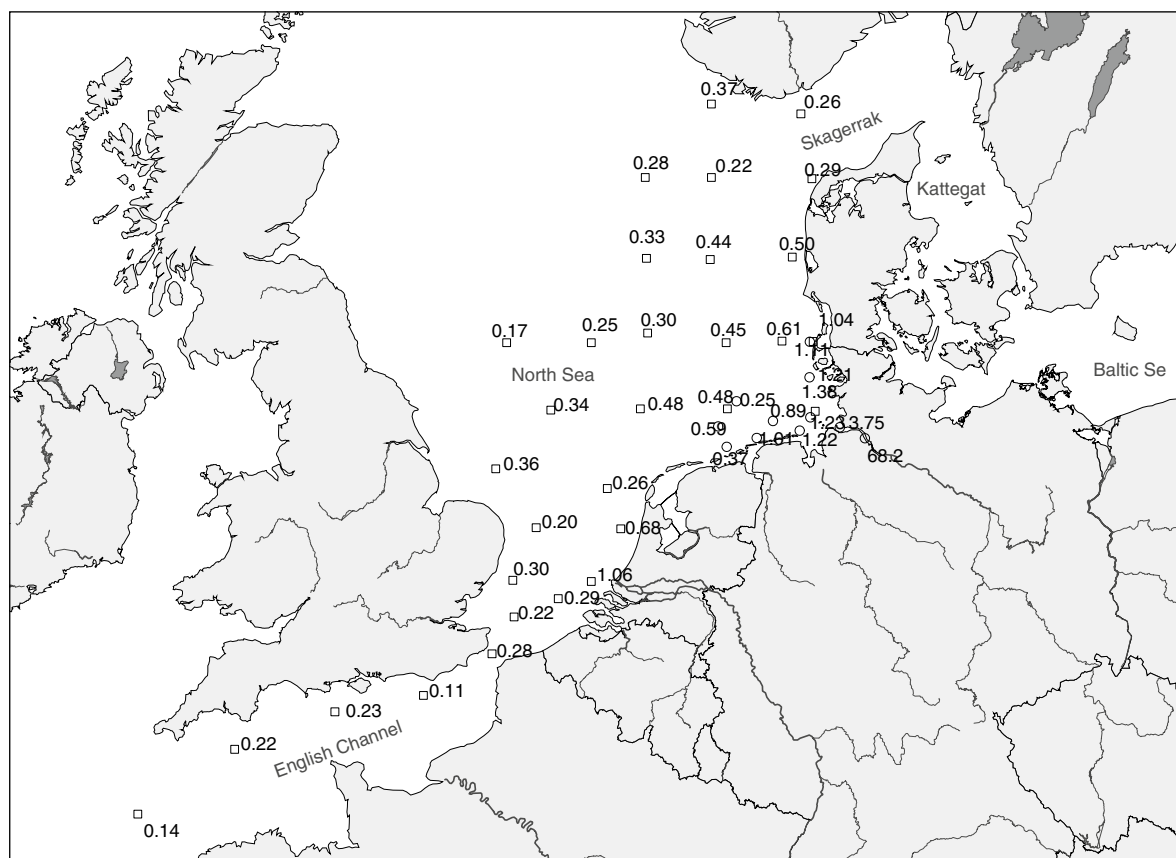


**Figure 15.1** Distribution of iodide and iodate in the surface water of the North Sea. The ratios of iodide/iodate in the surface water collected from the North Sea in 2005 are mapped; a high iodide concentration was seen in the coastal area, especially in the German Bight.

this method, iodide and iodate are separated by an anion exchange column. Due to different affinities, iodate passes through the column, while iodide is strongly adsorbed, which is then eluted from the column using a higher concentration of nitrate (2–2.5 mol/l). Organic iodine may not be absorbed on the column. After iodate is reduced to iodide, the water is passed through an anion exchange column; the inorganic iodine is absorbed onto the column, whereas the organic iodine remains in the effluent. The separated iodine is then detected using NAA or ICP-MS.

### Speciation analysis of volatile organic iodine

Volatile organic iodine compounds have been determined by gas chromatography (GC) with MS (Schall *et al.*, 1997). Figure 15.2 shows the schematic of the analytical procedure. Seawater (50–100 ml) is injected into the purging unit of sample treatment with a syringe, where it is degassed; the degassed substances are then transferred with helium into a cold trap, which is cooled with liquid nitrogen. After degassing, the trapped substances are transferred to the separation column by removing liquid nitrogen and heating the trap. The organic iodine compound is separated

using a capillary column in GC and heating the trap at different temperatures, ranging from 40 to 240°C. The detection is performed with an electron capture detector (ECD) and/or ICP-MS; the ICP-MS is more sensitive for iodine than the ECD. The absolute detection limit for ICP-MS is 0.5 pg for iodinated volatile organic compounds. Figure 15.3 shows a chromatographic spectrum of iodinated and brominated volatile organic compounds measured by GC-ICPMS/ECD (Schwarz and Heumann, 2002).

### Speciation analysis of iodine in freshwater

The concentration of iodine in freshwater is normally much lower than that in seawater; however, in some particular regions, the groundwater may contain higher levels of iodine. The iodine in precipitation and river water is normally 0.5–5 ng/l, which is more than 10 times lower than that in seawater. The more sensitive ICP-MS and NAA are normally used for the speciation of iodine in freshwater (Reifenhauer and Heumann, 1990; Wuilloud *et al.*, 2003; Hou, 2004). Reifenhauer and Heumann (1990) developed a method by combining isotope dilution mass spectrometry

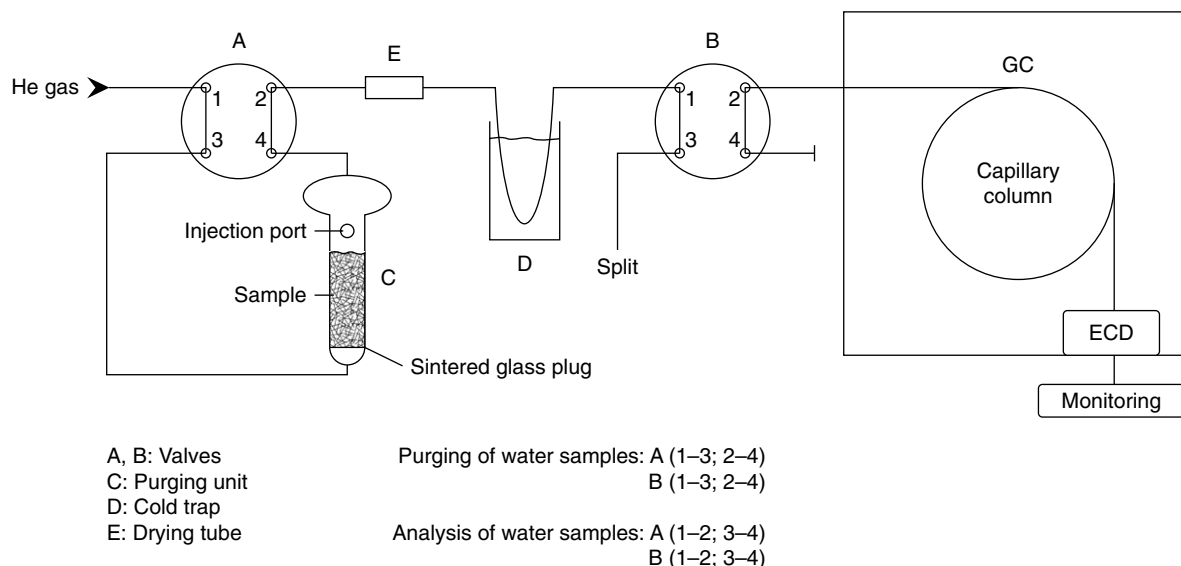


**Figure 15.2** A schematic of the analytical purge and trap – GC system for the determination of volatile organic iodine in seawater. Reproduced from Schall *et al.* (1997). The water sample is injected into column C with a syringe and then transferred with helium from valve A through column C and dry tube E and collected into a cold trap, D, which is cooled with liquid nitrogen. After degassing, the trapped substances are transferred to the separation column in a gas chromatography system by removing liquid nitrogen and heating the trap. The organic iodine compound is separated using a capillary column in a gas chromatograph and heating the trap at different temperatures from 40 to 240°C, and detected with an electron capture detector (ECD) and/or ICP-MS.

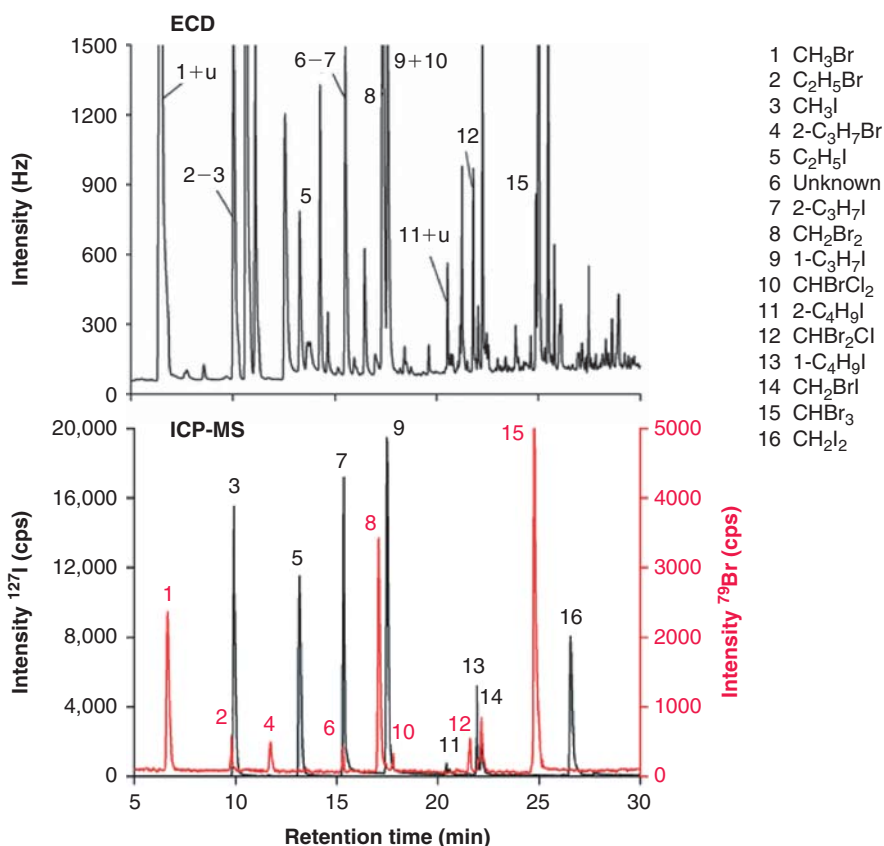


**Figure 15.3** Simultaneous ECD and ICP-MS chromatograms of a seawater sample for the determination of brominated and iodinated volatile organic compounds. Reproduced from Schwarz and Heumann (2002). The top figure shows the chromatograms of brominated and iodinated volatile organic compounds in seawater measured by ECD, the bottom figure shows the chromatogram measured by inductively coupled plasma mass spectrometry (ICP-MS).



(IDMS) with anion exchange separation to investigate the species of iodine in freshwater. Besides iodide and iodate, anionic organic iodine and nonelutable organic iodine were also determined. They observed that most iodine existed as organic iodine in lake and river water. Wuilloud *et al.* (2003) and Kannamkumarath *et al.* (2004) developed an analytical methodology using GC or capillary electrophoresis (CE) coupled to ICP-MS to analyze iodophenols, such as 2-iodophenol, 4-iodophenol, and 2,4,6-triiodophenol. Solid-phase microextraction (SPME) was used for preconcentration of the iodophenols from water samples; the concentrated substances were then desorbed from the GC injector at 290°C, or injected into a CE system for separation of different species of iodophenols. The separated species was then introduced to ICP-MS for quantitative detection of iodine. The method was applied for speciation analysis of iodophenols in river, tap and bottled water samples. Radlinger and Heumann (1997, 2000) developed a method for the separation of different fractions of humic substances (HS) by their molecular weight using size exclusion chromatography (SEC). The separated iodine in different species of HS was detected by online coupling of SEC with ICP-MS. The natural water and wastewater were analyzed. In the case of natural samples, iodide was exclusively fixed by HS fractions where natural HS/iodine species have also been observed in the original sample. In wastewater samples collected from sewage disposal plants, organoiodine compounds were also identified which were not affected by the transfer of iodide.

## Chemical Speciation of Iodine in Air

### Iodine species

The concentration of iodine in the atmosphere ranges from 0.2 to 10 ng/m<sup>3</sup>; a high iodine concentration is observed in urban areas due to combustion of oil and coal. In the atmosphere, iodine exists as particle-bound iodine (particulate iodine), inorganic gaseous iodine (I<sub>2</sub>, HI, HOI) and organic gaseous iodine (CHI<sub>3</sub>, CH<sub>2</sub>I<sub>2</sub>, CH<sub>3</sub>CH<sub>2</sub>CH<sub>2</sub>I); their concentrations vary with various parameters, such as location, season and climate (Noguchi and Murata, 1988; Gabler and Heumann, 1993; Yoshida and Muramatsu, 1995; Rahn *et al.*, 1976).

### Speciation analysis of iodine

A series filter was used to separate atmospheric particulate iodine, HI and I<sub>2</sub>, HOI and organic iodine. The particulate iodine is usually separated and collected using micropore filters or glass microfiber. The distribution of iodine in the different sizes of particulates is collected by a multi-stage cascade impactor. Wimschneider and Heumann (1995) used a six-stage slot cascade impactor to collect particulates

with an aerodynamic diameter of 7.2, 3.0, 1.5, 0.95, 0.45, and <0.45 μm. Iodine concentration in the collected particulates was measured by isotope dilution ICP-MS. The soluble species of iodine in the air particulates was investigated by leaching the particulates with water, and determination of iodide and iodate in the leachate. It was reported that iodide dominates the soluble iodine in the air particles (Baker, 2004; Baker *et al.*, 2001). I<sub>2</sub> and HI can be separated by adsorption using a LiOH (NaOH)-impregnated filter (Gabler and Heumann, 1993; Yoshida and Muramatsu, 1995) or silver screens (Noguchi and Murata, 1988). HOI is normally collected by tetrabutylammonium hydroxide (TBAH)-impregnated filter or charcoal filter, and organic iodine by a charcoal bed or triethylene diamine (TEDA)-impregnated charcoal bed (Noguchi and Murata, 1988; Gabler and Heumann, 1993; Yoshida and Muramatsu, 1995; Wershofen and Aumann, 1989). Figure 15.4 shows a diagram of a multi-stage sampler for iodine in air. The separated species of iodine were determined by NAA or ICP-MS.

### Speciation analysis of volatile iodine

GC combined with ICP-MS or ECD is quite often used for the determination of volatile organic iodine. A system similar to that used for seawater was used for the analysis of air samples (Schwarz and Heumann, 2002). Wevill and Carpenter (2004) reported a similar system for the speciation

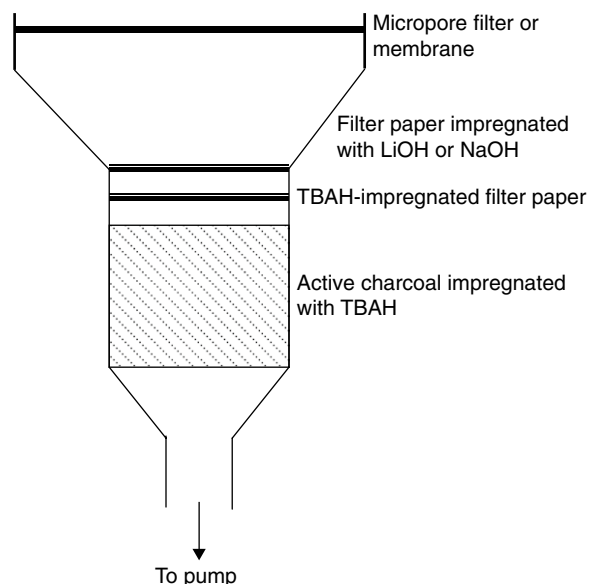


**Figure 15.4** A diagram of an air sampler for the collection of different species of iodine from air. The air is sucked by a pump through the system. The particle-associated iodine is collected in the first micropore filter; the gaseous elemental iodine I<sub>2</sub> and HI are absorbed in the second filter, made of cellulose and impregnated with LiOH or NaOH solution; the gaseous HOI is absorbed on the third filter, made of cellulose and impregnated with TBAH solution; and various volatile iodated organic compounds, such as CH<sub>3</sub>I and C<sub>2</sub>H<sub>5</sub>I, in the remaining gas are absorbed in an active charcoal column impregnated with TBAH.

analysis of volatile organic halocarbons, such as  $\text{CH}_3\text{I}$ ,  $\text{CHCl}_3$ ,  $\text{C}_2\text{H}_5\text{I}$ ,  $2\text{-C}_3\text{H}_7\text{I}$ ,  $\text{CH}_2\text{Br}_2$ ,  $\text{CH}_2\text{ClI}$ ,  $\text{CHBr}_2\text{Cl}$ ,  $1\text{-C}_3\text{H}_7\text{I}$ ,  $\text{CH}_2\text{BrI}$ ,  $\text{CHBr}_3$  and  $\text{CH}_2\text{I}_2$ . Detection limits were between 0.02 and 0.12 pptv (parts per trillion by volume).

The photolysis of volatile gaseous iodine could generate I, which would interact with atmospheric species such as  $\text{O}_3$ ,  $\text{H}_2\text{O}_2$ , and  $\text{NO}_x$  to produce IO, HOI,  $\text{ION}_2$  and  $\text{I}_2$ . Production and cycling back to I could cause catalytic removal of tropospheric  $\text{O}_3$ . A mixing ratio up to 6.6 ppt

has been measured at Mace Head, Ireland. Figure 15.5 shows a schematic of photochemical reaction of iodine species in the removal of ozone (Stutz *et al.*, 1999).

## Chemical Speciation of Iodine in Tissues and Biological Samples

### Species of iodine

Iodine is known to be utilized by the thyroid gland for biosynthesis of the thyroid hormones  $\text{T}_4$  and  $\text{T}_3$ . These hormones have an important influence on a wide of biochemical reactions. Besides  $\text{T}_3$  and  $\text{T}_4$ , iodine also exists as MIT, DIT,  $\text{T}_3$  and  $\text{rT}_3$ , which are mainly bound with proteins in thyroid, but also function as free  $\text{T}_3$  and  $\text{T}_4$ . Figure 15.6 shows the structure of iodinated hormones and their metabolism. Beside thyroid, iodine is also distributed in many other tissues (Hou *et al.*, 1997a).

### Speciation analysis of iodine in tissues

Radioimmunoassay methods are widely used for the determination of  $\text{T}_3$ ,  $\text{T}_4$  and  $\text{rT}_3$  in blood for diagnosis of thyroid diseases. Hou *et al.* (1999a) investigated the distribution of iodine in various subcellular fractions of human liver using gradient centrifugation coupled with NAA, and observed that iodine content is in the order of nuclei > cytosol > mitochondria > lysosome > microsome (Table 15.2). The proteins in the liver cytosol were fractionated by 2.0, 3.0 and 4.0 mol/l  $(\text{NH}_4)_2\text{SO}_4$  precipitation successively into four parts, including three precipitates and a supernatant. Each was dialyzed (MWCO = 8000–10 000) against distilled deionized water to remove the salt. They reported that most of the iodine bound to proteins mainly in the 4.0 mol/l  $(\text{NH}_4)_2\text{SO}_4$  precipitate; only a small part existed as inorganic ions or small molecular bound states. They further

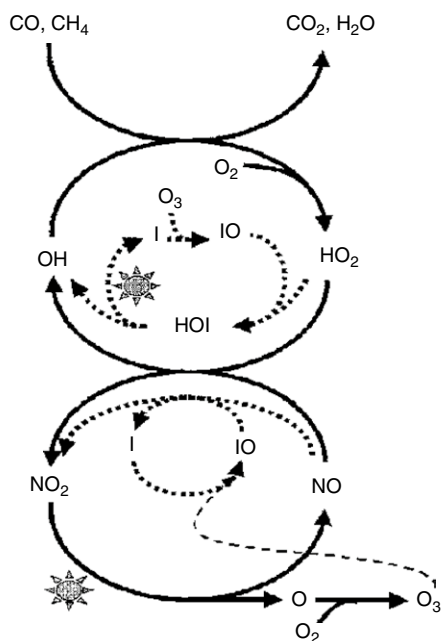


**Figure 15.5** A schematic of the photochemical reaction process of iodine species in the production and removal of ozone. The figure shows the reaction process of iodine species in the removal of  $\text{O}_3$ :  $\text{O}_3 + \text{I} = \text{IO} + \text{O}_2$ ;  $\text{HO}_2 + \text{HO}_2 + \text{IO} = \text{HOI} + \text{O}_2$ ;  $\text{HOI} + h\nu = \text{OH} + \text{I}$ ;  $\text{IO} + \text{NO} = \text{I} + \text{NO}_2$ .

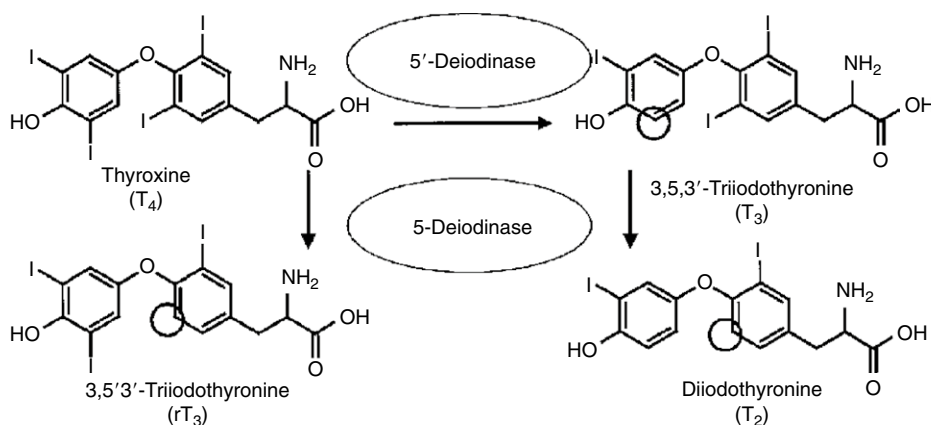


**Figure 15.6** Structure of iodinated hormones and their metabolism process. Thyroxine ( $\text{T}_4$ ) synthesized in the thyroid was deiodinated in the blood and tissues by 5-deiodinase to 3,5',3'-triiodothyronine ( $\text{rT}_3$ ) and by 5'-deiodinase to 3,5,3'-triiodothyronine ( $\text{T}_3$ ), which is then further deiodinated by 5-deiodinase to diiodothyronine ( $\text{T}_2$ ).

**Table 15.2** Distribution of iodine in subcellular fractions of human liver

Fraction	Weight percentage in total liver (%)	Iodine concentration ( $\mu\text{g/g}$ dry mass)		Percentage of iodine in total liver (%)
		Fraction	Protein	
Liver homogenization	–	0.321	4.472	–
Nuclei	26.0	0.932	6.413	48.0
Mitochondria	8.4	0.825	7.015	15.7
Lysosome	4.0	0.681	9.283	10.6
Microsome	3.3	0.171	1.471	1.0
Cytosol	58.3	0.135	1.120	17.7

Notes: The subcellular fractions of human liver were separated by ultracentrifuge. The second column shows the weight percentage of individual fractions in the entire liver sample. The third column shows the iodine concentration ( $\mu\text{g/g}$  dry mass) in different fractions as well as in the original liver homogenization. The fourth column shows iodine concentration in the proteins, which is calculated from the protein and iodine concentrations in the different fractions. The fifth column shows the percentage of iodine of the various fractions in the human liver sample.

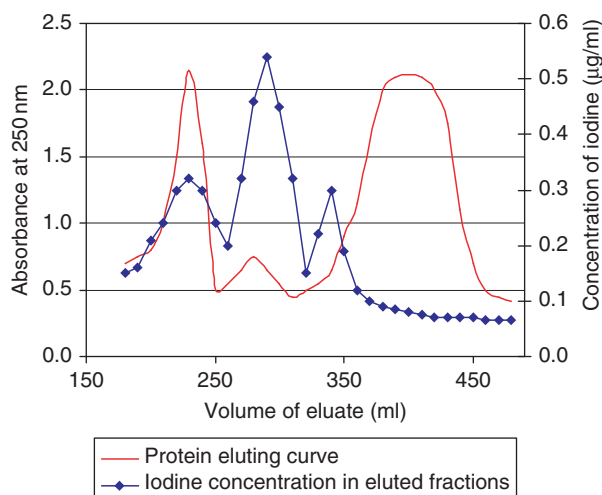


**Figure 15.7** Distribution of iodine-bound proteins in the cytosol of human liver. The protein in the cytosol of human liver was separated by gel chromatography (Sephadex G-2000); the protein was directly monitored by UV detector at 280 nm. The chromatogram of protein is shown in the protein elution curve; iodine-associated proteins are shown in the curve of the iodine in the eluted fraction.

investigated the iodine-bound proteins in the cytosol of human liver using gel chromatography and observed three iodine proteins, in which iodine is mainly bound with mid- and high-molecular-weight proteins (Figure 15.7).

#### Speciation analysis of iodine in hydrolyzed solution of tissues, urine and serum

Because most iodine is bound with macromolecular protein, the sample has to be enzymolyzed; then iodine ion and

various iodo-amino acids can be separated and measured for analysis of the concentrations of iodo-amino acids. High-performance liquid chromatography (HPLC) was successfully used to determine various chemical species of iodine, such as  $\text{I}^-$ , MIT, DIT,  $\text{T}_3$ ,  $\text{T}_4$ ,  $\text{rT}_3$  and iodo-polypeptide in hydrolyzed solution of thyroid, tissues, serum and urine (Meurizis *et al.*, 1982; Michalke *et al.*, 2000; Leiterer *et al.*, 2001; Takatera and Watanabe, 1993). Takatera and Watanabe (1993) used two similar RP-HPLC-ICP-MS methods to measure iodine species in thyroid gland protease digestion –  $\text{C}_{18}$   $3.5 \times 0.4$  cm CAPCELL column and a low MeOH concentration was used for the speciation analysis of small iodine species such as iodide, MIT and DIT, whereas a high MeOH concentration was used for speciating  $\text{rT}_3$ ,  $\text{T}_3$  and  $\text{T}_4$ . Michalke *et al.* (2000) modified this method to analyze six iodine species in a single run. The method was applied to urine and “normal” or pathological serum. In urine, predominantly iodide was seen. In human serum the six iodine species were seen in a range:  $10 \mu\text{g/l}$  for iodide;  $\sim 1.5 \mu\text{g/l}$ , MIT and DIT;  $3 \mu\text{g/l}$ ,  $\text{rT}_3$ ;  $5 \mu\text{g/l}$ ,  $\text{T}_3$ ; and  $45 \mu\text{g/l}$ ,  $\text{T}_4$ . However, the pathological serum was different.  $\text{T}_4$  was drastically reduced and  $\text{T}_3$  was almost totally lacking, which was considered a severe health risk. In contrast,  $\text{rT}_3$  was found in great excess.

Michalke and Schramel (1999) reported a method of CE coupled to ICP-MS for the speciation analysis of iodine. A buffer comprising phosphate (pH 2.3), NaOH, sodium dodecyl sulfate (SDS) and borate (pH 8.3) for stacking was employed for the separation of iodide, iodate,  $\text{T}_4$  and  $\text{T}_3$ . The separated four iodine species were subsequently detected during a pressure-driven detection step (baseline-separated) at 19.5, 29.1, 36.6 and 42.2 s. The detection limits were determined at  $0.08 \mu\text{g I/l}$  (iodide),  $0.3 \mu\text{g I/l}$  (iodate),  $3.5 \mu\text{g I/l}$  ( $\text{T}_4$ ) and  $2.5 \mu\text{g I/l}$  ( $\text{T}_3$ ). This method has been applied for iodine speciation in human serum and urine. The serum from a healthy person contained iodide ( $13 \mu\text{g I/l}$ ),  $\text{T}_4$  ( $61 \mu\text{g I/l}$ ) and  $\text{T}_3$  ( $7.5 \mu\text{g I/l}$ ), whereas the serum from a thyroid-operated person lacked  $\text{T}_3$ .

Speciation analysis of iodine in human urine samples has also been carried out by ion chromatography (IC) combined with ICP-MS (Stark *et al.*, 1997). Because of the possible interconversion of the iodine species, depending on the pH value, different eluent–column combinations were used for acidic or alkaline sample solutions. Iodide, iodate and several unidentified, presumably organo-iodine species could be separated and detected.

#### Chemical Speciation of Iodine in Foodstuffs and Environmental Samples

The source of iodine for humans is mainly foodstuffs, as well as drinking water. The investigation on speciation of iodine in foodstuffs mainly focused on milk and

seafood (seaweed and fish), because of the importance of milk iodine to humans, especially to infants, and the high concentration of iodine in these types of foodstuffs. In addition, lack of iodine supplementation to newborns can result in slow brain development, leading to severe damage to the central nervous system (Brätter *et al.*, 2000). It is therefore supposed that an iodine transporter and a peroxidase enzyme are involved in iodine accumulation in mammary glands. These facts make iodine speciation an important factor in human milk. Further, the bioavailability of various species of iodine may be quite different, especially for iodine-bound macromolecules. Investigation on speciation in different types of milk and formula, and other kinds of food, becomes important to accurately estimate the status of iodine nutrition.

### Speciation analysis of iodine in milk

Brätter *et al.* (1998) developed an online method for the investigation of iodine species in human milk – SEC separation coupled with ICP-MS detection. They reported that 80% of iodine in human milk was present as iodide; besides iodide, another six high-molecular-weight iodine-containing molecules (5–300 kDa) were also observed. The total iodine in European breast milk samples was determined to be  $95 \pm 60 \mu\text{g/l}$ .

Michalke (2006) also investigated iodine species in breast milk. He reported that total iodine varied according to lactation state, beginning at 60 mg/l on the 2nd day (postpartum) reaching 100  $\mu\text{g/l}$  on the 3rd day, and decreasing to 80 mg/l (6th day) or 60 mg/l constantly from 9th to the 60th day. A prefractionation by centrifugation showed that iodine is associated with fat at approximately 30%, and 70% of the low-molecular-weight fraction. Speciation analysis of iodine in milk whey (pooled human milk) was carried out by SEC-ICP-MS and IC using a strong anion exchange column combined with ICP-MS. The SEC showed predominantly iodide with about 37  $\mu\text{g/l}$ , as well as two more iodine species with 1.5 and 1.0  $\mu\text{g/l}$  having retention times pointing to  $T_4$  and  $T_3$ . IC-ICP-MS results indicated iodide to be the major iodine species in human milk. Leiterer *et al.* (2001) also used an IC coupled with ICP-MS for the speciation of iodine in human milk. They also observed that iodide is the main iodine species in milk, but in a few samples it also has traces of iodate and several unidentified, presumably organoiodine, compounds.

Sanandez and Szpunar (1999) determined iodine species in milk and infant formulas using SEC-ICP-MS. Iodine species were quantitatively eluted with 30 mM Tris buffer within 40 minutes and detected by ICP MS with a detection limit of 1  $\mu\text{g/l}$  (as I). A systematic study of iodine speciation in milk samples of different animals (cow, goat), humans of different geographic origin (several European

countries) and in infant formulas from different manufacturers was carried out. Whey obtained after centrifugation of fresh milk or reconstituted milk powders contained more than 95% of the iodine initially present in milk in all the samples investigated, with the exception of the infant formulas in which only 15–50% of the total iodine was found in the milk whey. An addition of sodium dodecyl sulfonate (SDS) considerably improved the recovery of iodine from these samples into the milk whey. Iodine was found to be present principally as iodide in all the samples except infant formulas. In the latter, more than half of the iodine was bound to a high molecular weight (>1000 kDa) organic molecules.

### Speciation analysis of iodine in fish

Simon *et al.* (2002), using LC-ICP-MS, investigated iodine speciation in whole-body homogenates of adult male and female zebrafish (*Danio rerio*) and tadpoles of the African clawed frog (*Xenopus laevis*) at two different developmental stages (NF58 and 61) according to Nieuwkoop and Faber. A Capcell-C18 column and a mobile phase comprising Tris-HCl and methanol were used for chromatographic separation. Iodide, MIT, DIT,  $T_4$ ,  $T_3$  and  $rT_3$  were observed in these samples. In addition, another five species of iodine were also identified in the samples.

### Speciation analysis of iodine in seaweeds

Due to the high concentration of iodine in marine vegetation, the chemical species of iodine in plants is mainly focused on seaweed. Hou *et al.* (1997b, 2000) developed a method for the determination of various chemical species of iodine in seaweed, such as water-soluble iodine, soluble organic iodine, iodide, iodate and protein-, pigment-, polyphenol-, or polysaccharide-bound iodine. First the soluble iodine was separated from the seaweed by water leaching. Then, iodide in the leachate was separated by  $\text{BiI}_3$  precipitation, while iodate in the filtrate was reduced to iodide and precipitated. Organic iodine remained in solution. The separated fractions were then analyzed by NAA for iodine concentration. They reported that 9–99% of iodine in seaweed is water soluble. In addition, the percentage of water-soluble iodine is the highest in brown algae and lowest in green algae. In the water leachate of seaweed, iodine exists mainly as iodide, the percentage of organic iodine ranges from 5 to 40%, and the iodate is lower than 5% in all 30 species investigated. In biological macromolecules, iodine is mainly bound with proteins, polyphenol and pigments, but few is bound with polysaccharide. Tables 15.3 and 15.4 show the iodine speciation in *Sargassum kjellmanianum* (a brown seaweed).

Shah *et al.* (2005) also investigated iodine species in commercially available commonly consumed seaweed samples



**Table 15.3** Leaching rate of iodine with various solvents from *Sargassum kjellmanianum* and spinach

Solvent	<i>S. kjellmanianum</i>		Spinach	
	Concentration ( $\mu\text{g/g}$ )	Leaching rate (%)	Concentration ( $\mu\text{g/g}$ )	Leaching rate (%)
Whole sample	140.6 $\pm$ 7.6	–	0.196 $\pm$ 0.043	–
Water (20°C)	149.7 $\pm$ 8.2	39.7	0.310 $\pm$ 0.032	29.4
Water (99°C)	153.2 $\pm$ 5.8	40.0	–	–
Ethanol	121.6 $\pm$ 6.4	27.8	0.231 $\pm$ 0.028	43.9
Ether	129.5 $\pm$ 5.2	8.9	–	–
0.1 mol/l HCl	151.9 $\pm$ 9.2	39.2	0.334 $\pm$ 0.029	28.4
0.1 mol/l KOH	66.0 $\pm$ 3.2	93.3	0.177 $\pm$ 0.017	70.3

Notes: The seaweed *S. kjellmanianum* and spinach were leached with various solvents. After leaching, the remaining samples were dried and the iodine concentrations in the leached and the original samples were measured by neutron activation analysis. The values are shown in the second and fourth columns. Due to the loss of salt and some components of seaweed after leaching, the weight of leached seaweed is less than that of the original. The percentage (or ratio) of total iodine that remained in the leached seaweed to that in the original seaweed was calculated; the values are listed in the third and fifth columns.

**Table 15.4** Concentration of iodine in biological macromolecules in *S. kjellmanianum*

Sample	Fractions		Iodine	
	Weight (g), dry	Percentage (%)	Concentration ( $\mu\text{g/g}$ )	Percentage (%)
Whole algae	20.0	100	153.5 $\pm$ 2.4	100
Algin	3.05	14.3	1.86 $\pm$ 0.30	0.185
Fucoidan	0.25	1.17	6.10 $\pm$ 0.25	0.05
Protein	1.30	6.5	403.2 $\pm$ 7.4	65.5
Polyphenol	0.53	2.50	178.7 $\pm$ 3.6	3.09
Pigment	0.35	1.64	138.7 $\pm$ 1.7	1.57

Notes: The different components of seaweed *S. kjellmanianum* were separated using different processes. The second column shows the weight of different components, and the third column shows the weight percentage of different components in the entire sample. The fourth column shows the iodine concentration in the different components, and the fifth column shows the percentage of iodine component in the entire sample. It shows that the iodine is mainly associated with proteins, pigments and polyphenol.

using a multidimensional chromatographic approach coupled with ICP-MS. A similar profile of iodine species such as those observed by Hou *et al.* (1997b, 2000) was found in the analysis of the alkaline extract (0.1 mol/l NaOH) by SEC-ICP-MS, where iodine associated with both high-, as well as low-molecular-weight fractions in Wakame, while in case of Kombu, only low-molecular-weight iodine species were found. A likely association of iodine with protein, as well as polyphenolic species, was indicated in the case

of Wakame. Anion-exchange chromatography coupled to ICP-MS confirmed that the most predominant inorganic iodine species present in both types of seaweeds is iodide. Protein-bound iodinated species were hydrolyzed by enzymatic digestion using proteinase K. Analysis of the hydrolyzate using reversed-phase HPLC-ICP-MS revealed the presence of MIT and DIT in Wakame.

## Bioavailability and Toxicity of Iodine Species

It is known that iodide or iodate have a high bioavailability (> 95%) in humans and animals. However, iodine in the diet may combine with different components and exist as organic iodine, which may have a low uptake in the digestive tract. During the last decade the iodine supply in many countries has increased significantly, but there is still a high frequency of goiter. This may be related to the iodine bioavailability in foodstuffs (Hurrell, 1997).

### Bioavailability of iodine species

It was reported that the bioavailability of pure mineral iodine, such as potassium iodide, was 96.4% in normal humans, while that of pure organic iodine, such as moniodotyrosine, was 80%. A higher bioavailability of iodine in the seaweeds *Gracilaria verrucosa* and *Laminaria hyperborea* (80–99%) was also observed (Aquaron *et al.*, 2002). A similar high bioavailability of iodine in the diet was also reported by Jahreis *et al.* (2001). They investigated the uptake of iodine in 12 women and found that 89% of the iodine was excreted in the urine and 11% in the feces. However, Wahl *et al.* (1995) reported a very low uptake of iodine from a normal diet; they observed that only 16–18% of the alimentary iodine was excreted with the urine. This may indicate that the type of diet and the species of iodine in the foodstuff are very important with respect to the nutritional status of iodine. A relatively lower water (or acid) leaching rate of iodine (28–40%) from vegetables (spinach and green seaweed) was reported by Hou *et al.* (1997b) (Table 15.2).

### Toxicity of excessive intake of iodine

It has been known that excessive iodine intake results in goiter, hypothyroidism, or hyperthyroidism in humans (Institute of Medicine, 2001). The biological basis for iodine-induced hyperthyroidism (IIH) appears most often to be mutational events in thyroid cells that lead to autonomy of function. When the mass of cells with such an event becomes sufficient, and the iodine supply is increased, the subject may become thyrotoxic. These changes may occur in localized foci within the gland or

during the process of nodule formation. IIH may also occur with an increase in iodine intake in those whose hyperthyroidism (Graves' disease) is not expressed because of iodine deficiency. The risks of IIH are principally for the elderly who may have heart disease and those who live in regions where there is limited access to medical care (Stanbury *et al.*, 1998).

Acute toxicity of iodine to animals has resulted in death at levels of 200–500 mg/kg-day, while levels of iodine greater than 10 mg/day, due to the intake of iodine-containing drugs or as a result of accidental poisoning, were toxic to some humans (Backer and Hollowell (2000). Forty-eight individuals were reported to have adverse effects, including goiter, hypothyroidism and sensitivity reactions, from iodine levels less than or equal to 10 mg/day (IPCS, 1988). One study reported that long-term intakes greater than 18 mg/day increased the risk of goiter (Wolff, 1969), while others demonstrated that high iodine intake is associated with an increased risk of thyroid papillary cancer in humans (Franceschi, 1988; Lind *et al.*, 1998). The WHO has set a PMTDI for iodine of 1 mg/day, which was based on the observation that an iodine intake of 1 mg/day or less is probably safe for the majority of the population, but may cause adverse effects in some individuals, e.g., people with thyroid disorders or those that are particularly sensitive to iodine (IPCS, 1988).

### Toxicity of iodine species

The observation of toxicity of iodine mainly focused on the iodide or iodate, which is normally present in iodized salt, milk, water and leachate of foodstuffs. However, the toxicity of some other species of iodine may be much higher than that of iodide and iodate. For the prevention of iodine deficiency disorders, iodized oil was used as an injection or administered orally in many countries: iodized oil is normally produced by binding iodine atoms to the polyunsaturated fatty acid in the oil (Zimmermann *et al.*, 2000). After administration, it was supposed that iodine is released gradually as iodide to maintain a constant supply of iodine to the body. Experience in the past decades shows that the utilization of iodized oil is safe. However, acute poisoning of iodized oil to children who are orally administered was reported in China in 1998; this may be related to the species of iodine, which may be more toxic than iodide or iodate. Iodine has been used as an effective, simple, and cost-efficient means of water disinfection (Backer and Hollowell, 2000), in which the active disinfectant species are elemental iodine and hypiodous acid. Doses of iodine below 1 mg/l kill bacteria within minutes. Elemental iodine and hypiodous acid remain in the disinfected water, which may be toxic to humans.

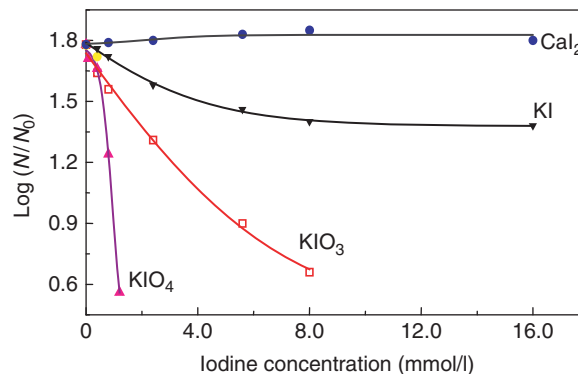


**Figure 15.8** The effect of iodine-containing compounds on the growth of *Tetrahymena pyriformis*. *T. pyriformis* is cultured in a solution of various iodine-containing compounds for 34 h. The growth of the cells in various solutions was shown as  $\log(N/N_0)$ , where  $N$  is the number of cells after 34 h culture and  $N_0$  is the number of cells at the beginning of the experiment. A high  $N/N_0$  indicates a lower toxicity of compound to the cells.

Laverock *et al.* (1995) have investigated the acute toxicity (96-h  $LC_{50}$ ) of aqueous stable iodine species (iodide, iodate and elemental iodine) to rainbow trout and *Daphnia magna*. They reported that rainbow trout was most sensitive to  $I_2$  ( $LC_{50}$  greater than or equal to 0.53 mg/l), and much less sensitive to  $IO_3^-$  ( $LC_{50}$  greater than or equal to 220 mg/l) or  $I^-$  ( $LC_{50}$  greater than or equal to 860 mg/l). *D. magna* was equally sensitive to  $I_2$  ( $LC_{50}$  greater than or equal to 0.16 mg/l) and  $I^-$  ( $LC_{50}$  greater than or equal to 0.17 mg/l), but less sensitive to  $IO_3^-$  ( $LC_{50}$  greater than or equal to 10.3 mg/l).

The author has investigated the biological toxicity of iodide, iodate, elemental iodine and periodate by exposing a single celled organism, *Tetrahymena pyriformis*, in various culture solutions with different concentrations and chemical species of iodine. He found that  $CaI_2$  slightly improves the growth of *T. pyriformis*, while other iodine-containing compounds inhibit its growth compared with the control group.  $KIO_4$  and  $I_2$  at high concentration seriously inhibit the growth of *T. pyriformis* in the initial stage; this inhibition was reduced in the later period because of the decomposition of  $KIO_4$  and  $I_2$ . Figure 15.8 compares the effect of iodine-containing compounds on the growth of *T. pyriformis*. It shows that the toxicity of five iodine compounds increases as follows:  $CaI_2 < KI < KIO_3 < I_2 < KIO_4$ .

### Summary Points

- In seawater, most iodine occurs as iodide and iodate, with minor amounts of organic iodine. In open and deep seawater (oxic) iodine mainly exists as iodate, while the iodide concentration is relatively higher in surface and coastal water.
- Titrimetry, colorimetry and differential pulse polarography methods are normally used for the determination of



iodate in seawater while cathodic stripping voltammetry is normally for iodide; the two species can also be separated by IC and determined by NAA or ICP-MS.

- In the air, iodine exists as particles associated, inorganic gaseous iodine ( $I_2$ , HIO) and organic iodine ( $CH_3I$ ,  $CH_2I_2$ , etc.). The different species of iodine in the air can be separated and collected in a series filter and then measured.
- The volatile iodine species in water and air are normally determined by GC combined with an ECD or ICP-MS.
- In the human and mammal body, iodine exists as thyroid hormones  $T_4$  and  $T_3$ , as well as MIT, DIT and  $rT_3$ , which are mainly bound with proteins in thyroid and other tissues.
- In milk and urine, most iodine occurs as iodide, but are some species of organic iodine also found. The iodine species in fish are similar to that in the human body.
- In seaweed, iodine species vary widely with the species of seaweed. In brown seaweed, most iodine exists as iodide; while in green seaweed, iodine is mainly bound to organic molecules, such as proteins and polyphenol.
- The most commonly used methods for speciation analysis of iodine in tissues and food are chromatographic techniques, such as anion exchange, size exclusion and reverse-phase chromatography, coupled with ICP-MS detection.
- Iodide and iodate have a low toxicity and high bioavailability, whereas the toxicity of elemental iodine and periodate is high. The bioavailability of organic iodine, especially iodine associated with macromolecules, is low.

## References

- Abdel-Moati, M.A.R. (1999). *Mar. Chem.* 65, 211–225.
- Anderson, G.W., Mariash, C.N. and Oppenheimer, J.H.O. (2000). The thyroid. In: (eds L.E. Braverman and R.D. Utiger), *A Fundamental and Clinic Text*. Lippincott, Philadelphia, PA, pp. 174–195.
- Anderson, K.A., Casey, B., Diaz, E., Markowski, P. and Wright, B. (1996). *J. AOAC. Int.* 79, 751–756.
- Aquaron, R., Delange, F., Marchal, P., Lognone, V. and Ninane, L. (2002). *Cell. Mol. Biol.* 48, 563–569.
- Backer, H. and Hollowell, J. (2000). *Environ. Health Perspect.* 108, 679–684.
- Baker, A.R. (2004). *Geophysical Research Letters* 31, Art. No. L23S02.
- Baker, A.R., Tunnicliffe, C. and Jickells, T.D. (2001). *J. Geophys. Res. Atmos.* 106, 28743–28749.
- Brandao, A.C.M., Buchberger, W.W., Bulter, E.C.V., Fagan, P.A. and Haddad, P.R. (1995). *J. Chromatogr. A* 706, 271–275.
- Brätter, P., Blasco, I.N., Negretti de Brätter, V.E. and Raab, A. (1998). *Analyst* 123, 821–826.
- Brätter, P., Blasco, I.N., Negretti de Brätter, V.E. and Raab, A. (2000). *Metal ions in Biology and Medicine*. John Libbey Eurotext, Montrouge, France, pp. 751–754.
- Campos, M.L.A.M., Nightingale, P.D. and Jickells, T.D. (1996). *Tellus* 48B, 106–114.
- Cook, P.L.M., Carpenter, P.D. and Butler, E.C.V. (2000). *Mar. Chem.* 69, 179–192.
- Franceschi, S. (1988). *Exp. Clin. Endocrinol. Diab.* 106, S38–S44.
- Gabler, H.E. and Heumann, K.G. (1993). *Fresenius J. Anal. Chem.* 345, 53–59.
- Gilfedder, B.S., Petri, M. and Biester, H. (2007). *J. Geophys. Res. Atmos.* 112, D07301.
- Herring, J.R. and Liss, P.S. (1974). *Deep-Sea Res.* 21, 777–783.
- Hou, X.L. (2004). *J. Radioanal. Nucl. Chem.* 262, 67–75.
- Hou, X.L., Aldahan, A., Nielsen, S.P., Possnert, G., Nies, H. and Hedfors, J. (2007). *Environ. Sci. Technol.* 41, 5993–5999.
- Hou, X.L., Chai, C.F., Qian, Q.F. and Li, C.S. (1997a). *Biol. Trace Elem. Res.* 56, 225–230.
- Hou, X.L., Chai, C.F., Qian, Q.F., Yan, X.J. and Fan, X. (1997b). *Sci. Total Environ.* 204, 215–221.
- Hou, X.L., Chen, C.Y., Ding, W.J. and Chai, C.F. (1999a). *Biol. Trace Elem. Res.* 69, 69–76.
- Hou, X.L., Dahlgard, H. and Nielsen, S.P. (2001). *Mar. Chem.* 74, 145–155.
- Hou, X.L., Dahlgard, H., Rietz, B., Jacobsen, U., Nielsen, S.P. and Aarkrog, A. (1999b). *Anal. Chem.* 71, 2745–2750.
- Hou, X.L., Fogh, C.L., Kucera, J., Andersson, K.G., Dahlgard, H. and Nielsen, S.P. (2003). *Sci. Total Environ.* 308, 97–109.
- Hou, X.L., Yan, X.J. and Chai, C.F. (2000). *J. Radioanal. Nucl. Chem.* 245, 461–467.
- Hurrell, R.F. (1997). *Eur. J. Clin. Nutr.* 51, S9–S12.
- Institute of Medicine. (2001). Dietary reference intakes for vitamin A, vitamin K, arsenic, boron, chromium, copper, iodine, iron, manganese, molybdenum, nickel, silicon, vanadium, and zinc. A Report of the Panel of Micronutrients, Subcommittees on Upper Reference Levels of Nutrients and of Interpretation and Uses of Dietary Reference Intakes and the Standing Committee on the Scientific Evaluation of Dietary Reference Intakes. National Academy Press, Washington, DC.
- IPCS International Programme on Chemical Safety. (1988). The 33rd Meeting of the Joint FAO/WHO Expert Committee on Food Additives, 1988. Toxicological Evaluation of Certain Food Additives and Contaminants. WHO Food Additive Series: 24.
- Jahreis, G., Hausmann, W., Kiessling, G., Franke, K. and Leitner, M. (2001). *Exp. Clin. Endocrinol. Diab.* 109, 163–167.
- Jones, S.D. and Truesdale, V.W. (1984). *Limnol. Oceanogr.* 29, 1016–1028.
- Kannamkumath, S.S., Wuilloud, R.G. and Jayasinghe, S. (2004). *Electrophoresis* 25, 1843–1851.
- Laverock, N.J., Stephenson, M. and Macdonald, C.R. (1995). *Arch. Environ. Contam. Toxicol.* 29, 344–350.
- Leitner, M., Truckenbrodt, D. and Franke, K. (2001). *Eur. Food Res. Technol.* 213, 150–153.
- Lind, P., Langsteger, W., Molnar, M., Gallowitsch, H.J., Mikosch, P. and Gomez, I. (1998). *Thyroid* 8, 1179–1183.

- Luther, G.W., III and Camobell, T. (1991). *Deep-Sea Res. Part A* 38, S875–S882.
- Luther, G.W., III, Ferdelman, T., Culberson, C.H., Kostka, J. and Wu, J.F. (1991). *Estuarine Coastal Shelf Sci.* 32, 267–279.
- Meurizis, J.C., Nicles, C. and Michelet, J. (1982). *J. Chromatogr.* 150, 129–135.
- Michalke, B. (2006). *Pure Appl. Chem.* 78, 79–90.
- Michalke, B. and Schramel, P. (1999). *Electrophoresis* 20, 2547–2553.
- Michalke, B., Schramel, P. and Witte, H. (2000). *Biol. Trace Elem. Res.* 78, 81–91.
- Moore, R.M. and Graszko, W. (1999). *J. Geophys. Res.* 104, 11163–11171.
- Noguchi, H. and Murata, M. (1988). *J. Environ. Radiat.* 7, 65–74.
- Radlinger, G. and Heumann, K.G. (1997). *Fresenius J. Anal. Chem.* 359, 430–433.
- Radlinger, G. and Heumann, K.G. (2000). *Environ. Sci. Technol.* 34, 3932–3936.
- Rahn, K.A., Borys, R.D. and Duce, R.A. (1976). *Science* 192, 549–550.
- Rasmussen, L.B., Larsen, E.H. and Ovesen, L. (2000). *Eur. J. Clin. Nutr.* 54, 57–60.
- Reifenhauser, C. and Heumann, K.G. (1990). *Fresenius J. Anal. Chem.* 336, 559–563.
- Sanandez, L.F. and Szpunar, J. (1999). *J. Anal. At. Spectrom.* 14, 1697–1702.
- Schall, C., Heumann, K.G. and Kirst, G.O. (1997). *Fresenius J. Anal. Chem.* 336, 559–563.
- Schwarz, A. and Heumann, K.G. (2002). *Anal. Bioanal. Chem.* 374, 212–219.
- Schwehr, K.A. and Santschi, P.H. (2003). *Anal. Chim. Acta* 482, 59–71.
- Shah, M., Wuilloud, R.G., Kannamkumaratha, S.S. and Caruso, J.A. (2005). *J. Anal. At. Spectrom.* 20, 176–182.
- Simon, R., Tietge, J.E., Michalke, B., Degitz, S. and Schramm, K.W. (2002). *Anal. Bioanal. Chem.* 372, 481–485.
- Solomon, S., Garcia, S.R. and Ravishankara, A.R. (1994). *J. Geophys. Res.* 99, 20491–20499.
- Stanbury, J.B., Ermans, A.E., Bourdoux, P., Todd, C., Oken, E., Tonglet, R., Vidor, G., Vidor, G., Braverman, L.E. and Medeiros-Neto, G. (1998). *Thyroid* 8, 83–100.
- Stark, H.J., Mattusch, J., Wennrich, R. and Mrocek, A. (1997). *Fresenius J. Anal. Chem.* 359, 371–374.
- Stipanicev, V. and Branica, M. (1996). *Sci. Total Environ.* 182, 1–9.
- Stutz, J., Hebestreit, K., Alicke, B. and Platt, U. (1999). *J. Atmos. Chem.* 34, 65–85.
- Takatera, K. and Watanabe, T. (1993). *Anal. Chem.* 65, 759–762.
- Tian, R.C. and Nicolas, E. (1995). *Mar. Chem.* 48, 151–156.
- Truesdale, V.W. and Jones, S.D. (1996). *J. Hydrol.* 179, 67–86.
- Truesdale, V.W., Nausch, G. and Baker, A. (2001). *Mar. Chem.* 74, 87–98.
- Wahl, R., Pilz-Mittenburg, K.W., Heer, W. and Kallee, E. (1995). *Z. Ernährungswiss.* 34, 269–276.
- Wershofen, H. and Aumann, D.C. (1989). *J. Environ. Radioact.* 10, 141–156.
- Wevill, D.J. and Carpenter, L.J. (2004). *Analyst* 129, 634–638.
- Wimschneider, A. and Heumann, K.G. (1995). *Fresenius J. Anal. Chem.* 353, 191–196.
- Windisch, W. (2002). *Anal. Bioanal. Chem.* 372, 421–425.
- Wolff, J. (1969). *Am. J. Med.* 47, 101–124.
- Wong, G.T.F. (1991). *Rev. Aquat. Sci.* 4, 45–73.
- Wong, G.T.F. and Cheng, X.H. (1998). *Mar. Chem.* 59, 271–281.
- Wuilloud, R.G., de Wuilloud, J.C.A., Vonderheide, A.P. and Caruso, J.A. (2003). *J. Anal. At. Spectrom.* 18, 1119–1124.
- Yoshida, S. and Muramatsu, Y. (1995). *J. Radioanal. Nucl. Chem. Art.* 196, 295–302.
- Zimmermann, M., Adou, P., Torresani, T., Zeder, C. and Hurrell, R. (2000). *Br. J. Nutr.* 84, 139–141.

## Article

## Modeling Fallout of Anthropogenic I

Edvard Englund, Ala Aldahan, Go#ran Possnert, Eeva  
Haltia-Hovi, Xiaolin Hou, Ingmar Renberg, and Timo Saarinen

*Environ. Sci. Technol.*, **2008**, 42 (24), 9225-9230 • DOI: 10.1021/es8009953 • Publication Date (Web): 18 November 2008

Downloaded from <http://pubs.acs.org> on March 11, 2009

### More About This Article

Additional resources and features associated with this article are available within the HTML version:

- Supporting Information
- Access to high resolution figures
- Links to articles and content related to this article
- Copyright permission to reproduce figures and/or text from this article

[View the Full Text HTML](#)

# Modeling Fallout of Anthropogenic $^{129}\text{I}$

EDVARD ENGLUND,<sup>\*,†</sup> ALA ALDAHAN,<sup>‡</sup>  
GÖRAN POSSNERT,<sup>†</sup> EEEVA HALTIA-HOVI,<sup>§</sup>  
XIAOLIN HOU,<sup>¶</sup> INGMAR RENBERG,<sup>||</sup> AND  
TIMO SAARINEN<sup>§</sup>

Tandem Laboratory, Uppsala University, Box 529, SE-751 20 Uppsala, Sweden; Department of Earth Sciences, Uppsala University, Villav. 16, SE-752 36 Uppsala, Sweden; Department of Quaternary Geology, 20014 University of Turku, Finland; Risø National Laboratory for Sustainable Energy, NUK-202, Technical University of Denmark, DK-4000 Roskilde, Denmark; and Environmental Assessment Group, Department of Ecology and Environmental Science, Umeå University, SE-901 87 Umeå, Sweden

Received April 10, 2008. Revised manuscript received September 5, 2008. Accepted September 9, 2008.

Despite the relatively well-recognized emission rates of the anthropogenic  $^{129}\text{I}$ , there is little knowledge about the temporal fallout patterns and magnitude of fluxes since the start of the atomic era at the early 1940s. We here present measurements of annual  $^{129}\text{I}$  concentrations in sediment archives from Sweden and Finland covering the period 1942–2006. The results revealed impression of  $^{129}\text{I}$  emissions from the nuclear reprocessing facility at Sellafield and La Hague and a clear Chernobyl fallout enhancement during 1986. In order to estimate relative contributions from the different sources, a numerical model approach was used taking into account the emission rates/estimated fallout, transport pathways, and the sediment system. The model outcomes suggest a relatively dominating marine source of  $^{129}\text{I}$  to north Europe compared to direct gaseous releases. A transfer rate of  $^{129}\text{I}$  from sea to atmosphere is derived for pertinent sea areas (English Channel, Irish Sea, and North Sea), which is estimated at 0.04 to 0.21  $\text{y}^{-1}$ .

## Introduction

The amount of naturally produced radioactive  $^{129}\text{I}$  ( $t_{1/2} = 15.7$  Myr) is presently overwhelmed by anthropogenic emissions of the isotope. Environmental hazards of the isotope are not clearly foreseeable, which imply that further evaluation is indispensable until a comprehensive assessment of the situation is established. Studies of  $^{129}\text{I}$  distribution in fresh and marine water and sediment of north Europe have revealed that the isotope is enriched by several orders of magnitude in comparison to the natural concentrations (1–8). Among the many anthropogenic  $^{129}\text{I}$  sources, emissions from the nuclear reprocessing facilities located at Sellafield (UK) and La Hague (France) are pointed out as the main ones. Emissions from these facilities started in 1952 (Sellafield) and 1966 (La Hague) and are still going on ((9), and

references therein). Additionally, two other facilities located in central Europe, at Karlsruhe in Germany (operated during 1970–1989) and at Marcoule in France (operated during 1959–1997), have released  $^{129}\text{I}$ . Gaseous emission from the Marcoule facility was as much or even higher than that from the Sellafield and La Hague, whereas emission from the Karlsruhe facility is considered negligible (10). Besides emission from the European facilities, there is a possibility that north Europe may have received an unquantified amount of  $^{129}\text{I}$  from the reprocessing facilities in Russia, particularly the Mayak (11).

Apart from the reprocessing facilities, the above-ground nuclear weapon tests that culminated during the early 1960s were also a source of radioactive  $^{129}\text{I}$ , but the contribution was insignificant compared to the emissions from the nuclear reprocessing facilities (9). Furthermore, large parts of Europe including Sweden were affected by fallout from the Chernobyl accident in 1986 (12). Although the total release of  $^{129}\text{I}$  from the Chernobyl accident was small in comparison to that from the reprocessing facilities, the fallout was strongly localized in time and space. The distribution pattern of the Chernobyl  $^{137}\text{Cs}$  fallout has been shown to vary by more than 100 times between low and high radioactively contaminated areas in Scandinavia. In comparison to the above-mentioned sources of  $^{129}\text{I}$ , emissions from conventional nuclear reactors seem to be negligible (13, 14).

Despite increasing concentrations of  $^{129}\text{I}$  in the environment, which today are up to  $10^6$  times the prenuclear values in north Europe, there is a limited number of published records about the temporal distribution of the isotope (6, 8). Here we present new results on  $^{129}\text{I}$  distribution in sediment archives from Sweden and Finland covering the period between 1942 and 2006 (Figure 1). The data from these archives together with that from Englund et al. (8) provided proxy information for  $^{129}\text{I}$  deposition from the atmosphere of north Europe over a period of 60 years. The proxy data were further utilized to numerically model the relative temporal variability of the  $^{129}\text{I}$  anthropogenic fallout over north Europe.

## Sampling and Analytical Techniques

The sediment archives used in this study were collected from two sampling sites (lakes) that were chosen for their

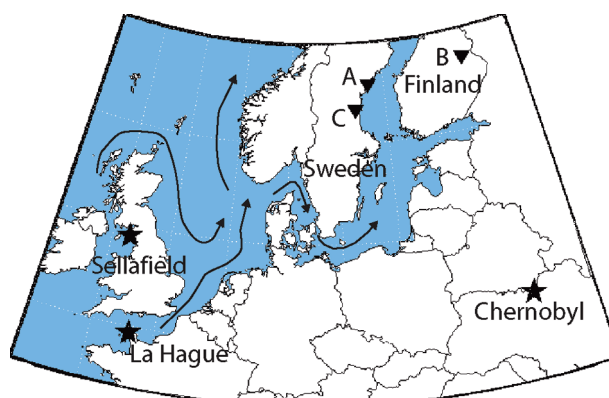


**FIGURE 1.** Location of the sampling sites: (A) Lake Nylandssjön, (B) Lake Lehmilampi, and (C) the additional modeled archive of Englund et al. (8) at Lake Loppesjön. The arrows indicate the general circulation pattern in the North Sea; see, e.g., Otto et al. (33). The main sources of  $^{129}\text{I}$  to the sampling sites are shown as stars, i.e., the nuclear fuel reprocessing facilities in Sellafield and La Hague, and the Chernobyl nuclear plant.

\* Corresponding author fax: +46-18-555736; phone: +46-18-4713899; e-mail: edvard.englund@angstrom.uu.se.

<sup>†</sup> Tandem Laboratory, Uppsala University.

<sup>‡</sup> Department of Earth Sciences, Uppsala University.

<sup>§</sup> University of Turku.

<sup>¶</sup> National Laboratory for Sustainable Energy, Denmark.

<sup>||</sup> Umeå University.

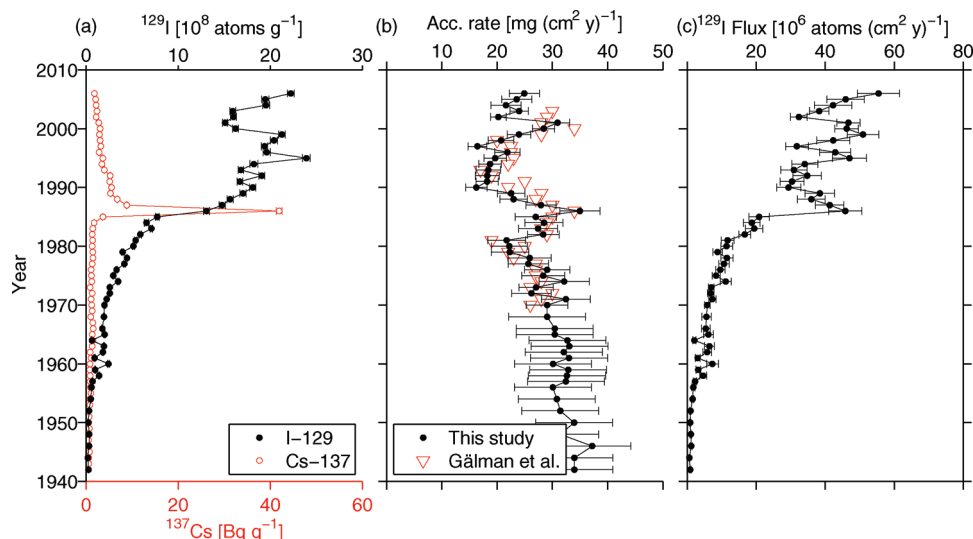


**FIGURE 2.** Sediment profiles for Lake Nylandssjön concentrations: (a)  $^{129}\text{I}$  and  $^{137}\text{Cs}$  concentrations ( $^{137}\text{Cs}$  is decay corrected to 1986), (b) dry mass accumulation rate, and (c)  $^{129}\text{I}$  flux in sediment as concentration ( $\theta$ )  $\times$  accumulation rate( $\theta$ ); the error margins include both accumulation and  $^{129}\text{I}$  concentration variability. Tabulated values are provided in the Supporting Information (Table S1).

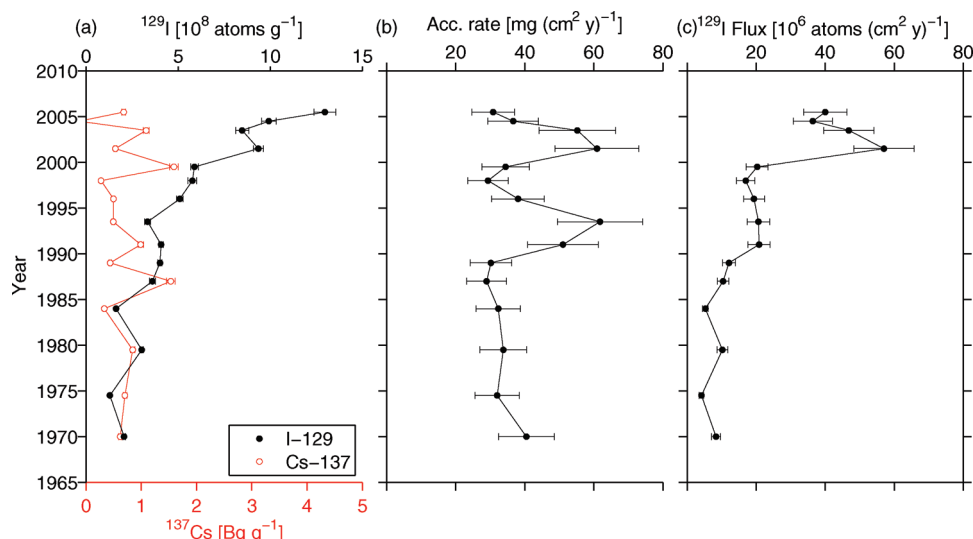


**FIGURE 3.** Sediment profiles for Lake Lehmilampi: (a)  $^{129}\text{I}$  and  $^{137}\text{Cs}$  concentrations, (b) dry mass accumulation rate, and (c)  $^{129}\text{I}$  flux in sediment. Measurements at the lower part are performed on merged samples of up to 5 years. Tabulated values are provided in the Supporting Information (Table S2).

undisturbed varved chronology and marked 32 kBq  $\text{m}^{-2}$  differences in  $^{137}\text{Cs}$  Chernobyl fallout (Figures 2 and 3). Considerably higher  $^{137}\text{Cs}$  fallout was received at Lake Nylandssjön (12) as opposed to the negligible fallout of  $\sim 0.5$  kBq  $\text{m}^{-2}$  at Lake Lehmilampi (15). Details of each sampling site are presented in Table 1. Both sites have been targeted for many years for the high-resolution varve chronology and environmental and paleoclimatic investigations (16–19). The sediment cores used in this study were collected in winters of 2006 and 2007 with a crust-freeze sampler. Subsamples (sediment varves) were sliced in a freeze room and subsequently freeze-dried. The varves were typically 3–4 mm thick in Lake Nylandssjön and 1–4 mm in Lake Lehmilampi.

In order to clearly mark the Chernobyl fallout peak during 1986, the  $^{137}\text{Cs}$  was measured on dried portions of the samples using  $\gamma$ -spectroscopy (error  $< 5\%$ ), and the results obtained were normalized to sample sizes and decay corrected to 1986. A  $^{129}\text{I}$  profile was measured at annual to biannual resolution in sediments from Lake Nylandssjön, whereas the  $^{129}\text{I}$  profile in Lake Lehmilampi was measured with somewhat coarser resolution. The extraction of  $^{129}\text{I}$  was performed by combustion of 100–400 mg of dry material mixed with a known

amount of iodine carrier ( $^{127}\text{I}$ , 1–2 mg) in a stream of oxygen, according to the procedure described in (20). Measurement of  $^{129}\text{I}/^{127}\text{I}$  was carried out at the Uppsala accelerator mass spectrometry facility. Procedural blank values of  $(2\text{--}3) \times 10^{-13}$  in  $^{129}\text{I}/^{127}\text{I}$  were at least 3 times lower than the ratio in the samples of  $10^{-12}$  to  $10^{-10}$ . Total iodine (referring to  $^{127}\text{I}$ ) was measured in 10 samples from Nylandssjön using ICP-MS after extraction by combustion at the Risø National Laboratory for Sustainable Energy (Denmark) (21). Total organic carbon was determined in sediment cores from Lake Nylandssjön taken between 1979 and 2007 using a Perkin-Elmer 2400-CHNS/O elemental analyzer, operated in CHN mode (includes combustion at 950  $^{\circ}\text{C}$ , knowing that calcium carbonate content is negligible in Lake Nylandssjön). Analytical quality was verified against certified standard material (LKSD-4 from National Resources Canada, lake sediment sample CCRMP from CANMET Mining and Mineral Sciences) and internal standards with replicate within 0.8%.

## Results and Interpretations

The  $^{137}\text{Cs}$  profile of sediments from Lake Nylandssjön exhibits a sharp activity peak in 1986, obviously associated with the

**TABLE 1. Lake Parameters,  $^{129}\text{I}$  Inventories and Concentrations<sup>a</sup>**

	Lake Nylandssjön	Lake Lehmilampi	Lake Loppesjön
coordinates	62°57' N, 18°17' E	63°37' N, 29°6' E	61°42' N, 16°48' E
precipitation (mm)	800	700	500
lake area (km <sup>2</sup> )	0.28	0.15	0.28
drainage area (km <sup>2</sup> )	0.95	~1	4.1
max depth (m)	17.5	11.6	14
above sea level (m)	34	150	97
time interval	1942–2006	1968–2005	1920–2003
total $^{129}\text{I}$ inventory (atoms cm <sup>-2</sup> )	$11 \times 10^8$	$6.8 \times 10^8$	$14 \times 10^8$
range of $^{129}\text{I}$ conc. (atoms g <sup>-1</sup> )	$(1.9 - 240) \times 10^7$	$(13 - 130) \times 10^7$	$(1.0 - 210) \times 10^7$
$^{129}\text{I}$ inventory down to 1968 (atoms cm <sup>-2</sup> )	$10 \times 10^8$	$6.8 \times 10^8$	$13 \times 10^8$
average $^{129}\text{I}$ conc. down to 1968 (atoms g <sup>-1</sup> )	$12 \times 10^8$	$4.1 \times 10^8$	$7.7 \times 10^8$
Chernobyl derived fallout (atoms cm <sup>-2</sup> )	$1.1 \times 10^8$	$<0.5 \times 10^8$	$3.0 \times 10^8$

<sup>a</sup> Chernobyl derived fallout is calculated on basis of the model output.

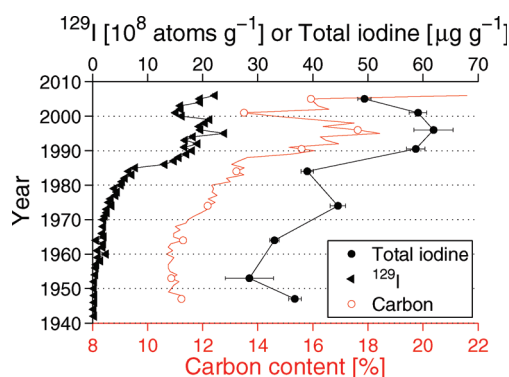


**FIGURE 4. Sediment profiles of total iodine,  $^{129}\text{I}$ , and carbon content in Lake Nylandssjön. The dots in the carbon curve mark the years of which total iodine are measured, the measurement uncertainties of carbon are within 0.8%. Tabulated values are provided in the Supporting Information (Table S1).**

fallout from the Chernobyl accident (Figure 2). As explained earlier in the text, the impact of Chernobyl in the region of Lake Lehmilampi was small which is also clearly reflected in the  $^{137}\text{Cs}$  profile of the sediment that shows reduced activity and no clear enhancement at year 1986 (Figure 3). The effect of Chernobyl fallout is apparently also identifiable in the  $^{129}\text{I}$  profile of the Swedish lake (Lake Nylandssjön) as shown by a sharp gradient at 1986. Unlike the  $^{137}\text{Cs}$  profile, the  $^{129}\text{I}$  profile remains at a high level after the Chernobyl accident, which is related to (1) input from the reprocessing facilities and (2) possibly delayed deposition from the lake and drainage area as well as postdepositional processes.

Dry mass accumulation rate varies between 15 and 40 mg (cm<sup>2</sup> y)<sup>-1</sup> in Lake Nylandssjön and between 20 and 60 mg (cm<sup>2</sup> y)<sup>-1</sup> in Lake Lehmilampi (details of calculating mass accumulation rates are given in the Supporting Information). The mass accumulation rates were used to estimate  $^{129}\text{I}$  fluxes in the sediment which seem to be rather comparable in both sites in the general range of  $(5-60) \times 10^6$  atoms (cm<sup>2</sup> y)<sup>-1</sup> for the period 1968–2006 (Figures 2 and 3).

Total iodine content in Lake Nylandssjön,  $\sim 30-60 \mu\text{g g}^{-1}$  (Figure 4), is relatively high in comparison with available data from soil (22). This feature may relate to incorporation of more iodine in the soils due to the fact that the region of the lake was under the Baltic Sea 5000 years ago (23). Additional sources of iodine can be the relatively high content of organic material and the proximity to the coast,  $\sim 4$  km, which imply addition of sea spray. The atomic ratios  $^{129}\text{I}/^{127}\text{I}$  in the top part of the sediment,  $\sim 1 \times 10^{-8}$ , is about the same as ratios in the Baltic Sea (from ref 5 together with the average iodine concentration in the brackish surface water of  $\sim 10 \mu\text{g}$

kg<sup>-1</sup>), but more than 10 times lower than average ratios in precipitation in north Sweden,  $2.5 \times 10^{-7}$  (24). This somewhat low  $^{129}\text{I}/^{127}\text{I}$  is in accordance with the high iodine content in the sediments and dilution effects by the relatively recent addition of  $^{129}\text{I}$  into an existing budget of  $^{127}\text{I}$  in soil and biota. The total organic carbon content at the top of sediment, 22% by weight (Figure 4), is at the upper bound of the concentration interval given for 32 Swedish lakes (25).

**Model Description and Outcome.** The  $^{129}\text{I}$  distribution patterns in the sediment archive of Lake Nylandssjön and Lake Lehmilampi (this study) and Lake Loppesjön (8) were used to numerically model deposition of  $^{129}\text{I}$  in the studied regions. Modeling of  $^{129}\text{I}$  fallout was accomplished by taking into account relative influence from emission rates, possible transport pathways, and the influences of the lake system (drainage and depositional effects). Major sources of emission were considered to be the following: (1) liquid and gaseous releases from the reprocessing facilities in Sellafield and La Hague (Figure S1 in the Supporting Information); the two facilities are here regarded as a single source, although different modes of release form (gaseous or liquid) are addressed; (2) fallout from the Chernobyl accident in 1986; and (3) fallout from the nuclear weapon tests during the late 1950s and early 1960s. Details of the modeling approach are explained in the Supporting Information.

Modeled and measured  $^{129}\text{I}$  deposition into the sediment archives at the three considered sites (Table 1) are shown in Figure 5. Among all sampling sites, the contribution from liquid emissions is predicted to be the dominating source of  $^{129}\text{I}$  in the sediments, varying between 50% and 71% of the total inventories (Table 2). By means of the model parameters, a transfer rate  $k$  of  $^{129}\text{I}$  from ocean to atmosphere range is estimated (in Supporting Information) to within 0.04 and 0.21 y<sup>-1</sup>.

## Discussion

Despite different geographical location, drainage area, lake surface area, and precipitation rates between the sites (Table 1), there is a rather similar range in the  $^{129}\text{I}$  flux for the period before 1986 (Figures 2 and 3). However, the strong impact of Chernobyl fallout is clearly demonstrated in the profile of Lake Nylandssjön compared to Lake Lehmilampi. At the beginning of the 1950s, the  $^{129}\text{I}$  fluxes in sediments of Lake Nylandssjön rise in a rather constant increasing trend until 1986. This pattern is also observed in the sediments of Lake Loppesjön (8).

Post-Chernobyl  $^{129}\text{I}$  fluxes differ somewhat among the sites,  $(30-50) \times 10^6$  atoms (cm<sup>2</sup> y)<sup>-1</sup> in Lake Nylandssjön,  $(50-60) \times 10^6$  atoms (cm<sup>2</sup> y)<sup>-1</sup> in Lake Loppesjön, and  $(20-70) \times 10^6$  atoms (cm<sup>2</sup> y)<sup>-1</sup> in Lake Lehmilampi, without significant trend at the former two sites. Although these fluxes are affected by both dry and wet fallout of  $^{129}\text{I}$ , a comparable



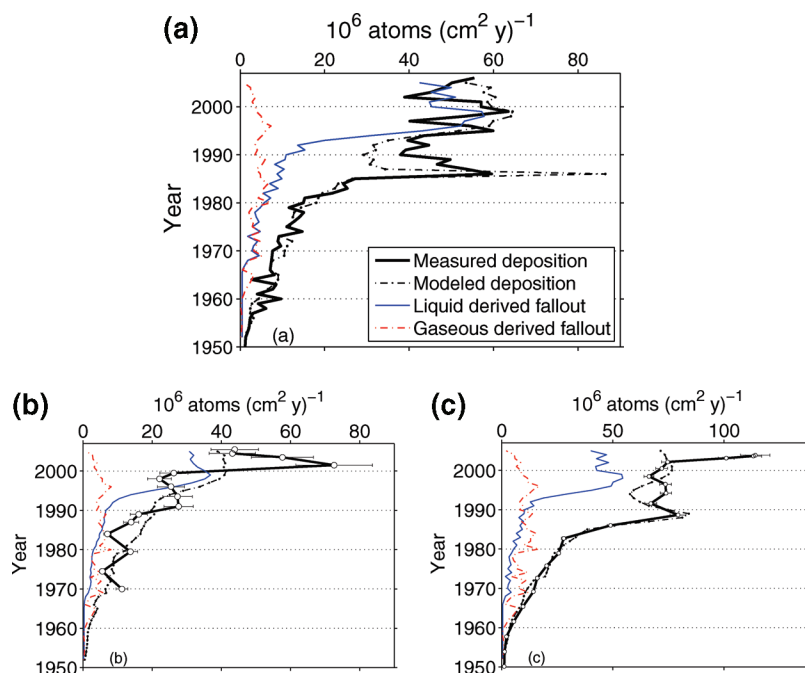


**FIGURE 5.** Modeled and measured  $^{129}\text{I}$  deposition in sediments from (a) Lake Nylandssjön, (b) Lake Lehmilampi, and (c) Lake Loppesjön. The measured  $^{129}\text{I}$  deposition is derived from the  $^{129}\text{I}$  flux as shown in Figures 2 and 3 and ref 8 divided by the diagenetic influence from eq 9 in the Supporting Information. The liquid and gaseous derived fallout (from the reprocessing facilities) are estimated according to eq 4 in the Supporting Information with the fallout constant  $\phi_{F_{129}}$  set to the respective total inventory of  $^{129}\text{I}$  in the sediments. The error margins were omitted in (a) in favor of clarity.

**TABLE 2.** Model Outcome on the Relative Contributions of  $^{129}\text{I}$  from Different Sources, from the Values of  $w_L$ ,  $w_G$ ,  $w_{Ch}$ , and  $w_{NW}$  in Eqs 4 and 7 in the Supporting Information

	Lake Nylandssjön	Lake Lehmilampi	Lake Loppesjön
liquid emissions (%)	70 ± 6	71 ± 18	50 ± 7
gaseous emissions (%)	16 ± 7	29 ± 20	28 ± 9
Chernobyl accident (%)	10 ± 4	<8	21 ± 6
nuclear weapon tests (%)	4 ± 1	—	1 ± 1
liquid time delay (years)	1 lb <sup>b</sup>	3 ub <sup>a</sup>	1 lb <sup>b</sup>

<sup>a</sup> Upper bound. <sup>b</sup> Lower bound.

measure of the wet fallout is obtained from numerous data in precipitation at Uppsala (59°51' N, 17°38' E) and Abisko (68°21' N, 18°49' E) (24). The average annual flux during 2001–2005 from precipitation data ranges between  $(30\text{--}60) \times 10^6 \text{ atoms (cm}^2 \text{ y)}^{-1}$  and  $30 \times 10^6 \text{ atoms (cm}^2 \text{ y)}^{-1}$ , without significant temporal trend. This implies that most of the  $^{129}\text{I}$  fluxes to the studied sites can be related to wet fallout likely due to the relatively high precipitation rate in this part of Europe.

The positive correlation observed between  $^{129}\text{I}$  and carbon ( $r^2 = 0.87$ ) and total iodine and carbon ( $r^2 = 0.85$ ), show that most of the  $^{129}\text{I}$  is associated with the organic material. The profiles of carbon and iodine in Lake Nylandssjön show a decreasing trend with depth that likely suggest some diagenetic effect. However, a diagenetic mobilization and/or changes in primary supply of organic materials cannot account for the 2 orders of magnitude ( $\times 100$ ) difference in  $^{129}\text{I}$  between the 1940s and present. This is because we would expect only a doubling in the concentrations of  $^{129}\text{I}$  if only organic matter is considered as the controlling factor. Accordingly, our data clearly demonstrate the impact of external sources on the  $^{129}\text{I}$  concentration.

On the basis of the acceptable correspondence between  $^{137}\text{Cs}$  fallout and inventory, as well as the temporal correspondence between Chernobyl derived fluxes of  $^{137}\text{Cs}$  and

$^{129}\text{I}$  in sediments from the Swedish lakes, we assumed similar depositional conditions for the two isotopes. The total fallout of  $^{129}\text{I}$  derived from a particular source is then calculated as (from eq 4 in the Supporting Information)

$$(\text{total fallout derived from } x) = \phi_{F_{129}} w_x \quad (1)$$

where  $w_x$  is the weight for either of the sources *Liquid*, *Gaseous*, *Chernobyl* or *Nuclear weapons* (Table 2), and  $\phi_{F_{129}}$  is the fallout given as the total inventory at the sampling site, approximated by the  $^{137}\text{Cs}$  depositional behavior.

According to the approach given in eq 1, influence of the Chernobyl fallout was considerable at Lake Nylandssjön and Lake Loppesjön,  $11 \times 10^7 \text{ atoms cm}^{-2}$  and  $30 \times 10^7 \text{ atoms cm}^{-2}$  respectively, while insignificant in Lake Lehmilampi (Table 1). These estimates are in accordance with the high  $^{137}\text{Cs}$  fallout in the former lakes ( $3.2$  and  $2.7 \text{ Bq cm}^{-2}$ ) and negligible in the latter. In order to obtain comparable estimates for the contribution from the reprocessing facilities (liquid and gas) at the three studied sites, the  $^{129}\text{I}$  inventories down to 1968 are calculated without the Chernobyl contribution (Table 1). The results indicate similar values for the Swedish lakes ( $9.2 \times 10^8 \text{ atoms cm}^{-2}$  in Lake Nylandssjön and  $10.5 \times 10^8 \text{ atoms cm}^{-2}$  in Lake Loppesjön) which may relate to proximity to the sources compared with the Finnish lake ( $6.8 \times 10^8 \text{ atoms cm}^{-2}$  in Lake Lehmilampi) (Figure 1).

Imprints of the nuclear weapon tests during the late 1950s and early 1960s vary between  $(4 \pm 1)\%$  in sediments from Lake Nylandssjön and  $(1 \pm 1)\%$  in Lake Loppesjön, which correspond to a fallout of  $4.4 \times 10^7$  and  $1.4 \times 10^7 \text{ atoms (cm}^2 \text{ y)}^{-1}$ , respectively. The section of Lake Lehmilampi covers only the period 1968–2005 and is thus beyond the weapon tests period. Deposition related to the nuclear weapon tests has been estimated to be  $\sim(1\text{--}2) \times 10^8 \text{ atoms (cm}^2 \text{ y)}^{-1}$  averaged over the north hemisphere (13, 27, 28). These estimates include assumptions about the fission yield of  $^{129}\text{I}$ , as well as assumption of the fraction of the fission yield entering the stratosphere. To our

knowledge, direct measurements of  $^{129}\text{I}$  have neither confirmed these estimates nor established the latitudinal dependence observed for other isotopes (29).

Studies in central Europe indicate that the gaseous emissions from the nuclear reprocessing facilities are the most important supplier of atmospheric  $^{129}\text{I}$  (30, 31). Our modeling approach shows that both liquid and gas emissions are contributing, with the liquid emissions accounting for ~50% to 70% of the total  $^{129}\text{I}$  inventory in the sediment archives (Table 2). Furthermore, the estimated transfer of stable iodine from the sea to atmosphere was used as a proxy for  $^{129}\text{I}$  (30, 31). The former author assumed the annual global transfer of  $1 \times 10^9$  kg of I occurred at 10% of the biologically active areas with an average flux of  $28.6 \text{ kg I (km}^2 \text{ y)}^{-1}$ , applied on areas of the English Channel/Irish Sea and North Sea with high  $^{129}\text{I}/^{127}\text{I}$  ratios. Here, we have used the transfer rate constant  $k$  ( $\text{y}^{-1}$ ), in order to compare values of the different hypothesis about source contribution. The transfer rate was calculated through the assumption that iodine flux is proportional to the concentration of stable iodine ( $c = \sim 50 \mu\text{g L}^{-1}$  (21)) in North Sea surface waters according to

$$\text{flux} = c \times h_v$$

which yields the constant value  $h_v = 0.57 \text{ m}$ . Let us denote  $\dot{m}_i$  ( $\text{kg y}^{-1}$ ) as the total annual emitted iodine for an area  $A$  of the above-mentioned territory with mean depth  $\bar{h} = 40 \text{ m}$  (32), and  $\text{Inv}_i$  the corresponding total iodine inventory in the water volume, then

$$\dot{m}_i = \text{flux} \times A = \frac{\text{Inv}_i}{A\bar{h}} \times h_v \times A = \text{Inv}_i \frac{h_v}{\bar{h}} = \text{Inv}_i \times 0.014$$

This  $(h_v)/(\bar{h}) = k = 0.014 \text{ y}^{-1}$  is comparable to the transfer rate derived in this study.

Reithmeier et al. (31) estimated the value of  $h_v = 0.12 \text{ m}$  based on the annual transfer of  $2 \times 10^9 \text{ kg I y}^{-1}$  averaged over the global oceanic surfaces (the mean iodine concentration of  $47 \mu\text{g L}^{-1}$  was assumed), which yielded a transfer rate of  $(h_v)/(\bar{h}) = 0.003$ .

Apart from the different approaches used to estimate transfer rates (biologically active areas or global averaged), our  $k$  value for  $^{129}\text{I}$  ( $0.04\text{--}0.21 \text{ y}^{-1}$ ) is much larger. Possible explanations for the difference may lie in the different chemical behavior between  $^{129}\text{I}$  and  $^{127}\text{I}$ , as already indicated by a study of the surface waters in the North Sea (21).

## Acknowledgments

Financial support from Carl Tryggers Foundation, Swedish Radiation Protection Authority, and Swedish Research Council is acknowledged. We also thank J.-E. Wallin for laboratory assistance and A. Broberg for help with the  $^{137}\text{Cs}$  measurements.

## Supporting Information Available

Model description and application to the studied archives, details of the dry mass accumulation calculation, and a derivation of the transfer factor  $k$  of  $^{129}\text{I}$  from ocean to atmosphere are presented. Tabulated values are given for all data from Lake Nylandssjön and Lake Lehmilampi. This material is available free of charge via the Internet at <http://pubs.acs.org>.

## Literature Cited

- Rucklidge, J.; Kilius, L.; Fuge, R.  $^{129}\text{I}$  in moss down-wind from the Sellafield nuclear fuel reprocessing plant. *Nucl. Instrum. Methods* **1994**, *92*, 417–420.
- Szidat, S.; Schmidt, A.; Handl, J.; Jakob, D.; Botsch, W.; Michel, R.; Synal, H. A.; Schnabel, C.; Suter, M.; Lopez-Gutierrez, J. M.; et al. Iodine-129: Sample preparation, quality control and analyses of pre-nuclear materials and of natural waters from Lower Saxony, Germany. *Nucl. Instrum. Methods* **2000**, *172*, 699–710.
- Buraglio, N.; Aldahan, A.; Possnert, G.; Vintersved, I.  $^{129}\text{I}$  from the nuclear reprocessing facilities traced in precipitation and runoff in northern Europe. *Environ. Sci. Technol.* **2001**, *35*, 1579–1586.
- Buraglio, N.; Aldahan, A.; Possnert, G.  $^{129}\text{I}$  in lakes of the Chernobyl fallout region and its environmental implications. *Appl. Radiat. Isot.* **2001b**, *55* (5), 715–20.
- Alfimov, V.; Aldahan, A.; Possnert, G.; Winsor, P. Anthropogenic Iodine-129 in seawater along a transect from the Norwegian coastal current to the North Pole. *Mar. Pollut. Bull.* **2004**, *49* (11–12), 1097–1104.
- Gallagher, D.; McGee, E. J.; Mitchell, P. I.; Alfimov, V.; Aldahan, A.; Possnert, G. Retrospective search for evidence of the 1957 Windscale fire in NE Ireland using  $^{129}\text{I}$  and other long-lived nuclides. *Environ. Sci. Technol.* **2005**, *39*, 2927–2935.
- Michel, R.; Handl, J.; Ernst, T.; Botsch, W.; Szidat, S.; Schmidt, A.; Jakob, D.; Beltz, D.; Romantschuk, L. D.; Synal, H. A.; et al. Iodine-129 in soils from northern Ukraine and the retrospective dosimetry of the iodine-131 exposure after the Chernobyl accident. *Sci. Total Environ.* **2005**, *340* (1–3), 35–55.
- Englund, E.; Aldahan, A.; Possnert, G. Tracing anthropogenic nuclear activity with  $^{129}\text{I}$  in lake sediment. *J. Environ. Radioact.* **2008**, *99* (2), 219–229.
- Aldahan, A.; Alfimov, V.; Possnert, G.  $^{129}\text{I}$  anthropogenic budget: Major sources and sinks. *Appl. Geochem.* **2007**, *22* (3), 606–618.
- Robens, E.; Aumann, D. C. Iodine-129 in the environment of a nuclear fuel reprocessing plant: I.  $^{129}\text{I}$  and  $^{127}\text{I}$  contents of soils, food crops and animal products. *J. Environ. Radioact.* **1988**, *7* (2), 159–175.
- Chamberlain, A. C. *Radioactive aerosols*; Cambridge University Press: London, 1991.
- Edvarson, K. In *The Chernobyl Fallout in Sweden. Results from a Research Program on Environmental Radiology*; Moberg, L., Ed.; Swedish Radiation Protection Institute: Stockholm, 1991; pp 47–65.
- Rao, U.; Fehn, U. Sources and reservoirs of anthropogenic Iodine-129 in western New York. *Geochim. Cosmochim. Acta* **1999**, *63* (13–14), 1927–1938.
- Hou, X. L.; Dahlgaard, H.; Nielsen, S. P.; Kucera, J. Level and origin of Iodine-129 in the Baltic Sea. *J. Environ. Radioact.* **2002**, *61*, 331–343.
- Paatero, J.; Kulmala, S.; Jaakkola, T.; Saxén, R.; Buyukay, M. Deposition of  $^{125}\text{Sb}$ ,  $^{106}\text{Ru}$ ,  $^{144}\text{Ce}$ ,  $^{134}\text{Cs}$  and  $^{137}\text{Cs}$  in Finland after the Chernobyl accident. *Boreal Environ. Res.* **2007**, *42*, 43–54.
- Renberg, I. Photographic demonstration of the annual nature of a varve type common in N. Swedish lake sediments. *Hydrobiologia* **1986**, *140* (1), 93–95.
- Pettersson, G.; Renberg, I.; Geladi, P.; Lindberg, A.; Lindgren, F. Spatial uniformity of sediment accumulation in varved lake sediments in northern Sweden. *J. Paleolimnol.* **1993**, *9* (3), 195–208.
- Gälman, V.; Pettersson, G.; Renberg, I. A comparison of sediment varves (1950–2003 AD) in two adjacent lakes in northern Sweden. *J. Paleolimnol.* **2006**, *35* (4), 837–853.
- Haltia-Hovi, E.; Saarinen, T.; Kukkonen, M. A 2000-year record of solar forcing on varved lake sediment in eastern Finland. *Q. Sci. Rev.* **2007**, *26* (5–6), 678–689.
- Englund, E.; Aldahan, A.; Possnert, G.; Alfimov, V. A routine preparation method for AMS measurement of  $^{129}\text{I}$  in solid material. *Nucl. Instrum. Methods.* **2007**, *259* (1), 365–369.
- Hou, X.; Aldahan, A.; Nielsen, S. P.; Possnert, G.; Nies, H.; Hedfors, J. Speciation of  $^{129}\text{I}$  and  $^{127}\text{I}$  in seawater and implications for sources and transport pathways in the North Sea. *Environ. Sci. Technol.* **2007**, *41*, 5993–5999.
- Fuge, R.; Johnson, Christopher, C. The geochemistry of iodine - a review. *Environ. Geochem. Health* **1986**, *8* (2), 31–54.
- Björk, S.; Svensson, N.-O. In *Rocks and soil*; Fredén, C., Ed.; Swedish National Atlas: Stockholm, 1998; pp 138–143.
- Persson, S. Licentiate thesis, Institution of Engineering Sciences, Uppsala University, 2007.
- Håkanson, L. Models to predict organic content of lake sediments. *Ecol. Modell.* **1995**, *82* (3), 233–245.

- (26) Håkanson, L.; Jansson, M. *Principles of Lake Sedimentology*; Springer-Verlag: New York, 1983.
- (27) Schink, D. R.; Santschi, P. H.; Corapcioglu, O.; Fehn, U. Prospects for "iodine-129 dating" of marine organic matter using AMS. *Nucl. Instrum. Methods* **1995**, B99, 524–527.
- (28) Oktay, S. D.; Santschi, P. H.; Moran, J. E.; Sharma, P. The <sup>129</sup>Iodine bomb pulse recorded in Mississippi River Delta sediments: results from isotopes of I, Pu, Cs, Pb, and C. *Geochim. Cosmochim. Acta* **2000**, 64, 989–996.
- (29) UNSCEAR; Sources and effects of ionizing radiation: Annex c: Exposures from man-made sources of radiation; Technical Report 2000 Report to the General Assembly, with scientific annexes United Nations Scientific Committee on the Effects of Atomic Radiation, 2000.
- (30) Schnabel, C.; Lopez-Gutierrez, J. M.; Szidat, S.; Sprenger, M.; Wernli, H.; Beer, J.; Synal, H. A. On the origin of <sup>129</sup>I in rain water near Zurich. *Radiochim. Acta* **2001**, 89, 815–22.
- (31) Reithmeier, H.; Lazarev, V.; Ruhm, W.; Schwikowski, M.; Gaggeler, H. W.; Nolte, E. Estimate of european <sup>129</sup>I releases supported by <sup>129</sup>I analysis in an alpine ice core. *Environ. Sci. Technol.* **2006**, 40, 5891–5896.
- (32) Nielsen, S. P. A box model for north-east Atlantic coastal waters compared with radioactive tracers. *J. Marine Syst.* **1995**, 6, 545–560.
- (33) Otto, L.; Zimmerman, J. T. F.; Furnes, G. K.; Mork, M.; Saetre, R.; Becker, G. Review of the physical oceanography of the North Sea. *Netherlands J. Sea Res.* **1990**, 26 (2–4), 161–238.

ES8009953

## On-line separation of Pu(III) and Am(III) using extraction and ion chromatography

J. Jernström,<sup>1\*</sup> J. Lehto,<sup>2</sup> M. Betti<sup>3</sup>

<sup>1</sup> Radiation Research Department, Risø National Laboratory, Technical University of Denmark, DK-4000 Roskilde, Denmark

<sup>2</sup> Laboratory of Radiochemistry, Department of Chemistry, P.O. Box 55, FI-00014 University of Helsinki, Finland

<sup>3</sup> European Commission, Joint Research Centre, Institute for Transuranium Elements, P.O. Box 2340, D-76125 Karlsruhe, Germany

(Received July 28, 2006)

An on-line method developed for separating plutonium and americium was developed. The method is based on the use of HPLC pump with three analytical chromatographic columns. Plutonium is reduced throughout the procedure to trivalent oxidation state, and is recovered in the various separation steps together with americium. Light lanthanides and trivalent actinides are separated with TEVA resin in thiocyanate/formic acid media. Trivalent plutonium and americium are pre-concentrated in a TCC-II cation-exchange column, after which the separation is performed in CS5A ion chromatography column by using two different eluents. Pu(III) is eluted with a dipicolinic acid eluent, and Am(III) with oxalic acid eluent. Radiochemical and chemical purity of the eluted plutonium and americium fractions were ensured with alpha-spectrometry.

### Introduction

Determination of plutonium and americium in environmental samples by alpha-spectrometry involves tedious radiochemical procedures to separate these radionuclides from the matrix.<sup>1</sup> In the case of soil or sediment samples several steps must be performed: conversion of the actinides associated with the matrix into acid-soluble form, separation of the actinides from the macro components of the sample and other radionuclides, purification of the actinides, and preparation of the source for measurement.<sup>2</sup> A traditional way to analyze plutonium and americium content in an environmental sample involves the use of anion-exchange. However, copious ion-exchange steps together with evaporation of large volumes of concentrated mineral acids lengthen the duration of the traditional procedure, and to perform the whole analysis lasts for several days.

Ion chromatography is a form of liquid chromatography that uses ion-exchange resins to separate ions or ionic compounds based on their interaction with the resin. Chelating ligands, such as oxalate and 2,6-pyridinedicarboxylate (dipicolinate or PDCA), which are used for eluting the analytes, form stable anionic complexes with trivalent actinide cations in appropriate pH and concentration conditions. Elution rate of these complexes in anion-exchange chromatography resin is related to the stabilities of the anionic complexes.

PERNA et al.<sup>3</sup> developed an on-line method in which americium was determined in sediment and soil samples using extraction chromatography, cation-exchange and ion chromatography. The separated americium fraction was measured by alpha-spectrometry. In the on-line procedure two methods were utilized in order to remove

interfering matrix components before the ion chromatography step. Co-precipitation with calcium oxalate was applied to remove the majority of matrix components, and extraction chromatography by using TEVA resin (Eichrom, USA) was applied for separating light lanthanides and americium in ammonium thiocyanate/formic acid media. After the purification steps americium was pre-concentrated in a cation-exchange column (TCC-II from Dionex). The final separation of americium was accomplished by using a mixed bed ion chromatography column (CS5A from Dionex), from which americium was eluted as a chemically and radiochemically pure fraction by using oxalate as the complexing ligand.

The preceding method for separation of americium has been modified in order to include the separation of plutonium, which is reduced to trivalent oxidation state to be recovered together with americium throughout the separation steps. The basic method is similar than the one for americium, i.e., the separation of lanthanides and trivalent plutonium and americium is done with TEVA resin in ammonium thiocyanate/formic acid media, and plutonium and americium are pre-concentrated in TCC-II cation-exchange column prior to the final separation in the CS5A ion chromatography column. The elution of plutonium from the CS5A column is performed with a dipicolinic acid eluent,<sup>4</sup> while americium, as in the on-line method of PERNA et al.,<sup>3</sup> is eluted with oxalic acid eluent. The radiochemical and chemical purity of the actinide fractions was ensured by measuring them with alpha-spectrometry.

This paper describes the behavior of plutonium in the different separation steps, and presents the entire procedure of separation of radiochemically pure plutonium and americium fractions.

\* E-mail: jussi.jernstroem@risoe.dk

## Experimental

The method steps being handled in the following sub-chapters are schematically illustrated in Fig. 1.

### Reduction of plutonium

Throughout the separation procedure plutonium was reduced to trivalent oxidation state. To achieve reducing conditions ascorbic acid and hydroxylamine hydrochloride was present in all solutions, except within the final step of elution of americium. The concentration of both reduction agents was constantly  $2 \cdot 10^{-3} \text{ mol} \cdot \text{dm}^{-3}$ .

### Sample preparation

Approximately 1 Bq of  $^{239}\text{Pu}$  and  $^{243}\text{Am}$  were added to 6 ml of  $2.0 \text{ mol} \cdot \text{dm}^{-3}$  ammonium thiocyanate in  $0.1 \text{ mol} \cdot \text{dm}^{-3}$  formic acid. Reduction agents were added, and the sample was left for reduction for 20 minutes. By

using that time for the reduction of plutonium the following separation step was quantitative, i.e., the reduction time was found to be appropriate for quantitative reduction of plutonium.

### Separation of light lanthanides and trivalent plutonium and americium

Preparing for the step of separation of light lanthanides and trivalent plutonium and americium TEVA extraction chromatography resin was dry-packed in a chromatography column. With length of 250 mm and inner diameter of 4 mm the column had a resin capacity of  $\sim 1.2 \text{ g}$ . Before introducing the sample the column was equilibrated with 20 ml ( $1 \text{ ml} \cdot \text{min}^{-1}$ ) of  $2.0 \text{ mol} \cdot \text{dm}^{-3}$  ammonium thiocyanate in  $0.1 \text{ mol} \cdot \text{dm}^{-3}$  formic acid.

After the 20 minutes of reduction time the sample was loaded ( $1 \text{ ml} \cdot \text{min}^{-1}$ ) in the TEVA column, and washed with 2 ml ( $1 \text{ ml} \cdot \text{min}^{-1}$ ) of  $2.0 \text{ mol} \cdot \text{dm}^{-3}$  ammonium thiocyanate in  $0.1 \text{ mol} \cdot \text{dm}^{-3}$  formic acid.

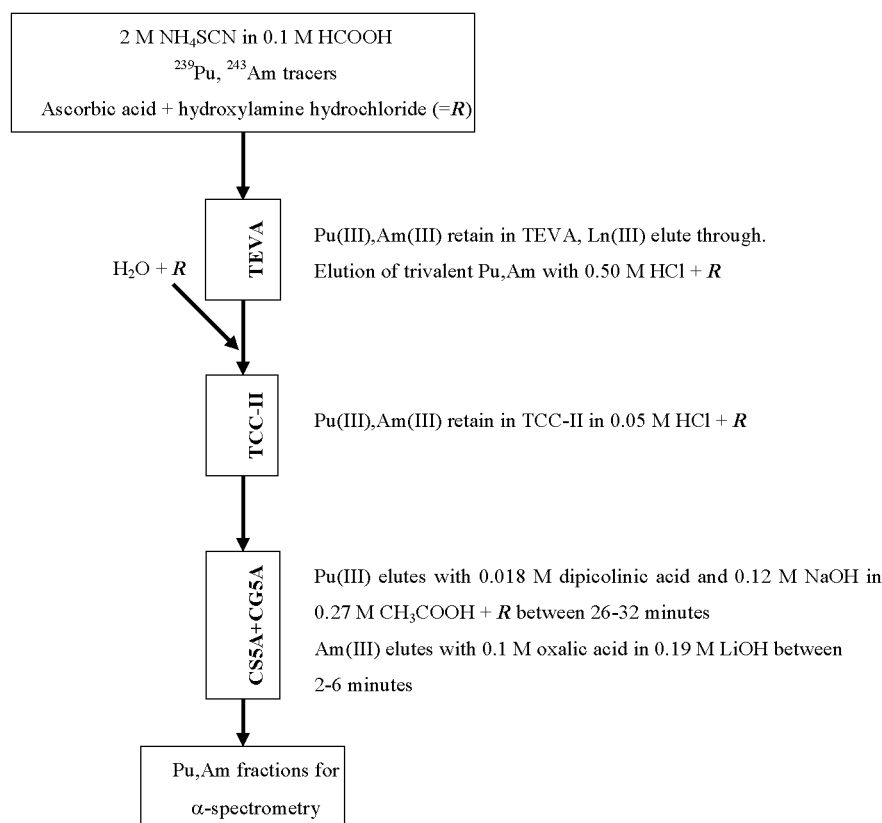


Fig. 1. A scheme of the separation procedure. The symbol *R* denotes the added reducing agents

*Pre-concentration of plutonium and americium*

Prior to the step of pre-concentration of plutonium and americium the TCC-II cation-exchange column was equilibrated with 20 ml ( $2 \text{ ml} \cdot \text{min}^{-1}$ ) of  $0.05 \text{ mol} \cdot \text{dm}^{-3}$  hydrochloric acid.

The TEVA column, containing Pu and Am sorbed in the resin as thiocyanate complexes, was connected with the TCC-II pre-concentrator column, and Pu and Am were subsequently eluted with 10 ml ( $0.2 \text{ ml} \cdot \text{min}^{-1}$ ) of  $0.5 \text{ mol} \cdot \text{dm}^{-3}$  hydrochloric acid. A flow of water with flow rate of  $1.8 \text{ ml} \cdot \text{min}^{-1}$  was connected to the eluent flow, which diluted the concentration of hydrochloric acid prior to entering to TCC-II column to  $0.05 \text{ mol} \cdot \text{dm}^{-3}$ . The water flow was pumped by using an external peristaltic pump.

*Separation in ion chromatography column*

During the loading in the TCC-II column plutonium and americium were concentrated in a compact band in the head of the column. That is why the elution of the actinides from the cation-exchange column was performed countercurrentwise by turning the TCC-II column when connecting it with the CS5A column. Plutonium was eluted ( $1 \text{ ml} \cdot \text{min}^{-1}$ ) with the dipicolinic acid eluent, i.e., a mixture of  $0.018 \text{ mol} \cdot \text{dm}^{-3}$  dipicolinic acid and  $0.12 \text{ mol} \cdot \text{dm}^{-3}$  sodium hydroxide in  $0.27 \text{ mol} \cdot \text{dm}^{-3}$  acetic acid, and the fraction of 26–32 minutes was collected for activity determination. After the elution of plutonium the columns were rinsed with the dipicolinic acid eluent for 10 minutes. After the rinsing, americium was eluted with a reductant-free mixture of  $0.1 \text{ mol} \cdot \text{dm}^{-3}$  oxalic acid in  $0.19 \text{ mol} \cdot \text{dm}^{-3}$  lithium hydroxide in a fraction between 2 and 6 minutes.

Prior to introducing the sample to the CS5A column it was equilibrated with 20 ml ( $2 \text{ ml} \cdot \text{min}^{-1}$ ) of mixture containing  $0.018 \text{ mol} \cdot \text{dm}^{-3}$  dipicolinic acid and  $0.12 \text{ mol} \cdot \text{dm}^{-3}$  sodium hydroxide in  $0.27 \text{ mol} \cdot \text{dm}^{-3}$  acetic acid.

*Activity determination*

The activity of the 2 ml eluate fractions was measured using liquid scintillation counting. In each fraction 18 ml of HiSafe 3 scintillation solution was added. Because the eluate fractions contained a heterogenous mixture of compounds which lower the counting efficiency with various degrees, a quenching curve was determined and used for efficiency corrections. The curve was determined by measuring a constant activity of  $^{239}\text{Pu}$  with different concentrations of carbon tetrachloride, which is a substance that has a significant quenching effect.

After optimizing the separation procedure by using LSC the eluted fractions were measured by alpha-

spectrometry to determine the radiochemical purity. The sources for alpha-spectrometry were prepared by precipitating the actinides with neodymium fluoride on a filter.<sup>6</sup> The precipitation of the oxalate-containing americium eluates was straightforward, following the procedure described by PERNA et al.<sup>3</sup> However, using the similar precipitation method for the dipicolinic acid eluates of plutonium was not possible. It was noticed that during the precipitation process, shortly after adding hydrofluoric acid to the sample, hair-like solid structures formed. These formations dissolved when heated, but reformed after cooling. Since dipicolinic acid decomposes at 243–245 °C, it was decided to destroy the dipicolinate complex by heating the sample at 350 °C for 1 hour. The charred sample was fumed several times with concentrated nitric acid and 30% hydrogen peroxide, and finally with concentrated hydrochloric acid. Prior to precipitating plutonium with neodymium fluoride Pu was stabilized to tetravalent oxidation state by heating the sample in concentrated nitric acid which contained  $0.1 \text{ mol} \cdot \text{dm}^{-3}$  of sodium nitrite. By this above-mentioned handling the measurement of plutonium with alpha-spectrometry was accomplished.

**Results and discussion**

A scheme illustrating the separation procedure is presented in Fig. 1. The separation steps being treated in the following sub-chapters describe the behavior of both plutonium and americium. The difference with the two elements is that the various steps related to Pu include the use of reducing agents. The separation quantitativity for both plutonium and americium was then verified after the whole method was firstly adjusted for plutonium.

*TEVA column for separating trivalent lanthanides and actinides*

Soil and sediment samples usually contain major amounts of lanthanide elements. Lanthanides exist mostly in trivalent oxidation state in solutions, and exhibit similar chemical behavior than americium and other trivalent actinides. Sources prepared for measurement by alpha-spectrometry need to be chemically pure. Impurities in the sources absorb the energy of the emitting alpha-particles, and therefore, degrade the spectral resolution. Because of their chemical similarity, trivalent lanthanides and actinides are frequently recovered together in chromatographic separations. Therefore, removal of lanthanides from the sample prior to alpha-spectrometry is required.

In the literature one can find several methods which exploit different stationary phases to achieve the separation of lanthanides and actinides.<sup>7–12</sup> TEVA



extraction chromatographic resin, which contains quaternary ammonium salt (Aliquat-336™, general formula  $R_3CH_3NCl$ ) as the extractant, has been applied in separating americium from lanthanide elements in thiocyanate/dilute acid media.<sup>7,13,14</sup> The moderately high separation factor for trivalent actinides and lanthanides is due to the increased partial covalent character of the bonds between actinides and soft ligand donor atoms.<sup>15</sup> KHOPKAR and MATHUR<sup>16</sup> found the distribution coefficients of some trivalent lanthanides obtained from  $1.0 \text{ mol} \cdot \text{dm}^{-3}$  ammonium thiocyanate, using quaternary ammonium (aliquat) thiocyanate as the extractant, increasing with atomic number. This was in contrast with trivalent actinides from plutonium to curium, which showed the inverse behavior ( $\text{Pu(III)} > \text{Am(III)} > \text{Cm(III)}$ ).

As regards to the investigated procedure, it was assumed that trivalent plutonium would behave similarly to americium in the TEVA/ammonium thiocyanate/formic acid system. As Fig. 2 presents, practically all of plutonium (98.5–99.1%) was sorbed in TEVA resin during loading and washing. For elution of plutonium from TEVA resin, and subsequent pre-concentration in the strong cation-exchange resin (TCC-II column), the elution needed to be performed with dilute acid. By eluting with hydrochloric acid it was found out that for quantitative elution of Pu(III) from TEVA resin the concentration and volume of hydrochloric acid should be no less than  $0.25 \text{ mol} \cdot \text{dm}^{-3}$  and 6 ml, respectively (Fig. 2). The use of nitric acid as eluent was out of question due to the sorption of trivalent actinides in the quaternary ammonium resin in nitrate solution.<sup>13</sup>

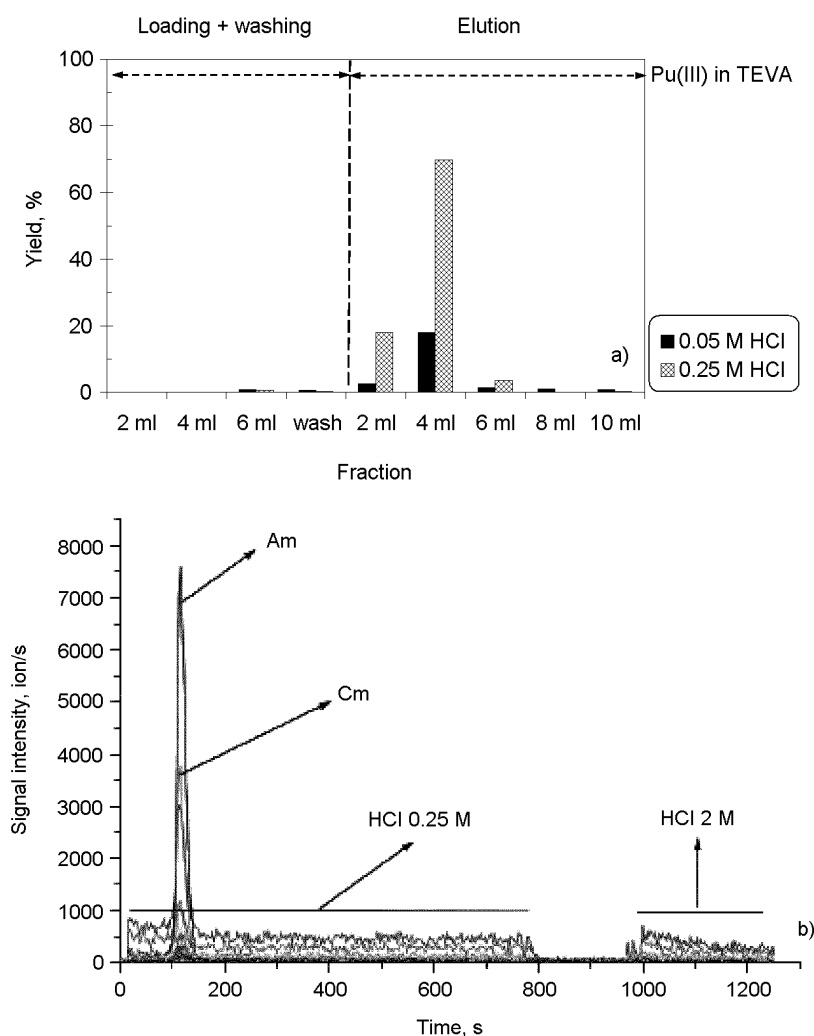


Fig. 2. Elution profiles of Pu(III) being eluted from TEVA resin with two different HCl molarities (a). The loading volume was 6 ml, and washing volume 2 ml, presents the Sharp elution peak of Am(Cm) (b) (taken from PERNA et al.<sup>3</sup>) being eluted with  $0.25 \text{ mol} \cdot \text{dm}^{-3}$  HCl. The position of the peak is within 150 s, which corresponds to 2.5 ml of HCl. The detector in the experiment with Pu was LSC, with Am(Cm) ICP-MS. The experiment with Am(Cm) did not contain any added reducing agents

The behavior of americium was studied previously in similar conditions except without the presence of the added reducing agents, as reported by PERNA et al.<sup>3</sup> Americium was found to be eluted from TEVA resin with 2.5 ml (150 s, 1 ml·min<sup>-1</sup>) of 0.25 mol·dm<sup>-3</sup> hydrochloric acid (Fig. 2).

*Cation-exchange column for pre-concentrating trivalent actinides*

The trace cation concentrator column (TCC-II) from Dionex is packed with surface sulfonated styrene/divinylbenzene co-polymer. The function of the TCC-II column in the on-line procedure is to remove the trivalent ions from solution during the elution from TEVA resin, and to concentrate the cations in a compact band in the head of the column. The subsequent elution of the trivalent ions from the TCC-II column is done countercurrentwise, which enables rapid release of the cations into the following ion-chromatography

column.<sup>17</sup> In the investigated procedure the load solution volume was 100 ml, therefore, as the elution of plutonium and americium occurred in the first 2 ml fraction, a concentration factor of minimum of 50 was achieved.

As can be seen in the Fig. 3, plutonium did not retain in the TCC-II column in 0.25 mol·dm<sup>-3</sup> hydrochloric acid, which was needed for quantitative elution of Pu from the TEVA resin. However, by diluting the acid concentration to 0.05 mol·dm<sup>-3</sup> quantitative concentration of plutonium in the TCC-II column was attained. The water flow for dilution was pumped with an external peristaltic pump.

As reported by PERNA et al.<sup>3</sup> in similar conditions except without the added reducing agents americium was found to be sorbed on TCC-II column in 0.25 mol·dm<sup>-3</sup> hydrochloric acid. The sorption was quantitative except of the end of the loading when some breakthrough was observed (Fig. 3).

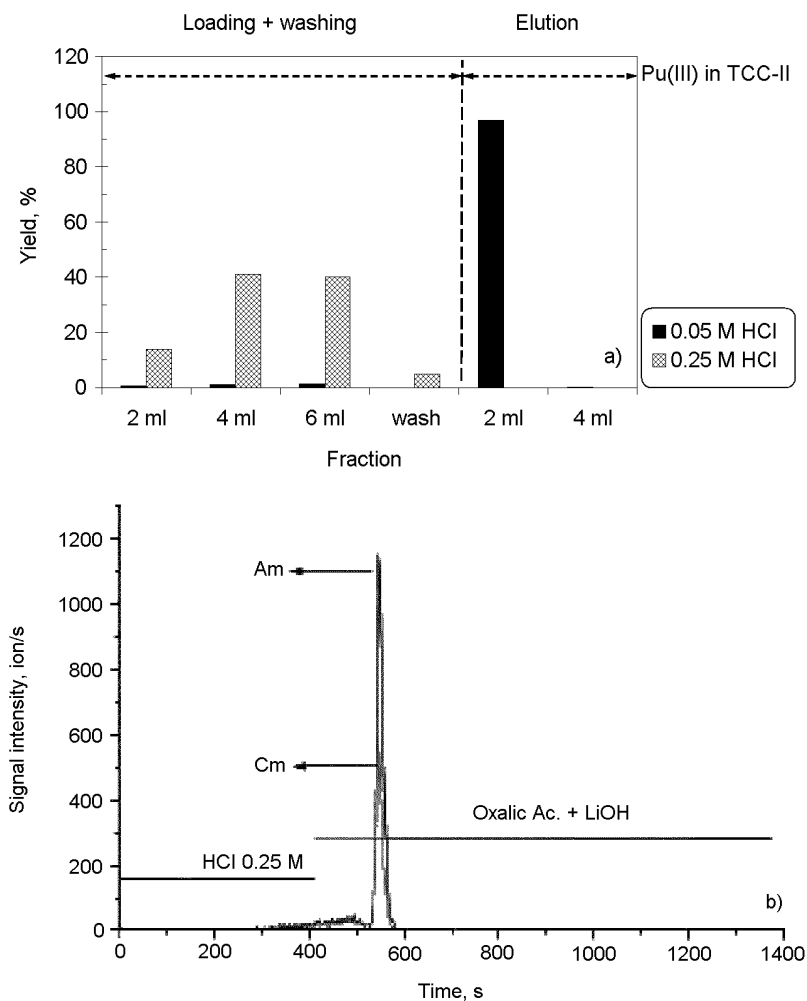


Fig. 3. Trivalent Pu is quantitatively sorbed on TCC-II column in 0.05 mol·dm<sup>-3</sup> HCl, but elutes through completely in 0.25 mol·dm<sup>-3</sup> HCl (a). The eluent consisted of 0.006 mol·dm<sup>-3</sup> dipicolinic acid and 0.04 mol·dm<sup>-3</sup> NaOH in 0.09 mol·dm<sup>-3</sup> CH<sub>3</sub>COOH. Am was found to be sorbed on the TCC-II column in 0.25 mol·dm<sup>-3</sup> HCl<sup>3</sup> (b). The experiment with Am did not contain any added reducing agent

*Ion-chromatography column for final separation of trivalent actinides*

The analytical chromatographic column CS5A from Dionex is a mixed bed anionic/cationic column. The column resin has 55% cross-linked microporous hydrophobic resin core that has been agglomerated with 2 layers of permeable latex particles. The latex particles carry the actual cation- and anion-exchange functionality. The first layer is a fully sulfonated latex for cation-exchange. The second layer is a fully aminated layer for anion-exchange.<sup>18</sup> The column is used together with a CG5A guard column, which is placed prior to the analytical column to prevent sample contaminants from eluting onto the CS5A analytical column.

The CS5A column has been applied for various analytical purposes, such as for analysis of metal species (Cr, Fe),<sup>19–21</sup> determination of transition and heavy metals,<sup>22–27</sup> lanthanides<sup>28,29</sup> and actinides<sup>3,29</sup> in environmental samples.

The separation of transition metals in CS5A column with oxalic acid ( $\log K_{a1,2}$ : 1.2, 3.8, 25 °C, 0.1 mol·dm<sup>-3</sup>) involves both cationic and anionic complexes, depending on ligand concentration and the strength of complexation between the metal and oxalate ligand.<sup>24,25,32</sup> Weakly complexing cations, such as Mn(II) and Cd(II), are separated by cation-exchange. Instead, trivalent lanthanides and actinides form moderately stable complexes with oxalate (Table 1), and the separation in CS5A column is anionic. PERNA et al.<sup>29</sup> found the elution order of lanthanides following the order of atomic numbers so that lanthanum, forming the weakest complex, eluted first. As was reported by PERNA et al.,<sup>29</sup> americium eluted between promethium and europium, which was expectable from the complex stabilities.

A mixture of 0.1 mol·dm<sup>-3</sup> oxalic acid in 0.19 mol·dm<sup>-3</sup> lithium hydroxide has been used in the on-line method developed for environmental samples in order to elute a pure fraction of americium from CS5A column for measurement by alpha-spectrometry.<sup>3</sup> The same eluent, additionally containing the ascorbic acid and hydroxyl amine hydrochloride reduction agents, was tested for trivalent plutonium. However, no sign of elution of plutonium was observed in the time frame of 60 minutes, while americium eluted quantitatively (~98%) between 2 and 6 minutes. Increasing the oxalate concentration up to 0.5 mol·dm<sup>-3</sup> did not have any effect on elution of plutonium. The database of NIST reports the  $\log \beta_3$  of 11.15 for  $\text{Am}(\text{C}_2\text{O}_4)_3^{3-}$ ,<sup>30</sup> as the corresponding  $\log \beta_3$  for  $\text{Pu}(\text{C}_2\text{O}_4)_3^{3-}$  has been determined as 9.39/10.65 (Table 1).<sup>31</sup> In the case of the elution behavior of oxalate complexes of Pu(III) and Am(III) in CS5A column follows that of lanthanides,

plutonium should have eluted prior to americium. The reason why trivalent plutonium was not observed to elute with oxalic acid is not clear.

As oxalic acid did not elute plutonium from the mixed bed column another eluent was needed. Like oxalic acid, 2,6-pyridinedicarboxylic acid (dipicolinic acid or PDCA,  $\log K_{a1,2}$ : 2.07, 4.66, 25 °C, 0.1 mol·dm<sup>-3</sup>) has been applied in separating transition and heavy metals in CS5A column.<sup>22,25–27</sup> The dipicolinate (2,6-pyridinecarboxylate) ligand is a tridentate ligand which is able to coordinate by an oxygen of each carboxylate group and by the nitrogen of the pyridine ring.<sup>33,34</sup> Dipicolinate reacts with transition and heavy metal cations, and lanthanide cations (Table 1) forming stable anionic complexes.

A mixture of 0.012 mol·dm<sup>-3</sup> dipicolinic acid and 0.08 mol·dm<sup>-3</sup> sodium hydroxide in 0.18 mol·dm<sup>-3</sup> acetic acid (solution pH 4.62) was found to elute Pu(III) from the column between 44 and 50 minutes (Fig. 4). By modifying the eluent and increasing dipicolinate concentration a solution of 0.018 mol·dm<sup>-3</sup> dipicolinic acid and 0.12 mol·dm<sup>-3</sup> sodium hydroxide in 0.27 mol·dm<sup>-3</sup> acetic acid was applied. As a consequence faster elution of plutonium between 26 and 32 minutes was achieved, as shown in Fig. 4. Further increase of dipicolinic acid concentration within a same pH range was not feasible, as the viscosity of the eluent increased too much for stable elution rate with the used HPLC pump.

No americium was found to elute with dipicolinic acid during time of 60 minutes. Observing the stability constants of anionic dipicolinate complexes of light lanthanides, collected in Table 1, a steady increase in  $\log \beta$  values from La to Gd is seen. No equivalent information on trivalent actinide complexes was found in the literature, nor was found any experimental data dealing with elution behavior of trivalent lanthanides or actinides in CS5A column in dipicolinate media. However, in the case of the stability order of anionic dipicolinate complexes of trivalent actinides follows that of trivalent lanthanides, as is the case with oxalate complexes, Pu(III) should form weaker complexes with dipicolinate than Am(III). Consequently, assuming that the elution behavior of anionic dipicolinate complexes of trivalent actinides follows that observed by PERNA et al.<sup>29</sup> as regards to oxalate complexes of trivalent americium and lanthanides, Pu(III) should elute before Am(III) with dipicolinic acid eluent. In the experiments no elution of americium was observed, before or after the elution of plutonium. However, as the elution dynamics of americium in the studied dipicolinic acid system are not known, it is possible that the elution of americium would have taken place beyond the time (60 minutes) used in the experiments.

Table 1. Various stability constants of oxalate and dipicolinate ligands of trivalent light actinides and lanthanides

Cation	Oxalate			Dipicolinate		
	$\log \beta_1$	$\log \beta_2$	$\log \beta_3$	$\log \beta_1$	$\log \beta_2$	$\log \beta_3$
Ac(III)	4.36 <sup>1</sup>	7.08 <sup>1</sup>				
Pu(III)	—	—	9.39 <sup>5</sup> 10.65 <sup>6</sup>	—	—	—
Am(III)	5.25 <sup>1</sup>	8.85 <sup>1</sup>	11.15 <sup>2</sup>	—	—	—
Cm(III)	5.25 <sup>1</sup>	8.85 <sup>1</sup>	—	—	—	—
Bk(III)	5.45 <sup>1</sup>	9.14 <sup>1</sup>	—	—	—	—
Cf(III)	5.50 <sup>1</sup>	9.37 <sup>1</sup>	—	—	—	—
La(III)	4.71 <sup>1</sup>	7.83 <sup>1</sup>	10.3 <sup>2</sup>	7.94 <sup>3</sup>	13.71 <sup>3</sup>	17.95 <sup>3</sup>
Ce(III)	4.90 <sup>1</sup>	8.26 <sup>1</sup>	10.2 <sup>4</sup>	8.29 <sup>3</sup>	14.33 <sup>3</sup>	18.67 <sup>3</sup>
Pr(III)	—	—	—	8.58 <sup>3</sup>	15.00 <sup>3</sup>	19.80 <sup>3</sup>
Nd(III)	—	—	—	8.73 <sup>3</sup>	15.40 <sup>3</sup>	20.41 <sup>3</sup>
Pm(III)	5.18 <sup>1</sup>	8.78 <sup>1</sup>	—	—	—	—
Sm(III)	—	—	—	8.81 <sup>3</sup>	15.77 <sup>3</sup>	21.06 <sup>3</sup>
Eu(III)	5.36 <sup>1</sup>	9.04 <sup>1</sup>	11.4 <sup>2</sup>	8.79 <sup>3</sup>	15.86 <sup>3</sup>	21.32 <sup>3</sup>
Gd(III)	4.77 <sup>3</sup>	8.66 <sup>3</sup>	—	8.68 <sup>3</sup>	15.95 <sup>3</sup>	21.66 <sup>3</sup>

All values are obtained from SMITH et al.<sup>30</sup> except those of Pu(III) oxalate, which are taken from CLEVELAND.<sup>31</sup>

<sup>1</sup> 25 °C, 0.1 mol·dm<sup>-3</sup>.

<sup>2</sup> 25 °C, 1.0 mol·dm<sup>-3</sup>.

<sup>3</sup> 25 °C, 0.5 mol·dm<sup>-3</sup>.

<sup>4</sup> 25 °C, 0.7 mol·dm<sup>-3</sup>.

<sup>5</sup> 25 °C, 3.0 mol·dm<sup>-3</sup>.

<sup>6</sup> 25 °C.

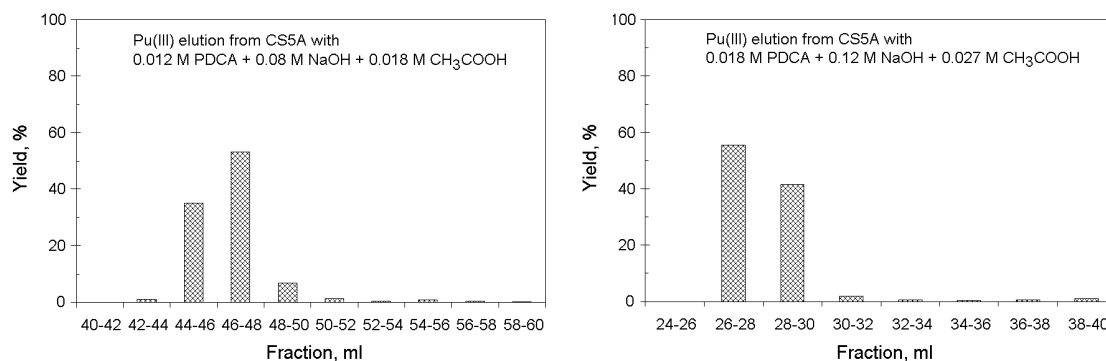


Fig. 4. Elution of Pu(III) from CS5A column using two different concentrations of dipicolinate ligand

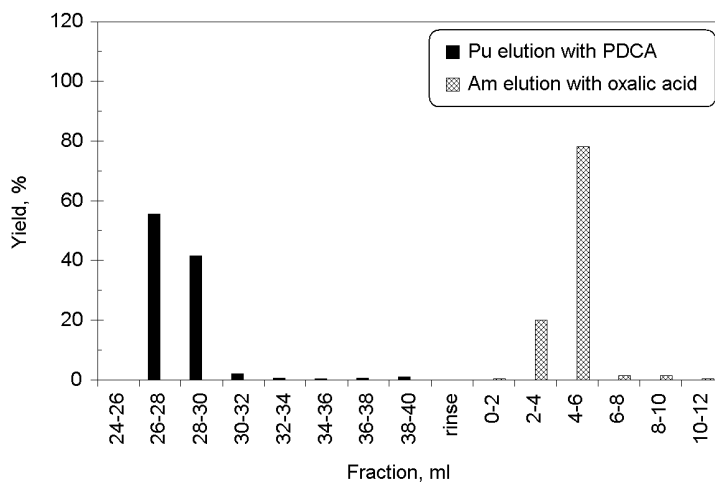


Fig. 5. Separation of Pu(III) and Am(III). Plutonium is firstly eluted from CS5A column with solution of 0.018 mol·dm<sup>-3</sup> dipicolinic acid and 0.12 mol·dm<sup>-3</sup> NaOH in 0.27 mol·dm<sup>-3</sup> CH<sub>3</sub>COOH, including the reduction agents. After washing the column, americium is eluted with reductant-free solution of 0.1 mol·dm<sup>-3</sup> oxalic acid in 0.19 mol·dm<sup>-3</sup> LiOH

In order to quantitatively separate trivalent plutonium and americium in CS5A column it was therefore, necessary to use two different eluents. ~99% of Pu eluted from the column between 26 and 32 minutes by using dipicolinic acid eluent; ~98% of Am eluted between 2 and 6 minutes with oxalic acid eluent (Fig. 5). The elution of plutonium was followed by rinsing the column for 10 minutes with dipicolinic acid solution, after which the elution of americium followed. The eluted plutonium and americium fractions were measured with alpha-spectrometry, and were found to be radiochemically and chemically pure.

### Conclusions

A previously developed on-line method for separation of americium from environmental samples has been modified to include separation of plutonium. The novel procedure is based on reducing plutonium to trivalent oxidation state, when it follows the behavior of americium throughout the separation processes. The elution of Pu and Am from the final separation column was done with two different eluents, and radiochemically pure quantitative separation of both elements was achieved. Further studies are needed for testing the method with environmental samples.

\*

The authors would like to thank Dr. Lorenzo PERNA and Dr. Laura ALDAVE DE LAS HERAS for the supportive ideas during the work. The valuable help of Mr. Ramon CARLOS-MARQUEZ and Ms. Ylva RANEBO is gratefully acknowledged.

### References

1. Y. YU-FU, B. SALBU, H. E. BJORNSTAD, J. Radioanal. Nucl. Chem., 148 (1991) 163.
2. M. P. RUBIO MONTERO, A. MARTIN SÁNCHEZ, M. T. CRESPO VÁZQUEZ, J. L. GASCÓN MURILLO, Appl. Radiation Isotopes, 53 (2000) 259.
3. L. PERNA, J. JERNSTRÖM, L. ALDAVE DE LAS HERAS, J. DE PABLO, M. BETTI, Anal. Chem., 75 (2003) 2292.
4. Determination of Trace Transition Metals in Reagent Grade Acids, Bases, Salts, and Organic Solvents Using Chelation Ion Chromatography, Application Note 75, Dionex Corporation, Sunnyvale, CA, USA, 2000.
5. A. MORGENSTERN, C. APOSTOLIDIS, R. CARLOS-MARQUEZ, K. MAYER, R. MOLINET, Radiochim. Acta, 90 (2002) 81.
6. F. D. HINDMAN, Anal. Chem., 55 (1983) 2460.
7. E. P. HORWITZ, M. L. DIETZ, R. CHIARIZIA, H. DIAMOND, S.L. MAXWELL, M. R. NELSON, Anal. Chim. Acta, 310 (1995) 63.
8. C. HILL, C. MADIC, P. BARON, M. OZAWA, Y. TANAKA, J. Alloys Comp., 271–273 (1998) 159.
9. G. MODOLO, R. ODOJ, J. Alloys Comp., 271–273 (1998) 248.
10. E. HRNECEK, K. IRLWECK, Determination of Am and Pu in Contaminated Soil Samples. Environmental Radiochemical Analysis, Royal Society of Chemistry, UK, 1999.
11. H. HOSHI, A. TSUYOSHI, K. AKIBA, J. Radioanal. Nucl. Chem., 249 (2001) 547.
12. M. PIMPL, R. H. HIGGY, J. Radioanal. Nucl. Chem., 248 (2001) 537.
13. R. CHIARIZIA, R. C. GATRONE, E. P. HORWITZ, Solvent Extr. Ion Exch., 13 (1995) 615.
14. M. SCHULTZ, W. BURNETT, T. HINTON, J. ALBERTS, M. TAKACS, Analysis of Am, Pu and Th in large volume water samples in the presence of high concentrations of iron, Special Publication, Royal Society of Chemistry, 291 (2003) 197.
15. G. CHOPPIN, Radiochim. Acta, 92 (2004) 519.
16. P. K. KHOPKAR, J. N. MATHUR, J. Inorg. Nucl. Chem., 36 (1974) 3819.
17. IonPac TCC-II Trace Cation Concentrator Column, Document No. 034466, Dionex Corporation, Sunnyvale, CA, USA, 1998.
18. IonPac CS5A Analytical Column, Document No. 031188, Dionex Corporation, 1999.
19. M. ŠIKOVEC, M. FRANKO, M. NOVIČ, M. VEBER, J. Chromatogr., A920 (2001) 119.
20. F. SEBY, S. CHARLES, M. GAGEAN, H. GARRAUD, O. F. X. DONARD, J. Anal. At. Spectrom., 18 (2003) 1386.
21. R. MICHALSKI, Acta Chromatogr., 15 (2005) 322.
22. N. CARDELLICCHIO, P. RAGONE, S. CAVALLI, J. RIVIELLO, J. Chromatogr., A770 (1997) 185.
23. B. DIVJAK, M. FRANKO, M. NOVIČ, J. Chromatogr., A829 (1998) 167.
24. H. LU, S. MOU, Y. YAN, S. TONG, J. RIVIELLO, J. Chromatogr., A800 (1998) 247.
25. N. CARDELLICCHIO, S. CAVALLI, P. RAGONE, J. RIVIELLO, J. Chromatogr., A847 (1999) 251.
26. X.-J. DING, S.-F. MOU, K.-N. LIU, A. SIRIRAKS, J. RIVIELLO, Anal. Chim. Acta, 407 (2000) 319.
27. M. R. VAN PAEMEL, H. DE RYCKE, S. MILLET, M. HESTA, G. P. J. JANSSENS, J. Agric. Food. Chem., 53 (2005) 1873.
28. E. H. BORAI, M. A. EID, H. F. ALY, Anal. Bioanal. Chem., 372 (2002) 537.
29. L. PERNA, F. BOCCI, L. ALDAVE DE LAS HERAS, J. DE PABLO, M. BETTI, J. Anal. At. Spectrom., 17 (2002) 1166.
30. R. M. SMITH, A. E. MARTELL, R. J. MOTEKAITIS, NIST Standard Reference Database 46, NIST Critically Selected Stability Constants of Metal Complexes Database, Version 8.0 For Windows, U.S. Department of Commerce, Technology Administration, National Institute of Standards and Technology, Standard Reference Data Program, Gaithersburg, MD, USA, 2004.
31. J. M. CLEVELAND, The Chemistry of Plutonium. American Nuclear Society, La Grange Park, IL, USA, 1979.
32. X. DING, S. MOU, J. Chromatogr., A920 (2001) 101.
33. D. H. METCALF, J. M. MCD. STEWART, S. W. SNYDER, C. M. GRISHAM, F. S. RICHARDSON, Inorg. Chem., 31 (1992) 2445.
34. K. BINNEMANS, K. VAN HERCK, C. GÖRLLER-WALRAND, Chem. Phys. Lett., 266 (1997) 297.

